FILM CONDENSATION OF STEAM IN THE PRESENCE OF NON-CONDENSING GASES

by

Hady Karim Al-Diwany

A thesis submitted for the Degree of
Doctor of Philosophy
in the Faculty of Engineering of the
University of London

Queen Mary College
December 1969.

ACKNOWLEDGEMENTS

The work here described has been wholly carried out in the Department of Mechanical Engineering, Queen Mary College, University of London.

The author wishes to express his sincere gratitude to Professor E.J. Le Fevre for his encouragement throughout the progress of this work and to Dr. J.W. Rose, who initiated the project, for his advice and help in the experimental work and in the preparation of this thesis.

The thesis was typed by Mrs Pearl Waterhouse to whom the author wishes to express his thanks and appreciation.

Thanks are also due to Mr F.C. Newman and the workshop staff of the Mechanical Engineering Department, Queen Mary College, for collaboration and co-operation in building the apparatus.

ABSTRACT

Considerable progress has been made in recent years towards the understanding of the mechanism of heat transfer by condensation in the presence of non-condensing gases. For the case of laminar film condensation on a plane vertical surface and for laminar flow of the vapour-gas mixture, boundary layer solutions have been given [22,43,44]. In the present work these are reviewed and modifications to the approximate solutions are suggested.

Such limited experimental data (for condensation on vertical flat plates under conditions of free convection) as was available at the outset of the present study, disagreed widely with theory. In the present work further careful measurements were made to test the validity of the theory. The condensing chamber (i.e. the steam chamber) was large in comparison to the condensing surface and care was taken to avoid forced convection effects associated with the vapour supply to the condenser. The vertical test plate was water-cooled and the surface temperature and the heat flux measured by thermocouples precisely located in isothermal planes at different depths.

Steam was condensed in the presence of air, argon, neon and helium. The pressure in all cases was near to atmospheric. Tests were carried out for a range of gas concentrations and coolant flow rates. The present results, in general, give good support to the boundary layer theory, as do other data [44] for air-steam mixtures at low pressures, published during the course of the

present work.

The theoretical solutions available at present (for free convection conditions) are not valid for the case where the non-condensing gas has a molecular weight smaller than that of the vapour (i.e. when the convective motion of the vapour-gas mixture near the condensing surface is in the opposite direction to that of the condensate). The present results for steam-helium mixture were used to obtain a semi-empirical equation for this situation.

Note on Presentation

Graphs, diagrams, photographs and tables, except when these are close to the text, will be found at the end of the relevant chapter.

Principal Symbols Used

D	diffusion coefficient
g	gravitational acceleration
Gr	$\rho_\infty(\rho-\rho_\infty)x^3 g/\mu^2$ (Grashof number)
h	height
h_{fg}	specific latent heat of vaporization
k	thermal conductivity
k	diffusion masstransfer coefficient (see ref 49, k_i)
$\dot{m}''$	mass flux (mass transfer rate per area)
p	absolute pressure
P_{tot}	steam-gas mixture total pressure
Q	heat flux (heat transfer rate per area)
Q_{nu}	heat flux given by simple Nusselt theory in the absence of a non-condensing gas
Sc	ν/D (Schmidt number)
Sp	$(T_o-T_w)k_f/(h_{fg}\,\mu_f)$
T	absolute temperature in Kelvin
t_p	steam-gas temperature measured by the probe, in Celsius
t_h	steam-gas temperature half way between the test plate and the flow dispersing section, in Celsius
t_f	steam-gas temperature near the flow dispersing section, in Celsius
u	x-component of velocity
$\tilde{u}$	a function of x having dimensions of velocity
v	y-component of velocity
W	non-condensing gas concentration
x	distance, along the condensing surface, from the leading edge
y	distance normally from the condensing surface

Greek Symbols

μ	absolute viscosity
ν	kinematic viscosity

α	thermal diffusivity
ρ	density
Δ	Condensate film thickness

<u>Subscripts</u>

f	condensate
g	gas(i.e. non-condensing component of mixture)
m	mean value
p	the probe
v	vapour(i.e. condensing component of mixture)
w	wall-condensate interface
o	condensate-mixture interface
∞	in vapour-gas mixture, remote from the interface (i.e. in the bulk, at mid hieght)

INDEX

Acknowledgements			2
Abstract			3
Note on Presentation			5
Principal Symbols Used			6
Chapter 1		Introduction	11
Chapter 2		Literature Survey	15
2.1		Introduction	16
2.2		Film condensation of vapours from vapour-gas mixtures	19
2.2.1		Condensation on flat plates	19
	a	Theoretical Analyses	20
	b	Experimental Investigations	31
2.2.2		Condensation on tubes	36
	a	Theoretical analyses and condenser design methods	36
	b	Experimental Investigations	38
2.3		Conclusion	46
Chapter 3		Theoretical Considerations	58
3.1		The effect of including the variation of condensate film thickness with height in Rose's analysis	60
3.2		Condensation from a mixture containing a gas lighter than vapour	65
3.3		Condensation from a mixture whose bulk temperature varies with height	68
Chapter 4		Apparatus	71
4.1		General	72

4.2 Test Plate.............................. 73

4.3 The Flow Dispersing Section.............. 76

4.4 Temperature and pressure measurements of the vapour-gas mixture................ 78

4.5 Non-Condensing Gas Injection and Concentration Measurements............ 80

4.6 Measurement of the Thermo Electrical potential difference.................... 81

4.7 Thermocouple Calibration................. 82

4.8 Apparatus Cleansing...................... 84

4.9 Leak Testing Technique................... 85

Chapter 5 Observations and Results................... 101

5.1 Experimental Procedure................... 102

a Temperature Profiles..................... 102

b Variation of heat flux with temperature difference (i.e. between the steam-gas mixture and the metal surface)............ 103

5.2 Accuracy of Observations................. 104

a Plate Thermocouple Positions............. 104

b Temperatures............................. 104

c Pressures................................ 105

d Mean Gas Concentration................... 105

5.3 Results................................... 105

Chapter 6 Discussion................................ 147

6.1 Mechanism of condensation in the presence of a non-condensing gas.................. 148

6.2 Comparison of present and other approximate analyses [43,44] with the "exact" variable property" analyses[22]. 149

6.3 Present Experimental Results.............. 150

6.3.1 Condensation of steam from steam-gas mixtures when maximum coolant flowrate was used.................................. 150

6.3.2 Effect of mixture-to-surface temperature difference on the fractional reduction in heat flux............................ 153

6.3.3 Effect of variation of mixture temperature with height on heat flux...... 155

6.4 Comments on the different gases used...... 155

6.5 Comparison between present esperimental results and equation 3.27 with earlier experimental work................ 157

Chapter 7 Concluding Remarks........................ 186

Appendices 189

Appendix 1 Velocity measurements and temperature profiles in the steam-gas mixture......... 190

Appendix 2 Vertical temperature variation in the steam chamber...................... 203

Appendix 3 Specimen Calculation...................... 210

Appendix 4 Experimental Errors...................... 215

Appendix 5 Condensation of steam from steam-carbon dioxide mixture............. 217

Appendix 6 Consideration of Sledgers analysis [44]... 218

Appendix 7 Computation of the theoretical results.... 221

References 231

Chapter 1

Introduction

A vapour may condense on a cooled surface in either of the two modes known as film and drop condensation. The mode prevailing depends primarily on the wettability of the condensing surface. A continous condensate film results when the surface is wetted by the condensate, while condensation may occur in the form of drops on a non-wettable surface. On a surface over which the degree of non-wettability varies, both drops and patches of film may be seen. The drops are usually less regular in shape than those associated with the term "ideal drop condensation" and falling drops tend to leave streaks of condensate behind them. This is termed "mixed" condensation.

Considerable progress has been made towards understanding the mechanism of heat transfer by film condensation and to a lesser extent that of the more complex phenomenon of drop condensation. It is known that the thermal resistance associated with drop condensation is, for the case of water at least, much lower than that associated with film condensation. Thus, for the same vapour-to-surface temperature difference, the heat flux during drop condensation is considerably higher than that during film condensation.

In addition to the mode of condensation, the heat transfer during the condensation process is affected by many other factors. One of these, the primary concern of the present work, is the presence of non-condensing gas in the condensing vapour. When a vapour, containing a non-condensing gas, condenses on a cooled surface, the concentration of the gas in the immediate vicinity of the surface is greater than that in the remoter vapour. In consequence of the increased gas concentration, the partial pressure, and hence temperature, of the vapour near the surface, is diminished. This, in turn, reduces the temperature difference across the condensate layer, and thereby diminishes the heat flux.

The reduction in heat flux due to the presence of non-condensing gas may be severe. For instance, recent analyses on the effect of the gas on film condensation on a flat plate and in the absence of forced convection (i.e. under natural convection conditions), have indicated that gas concentrations as little as 0.005 can cause a reduction of about 50% in heat flux.

With drop condensation the vapour-to-surface temperature difference is very small and consequently its measurement is very susceptible to errors arising from the presence of a non-condensing gas. The wide discrepancies between the results of different workers, which for a considerable time hindered progress towards understanding the mechanism of drop condensation, are now thought to be due to errors resulting from the presence of non-condensing gases.

Considerable progress has been made in recent years towards the theoretical understanding of the effect of non-condensing gas for the case of film condensation on a vertical flat plate. Conversely most of the experimental effort has been directed towards the practically more relevant case of the tube. Such limited data as was available for the flat plate prior to the present work indicated, for conditions of free convection, vapour-side heat transfer coefficients about an order of magnitude higher than those given by the theory.

The theory invokes the boundary layer approximation and is closely similiar to the well established solution for single phase free convection. A detailed study of the theory failed to reveal an explanation for the apparent discrepancy between theory and experiment. It was thus decided to undertake further careful experimental investigation.

The present thesis describes an experimental investigation on film condensation of steam in the presence of different gases. The condensation took place on a vertical flat plate and in the absence of forced convection. The object of this investigation was to provide heat-transfer data to assist in the development of the theoretical understanding of the influence of non-condensing gas on the process of heat-transfer by condensation.

It was hoped to resolve the above mentioned discrepancy between theory and experiment for the flat plate and thus to clear the way for theoretical study of the less mathematically tractable but practically more important case of condensation on tubes.

Chapter 2

Literature Survey

2.1. Introduction

2.2. Film condensation of vapours from vapour-gas mixtures

2.2.1 Condensation on flat plates

a Theoretical analyses

b Experimental **investigations**

2.2.2 Condensation on tubes

a Theoretical analyses and condenser design methods

b Experimental investigations

2.3 Conclusion

X

2.1 Introduction

Early theoretical investigators in the field of film condensation were primarily concerned with the mechanism of the processes that take place in the condensate film. The first major step forward in the study of the condensate film was made in 1916 when Nusselt [1,2] proposed simple theories for the laminar film condensation on vertical planes and horizontal cylindrical surfaces. These theories were based on the assumptions that the flow of the condensate film was controlled by gravitational and viscous forces. The condensation took place at the surface of the film and heat transfer through the film was solely by conduction. These theories, within their limits, found considerable experimental support particularly for systems where the vapour at the bulk is either stagnant or has a low velocity.

Recently Sparrow and co-workers [3,4,5] have formulated a laminar boundary layer film theory, taking into account convection and inertia effects in the film. Comparison between the heat transfer results obtained by these treatments and those of the Nusselt analyses has lent support to the reliability of the Nusselt analyses.

In many instances, when the condensation rates are high or the condensing surfaces are long or vapour bulk velocity is high, the Nusselt's analyses were found to underestimate the heat fluxes [6,7]. In these cases it was observed that although laminar flow is present at the upper edge of the condensing surface, ripples begin to form on the film surface and at some distance from the leading edge, the film becomes turbulent [7,8,9,10]. Various analyses were proposed for this type of condensation [11,12,13]. For a turbulent condensate film in the absence of forced convection in the vapour, an analysis was developed incorporating the Nusselt analysis for the laminar region with an analysis for the turbulent region. The analysis for the turbulent region was based on an analogy with single phase flow, accompanied by heat transfer, in a duct or a pipe. For moving vapours, analyses similiar to the Nusselt analysis, were proposed which took into account the vapour interfacial stress [12,13]. Experimental data, though limited, gives reasonable support to these analyses [14,15,16].

As the processes in the condensate film became better understood attention was directed to the processes in the vapour. Some progress has been made and investigations are continuing to understand more fully the roles of such effects as vapour velocity, superheat, interphase matter transfer effects and also the effect of the presence in the vapour of non-condensing gases.

In most industrial applications, the vapour flows over the cooling surface with a significant velocity (i.e. forced convection flow). This can have an appreciable effect on the processes of condensation. While the effect of vapour velocity is still not fully understood, it has been found that heat **flux increases** appreciably with increasing vapour velocity [17,18,19].

When the condensing vapour is superheated, the interface remains very nearly at saturation temperature [20]. Theoretical analyses have shown that heat flux increases only slightly with increasing superheat [13,20,21,22]. These analyses were either based on modifying the Nusselt analysis by accounting only for the enthalpy change, from superheat to saturation, at the interface [13,20], or by employing the boundary layer theory to both phases, thereby taking account of the convection effects and the sub-cooling in both phases [21,22]. Most experiments indicate similiar modest increases in heat flux to those obtained in the analyses[23,24,2

Recently attention has been given to the processes at the liquid-vapour interface [22,26,27,28,29]. When a vapour and its liquid are in equilibrium, the temperatures of liquid and vapour phases at their interface are the same. Condensation takes place only if the liquid interfacial temperature is less than that of the vapour. More precisely, during condensation or evaporation, there are changes of temperature, pressure and density in both phases in the immediate vicinity of the interface(i.e. within a few mean free paths). The temperature difference at the interface is often referred to as the "temperature jump" and the phenomenon as the "interfacial resistance". While this effect is not fully understood, there is a clear indication that the "temperature jump" increases with decreasing pressure and increasing heat flux [26]. For most cases, except at very high fluxes or low pressures this effect is thought to be small [22,27]. It could, however, be significant for dropwise condensation and for condensation of liquid metals where the resistance offered by the condensate is small.

A further area of interest which has received considerable attention on account of its practical importance, but is still not fully understood, is the effect of the presence of non-condensing gases in the vapour phase. The presence of such gases, as pointed out in chapter 1, causes a reduction in heat flux. This aspect of condensation heat transfer is the subject of the present study and in consequence the literature on it will be reviewed in more detail.

2.2 Film condensations of vapours from vapour-gas mixtures

Investigations have been carried out on flat plates under conditions of both free and forced convection. Owing to the practical application, most of the experimental investigations have been carried out using tubes. Condensation on flat plates, however, has received extensive theoretical treatments since it is more amenable to analysis. Details of the various experimental arrangements and conditions, prevailing in the experimental investigations for mixtures in the absence of forced convection, are tabulated at the end of this chapter.

2.2.1 Condensation on flat plates

a-Theoretical analyses

Early analyses in this field were based on consideration of the process in the mixture as that of a one-dimensional diffusion (i.e. the vapour diffusing through a film of stagnant non-condensable gas)[30,31,32] . The earliest of these analyses is that of Stefan [31,32] , this was based on the Maxwell equation of diffusion [33,34] and yielded the following expression for the mass transfer rates.

$$\dot{m}_w = \frac{D}{\delta} \frac{P_m}{RT} \ln \left[\frac{P_{gs}}{P_{gm}}\right] \qquad 2.01$$

where P_m is mixture pressure.

P_{gs} is gas partial pressure relative to the condensing surface temperature.

P_{gm} is gas partial pressure in the bulk.

δ is diffusion layer thickness.

In more recent analyses, many problems in heat and mass transfer have been formulated in terms of boundary layer theory [e.g. 5,35,36,37,38,39] . The boundary layer partial differential equations may sometimes be solved by using the so called similarity transformations. This technique involves the transformation of the rélevant partial differential equations into fewer ordinary differential equations by introducing new variables. The resulting equations are generally non-linear and are usually solved, for given boundary conditions, by numerical methods [40,41].

In the present problem, two interacting boundary layers exist, the condensate layer and the vapour-gas mixture layer. In order to solve the differential equations of these layers certain boundary conditions at the condensing surface and outside the mixture layer must be specified, in addition the interfacial conditions of both layers must be matched in such a way that the physical laws are satisfied.

Sparrow and co-workers have used the similarity transformation technique in their analyses for the condensation of vapours from mixtures, in the absence of forced convection, over vertical plates [21,22,35] and from moving mixtures over a horizontal plate [27].

Sparrow & Eckert [21] proposed an analysis for condensation from a mixture, in the absence of forced convection, on a vertical plane surface, in which the condensate and the mixture film were treated as boundary layers. The analysis did not take into account the effect of natural convection in the mixture due to density differences. The heat transfer results, computed for steam-air mixture, while affirming the role of the non-condensables in drastically reducing the heat fluxes, indicated a much higher reduction in these fluxes than that found experimentally [42] (these experiments were carried out on a horizontal tube). This discrepancy was attributed to the exclusion of the free convection which would aid the removal of non-condensables by increasing the flow in the direction parallel to the plate surface. In conclusion Sparrow & Eckert regarded their results as qualitative rather than quantitative and suggested the need for more detailed analysis in which free convection effect is included. This suggestion was taken up by Sparrow and Lin [37]. The Nusselt analysis for the condensate film was employed while boundary layer approach was applied to the vapour-gas layer. The properties of the latter were assumed to be constant, except in the buoyancy term of the momentum equation. The relevant boundary layer equations for continuity, momentum and diffusion are, respectively, as follows, referring to fig 2.01.

$$\frac{\partial u}{\partial x} + \frac{\partial v}{\partial y} = 0. \qquad 2.02$$

$$u\frac{\partial u}{\partial x} + v\frac{\partial u}{\partial y} = g\left(1-\frac{\rho}{\rho_\infty}\right) + \nu\frac{\partial^2 u}{\partial y^2} \qquad 2.03$$

$$u\frac{\partial W}{\partial x} + v\frac{\partial W}{\partial y} = D\frac{\partial^2 W}{\partial y^2} \qquad 2.04$$

Equations 2.02, 2.03 & 2.04 were reduced to ordinary differential equations using the following similarity transformation.

(a) Similarity variable

$$\eta = c(y-\delta)/x^{\frac{1}{4}}$$

where $c = \left[\dfrac{g(M_g - M_v)/4\nu^2}{M_g - (M_g - M_v)W_\infty}\right]^{\frac{1}{4}}$

δ is the condensate layer thickness.

M_g and M_v are the molecular weights of gas and vapour respectively.

(b) Stream function and mass fraction respectively

$$\psi = 4\,Cx^{\frac{3}{4}}f(\eta), \qquad W - W_\infty = \phi(\eta)$$

The resulting ordinary differential equations were

$$f''' + 3ff'' - 2(f')^2 + \phi = 0 \qquad 2.05$$

$$\phi'' + 3Sc\, f\, \phi' = 0 \qquad 2.06$$

where the primes denote differentation with respect to η and Sc is the Schmidt number.

To solve equations 2.05 & 2.06 numerically, Sparrow & Lin specified five boundary conditions, these were

(1) Prescribed value for W at the bulk.

(2) Vanishing longitudinal velocity in the bulk as $y \rightarrow \infty$

(3) For condition of no slip at the interface the interfacial velocities of condensate and mixture are the same.

(4) By continuity the vapour and condensate interfacial mass transfers are the same.

(5) The impermeability of the interface to the non-condensing gas.

From the mathematical representation of these conditions the following parameters emerged as freely disposable parameters:-

$$M_g,\ M_v,\ W_\infty,\ Sc,\ (\rho\mu)_L/(\rho\mu),\ c_{p_L}(T_\infty - T_w)/(h_{fg}\ Pr_L)$$

For various values of W_∞, Sc, $(\rho\mu)_L/(\rho\mu)$, equations 2.05 & 2.06 were solved to determine the relationships between the interfacial gas concentration and partial pressure and the group $c_{p_L}(T_\infty - T_w)/(h_{fg}\ P_{r_L})$, the mixture being steam-air at atmospheric pressure. From these results the interfacial temperature was computed for various mixture-to-surface temperature difference and hence the heat flux was determined using the appropriate Nusselt expression.

Sparrow & Lin presented their heat transfer results as a plot of fractional reduction in heat transfer rates against mixture-to-surface temperature differences, fig 2.02. These results have shown that the presence of a few per cent of air causes a reduction of 50% in the heat flux. No comparison with experimental data on flat plates was made, instead Othmer's data [40] were used for comparison. For this comparison, fractional reduction in heat fluxes were computed on the basis of Sc=0.5, & $(\rho\mu)_L/(\rho\mu) = 150$.

Although Sparrow & Lin concluded that there was good agreement between theory and experiment, his comparison could not be considered as satisfactory since in any situation, the values of Sc and the viscocity ratio (i.e. $(\rho\mu)_L/(\rho\mu)$) vary widely within the mixture. Therefore it is difficult to use this theory for comparison with experiments.

A more rigorous and comprehensive analysis was presented by Minkowycz and Sparrow [22]. The boundary layer treatment was again applied to both the condensate and the mixture layers. The analytical model included, in addition to the effect of non-condensing gas, the effects of interfacial resistance (i.e. the existence of temperature jump at the interface), superheating, free convection due to concentration gradients, "thermal diffusion" (defined as the transport of mass due to temperature gradients), "diffusion thermo " (defined as the energy transport due to concentration gradients) and variable properties for both layers. The governing equations for the condensate layer were simplified by neglecting the inertia and natural convection terms in them (as in the simple Nusselt theory), since these effects have been shown in an earlier paper, ref [5], to be of negligible effect on the heat transfer.

The condensate equations are

$$\frac{\partial}{\partial x}(\rho u) + \frac{\partial}{\partial y}(\rho v) = 0 \qquad 2.07$$

$$\rho g + \frac{\partial}{\partial y}\left(\mu \frac{\partial u}{\partial y}\right) = 0 \qquad 2.08$$

$$\frac{\partial}{\partial y}\left(k \frac{\partial T}{\partial y}\right) = 0 \qquad 2.09$$

and the equations for the mixture layer are

$$\frac{\partial}{\partial x}(\rho u) + \frac{\partial}{\partial y}(\rho v) = 0 \qquad 2.10$$

$$\rho\left(u\frac{\partial W}{\partial x} + v\frac{\partial W}{\partial y}\right) = -\frac{\partial j_g}{\partial y} \qquad 2.11$$

$$\rho\left(u\frac{\partial u}{\partial x} + v\frac{\partial u}{\partial y}\right) = g(\rho-\rho_\infty) + \frac{\partial}{\partial y}\left(\mu\frac{\partial u}{\partial y}\right) \qquad 2.12$$

$$\rho c_p\left(u\frac{\partial T}{\partial x} + v\frac{\partial T}{\partial y}\right) + (c_{pg}-c_{pv})j_g \frac{\partial T}{\partial y} = -\frac{\partial q^*}{\partial y} \qquad 2.13$$

where j_g and q^* are the generalized diffusive mass flux and heat flux respectively.

Th[illegible] [illegible]uations were transformed into the following ordina[illegible] [illegible]ions.

For the con[illegible] [illegible]yer.

$$\left[\varphi_\mu\left(\frac{f'}{\varphi_\rho}\right)'\right]' + \varphi_\rho = 0 \qquad 2.14$$

$$(\varphi_k\, \theta')' = 0 \qquad 2.15$$

where f' is dimensionless stream function

$$\theta = T/T_\infty, \quad \varphi_\rho = \rho/\rho_w, \quad \varphi_\mu = \mu/\mu_w, \quad \varphi_k = k/k_w$$

For the vapour-gas layer,

$$\left[\frac{W'}{Sc}\right]' + 3Sc\, F\left(\frac{W'}{Sc}\right) = -\Gamma' \qquad 2.16$$

$$\left[\frac{F'}{\Phi_\mu \Phi_\rho}\right]'' + 3F\left[\frac{F'}{\Phi_\mu \Phi_\rho}\right]' - \left[\frac{2F'^2}{\Phi_\mu \Phi_\rho} + \Phi_\mu(1-\Phi_\rho)\right] = 0 \qquad 2.17$$

$$\left[\frac{\Phi_k}{\Phi_\mu}\theta'\right]' + Pr_\infty\left(3\Phi_c F + \Phi_{cgv}\frac{W'}{S_c}\right)\theta' = -Pr_\infty\left(\Lambda' + \Phi_{cgv}\Gamma\theta'\right) \qquad 2.18$$

where F, θ are dimensionless stream function and temperature respectively.

$$\Gamma = \frac{a}{Sc} W(1-W)\frac{\theta'}{\theta}$$

$$\Lambda = \frac{a\theta}{c_{p_\infty}} \frac{M^2}{M_g M_v}\left(\frac{W'}{Sc} + \Gamma\right)$$

$$\Phi_\rho = \rho/\rho_\infty, \quad \Phi_k = \frac{k}{k_\infty}, \quad \Phi_\mu = \mu/\mu_\infty, \quad \Phi_c = \frac{c_p}{c_{p_\infty}}, \quad \Phi_{cgv} = \frac{c_{pg} - c_{pv}}{c_{p_\infty}}$$

M is mixture molecular weight.

Kho, Sparrow & Hartnett[5], when dealing with the condensation of pure vapours, concluded that the neglect of continuity of interfacial shear has completely negligible effect on the heat transfer results for the range of parameters appropriate to steam under free convection. This conclusion was implemented in this analysis when dealing with the coupling of the condensate and mixture equations at the interface.

Dealing with steam-air mixture and for all cases other than those which included interfacial resistance, similarity solutions were obtained for these equations.

This is done by replacing them in to integral forms. In these numerical solutions a special iterative method was used [41]. When interfacial resistance was included Minkowycz & Sparrow found that the similarity solutions only exist for pure vapour; in all other cases local similarity was employed (i.e. the application of similarity at a certain height from the leading edge).

To evaluate the necessary thermal and transport properties for the condensate layer, a reference temperature was derived. Sparrow & Minkowycz found that a virtual coincidence between heat transfer rates evaluated by solving the condensate layer equations and those using the Nusselt analysis was achieved, for the range of parameters used in the analysis, if all the properties appearing in the Nusselt expression were evaluated at the reference temperature defined by

$$T^* = T_w + 0.31\ (T_o - T_w) \qquad 2.19$$

Heat transfer results were obtained for a wide range of parameters including bulk gas concentration, system pressure level, wall to bulk temperature difference and degree of superheat. The results, presented as fractional reductions in heat flux against mixture-to-surface temperature difference, have shown that for a bulk air concentration of 0.5% the heat flux drops by about 50% below that of pure vapour condensation, also the influence of the non-condensing gas is strongly accentuated as bulk temperature decreases. The results also demonstrated that the interfacial resistance, thermal diffusion and diffusion thermo are second order effects and the effect of superheat is more important when non-condensing gases are present than in the case of pure vapour.

Comparisons of Minkowycz & Sparrow's analysis with Othmer's data and the Sparrow & Lin analysis, fig 2.03, show that the first analysis predicted higher reduction in heat transfer than those obtained experimentally and those predicted by the Sparrow & Lin analysis. The lack of agreement between the two analyses was attributed to the difference in evaluating the properties of the condensate and the mixture

The effect of the non-condensing gas and interfacial resistance in the condensation of moving mixtures on a horizontal plate was recently investigated by Sparrow, Minkowycz and Saddy [27]. As in ref [37], the fluid properties of both the condensate and the mixture were assumed to be constant. The effects of inertia and natural convection in the condensate layer were neglected. Numerical solutions were obtained for the relevant ordinary differential equations, and in evaluating the heat transfer results for steam-air mixture, the reference temperature derived in ref [22] was used to evaluate the relevant properties of the condensate.

The heat transfer results indicated a much smaller reduction in heat fluxes when compared with those obtained by Minkowycz & Sparrow for mixtures in the absence of forced convection, fig 2.04.

Although the numerical methods in solving the boundary layer differential equations employed in the foregoing analyses produced " xact" solutions, these methods are laborious and require extensive computation. Consequently in recent literature, approximate solutions were obtained for these differential equations [27,43,44] . These solutions were based on assigning suitable profiles for the temperature, gas concentration and the longitudinal velocity in the mixture.

Rose [43] and Sledgers [44] considered the condensation from mixtures, in the absence of forced convection, over vertical plates while Sparrow and others [27] dealt with moving mixtures on horizontal plates. Rose & Sledgers applied the Nusselt's analysis to the condensate film and obtained equations, relating heat and mass transfer parameters and the relevant fluid properties.

Rose proposed the following profiles

$$u = u_o(1-y/\delta)^2 + \tilde{u}(y/\delta)(1-y/\delta)^2$$

$$\frac{W-W_\infty}{W_o-W_\infty} = (1-y/\delta)^2$$

where u_o, W_o are the interfacial velocity and gas concentration respectively, δ is the mixture boundary layer thickness $\tilde{u}$ is a function of the normal distance to the plate, having dimensions of velocity.

Rose deduced the following equation

$$10\,Sp\,Sc[(\mu_f\rho_f/(\mu\rho))[W_\infty/w_o]^2[20/21+W_o Sc/W_\infty]$$
$$+8/(Sp^2 Sc)[\mu\rho/(\mu_f\rho_f)][w_o/W_o]^2[5Sp/28-Xw_o/3]$$
$$=(100/21)(W_\infty/W_o)-2w_o/W_o+8Sc \qquad 2.20$$

where $X=(M_g-M_v)/[M_g-(M_g-M_v)W_\infty]$ ~~2.20~~

$w_o=W_o-W_\infty$

For given surface-to-bulk temperature difference, W_∞ and T_∞, equation 2.20 may be used to determine the interfacial temperature, hence the heat flux is determined using the Nusselt expression.

Sledgers proposed the following profiles:-

$$u/u_\delta=1-F(\eta)-\lambda G(\eta),\ \phi=\theta=1-F(\eta)$$

where $F(\eta)=2\eta-2\eta^3+\eta^4$

$G(\eta)=(\eta(1-\eta)^3)/6$

ϕ and θ are dimensionless gas concentration and mixture temperature respectively

$\eta=(y-\delta)/(\Delta-\delta)$

δ & $(\Delta-\delta)$ are the condensate and the mixture layer thicknesse respectively

λ is a constant

The following equations were deduced by Sledgers

$$I_3=W_\infty KN/(W_o\cdot 12) \qquad 2.21$$

$$N\left[1-\frac{\rho_\infty}{\rho_o}\right]=\frac{144}{64}\frac{I_3^2}{I_2}\left[\frac{W_o}{W_\infty}\right]^2\left[\frac{5}{3}\frac{I_1}{I_3}\frac{W_\infty}{W_o}+1-\frac{W_\infty}{W_o}-Sc(1+\frac{\lambda}{12})\right] \qquad 2.22$$

where $K=4k_f(T_o-T_w)/(\rho_f\nu_f h_{fg})$

$N=(\rho_f/\rho_o)^2\nu/(D(1-W_\infty/W_o)^2)$

$I_2=0.3$

I_1 and I_3 are known functions of λ

For given W_∞, T_∞, and T_o, equation 2.22 may be solved for λ, hence T_w is determined from equation 2.21. The heat flux is determined using the Nusselt expression.

Comparison with the results of the exact solutions of ref[22], for air-steam mixture, shows that, at low air concentrations(i.e. less than 0.0050), the results of both equations 2.20 and 2.22, underestimate the heat flux while at higher air concentrations, the three solutions virtually coincide.

Sparrow and others[27] compared their results, obtained from exact solutions, with the results they obtained by the approximate solution and found virtual coincidence between the two.

It should be noted that all of the above analyses which were based on the boundary layer theory are only valid for cases where the molecular weight of the non-condensing gas is greater than that of the vapour. The results of these analyses hold only for mixture Grashof numbers above those necessary for the validity of the boundary layer approximations and below those at which turbulence occurs.

(b)-Experimental investigations

In contrast to the extensive theoretical treatment, the experimental investigations on the condensation on flat plates are only few [44,45,46,47,48]. These investigations are all on mixtures in the absence of forced convection.

In these investigations, unless it is stated otherwise, the heat flux was determined from the coolant temperature rise and its mass flowrate and the gas concentration was determined by measuring the mixture temperature and pressure and employing the ideal-gas mixture relations.

Hampson [45] investigated the effect of nitrogen on the film and the drop condensation of steam on a vertical copper plate. The condensing surface temperature was measured by means of six thermocouples embedded, in solder, in grooves parallel to the horizontal edge of the surface (i.e. isotherms) at a depth of 0.025in below the surface. The gas was fed continously, and together with excess steam, was vented at the base of the test plate. For the film condensation, Hampson deduced the following empirical expression for the steam-side heat-transfer coefficient,

$$h_s = C\left[\frac{k_f^3 \rho_f^2 h_{fg} g}{L \mu_f \Delta\theta_s}\right]^{\frac{1}{4}} \left(\frac{1}{W}\right)^{0.11} \qquad 2.23$$

where $\Delta\theta$ is the mixture-to-surface temperature difference

L is the height of the plate

W is the ~~percentage~~ gas concentration by mass

C = 0.604 for ~~1>W>0.1~~ 0.01 > W > 0.001

and = 0.64 for 4>W>0.5 0.04 > W > 0.005

Brdlik [46] investigated the condensation of steam from steam-air mixture over a horizontal plate. The plate was cooled by water circulating in channels passing through the plate. The condensate was drained through a central hole in the plate. The mixture and the interface temperatures were measured by a vertically moveable thermometer. The gas concentration was determined from the measured condensate and gas flowrates. Using his experimental data (in which the gas concentration were greater than 3%), Brdlik obtained the following expression for the condensate mass flowrate.

$$\dot{m}_c = \frac{135D}{LR_vT}\,\frac{P_{vm}}{P_a}\,(P_{vm}-P_v) \qquad 2.24$$

where R_v is the gas constant for the steam

P_v & P_{vm} are the steam partial pressure at the bulk and relative to the condensing surface temperature

P_a and L are ambeint pressure and plate length respectively

The effects of nitrogen, helium and carbon dioxide on the condensation of ethanol and of nitrogen and carbon dioxide on the condensation of carbon tetrachloride were investigated by Akers, Davis and Crawford [47]. The vapours condensed on two faces of a vertical copper plate which was cooled by water passing through channels in the plate. The plate was mounted in a 4300ml flask which contained the evaporating liquid. The condensing surface temperature was measured by means of a thermocouple located at the mid point of the condensing plate. The experimental results were expressed in the form of dimensionless groups. In deriving these groups Akers, Davis and Crawford integrated the differential equation of the one dimensional diffusion to produce the following expression

$$\frac{K_g\, LRT}{D}\,\frac{P_{bm}}{P} = \frac{L}{Z}$$

where $K_g = \dfrac{Q}{h_{fg}\cdot M\cdot A(P_{go} - P_{g\infty})}$

Q is the heat flux

P_{go} and $P_{g\infty}$ are the gas partial pressure at interface and bulk respectively

P is mixture total pressure

$$P_{bm} = \frac{P_{go} - P_{g\infty}}{\ln\left[P_{go}/P_{g\infty}\right]}$$

L is the height of the condensing plate

Z is the mixture layer thickness

M is the mixture molecular weight

A is the condensing surface area

In analogy to the natural convection heat transfer the ratio L/Z was taken as a function of the Grashof and Schmidt numbers. The relationship obtained, fitting their data, was, fig 2.05

$$\frac{K_g\, LRT}{D}\,\frac{P_{bm}}{P} = 1.02(Gr.Sc)^{0.373} \qquad 2.25$$

Kroger & Rohsenow [48] performed experiments for the condensation of potassium from mixtures with helium and argon on the underside of a horizontal disc, the disc was cooled by boiling water. The temperature distribution across the thickness of the plate was determined by means of thermocouples located in holes, drilled at various depths in the plate, parallel to its surface. The surface temperature was determined by extrapolation and the heat flux was determined from the temperature gradient across the plate thickness and its thermal conductivity. Two thermocouples were located at two different depths in the vicinity of the condensing surface to determine the temperature profiles in the mixture layer. Heat fluxes were determined for various known amounts of injected helium or argon. Kroger & Rohsenow expressed their experimental results in terms of, and compared them with, a simple analysis they developed for the heat transfer coefficient. This was based on the one dimensional diffusion of a gas through another, stagnant gas. This comparison showed a good agreement between theory and experiment for potassium-helium system and a poor agreement for potassium-argon system. The discrepancy for the second system was attributed to the influence of the convective currents which were not included in the analysis and which were more important in the second system than in the first (since potassium and argon are of approximately the same molecular weight).

Sledgers [44] carried out a systematic investigation in which, for constant bulk temperature and gas concentration, fractional reductions in heat flux were determined for different surface-to-bulk temperature differences. In this investigation steam was condensed from steam-air mixture on a vertical plate, the plate was cooled by freon 12 vapour. The temperature distributions across the plate thickness and along its height were determined by means of two rows of thermocouples located in holes, drilled in the plate, parallel to its surface. The surface temperature was determined by extrapolation and the heat flux from the temperature gradient across the plate. The gas concentration was measured by sampling using a specially adapted McLeod gauge. The experimental results were compared with Sledger's approximate analysis and with the exact analysis of ref [22]. This comparison showed an agreement to within 30% with the theoretical analyses.

2.2.2 Condensation on tubes

a-Theoretical analyses and condenser design methods

The simplicity of the surface geometry of the flat plate made it amerable to analysis. With tubes, however, the surface geometry makes the formulation of an analysis more difficult. Only one theoretical analysis or tubes could be found in the literature [49], this is on mixtures in the absence of forced convection. In most practical applications, the mixture at the bulk has a finite velocity. In the design of condensers for such mixtures, various methods of calculation of the surface area have been proposed [e.g. 50,51,52].

Thain [49] applied the boundary layer theory to the condensation of vapour, a horizontal tube, from vapour-gas mixtures in the absence of forced convection. Nusselt's analysis was employed for the condensate layer. The relevant constant property partial differential equations for the mixture layer were transformed into ordinary differential equations. These ordinary differential equations were exactly the same as those obtained by Sparrow and Lin[37]. By making some approximations, the boundary conditions were also the same as those of Sparrow and Lin, consequently Thain used the solutions obtained by Sparrow and Lin for the steam-air mixture. Thain, however, found that his analysis consistently under-estimates the heat flux when compared with the experimental results he obtained for the steam-air mixtures. This discrepancy was attributed to the assumption he made, when formulating his boundary layer equations, that normal velocity to the condensing surface is of an order of magnitude less than the tengential velocity. Accordingly, Thain neglected some of the normal velocity terms. However, in estimating the values of these velocities at the interface, Thain found that they are of the same order of magnitude at some parts of the interface.

The calculation methods for surface area of industrial condensers are based on semi-empirical analyses and most of these methods involved graphical solutions. The most commonly referred to of these methods is that of Colburn and Hougen[50]. Colburn and Hougen suggested that the local heat transfer rate for mixtures could be evaluated from the following energy balance equations:

$$h_s(t_v-t_c) + K\,M_v\,h_{fg}\,(P_v-P_c) = h_o(t_c-t_w) = U\,\Delta T \qquad 2.26$$

where t_v, t_c, t_w are the mixture temperature at the bulk, the interfacial temperature and the surface temperature respectively

P_v and P_c are the vapour partial pressures at the bulk and at the interface respectively

h_o is the vapour-side heat-transfer coefficient

U is the overall heat-transfer coefficient

ΔT is the overall temperature difference

h_s and K are determined from the following relationships:

$$J_h = \frac{h_s (c\mu/k)^{\varepsilon}}{c\ G}$$

$$J_m = \frac{K \cdot M_m \cdot P_{gf} (\mu/\rho d)^{\xi}}{G}$$

where J_h and J_m are determined from suitable graphs relating these factors to the mixture Reynolds number[53]

c is the mixture specific heat at constant pressure

d is the tube diameter

μ is the mixture viscosity

G is the mixture mass flowrate

M_m is the mean molecular weight of the mixture

P_{gf} is the log mean partial pressure of the gas relative to P_v and P_c

By graphical integration the average value for $U\Delta T$ is found hence the required area.

b- Experimental investigations

Various investigators examined the process of condensation from mixtures in the absence of forced convection [25, 42, 59, 54, 55, 56, 57, 58, 59] and from mixtures under forced convection conditions [e.g. 19, 60, 61, 62]. The majority of these investigations dealt mainly with steam-air mixtures and except in four cases [57, 60, 61, 62], the tubes were horizontal. In some investigations the data of other investigators were used to verify some empirical expressions [46,47]. In all these investigations, unless it is stated otherwise, the heat flux was determined from the coolant temperature rise and its mass flowrate and the gas concentration by measuring the mixture temperature and pressure and using the-ideal-gas mixture relation

Condensation of vapours from mixtures in the absence of forced convection

Othmer [42] carried out a series of tests in which he examined the dependence of the steam-side heat-transfer coefficient on three variables, during the condensation of steam from steam-air mixture. These variables were air concentration, mixture-to-surface temperature difference and the mixture temperature. By keeping two of these variables constant he determined the variation of the coeffici with the third variable. The apparatus consisted of four tubes, the outer one in which water was boiled at atmospheric conditions, the generated steam condensed on an inner tube (the test tube). Inside the test tube water was boiled at sub-atmospheric conditions (this was to insure a constant surface temperature). The steam generated at the sub-atmospheric conditions, condensed on two tubes passing through the test tube; Water at room temperature passed through these two tubes. The surface temperature was measured by a thermocouple embedded in the surface. The gas concentration was determined from the gas partial pressure, which was directly measured by a specially designed manometer [63], and the vapour partial pressure. Othmer deduced the following empirical expression for the coefficient of heat transfer.

$$\log h_c = \log\Delta T(1.213-0.00242T) + \left[\log\Delta T/3.439 - 1\right]\left[\log(W+0.505)-1.551-0.009T\right] \qquad 2.27$$

where ΔT is the mixture-to-surface temperature difference

T is the mixture temperature

W is the percentage gas concentration by volume

Langen [54] carried out a similiar but less detailed examination to that of Othmer. In some tests the pressure and wall temperature were held constant while varying the air concentration and in other tests the pressure and gas concentration were held constant while varying the wall temperature. Mixed condensation prevailed in all the tests that Langen performed. The surface temperature was measured by a resistance wire thermometer embedded in grooves along the surface. The gas was fed continously into the system and the gas concentration was determined from the measured mass flowrates of the gas and the collected condensate. Langen obtained the following expression for the condensate mass flux:-

$$\dot{m}''_c = 14.5(W)^{-0.6}(P_{v\infty}-P_{vo})^{0.5} \qquad 2.28$$

where W is air concentration by mass

$P_{v\infty}$ and P_{vo} are the vapour partial pressure at the bulk and the interface.

Luder [56] investigated the condensation of steam and carbon tetrachloride from mixtures with various gases, mainly air, hydrogen and methane. Although Juder calculated the vapour-side heat transfer coefficient and the vapour partial pressure relative to the surface temperature, he did not explain the methods he used in these calculations. The following expression was deduced for the vapour-side heat transfer coefficient, fig 2.06 .

$$\frac{h_c}{D} = C\left[\frac{P_o}{P_1 \cdot P_2}\right] \ln\left[\frac{P_o - P_1}{P_o - P_2}\right] \qquad 2.29$$

where D = the diffusion coefficient

C = a constant which varies from one vapour-gas mixture to another

P_o = mixture pressure

P_1 & P_2 are the vapour partial pressu[illegible] [illegible]e bulk and relative to the surface temperature respectively

The right hand side of equation 2.29 is a function of the gas concentration, therefore fig 2.06 indicates that for a given concentration, the reduction in heat flux when the air is present is less tha[n] that when methane is present and more than that when the hydrogen is present.

Tolouhirskii and Yampolskii [57] investigated the condensation of steam from steam-air mixtures over a vertical tube. The surface temperature was measured by means of thermocouples embedded in grooves along the height of the tube. The gas concentration was determined from the measured flowrates of the condensate and the gas. The following expression was deduced for the steam-side heat transfer coefficient.

$$h_c = 0.48\ h_{nu}/(W)^{\frac{1}{3}} \qquad 2.30$$

where h_{nu} is the heat transfer coefficient corresponding to the condensation of pure vapour with the same mixture-to-surface temperature difference.

De Friece [55] investigated the condensation of n-heptane from mixtures of n-heptane and methane. The heat flux was determined from the cooling water inlet and outlet temperature difference and its mass flowrate. To determine the vapour-side coefficient the Wilson plot was used. This entailed the plotting of the reciprocal of the overall coefficient against the reciprocal of 0.8 power of the cooling water velocity and by extrapolating to zero value for the abscissa the vapour-side coefficient was determined for each gas concentration. De Friece did not present his data in any mathematical form. Akers, Davis and Crawford [47], however, fitted Langen's [54] and De Friece's [55] data by the following correlation.

$$\frac{K_g\ LRT}{D}\ \frac{P_{bm}}{P} = 0.62(Gr.Sc)^{0.373} \qquad 2.31$$

Brdlik [46] used the data of Othmer [42] Langen [54] Toloubinskii and Yampolskii [57] and Gudenchuk [67] to obtain the following expression for the heat transfer coefficient when the gas concentration by volume is less than 0.03

$$h_c = 0.43\ h_{nu} \left[\frac{P_t}{P_a}\right]^{0.1} (W)^{-0.28} \qquad 2.32$$

where h_{nu} = the Nusselt coefficient for the condensation of pure vapours

P_t = the mixture pressure

P_a = the barometric pressure

W = the gas concentration by volume

Mazyrkevich [58] investigated the effect of air on the condensation of ammonia from ammonia-air mixtures over a horizontal tube. The surface temperature was measured by thermocouples fitted in grooves on the tube surface. Thermocouples were held in various positions, in the mixture, around the periphery of the tube to examine the temperature of mixture distribution around the tube. The gas concentration was determined by venting and sampling the mixture from three various points in the mixture chamber. The investigation indicated a marked variation in the mixture temperature, around the tube, fig 4.07. However, no variation in the mixture concentration was detected. Mazyrkevich compared his results with those he obtained for the condensation over a vertical tube [64,65] . This comparison, fig 2.08, shows that, for gas concentration greater than 0.1 by volume, there is very little difference in the heat transfer coefficient, whether the tube was horizontal or vertical. For concentrations less than 0.1 the coefficient for the horizontal tube is greater than that for the vertical tube.

Hampson [59] examined the effect of air on the steam-side heat-transfer coefficient in the film and drop condensation of steam on a horizontal tube. The steam-side coefficient was determined from the overall coefficient using the "Wilson" plot. The mixture was vented to determine the gas concentration by sampling. Hampson found that the overall heat transfer coefficient varied when varying the position of the vent.

Provan [25] investigated the effect of superheat and non-condensing gases (namely air and argon) on the condensation of steam on a horizontal tube. The surface temperature was determined from the heat flux, the tube thermal conductivity and the cooling water mean temperature. Provan expressed his data in terms of equation 2.31 and deduced that this equation underestimated the resistance to mass transfer. He also found that a slight improvement in heat flux resulted when the mixture was superheated and that for a given gas concentration, the reduction in the heat fluxes is the same whether the gas is air or argon.

Thain [49] examined the effect of air, argon and helium on the steam condensation on a horizontal tube. The tube was used as a resistance thermometer which enabled Thain to measure the tube mean temperature. The mixture gauge pressure was kept at 10in of water. For various gas concentrations, the variation in heat flux with varying mixture-to-surface temperature difference was determined. Temperature profiles in the mixture layer were also determined. Thain compared his results, as well as those of Othmer [42] Kelman [66] and Provan [25], with the equations deduced by

Othmer [42], Langen [54], Luder [56], Brdlik [46] and Aker, Davis and Crawford [47]. These comparisons indicated that these equations are not valid except for the data they were derived from. The failure of all these equations to correlate his results satisfactorily prompted Thain to develop his own correlation. He deduced dimensionless groups from the boundary layer theory equations and the equation for the gas-vapour interfacial mass transfer rate. He then correlated his own data and those of Othmer [42], Provan [25] and Kelman [66] by the following equation, fig 2.09:-

$$\frac{Nu_{vg}}{(1+\dot{m}''/k)^{1.1}} = 0.73(Sc.Gr_{vg})^{\frac{1}{4}}$$

where $\dot{m}''$ is the condensate mass flowrate

$$Nu_{vg} = \dot{m}\left[\frac{W_i}{W_\infty - W_i}\right]\frac{d}{\rho D}$$

W_i and W_∞ are the gas concentration at interface and bulk respectively

d is the tube diameter

ρ is the mixture mean density

D is the diffusion coefficient

Gr_{vg} & Sc are the mixture mean Grashof and Schmidt numbers respectively

Condensation from mixtures in the presence of forced convection

Although there is a considerable number of investigations on the condensation from moving mixtures, the majority of these investigations were performed on industrial condersers. The object in each of these investigations being either to obtain heat transfer data for design purposes or to test the reliability of a method of calculation for the surface area.

In some investigations, the effect of mixture velocity on heat transfer was examined [18,19,60,61,62], these investigations have shown that heat flux increases rapidly with increasing mixture velocity.

Comparison of heat transfer results for mixtures in the absence of forced convection and for mixtures in the presence of forced convection, (shown in fig 2.10), indicates that heat flux is much less susceptible to the non-condensing gases when the mixtures are flowing with a finite velocity than when they are stagnant.

2.3 Conclusion

Film condensation in the presence of non-condensing gases on plane surfaces has received extensive theoretical treatment. In all cases the boundary layer approximation was used for the conservation equations in the gas-vapour mixture and only laminar flow conditions were considered. To obtain "exact" solutions of the laminar boundary-layer equations, the so-called similarity transformation technique was used (for these solutions it was necessary to use numerical methods) and to date, detailed solutions have been obtained only for steam-air mixture . To obtain such solutions the time requirement, even with modern computers, is considerable and consequently approximate solutions have been developed leading to closed-form solutions. For air-steam mixtures agreement between the exact and approximate solutions is satisfactory.

As might have been expected, theory indicates that the reduction of heat transfer due to the presence of non-condensing gases is much smaller when forced convection is present.

The detailed exact solutions of Minkowycz and Sparrow [22], in which the effects of interfacial resistance, superheating, free convection due to concentration gradients, thermal diffusion, diffusion thermo and variable properties of both layers indicated that, when a non-condensing gas is present, these other factors are generally of secondary importance.

Relatively few experimental investigations into the effect of non-condensing gases on heat-transfer during condensation have been reported. All these investigations were carried out under free convection conditions (i.e. in the absence of forced convection). In the most recent of these investigation [44], the experiments were compared with theory and good agreement was found.

In contrast to the flat plate, the analytically less tractable case of condensation on tubes has received very little theoretical treatment. An analysis [49], based on the boundary layer approximation, has been proposed for condensation on horizontal tubes from gas-vapour mixtures in the absence of forced convection. This analysis, however, was found to consistently under-estimate the heat flux when compared with experiment. This was attributed mainly to the errors resulting from the simplified assumption made in the analysis, that the mixture normal velocity to the condensing surface is an order of magnitude less than the tangential velocity.

Many experimental investigations have been reported on the condensation on tubes from mixtures in the absence of forced convection. The heat transfer results in many cases have been summarised in the form of empirical or semi-empirical expressions. However, the data obtained in the various investigations are not in good agreement with each other, and consequently there is no satisfactory general correlation.

Few experimental investigations have been carried out on the effect of mixture velocity on the condensation on tubes, in the presence of non-condensing gases. As would be expected, and as theory indicates for the flat plate case, vapour-gas mixture velocity markedly reduces the effect of the non-condensing gas in reducing the heat flux.

Table 3.01

Reference	Vapour-gas mixture	Gas concentration range	Type of⁺ system	Condensing surface	Mixture pressure of temperature at the bulk
Hampson [45]	steam-N_2	0-0.04 by mass	open	3in wide x 5in high vertical copper plate	10in water gauge pressure
Brdlik [46]	steam-air	0.002-0.02 by mass	closed	180mm x 150mm horizontal copper plate	1.0-1.07 atmosphere
Aker, Davis and Crawford [47]	ethanol-N_2 ethanol-H_2 ethanol-CO_2 CCl_4-N_2 CCl_4-CO_2	0-0.7 by volume	closed	1.5in wide x 3in high vertical copper plate	0.0521-0.97 atmosphere
Kroger and Rohsenow [48]	potassium-He potassium-Ar		closed	4in dia x 0.75in thick nickel or stainless steel horizontal disc	1108° F-1414° F
Sledgers [44]	steam-air	0-0.01 by mass	closed	2in wide x 5in high x 2in thick vertical copper plate	80° F-150° F
Othmer [42]	steam-air	0-0.1144 by volume	closed	3in od x 47in long horizontal nickel plated tube	atmospheric
Langen [54]	steam-air	0.002-0.2 by mass	open	30mm od x 900mm long horizontal brass tube	0.15-0.65 atmosphere

contd............

Reference	Vapour-gas mixture	Gas concentration range	Type of+ system	Condensing surface	Mixture pressure of temperature at the bulk
Defriece [55]	N-heptane methane	0-0.18 by mass	closed	0.84in od x 4.03ft long horizontal copper tube	970-1500mm Hg
Luder [56]	steam-air steam-H_2 steam-methane steam-SO_2 steam-(H_2 N_2) CCl_3-air		closed	26mm od x 1280mm long, horizontal steel tube	75lbf/in^2 maximum
Tolubinskii and Yampolskii [57]	steam-air	0.004-0.02 by mass	closed	38mm od x 1500mm long vertical steel tube	
Mazyukevich [58]	ammonia-air	0-0.055 by mass	closed	30mm od x 1280mm long horizontal steel tube	
Hampson [59]	steam-N_2	0.002-0.012 by mass	open	1in od x 24in long horizontal copper tube	10in water gauge pressure
Provan [25]	steam-air steam-Ar	0-0.055 by volume	closed	0.754in od x 36in long horizontal titanium tube	1.13 atmosphere maximum
Thain [49]	steam-air steam-Ar	0-0.18 by mass	closed	1in od x 48in long horizontal copper tube	10in water gauge pressure

+ An "open" system is one in which a vent is provided. Therefore, to maintain constant conditions in the system (i.e. constant mixture pressure and bulk temperature and gas concentration), gas is fed continously to the system.

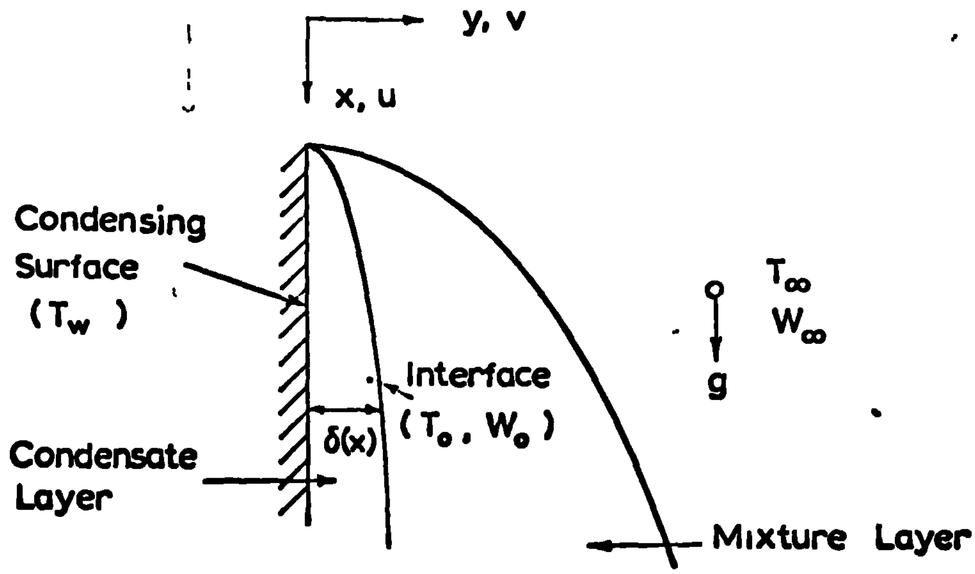

Fig. 2.01 Schematic of the Physical System for the Boundary layer analyses

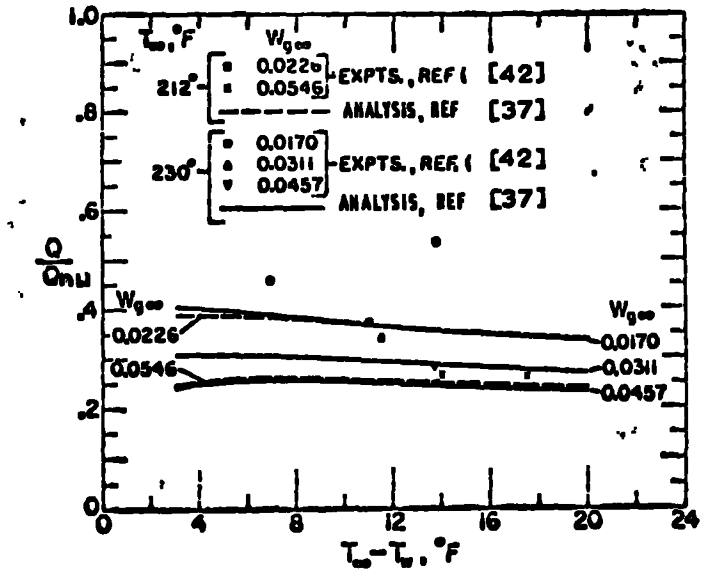

Fig. 2.02 Sparrow & Lin results [37]

Comparison of analytically predicted heat transfer reductions with experiments

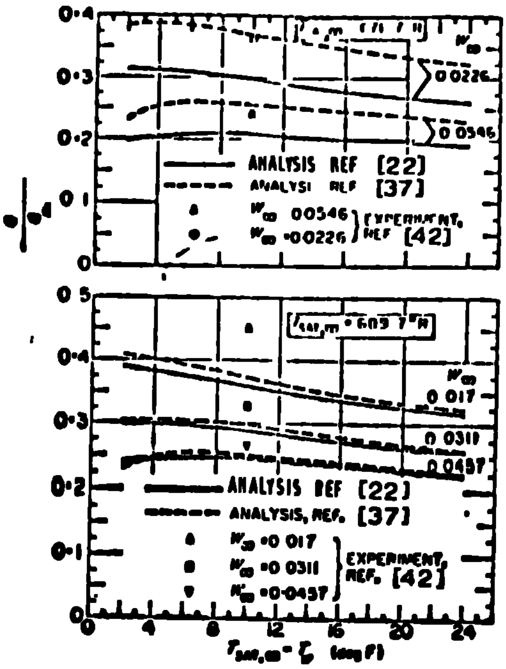

Fig. 2.03 Minkowycz & Sparrow [22]
Comparison of analytical (constant properties [37] and variable properties [22]) and experimental [42] heat transfer results.

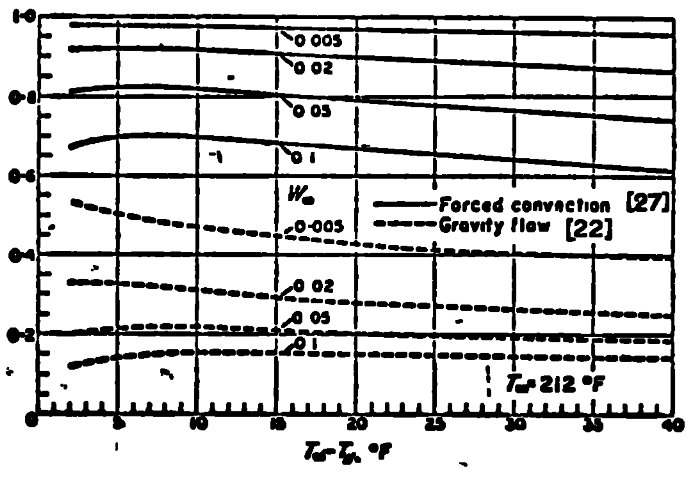

Fig. 2.04 Sparrow, Minkowycz & Saddy [27]
Comparison of heat transfer results for mixtures in the absence of forced convection [22] and in the presence of forced convection [27].

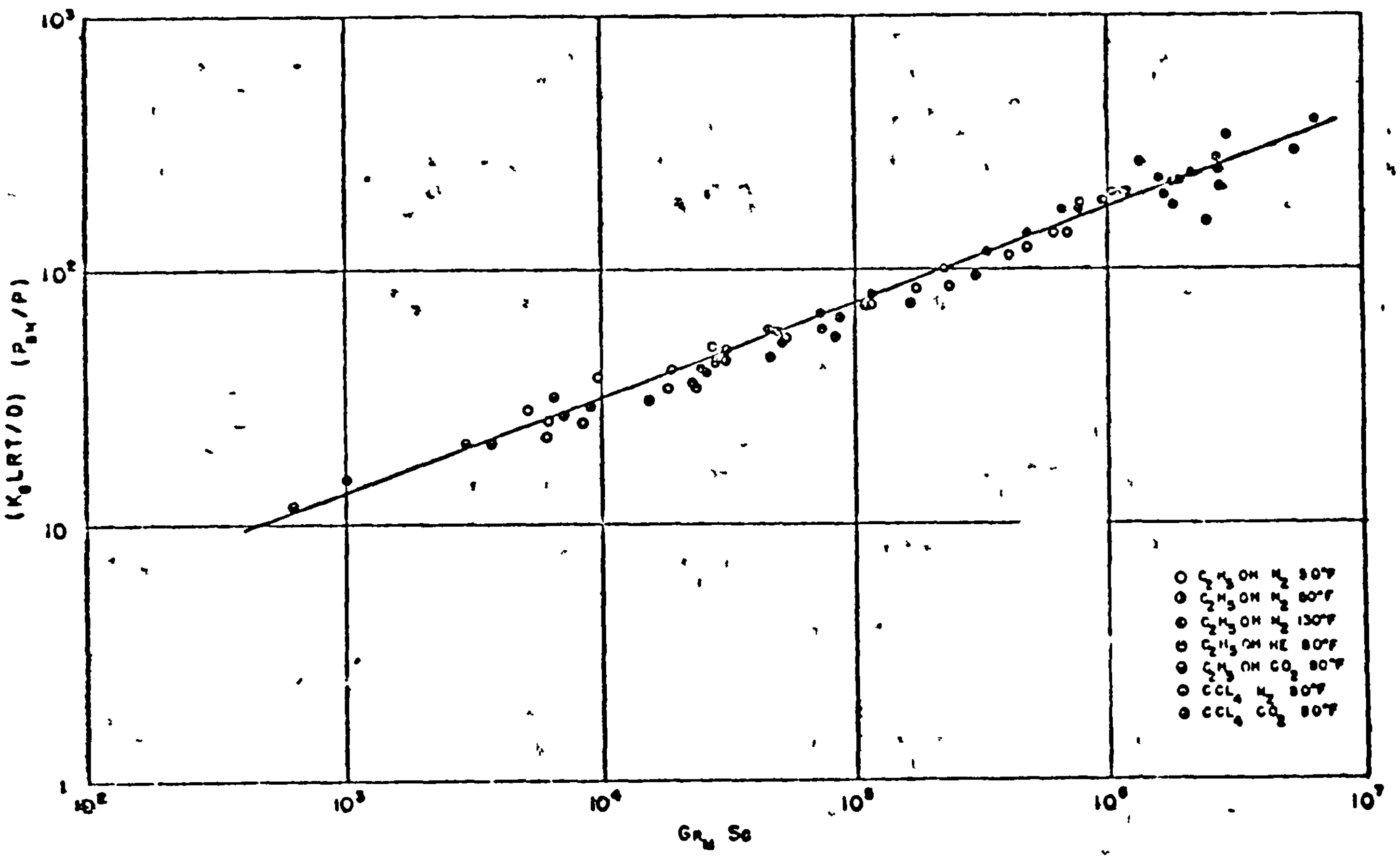

Fig 2.05 Akers, Davies & Crawford [47]
Correlation of Experimental Data

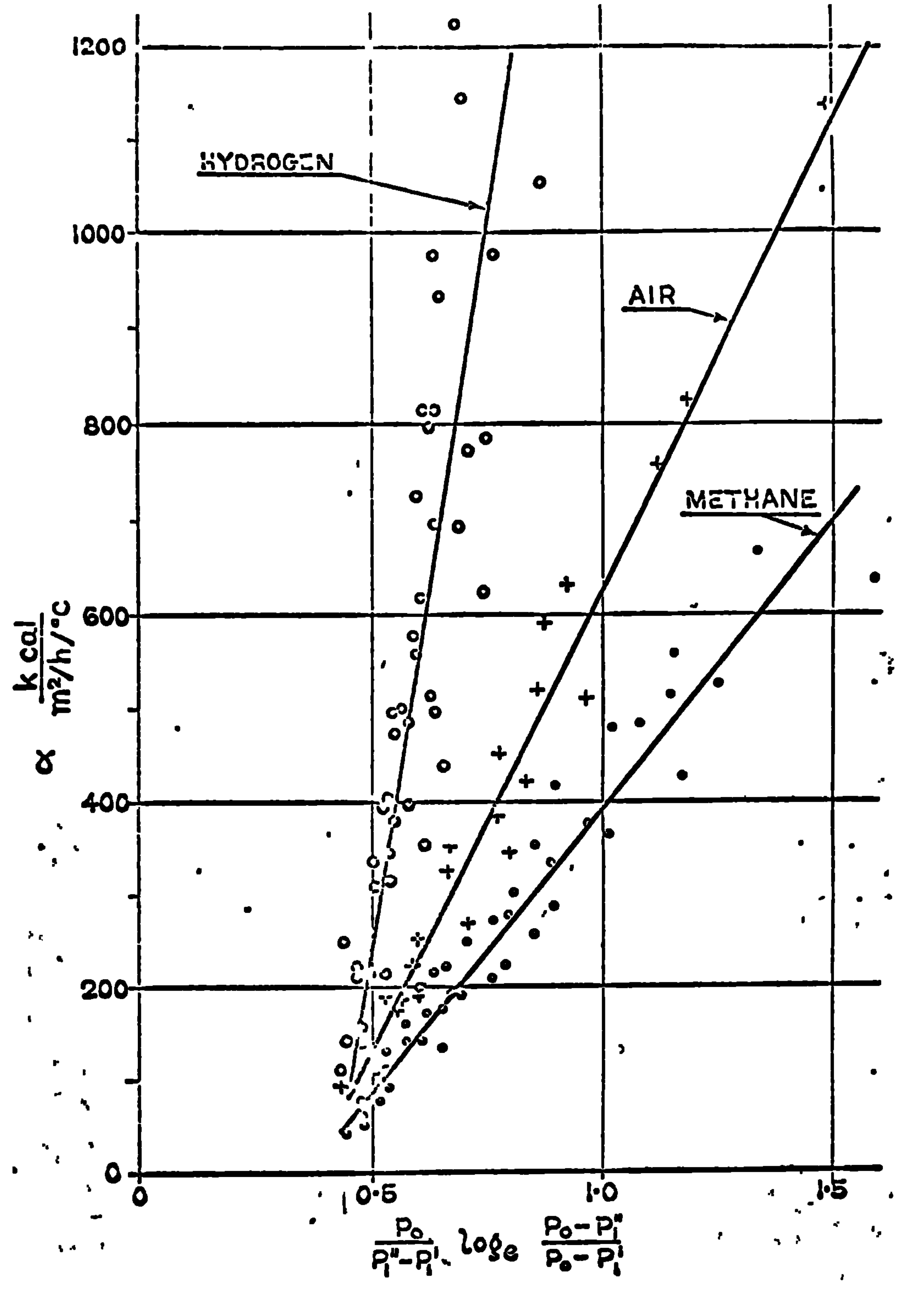

Fig. 2.06 Luder [56]

Comparison of the variation in heat transfer coefficient for various steam-gas mixtures.

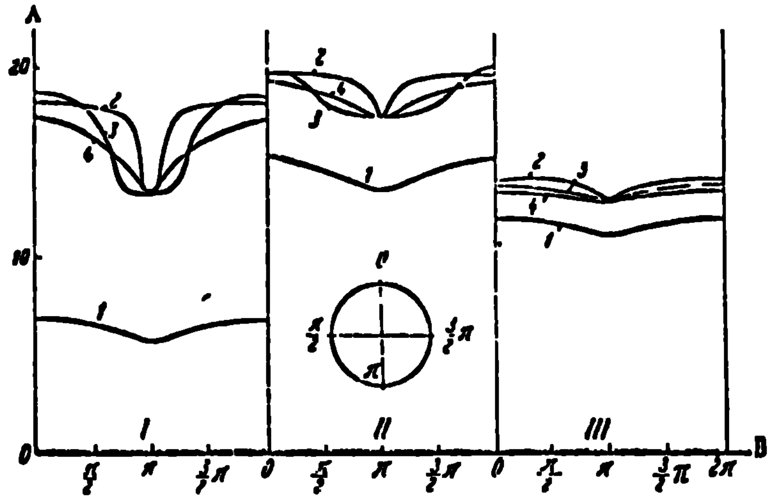

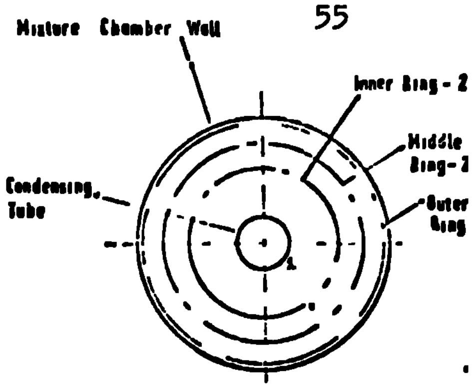

Position of the mixture thermocouples

Temperature distribution in the mixture in the condenser vapor space. A) Temperature (°C). B) positions of thermocouples relative to the condenser periphery. Heat flow rate q (kcal/m²·hr) and air content r of mixture (% by volume): I) 11,200, and 40, II) 4,100 and 40. III) 2,200 and 26. Temperature (°C): 1) Wall 2) inner ring; 3) middle ring; 4) outer ring.

Fig. 2.07 Mazyukevich [58]

Temperature distribution in the mixture chamber

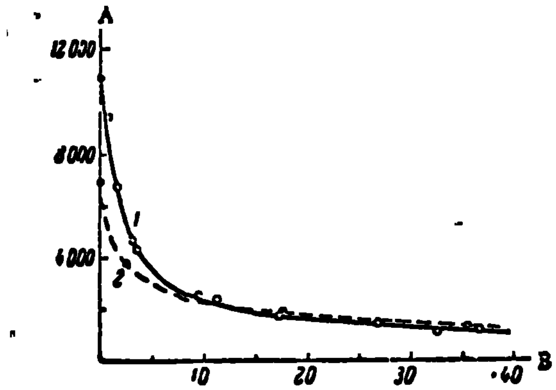

Variations of the heat transfer coefficient with mixture composition for tubes in horizontal and vertical positions, at a heat flow rate of 10,000 kcal/m²·hr. A) Heat transfer coefficient α (kcal/m²·hr·degree). B) air content of mixture (% by volume). Tube: 1) Horizontal, 2) vertical.

Fig. 2.08 Mazyukevich [58]

Comparison of experimental heat transfer results for horizontal and vertical tubes.

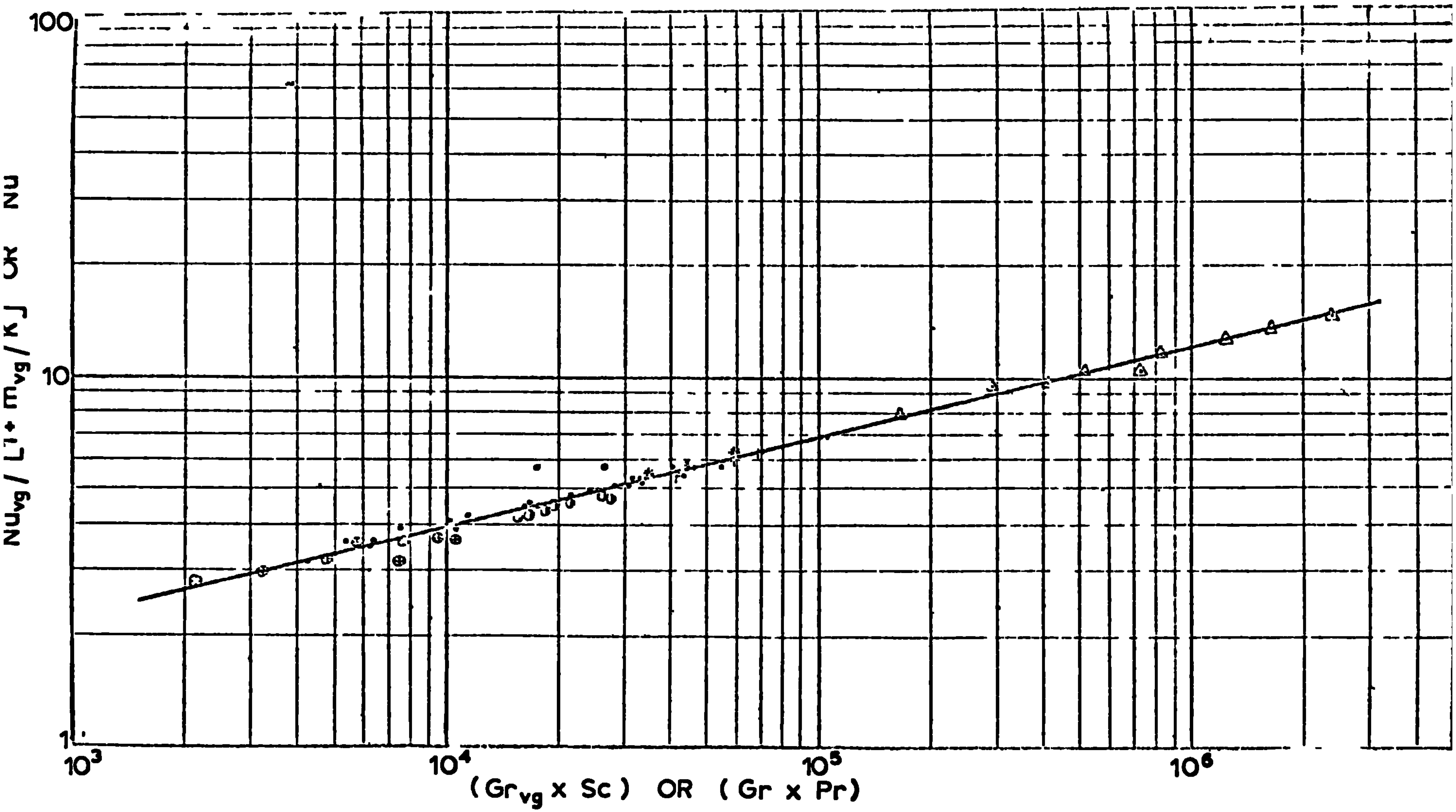

Fig 2.09 Thain [49]

Correlation of experimental data of refs. [25], [42], [49], [66]

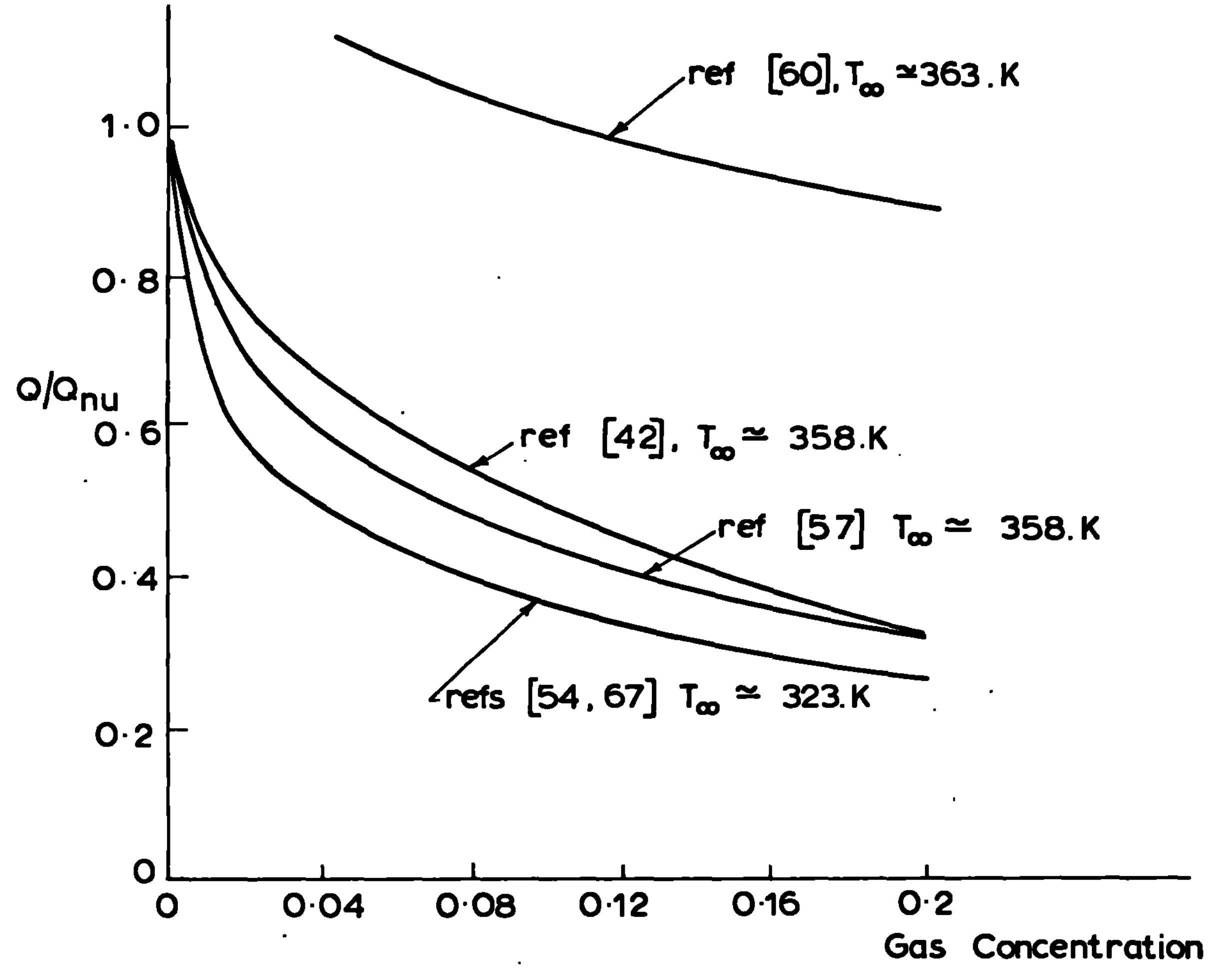

Fig. 2. 10. Comparison of experimental heat transfer results for mixtures in the presence of forced convention [60] and in the absence of forced convention [42, 54, 57, 67].

Chapter 3

Theoretical Considerations

3.1 The effect of including the variation of condensate film thickness with height in Rose's analysis

3.2 Condensation from a mixture containing a gas lighter than vapour

3.3 Condensation from a mixture whose bulk temperature varies with height

As indicated in chapter 2, the exact solutions for the present problem are laborious and require extensive computation. For instance Minkowycz and Sparrow [22] indicated, in their variable property solutions, that even with a "large" computer (type CDC 1604) the time requirement is measurable in terms of hours. Consequently approximate integral solutions which give relatively simple and more easily employable results have been proposed [43,44]. In these solutions the mixture properties were taken to be constant. These approximate analyses, however, underestimate the heat flux when compared with the "exact" analysis of Minkowycz and Sparrow [22]. Rose [43] suggested that a closer agreement with the exact analysis results might be obtained if a different method of estimating the average properties of the gas-vapour mixture is employed in the results of his approximate analysis.

In his analysis, Rose neglected the thickening of the condensate film with distance down the plate. This might contribute to the disagreement with the exact analysis, though it would not be expected to affect the results strongly since thickness of condensate layer varies only as the 0.25 power of distance down the plate. Sledgers [44] took this variation into account, but other aspects of this analysis seem, to the present writer, to be questionable, (see appendix 6). Consequently it is proposed here to include the variation of condensate film thickness with height in Rose's analysis [43] to investigate the extent to which this influences the result.

3.1 The effect of including the variation of condensate film thickness with height in Rose's analysis

The situation considered is that of a vapour condensing on a vertical isothermal plate from a mixture in the absence of forced convection. It is assumed that both the condensate and the mixture layers are laminar and that Nusselt's analysis holds for the condensate layer. Except for the density in the buoyancy term of the mixture momentum equation, the mixture and the condensate properties are taken as constant.

The procedure, to be followed here, in solving the mixture equations is the same as that employed by Rose [43], except that the variation of the condensate film thickness will be included. This is to be taken into account in the assumed concentration and velocity profiles, when integrating the mixture equations and in the interfacial velocity, mass and gas impermeability conditions.

With the co-ordinate system represented in fig 3.01, the relevant boundary layer equations of continuity, momentum and diffusion are respectively [37],

$$\frac{\partial u}{\partial x} + \frac{\partial v}{\partial y} = 0 \qquad 3.01$$

$$u\frac{\partial u}{\partial x} + v\frac{\partial u}{\partial y} = g\left(1 - \frac{\rho_\infty}{\rho}\right) + \nu\frac{\partial^2 u}{\partial y^2} \qquad 3.02$$

$$u\frac{\partial W}{\partial x} + v\frac{\partial W}{\partial y} = D\frac{\partial^2 W}{\partial y^2} \qquad 3.03$$

For the condensate layer, the simple Nusselt theory[1] gives the following expression for the interfacial velocity, condensate layer thickness and mass flow rate respectively:-

$$u_o = (g.Sp)^{\frac{1}{2}} x^{\frac{1}{2}} \qquad 3.04$$

$$\Delta = \left[\frac{4\mu_f^2 . Sp}{\rho_f^2 g}\right]^{\frac{1}{4}} x^{\frac{1}{4}} \qquad 3.05$$

$$\dot{m} = \left[\frac{g\rho_f^2\mu_f^2 Sp^3}{4}\right]^{\frac{1}{4}} x^{-\frac{1}{4}} \qquad 3.06$$

where $$Sp = \frac{(T_o - T_w)\, k_f}{h_{fg} . \mu_f}$$

Assuming the vapour and the gas to be perfect gases, and using the Gibbs-Dalton mixture equations, the buoyancy term in equation 3.02 may be written:-

$$g\left(1 - \frac{\rho_\infty}{\rho}\right) = gXw \qquad 3.07$$

where $X = (M_g - M_v) / \left[M_g - (M_g - M_v)\, W_\infty \right]$

$w = W - W_\infty$

Using 3.01 and 3.07 equations 3.02 and 3.03 may be re-written as follows,[43],

$$\frac{\partial}{\partial x}(u^2) + \frac{\partial}{\partial y}(uv) = gXw + \nu\frac{\partial^2 u}{\partial y^2} \qquad 3.08$$

$$\frac{\partial}{\partial x}(uW) + \frac{\partial}{\partial y}(vW) = D\frac{\partial^2 W}{\partial y^2} \qquad 3.09$$

Equations 3.08 and 3.09 may be integrated, with respect to y, across the mixture layer thickness to give respectively

$$\frac{d}{dx}\left(\int_{\Delta}^{\delta+\Delta} u^2\, dy\right) + (v_\infty v_\infty - u_\Delta v_\Delta) = gX\int_{\Delta}^{\delta+\Delta} w\, dy + \nu\left[\frac{\partial u}{\partial y}\right]_{\Delta}^{\delta+\Delta} \quad 3.10$$

$$\frac{d}{dx}\left(\int_{\Delta}^{\delta+\Delta} u\, W\, dy\right) + v_\infty W_\infty - v_\Delta W_\Delta = D\left[\frac{\partial W}{\partial y}\right]_{\Delta}^{\delta+\Delta} \quad 3.11$$

But since $u = \left[\frac{\partial u}{\partial y}\right]_{\delta+\Delta} = \left[\frac{\partial W}{\partial y}\right]_{\delta+\Delta} = 0$, for the condition of no slip at the interface, $u_\Delta = u_o$ (see ref [5]), and, in integrating equation 3.01, $v_\infty = v_\Delta - \frac{d}{dx}\left(\int_{\Delta}^{\delta+\Delta} u\, dy\right)$, equations 3.10, 3.11 are reduced to the following,

$$\frac{d}{dx}\left(\int_{\Delta}^{\delta+\Delta} u^2\, dy\right) - u_o\, v_\Delta = gX\int_{\Delta}^{\delta+\Delta} w\, dy - \nu\left[\frac{\partial u}{\partial y}\right]_{\Delta} \quad 3.12$$

$$\frac{d}{dx}\left(\int_{\Delta}^{\delta+\Delta} u\, w\, dy\right) + w_o\, v_\Delta = -D\left[\frac{\partial w}{\partial y}\right]_{\Delta} \quad 3.13$$

where $w_o = W_o - W_\infty$

Equations 3.12 and 3.13 may be solved by assuming suitable profiles and specifying some interfacial conditions. In analogy with the solution of the temperature induced natural convection [70,71,72], the following velocity and concentration profiles may be assumed, [43]:-

$$u = (u_o + \tilde{u}t)(1 - t^2) \quad 3.14$$

$$w = w_o\,(1 - t)^2 \quad 3.15$$

where $\tilde{u}$ is a function of x having dimensions of velocity

$$t = \frac{y - \Delta}{\delta}$$

As in [43] δ is taken to have the same value for both velocity and concentration boundary layer.

Considering the interface to be impermeable to the non-condensing gas,

$$m''_g = \left[\rho g\left(u\frac{d\Delta}{dx} - v\right) + \rho D\frac{\partial W}{\partial y}\right]_\Delta = 0 \qquad 3.16$$

The first term of the right hand side of equation 3.16 is the natural convection contribution to the mass transfer while the second term is the diffusion contribution (for the derivation of 3.16 see ref [44]).

$$\therefore \quad v_\Delta = +\frac{D}{W}\left(\frac{\partial W}{\partial y}\right) + u_o\left(\frac{d\Delta}{dx}\right) \qquad 3.17$$

In differentiating equations 3.14 and 3.15 we have

$$\nu\left[\frac{\partial u}{\partial y}\right]_\Delta = \frac{\nu}{\delta}(\tilde{u} - u_o) \qquad 3.18$$

$$D\left[\frac{\partial W}{\partial y}\right]_\Delta = \frac{-2\,Dw_o}{\delta} \qquad 3.19$$

$$v_\Delta = \frac{-2Dw_o}{\delta W_o} + u_o\left(\frac{d\Delta}{dx}\right) \qquad 3.20$$

The other interfacial condition to be used is that the mixture mass flux to the interface must equal the condensate mass flux leaving the interface into the liquid,

$$\left[\rho u\frac{d\Delta}{dx} - \rho v\right]_\Delta = m''(x) = \left[\frac{g\rho_f^2\mu_f^2 Sp^3}{4}\right]^{\frac{1}{4}} x^{\frac{1}{4}} \qquad 3.21$$

For the derivation of 3.21 see ref[5]. In combining 3.20 and 3.21 we have:-

$$\delta = \left[\frac{g\rho_f^2\mu_f^2 Sp^3}{4}\right]^{-\frac{1}{4}} \frac{2Dw_o}{W_o}\, x^{-\frac{1}{4}} \qquad 3.22$$

Using 3.14, 3.15, 3.19, 3.20 and 3.21 equations 3.12 and 3.13 may be re reduced to :-

$$\frac{d}{dx}\left(\delta\int_0^1 u^2 dt\right) - u_o^2\left(\frac{d\Delta}{dx}\right) + \frac{2u_o}{\delta}\,\frac{Dw_o}{W_o} = \qquad 3.23$$

$$= g\,x\,\delta \int_0^1 w\,dt - \frac{\nu}{\delta}(\tilde{u} - 2u_0)$$

$$\frac{d}{dx}\left(\delta \int_0^1 uw\,dt\right) - w_0 u_0 \frac{d\Delta}{dx} - \frac{2rDw_0}{\delta} = 0 \qquad 3.24$$

where $r = W_\infty / W_0$

In integrating 3.23 and 3.24 in conjunction with 3.14 and 3.15 we have:-

$$\frac{d}{dx}\left[\delta\left(\frac{u_0^2}{5} + \frac{u_0\tilde{u}}{15} + \frac{\tilde{u}^2}{105}\right)\right] = u_0^2 \frac{d\Delta}{dx} + \frac{2u_0 Dw_0}{W_0}$$

$$= gX\,\frac{\delta w_0}{3} - \frac{\nu}{\delta}(\tilde{u} - 2u_0) \qquad 3.25$$

$$\frac{d}{dx}\left[\delta\left(\frac{w_0 u_0}{5} + \frac{w_0\tilde{u}^2}{30}\right)\right] + w_0 u_0 \frac{d\Delta}{dx} - \frac{2Dw_0\,r}{\delta} = 0 \qquad 3.26$$

The solutions take the form:-

$u = Ax^{\frac{1}{2}}$

$\delta = Bx^{\frac{1}{4}}$

$U_0 = cx^{\frac{1}{2}}$ } Nusselt theory

and $\Delta = dx^{\frac{1}{4}}$

where A,B,c, and d are constants, c and d are determined from equations 3.04 and 3.05 as follows:-

$$c = \left[g.Sp\right]^{\frac{1}{2}}$$

$$d = \left[\frac{4\mu_f^2}{\rho_f^2 g}\right]^{\frac{1}{4}} Sp^{\frac{1}{4}}$$

Substituting for δ in equation 3.22 we have

$$B = \frac{2\rho_0 w_0 D}{W_0} \Big/ \left[\frac{g\rho_f^2\mu_f^2}{4}\,Sp^3\right]^{\frac{1}{4}}$$

substituting for B, c and d and in eliminating A from equations 3.25 and 3.26 we have

$$10Sp.Sc\left(\frac{\rho_f\mu_f}{\rho\mu}\right)\left[\frac{W_o r}{w_o}\right]^2\left(\frac{20}{21}+\frac{Sc}{r}\right)+\frac{}{Sp^2Sc}\left(\frac{\rho\mu}{\rho_f\mu_f}\right)\left[\frac{W_o}{w_o}\right]^2 x$$

$$\left(\frac{5}{28}Sp-\frac{Xw_o}{3}\right)+Sp.Sc\left(\frac{W_o}{w_o}\right)\left(\frac{\mu_f}{\mu}\right)\left(5Sc+\frac{200}{21}r\right)+$$

$$\frac{50}{21}Sp.Sc\left(\frac{\mu_f}{\mu}\right)\left(\frac{\rho}{\rho_f}\right)-\frac{71}{21}\left(\frac{W_o}{w_o}\right)\left(\frac{\rho}{\rho_f}\right)=$$

$$\frac{100}{21}r-\frac{2W_o}{w_o}+8\,Sc \qquad 3.27$$

For given W_∞, T_∞ and mixture-to-surface temperature difference, equation 3.27 may be solved to obtain the interfacial temperature. The heat flux is then calculated from the Nusselt expression.

Using equation 3.27, heat transfer results were computed for various steam-gas mixtures. These results will be discussed in chapter 6.

3.2 Condensation from a mixture containing a gas lighter than vapour

The analyses (exact and approximate including that of section 3.1) referred to earlier, are only applicable in situations where the boundary layers of both the condensate and gas-vapour mixture layers have the same leading edge (i.e. for a vertical plate, where the non-condensing gas is heavier than the vapour). For the reverse case a semi-empirical analysis will be developed here.

In this case there is no common "leading edge" for the gas mixture and condensate layers. The mixture, as before, is richer in gas (i.e. the gas concentration increases) nearer to the surface than in the bulk and since the gas is lighter than the vapour, the mixture density becomes smaller. Therefore, in a gravitational field, the mixture tends to move upwards, near the interface, as well as towards the interface. It is thus not possible to match the interfacial conditions.

As a first approximation we regard the interface as a stationary plane vertical isothermal surface, permeable to the vapour only. The influence of the condensate motion on the problem is thus initially ignored. This approximation removes the above mentioned difficulty and leads to a special case of the situation where the gas is heavier than the vapour. An empirical correction for the condensate motion is included later.

With the co-ordinate system represented in fig 3.02 the mixture boundary layer equations are

$$\frac{\partial u}{\partial x} + \frac{\partial v}{\partial y} = 0 \qquad 3.28$$

$$u\frac{\partial u}{\partial x} + v\frac{\partial u}{\partial y} = -g\left(1 - \frac{\rho}{\rho_\infty}\right) + \frac{\partial^2 u}{\partial y^2} \qquad 3.29$$

$$u\frac{\partial w}{\partial x} + v\frac{\partial w}{\partial y} = \frac{D\partial^2 w}{\partial y^2} \qquad 3.30$$

The procedure of solving 3.29 and 3.30 is the same as that for equations 3.02 and 3.03, however the velocity and concentration profiles become

$$u = \tilde{u}t(1 - t)^2 \qquad 3.31$$

$$w = w_o(1 - t)^2 \quad 3.32$$

where $t = y/\delta$

The procedure yields the following equation:-

$$\left[\frac{75}{21}\frac{W_\infty}{W_o} + \frac{15}{4}\,Sc.\right] \cdot \left[\frac{\rho_f \mu_f}{\rho \mu}\right]^2 .Sc.Sp^3 \;\; W_\infty = .\frac{-x w_o^5}{W_o^3} \quad 3.33$$

For given W_∞, T_∞ and mixture-to-surface temperature difference, equation 3.33 may be solved to obtain the interfacial temperature. The approximate heat flux is then calculated from the Nusselt expression.

Now, the effect of the condensate motion is to drag the mixture downwards at the interface so that the mixture moves downwards near the interface. However, further away from the interface, the mixture tends to move upwards. One might expect these complicating effects to impede convection and thus ultimately diminish heat transfer. Therefore, as a rough approximation, the ratio of the theoretical mixture velocity to the condensate velocity could serve as a variable upon which the required correction may be made. In including the condition that as $u_o \rightarrow \delta$ the correction factor $\rightarrow$ 1, this correction factor may be taken as:-

$$\left[1 + \frac{u_o}{u_{max}}\right]^n \quad 3.34$$

where u_{max} is the maximum mixture velocity according to the theoretical analysis

u_o is the condensate velocity at the interface

n is a constant to be determined by comparison with experimental data

When u_{max} and u_o are evaluated from the analysis and Nusselt expression, expression 3.34 reduces to

$$\left[1+\frac{4}{5.Sp.Sc}\;\frac{\rho\mu}{\rho_f\mu_f}\;\frac{w_0^2}{W_\infty W_C}\right]^n \qquad 3.35$$

Using the present experimental data for steam-helium mixture, (see chapter 5), satisfactory agreement with data was obtained when n=-0.355. These semi-theoretical results are discussed in chapter 6.

3.3 Condensation from a mixture whose bulk temperature varies with height

Existing theoretical treatments for the present problem (including those of sections 3.1 and 3.2) are based on the assumption that the temperature outside the boundary layer is constant. In the present experimental work, this temperature was found to vary with height (see Appendix 2). Consequently an attempt was made to include the variation of temperature outside the boundary layer in the theory. However, it was not possible to obtain similarity solutions for this case as was found for the case of single phase free convection [73]. This is because when matching conditions at interface, the equations obtained were not independent of the plate height (to obtain similarity solutions these equations must be independent of the plate height).

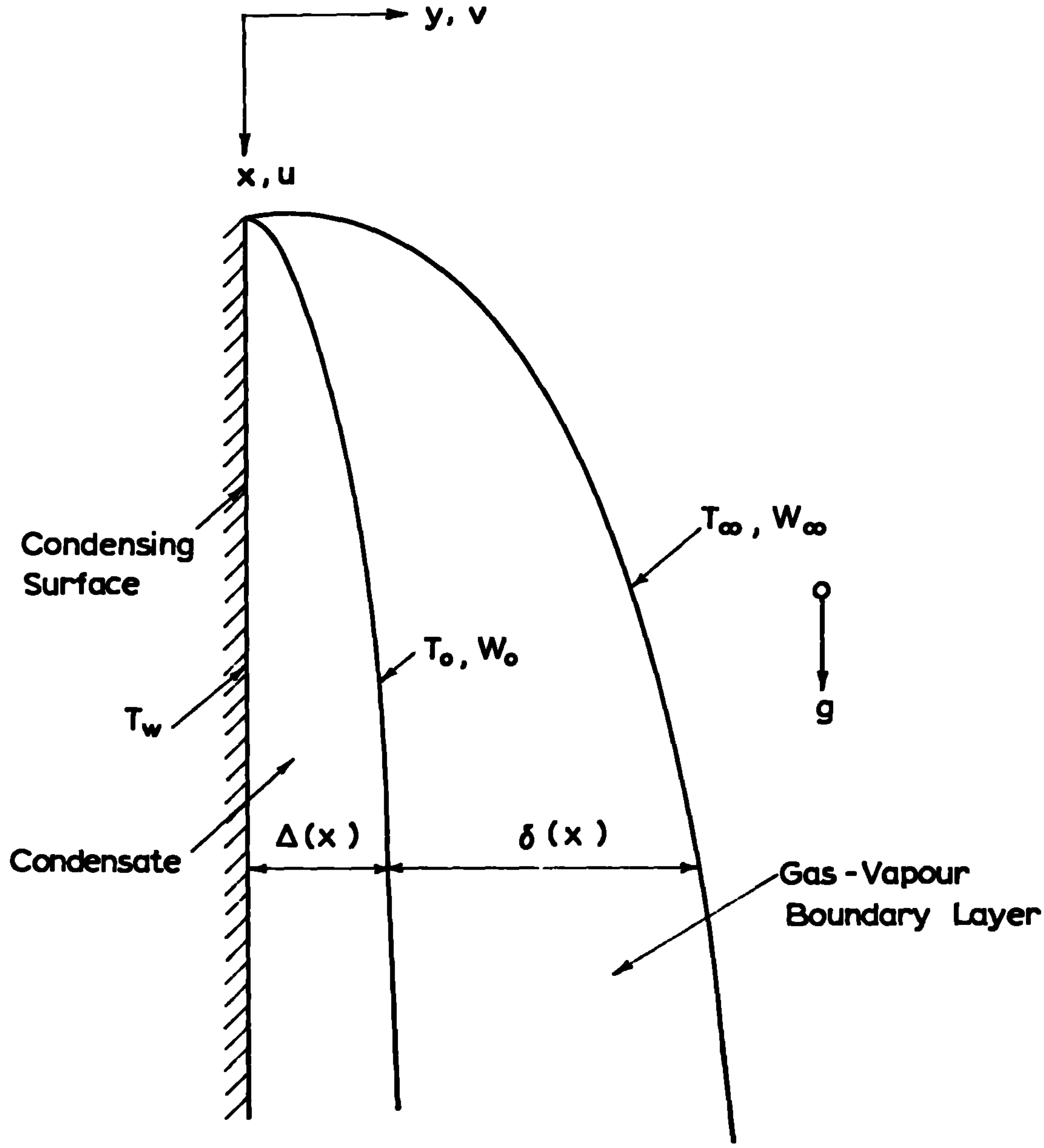

Fig. 3.01. CO-ORDINATE SYSTEM ($M_v < M_g$)

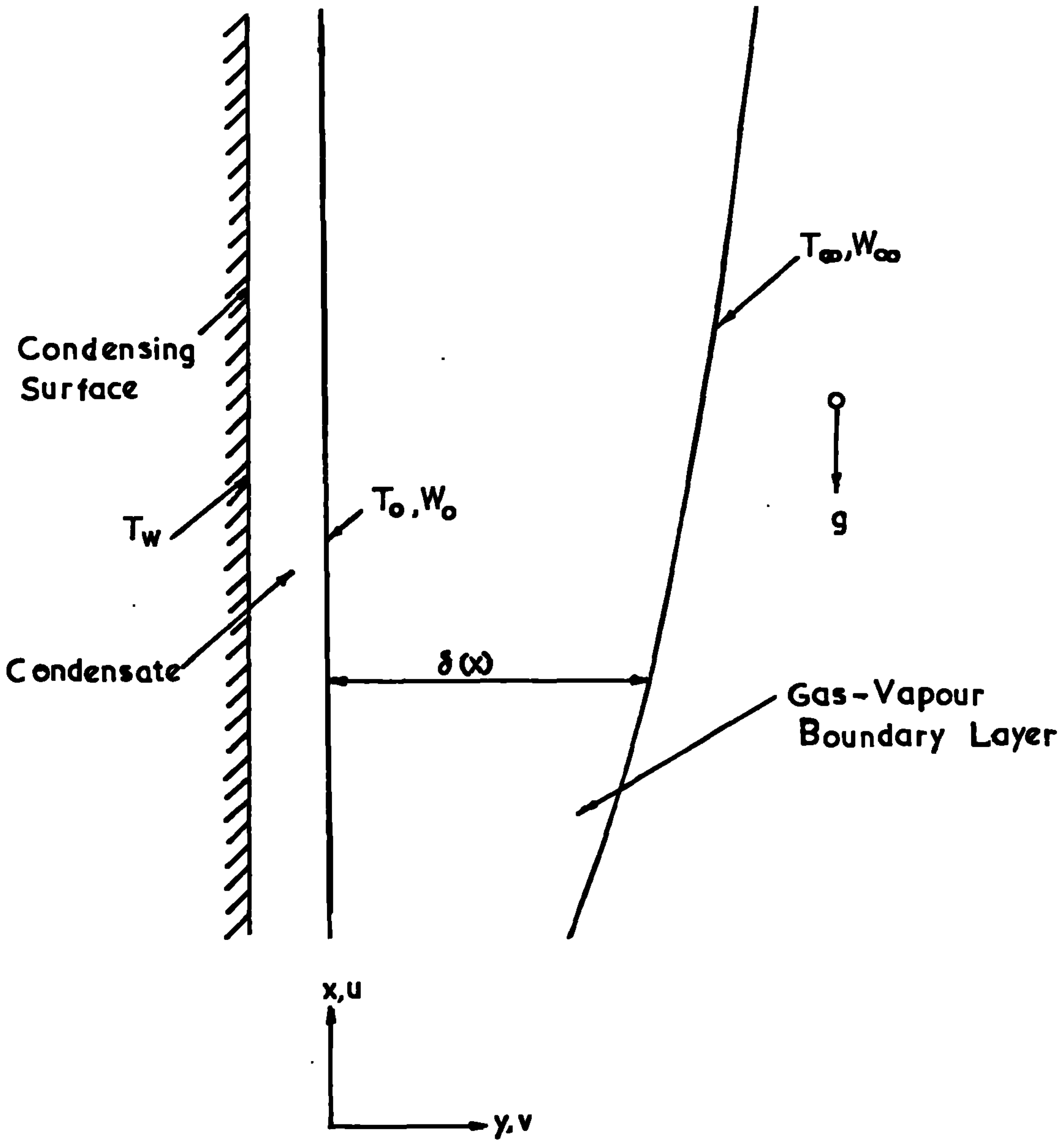

Fig. 3.02. CO-ORDINATE SYSTEM ($M_v > M_g$)

Chapter 4

Apparatus

4.1 General

4.2 Test Plate

4.3 The Flow Dispersing Section

4.4 Temperature and pressure measurements of vapour-gas mixture

4.5 Non-Condensing Gas Injection and Concentration Measurements

4.6 Measurement of the Thermo Electrical potential difference

4.7 Thermocouple Calibration

4.8 Apparatus Cleansing

4.9 Leak Testing Technique

4.1 General

With reference to fig 4.01, steam was generated from de-ionized water in the boiler. A measured quantity of non-condensing gas could be introduced to the boiler through the gas injection system (3). The mixture then passed into the steam chamber entering via the flow dispersing section (1). The steam condensed on the vertical test plate (8) which was cooled on the reverse side by water passing through the box (9). The condensate returned to the boiler via the steam supply line.

For cleanliness, all parts of the apparatus which came in contact with water or mixture were either glass, stainless steel or monel. All parts of the apparatus were stainless steel unless indicated differently.

The boiler consisted of a vertical cylindrical glass vessel 12in in diameter and 30in high, closed at both ends with stainless steel sheets 0.063in thick backed by mild steel plates 0.5in thick. (fig 4.03 shows details of the top of the boiler). The boiler was fitted with two immersion heaters of 5kW(5) and 2.5kW(4) each was supplied through a variable transformer. The boiler was lagged by boxing in with granular vermiculite. A narrow slit (2) was cut out from one side of the box to allow visual observation of the water level.

The steam chamber was a horizontal cylindrical glass vessel of 18in diameter. A smaller cylinder branched at right angles from the upper surface of the cylinder to which a double-glazed electrically heated window (11) was bolted. A stainless steel plate of thickness 0.5in (6) was bolted to the front end of the vessel (see fig 4.04). This end plate carried two thermocouple-carrying tubes and a "probe", all mounted on a monel plate (10) which could be moved vertically (see fig 4.10). The probe could be traversed horizontally, (details of the thermocouples and the probe will be given later). A small double-glazed electrically heated window was fixed to the middle of the monel plate, this allowed visual observations of the condensing surface, situated opposite to the monel plate.

An assembly carrying the test plate and the cooling box was bolted to the back end of the vessel. The assembly consisted of a stainless steel tube 14in internal diameter, soldered at one end to a stainless steel sheet backed by a mild steel disc (7). At the other end of the tube, which extended into the steam chamber, a stainless steel disc is bolted. The disc carried the test plate and the cooling box.

4.2 Test Plate

This plate was a high purity copper disc (99.9%), 6.125in diameter and 0.489in thick. It was machined from one face down to a depth of 0.187in leaving a central square of side 3.01in which formed the condensing surface, fig 4.05. A horizontal groove of 0.020in width and 1.75in length was machined centrally in the back of the plate to a depth of 0.420in. This groove housed an accurately located "Araldite" strip containing butt-welded thermocouples so that these thermocouples ran along lines parallel to the surface (i.e. isotherms during operation). The distances of these thermocouples from the condensing surface were accurately measured by a travelling microscope before the strip was inserted into the plate.

The thermocouples were Nicrom-Constantan of about 0.0085in diameter. They were butt-welded in a Spembly arc welding instrument type WI4. Good non-oxidised junctions were obtained when Argon was sprayed over the area where welding took place. The Araldite strip was cast in a specially designed mould (shown in fig 4.08). The thermocouples were held taut and parallel in the mould, with the junctions at its centre. Liquid Araldite was then poured over the junctions to form a 0.020in thick layer enclosing the thermocouples and extending 0.625in on either side of the junctions. To prevent the Araldite from sticking to the mould, all surfaces coming into contact with the layer were P.T.F.E. surfaces. The mould was then placed in an oven to cure and anneal the Araldite. When the Araldite strip was in position in the test plate, The thermocouple leads, insulated with P.V.C. sleeving (not shown in figs 4.05 and 4.07), were taken out of the plate through two shallow grooves, extending on either side of the groove carrying the Araldite strip, along the entire diameter of the plate, fig 4.06. To prevent water leaks in to these grooves, a tapered sliding copper strip, figs 4.05 and 4.06, was fitted tightly in a tapered groove machined over the earlier one. For sealing purposes silicone rubber paste was spread over the thermocouples leads filling the spaces in the shallow grooves before inserting the copper strip.

The cooling box, fig 4.07, was designed so that the cooled region of the plate had the same dimensions as those of the condensing surface. The depth of the cooling water channel was 0.020in. The cooling water passed through two heaters, each of 2kW, before entering the cooling box.

A P.T.F.E. frame fitted over the front face of the test plate so as to leave only the square condensing area exposed. Along the vertical edges of the condensing area, P.T.F.E. strips extended a distance of 0.25in into the steam chamber to form boundary layer guides.

The heat flux was determined from the temperature gradient through the test plate. Temperatures at six different depths were measured by the thermocouples in the Araldite strip. The condensing surface temperature was determined by extrapolation.

To determine the thermal conductivity of the plate, a specimen was machined from the same block of copper used to make the test plate. The dimensions of the specimen were

6in x 0.125in x 0.065in. Its electrical conductivity was measured by means of a Kelvin Double Bridge. Using Smith and Palmer method[68]. The thermal conductivity of the specimen at room temperature was calculated. This was found to be 3.84 W/(cm K). This figure agrees well with the suppliers of the metal recommendation of 3.85 W/(cm K). Although the thermal conductivity is dependent on temperature, a constant value was used for the heat transfer calculation (i.e. 3.85 W/(cm K)), since the variation of this value (9×10^{-4} W/(cm K)/K for the range 0-200°C, as indicated in ref[69]), over our range of temperature was negligible compared with the accuracy with which it was measured; moreover, the precision with which the heat flux is required does not warrant minor corrections.

4.3 The flow dispersing section

This part of the apparatus, fig 4.01, is fitted to the inside of the steam chamber front plate. The function of this section was to provide uniform flow towards the condensing plate. The section contains three vertical screens of fine stainless steel mesh, parallel to the condensing surface. This number of screens and their location in the section were determined experimentally using air. The unifomity of flow of air through the steam chamber, was studied as follows:-

The probe was replaced by the fibre anemometer discribed in appendix (1) so that the fibre, laid in a horizontal plane, parallel to the test plate. Two telescopes with graduated eye pieces were located as shown in fig 4.02. The vertical and horizontal deflections of the fibre could be determined by these telescopes.The test plate was dismantled from the steam chamber. The air was introduced through the boiler and was allowed to pass into the steam chamber. In entering the steam chamber the air passed through a preliminary cardboard box,fig 4.17, attached to the front plate of the steam chamber(this box was used for ease of modification). After passing over the fibre, the air issued through a square hole in the steam chamber back plate(the location of the condensing plate in actual tests). The pattern of flow of air through the steam chamber was therefore, similar to that of the steam-gas mixtures in the heat transfer tests.

For a range of air flow rates, the fibre deflections were measured. These measurements were made over a height range equivalent to that of the square hole and within a horizontal distance range of 8in from the vertical plane containing the square hole. This range of flowrates was comparable to that of the steam-gas mixtures to be used in the actual tests (the steam-gas mixture flowrates were estimated from the analysis of chapter 3). Various combinations of screens with different spacings were used to obtain a uniform flow of air. However, a uniform air velocity distribution was obtained when fitting the cardboard box with three equispaced (1in apart) screens. In each of the flowrates used, the air velocity was found to be constant over a height range equivalent to that of the square hole and within a distance of 6in from it.

A stainless steel flow dispersing section was then constructed having the same dimensions and number of screens as those found satisfactory when using the cardboard box.

4.4 Temperature and pressure measurements of the Steam-Gas-mixture

The gauge pressure of the mixture was measured by a water manometer, fig 4.04. This was connected by a rubber tubing to a tube passing through the front plate of the steam chamber, and extending to just below the top window, fig 4.01, (so that this could be used for purging gases lighter than steam).

Temperature profiles normal to the condensing surface were measured by the thermocouple of the probe, fig 4.12. Temperatures of the mixture half way between the test plate and the flow dispersing section and near this section were measured by the thermocouples in the fixed tubes . Since these parts are carried by the moveable monel plate, these temperatures and profiles could be measured at various horizontal planes.

The stem of the probe was 0.187in o.d. stainless steel tube with a stainless steel piece fitted tightly over one of its ends. This piece supported two hypodermic tubes which formed a horizontal U-shape at exit from stem. The ends of this U-shape were 3in apart. A Nicrom-Constantan 0.0085in diameter thermocouple was stretched between the arms of the U so that the junction was in the middle of the span between the arms. The wire passed through the hypodermic tubes and via a slot in the probe and along its entire length, out of the chamber. Except for the exposed portions, both wires were lagged with P.V.C. sleeving. The exposed part was insulated with varnish. This insulation was tested after immersion in boiling water for an hour and exposure to steam for another hour and found to be satisfactory.

The probe could be traversed horizontally and with a precision of 0.05mm, through a distance of 2cm. This was achieved by a vernier scale on the probe outside the steam chamber, fig 4.11.

The other two thermocouple tubes were stainless steel, each 0.125in diameter and closed at the end which is inside the steam chamber. To insure that the thermocouples carried by these tubes were sufficiently immersed the tubes were each bent to form a horizontal L. The base of the L being parallel to the condensing surface.

For sealing purposes "O" rings were located in the monel plate through which the thermocouple tubes and the probe passed.

The monel sliding plate covered a rectangular hole machined in the front plate of the steam chamber, the plate could be moved vertically by means of a screw anchored to the steam chamber front plate. This movement and hence the vertical location of the probe and the two tubes was indicated on the scale engraved on the monel plate's guides with a precision of 1mm, fig 4.07.

4.5 Non-Condensing Gas Injection and Concentration Measurements

The gas injection system, fig 4.09, consisted of two vertical glass cylinders of 2.5in diameter, one of which was graduated. The graduated cylinder was fixed while the other one could be moved vertically. The two cylinders were connected at their lower ends by rubber tubing. The sliding cylinder was open to atmosphere at its upper end. The graduated cylinder had a three way stop cock at its upper end. One outlet branch of this stop cock was connected to the gas cylinder while the other branch was connected to a three-way leak-proof stainless steel valve which led to the boiler (the other branch of this valve was connected to a vacuum pump). The two cylinders contained distilled water with the graduated one initially filled.

The injection procedure was as follows:-

That part of the system between the stainless steel valve and the boiler was first evacuated. The gas was then allowed to flow from its cylinder into the evacuated space and into the graduated cylinder thereby displacing some of the water into the other cylinder. The gas supply was then closed (at the gas cylinder) and by sliding the moveable cylinder, the water levels in both cylinders were made to lie in the same horizontal plane, thereby ensuring that the gas pressure was atmospheric. The volume of enclosed gas was then observed. To inject the gas into the boiler, the stainless steel valve was opened and the moveable cylinder was raised until the water filled the graduated cylinder. The stainless steel valve was finally closed. The displaced volume of the gas in the graduated cylinder represented the volume of the gas injected into the boiler.

The average gas concentration was found using the known dimensions of the boiler, steam chamber and pipes and the observed water level in the boiler (see specimen calculation appended 3).

4.6 Measurement of the thermo electrical potential difference

The leads of both the Nicrom and Constantan from all the measuring junctions were soldered to thicker enamelled copper wires, fig. 4.14, which were sleeved in pairs by figure 8 shaped sleevings (one pair for each thermocouple), fig 4.15. These wires were taken to the selector switch. The two junctions involving the copper leads were placed in closely fitting thin walled glass tubes. The glass tubes (one for each thermocouple) were immersed to a depth of about 10in in finely ground, closely packed, melting, distilled-water ice contained in a large Thermos. The ice formed the reference junction and at the same time eliminated any e.m.f. due to the lead wires. Care was taken to insure that the cold junction tubes were not clustered in bundles. It should be mentioned that the cold junction tubes for the test plate thermocouples were not made with the actual thermocouple leads but with the wires from the same reels. These wires were twisted with their corresponding thermocouple leads and held by a terminal when the test plate had been assembled with the steam chamber. This avoided making new cold junctions each time the plate was assembled with the steam chamber.

The selector switch was covered by an aluminium box to avoid draught. The leads from the selector switch were taken through a reversing switch to the potentiometer. By taking forward and reverse readings errors due to spurious e.m.fs. were minimised. The calibration of potentiometer, measuring to 0.1μV, had been newly checked. The sensitivity of the galvanometer was approximately 0.5 cm/μV. Fig 4.13. shows the measuring instrument panel.

4.7 Thermocouple Calibration

The calibrating tank was as shown in fig 4.16. It consisted of a large Thermos, D. The half-in-thick asbestos top was held down by spring clips. The variable speed electric motor V, mounted on the top, drove the stirrer S. The immersion heater H and radiation shield R were both screwed into the asbestos top. The heater was supplied through a variable transformer. A mercury-in-glass thermometer M was included to give an approximate indication of the tank temperature. The vessel was filled to about half an inch from the top with water.

Calibration was carried out against a thermocouple calibrated by the National Physical Laboratory. The junctions of the N.P.L.'s and that to be calibrated were soldered together and placed in the same tightly fitting copper tube G. The tube was full of oil and was immersed to a depth of about 10inches.

Calibration points were obtained by using a heater current just sufficient to keep the temperature constant at the desired level. The potential difference of the N.P.L. thermocouple was first measured in the forward and reversed directions. The thermocouple being calibrated was then read in both directions (the difference never exceeded 2μV). The N.P.L. thermocouple was then re-read. If the first and second readings of this thermocouple agreed to 1μV the reading was accepted; otherwise the heater current was adjusted and the procedure repeated until such agreement was obtained. The temperature was then adjusted to the new desired level and the procedure repeated. The calibration carried out in this way was found to be reproducible to within 1μV on different occasions.

4.8 Apparatus Cleaning

Before assembling, the glassware of the apparatus was cleaned with sodium diocromate solution, rinsed with tap water and finally with de-ionized water. The metallic parts of the apparatus were cleaned first with acetone, followed by carbon tetrachloride, rinsed with tap water and finally with de-ionized water.

After assembling, water was boiled and condensed on the test plate. Although a continuous condensate film initially appeared on the test plate, this changed gradually in to areas of dropwise indicating that the system was still not clean.

To clean the system again the water was replaced by carbon tetrachloride. This was boiled and condensed on the test plate. The carbon tetrachloride was then removed and water was again boiled and condensed on the test plate. Following this treatment, film condensation for periods in excess of five hours could be obtained.

The condensing surface was cleaned first by rinsing with tap water and rubbing with fine emery paper wetted with dilute sodium hydroxide solution. The condensing surface was finally rinsed thoroughly first with tap water, followed by de-ionized water.

4.9 Leak Testing Technique

Considerable time was spent in getting the apparatus satisfactorily leak proof. To test for leaks a "Laybold" halogen leak detector was used. When the system is completely evacuated, this instrument could detect leak rates down to 10^{-6} Torr/second. Periodic checks showed that at no time, during the whole experimental performing period, did the leak rate exceed 1Torr/hour when the system was tested under vacuum. This corresponded to less than 0.1% of air leak per hour. It is thought that this leak rate is much smaller when the system was under experimental operating conditions since the leak would be only due to diffusion and not due to differential pressure as was the case when the system was under vacuum,. Under condensing conditions with pure steam the saturation temperature corresponding to the observed pressure and the steam temperature agreed to within the precision of their measurement over periods of several hours, i.e. over periods longer than those subsequently used in tests.

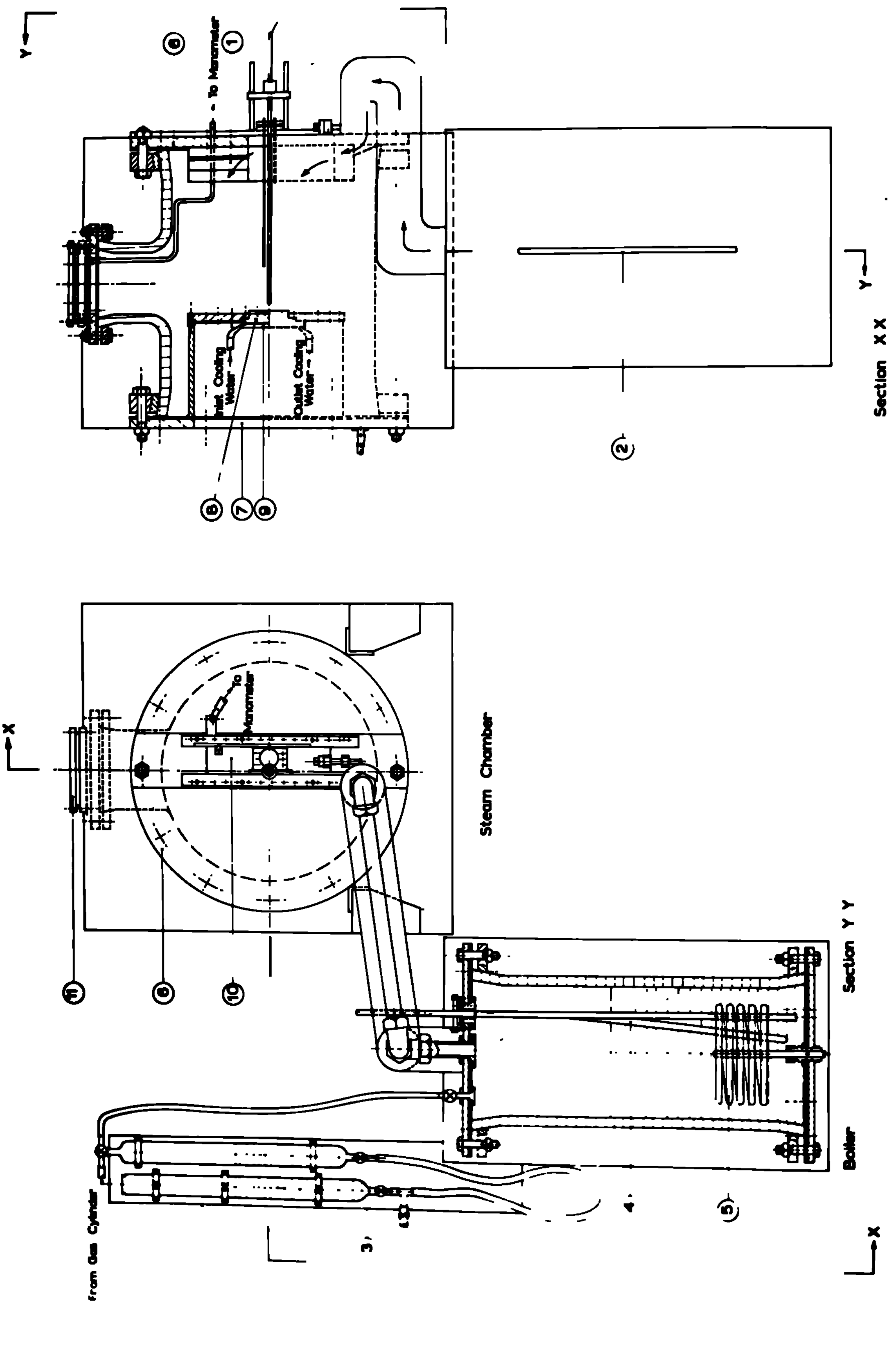

Fig. 4·01. APPARATUS LAYOUT

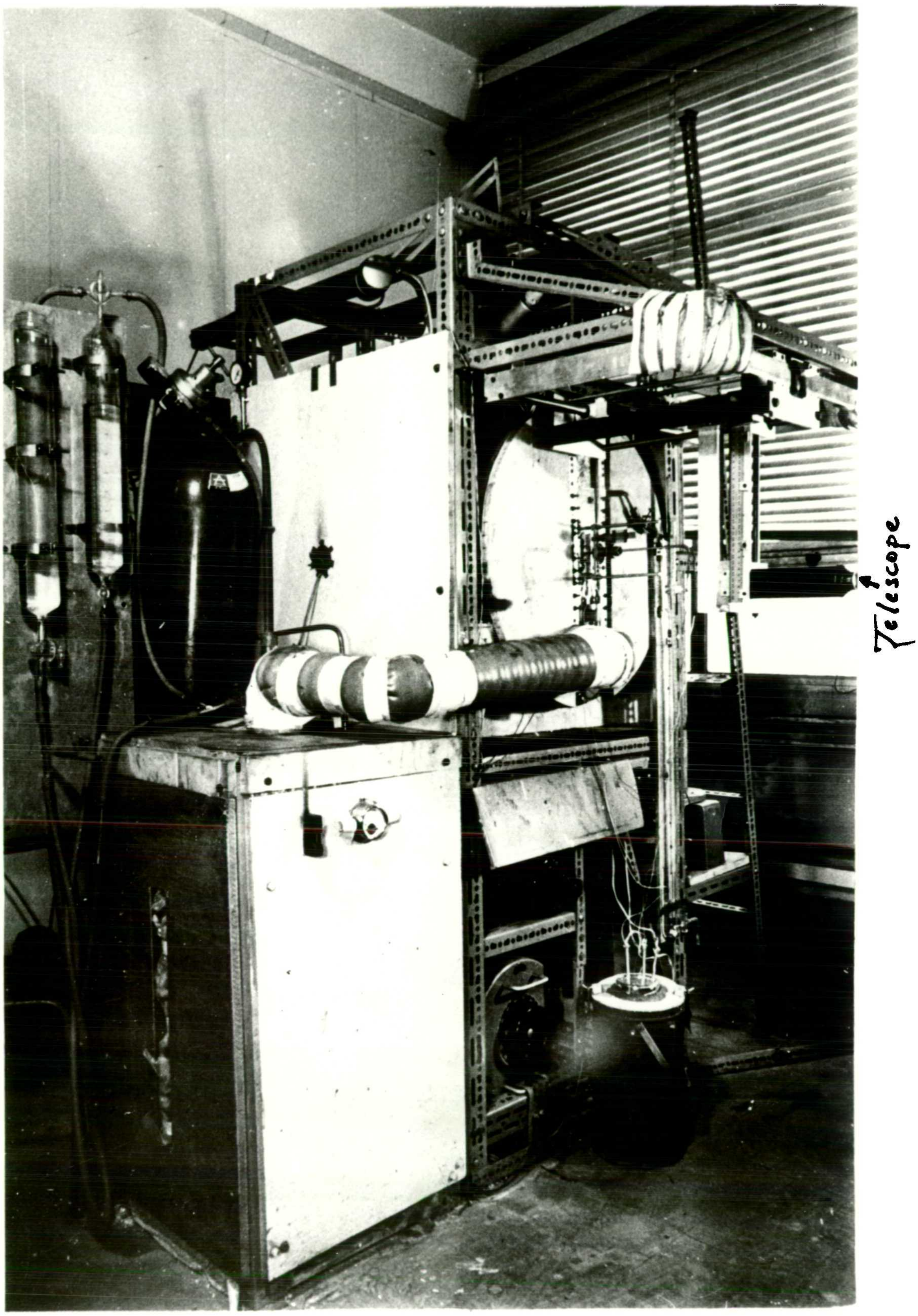

Fig 4.02. GENERAL VIEW OF THE APPARATUS.

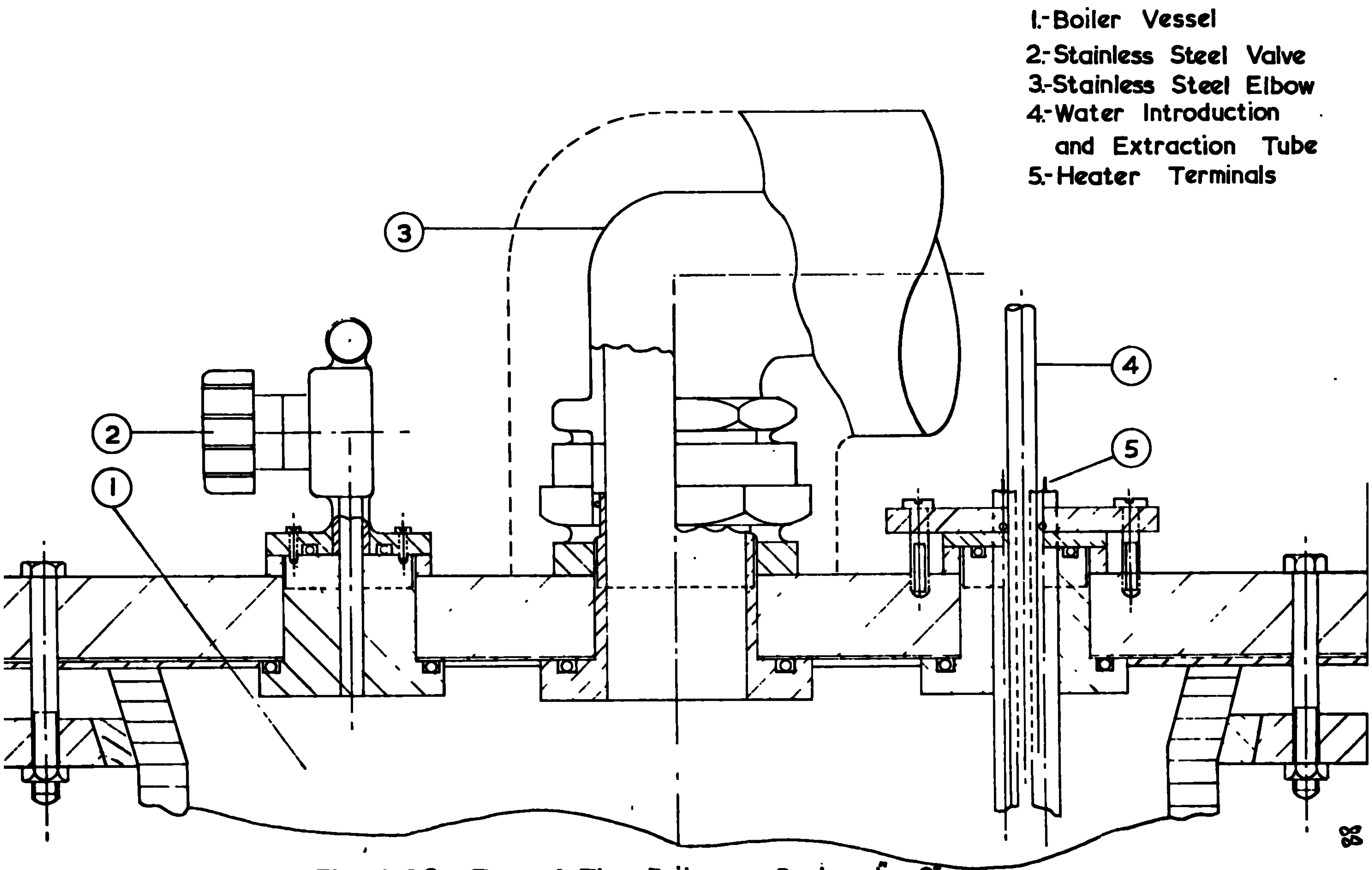

Fig. 4·03. Top of The Boiler. Scale 1" = 2"

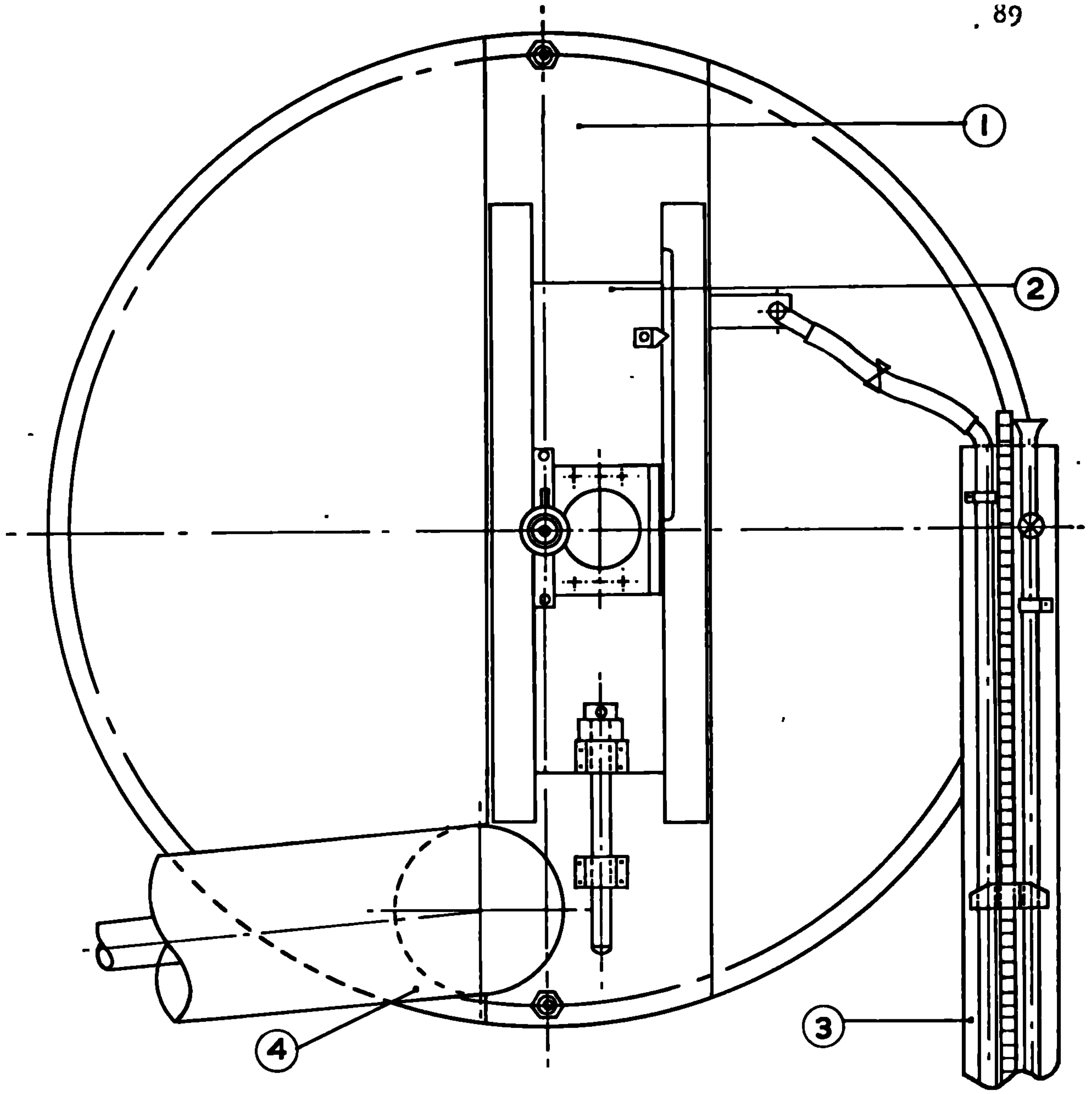

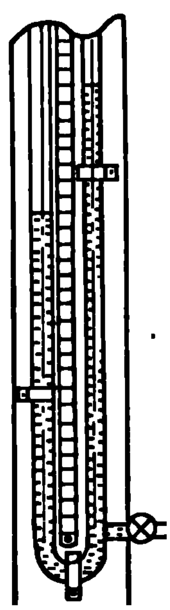

1. The Stainless Steel. Front Plate.
2. The Sliding Plate
3. The Manometer
4. Pipe Connection to Boiler

Fig. 4. 04. Steam Chamber. Front Plate. Scale 1" = 4"

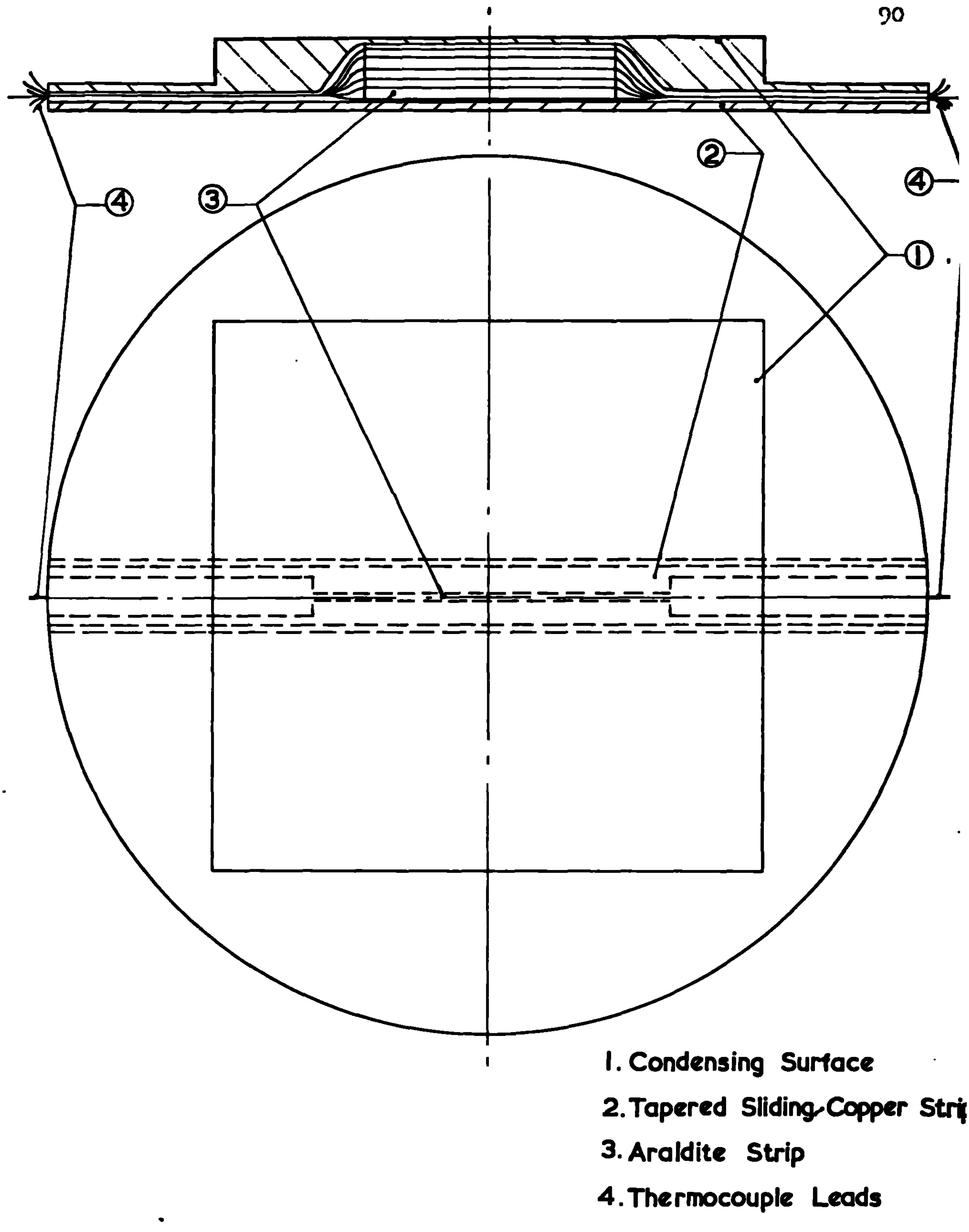

Fig. 4·05. The Condensing Plate. Full Size.

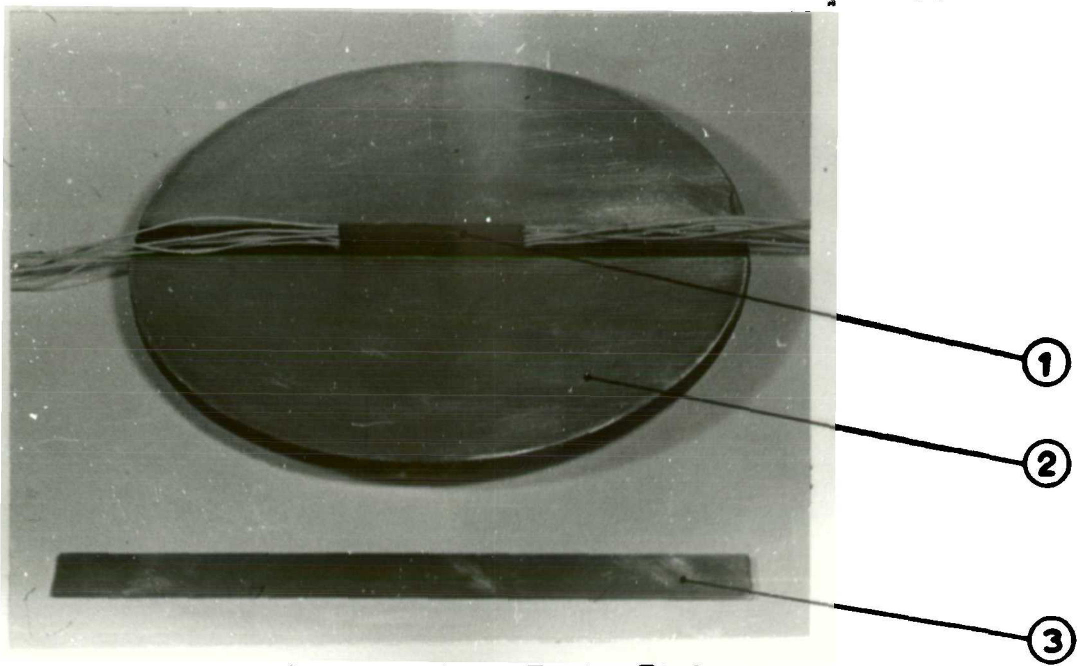

1- Araldite Strip. 2 - The Test Plate.
3- Copper Strip.

Fig 4 06a POSITIONING OF THE ARALDITE STRIP.

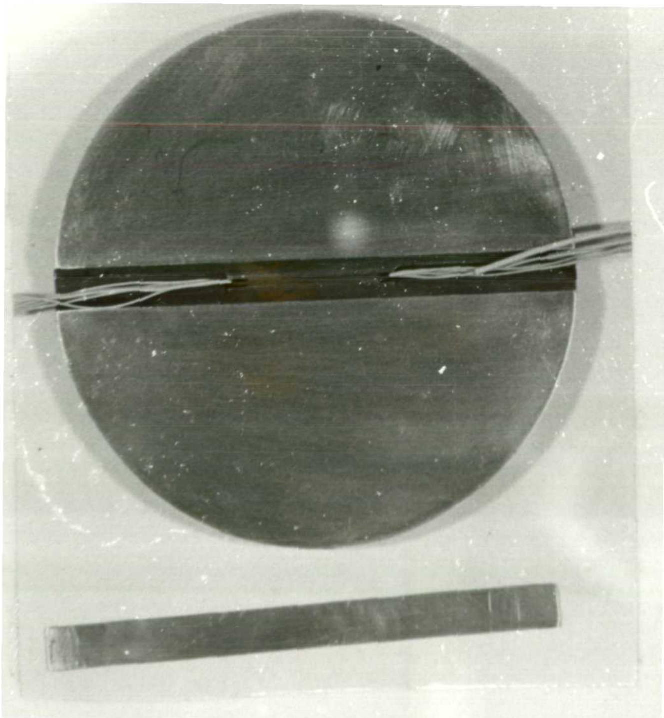

FIG. 4 06b. THE ARALDITE STRIP IN POSITION.

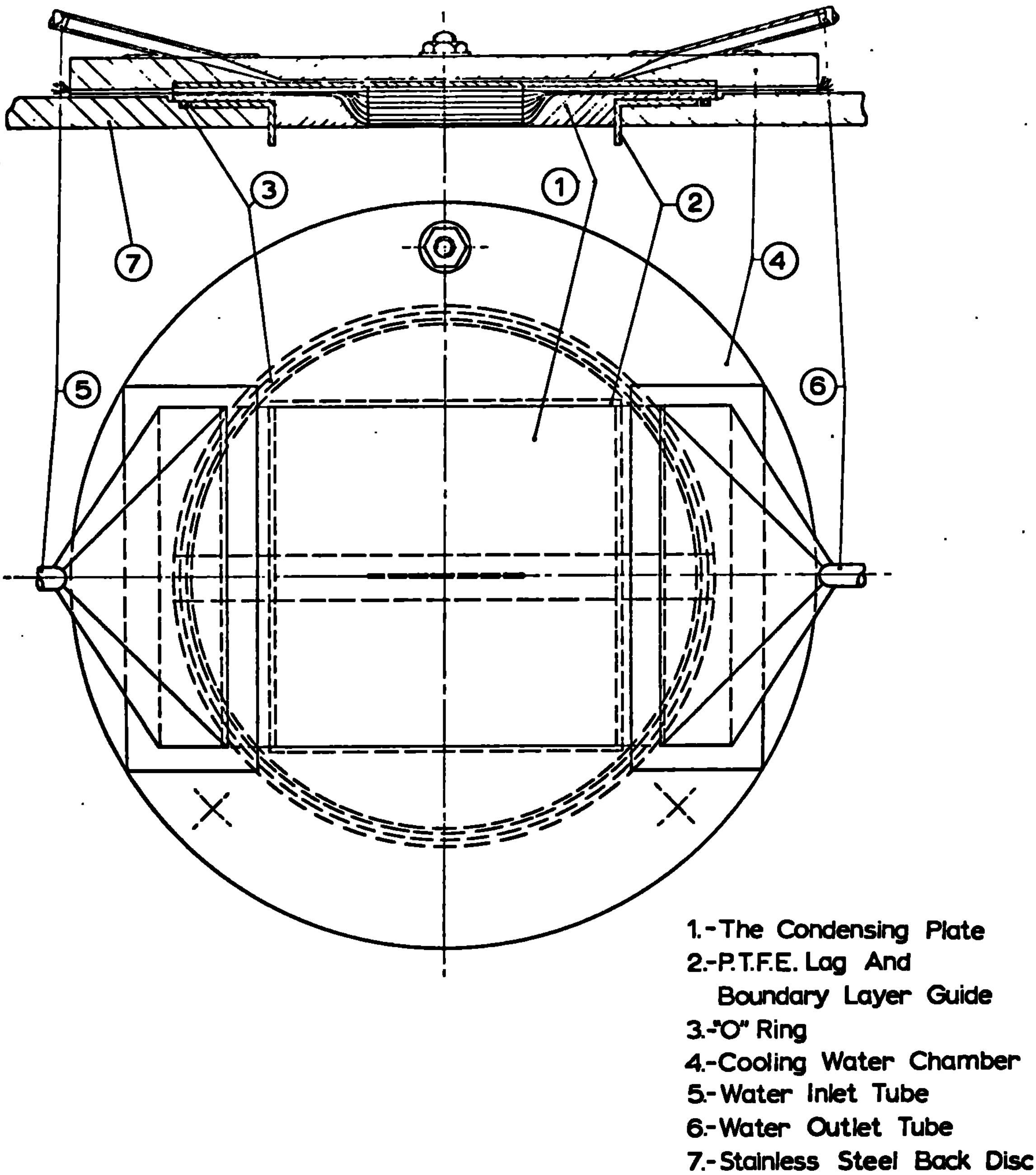

THE CONDENSING PLATE AND COOLING WATER CHAMBER ASSEMBLY SCALE 1: 2

Fig. 4.07.

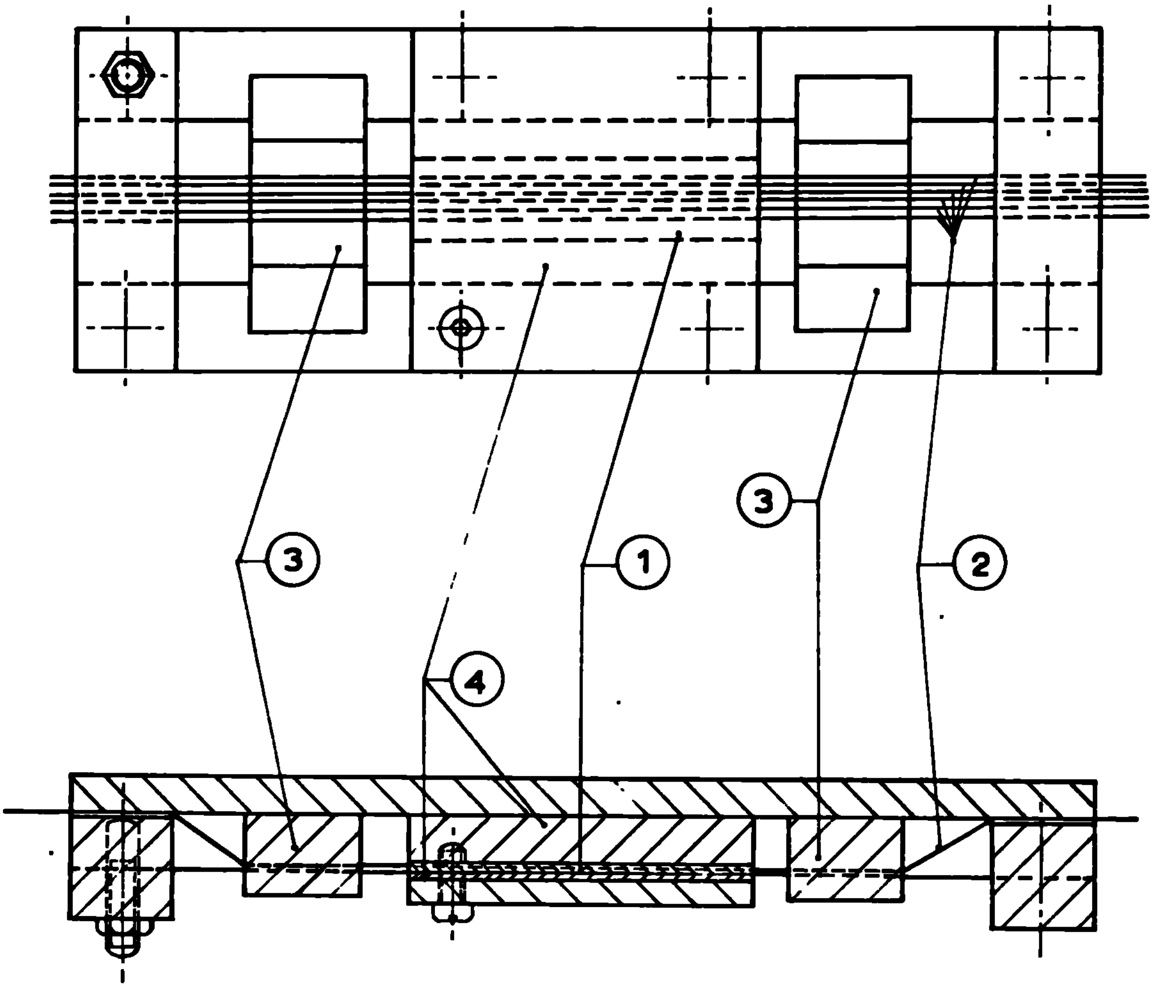

1 – The Araldite Strip
2 – The Test Plate Thermocouples
3 – Horizontally Movable Guide to keep the Thermocouples stretched and in position
4 – P. T. F. E. Strips

Fig. 4.08 THE ARALDITE STRIP MOULD. FULL SIZE.

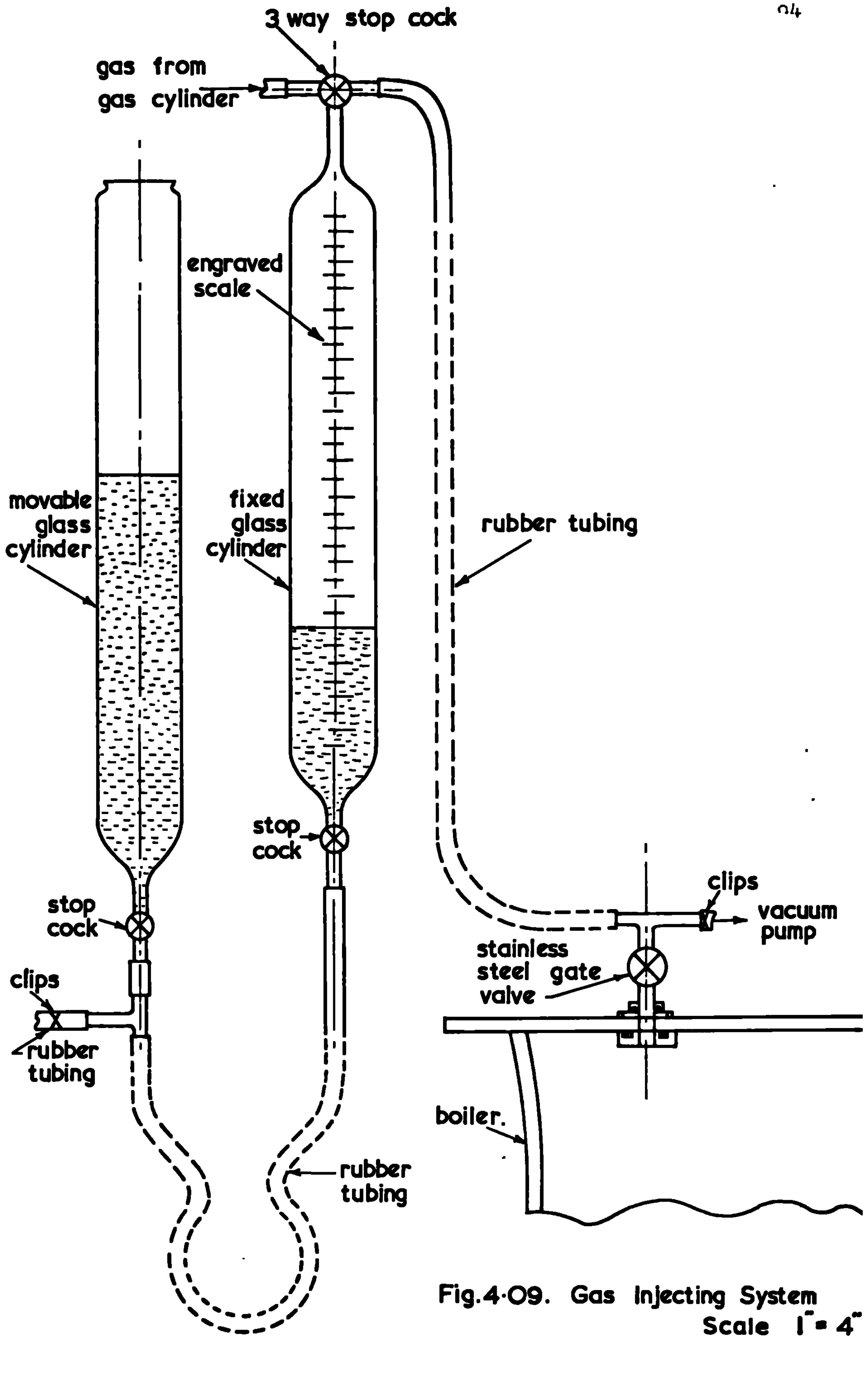

Fig.4·09. Gas Injecting System
Scale 1" = 4"

1. - The Sliding Plate
2. - Window
3. - "O" Rings
4. - Guides
5. - Pointer
6. - Scale
7. - Probe
8. - Probe Holder
9. - Heating Element
10. - Glass Discs

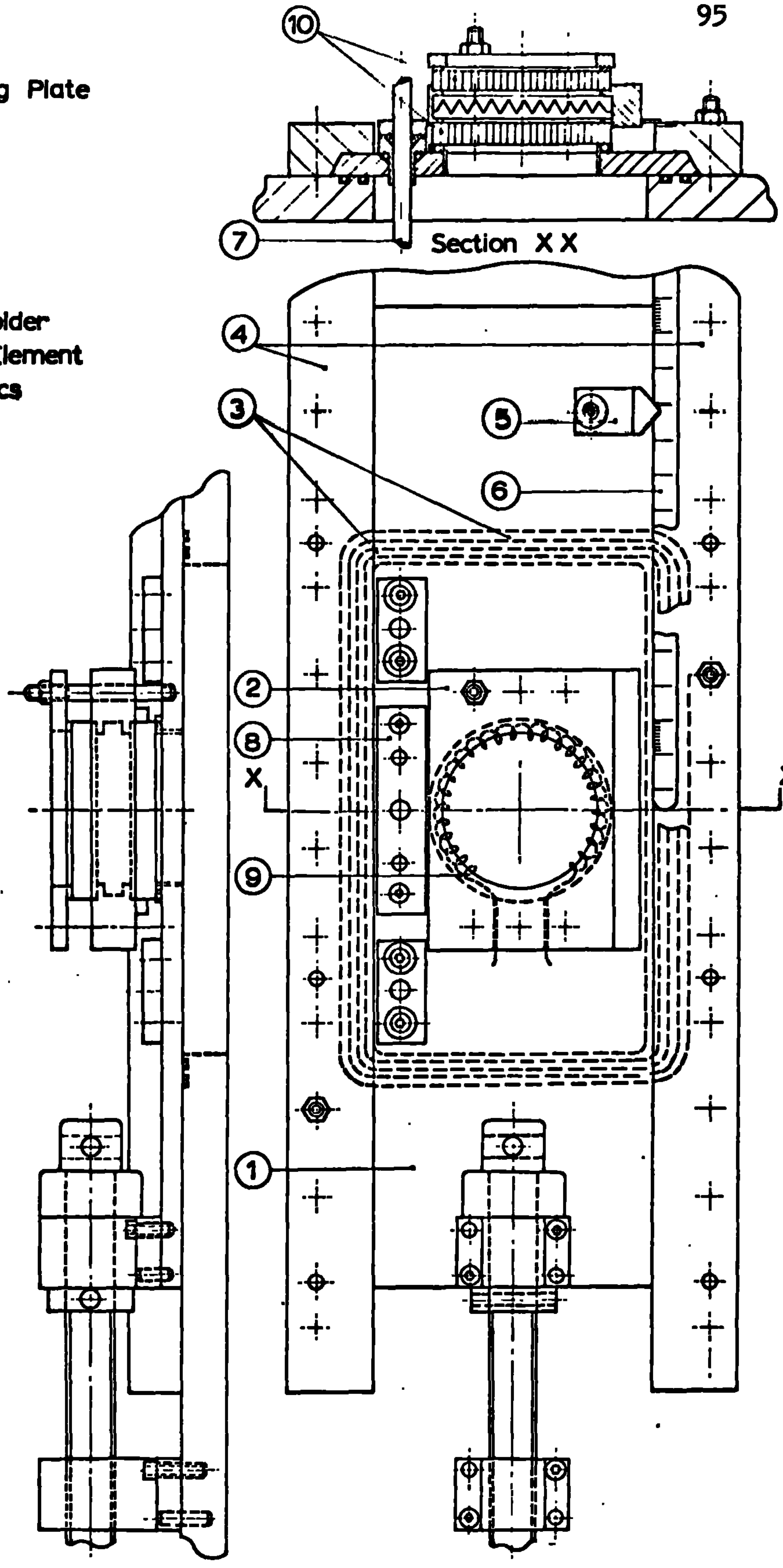

Fig. 4.10. THE SLIDING PLATE ASSEMBLY SCALE 1 : 2

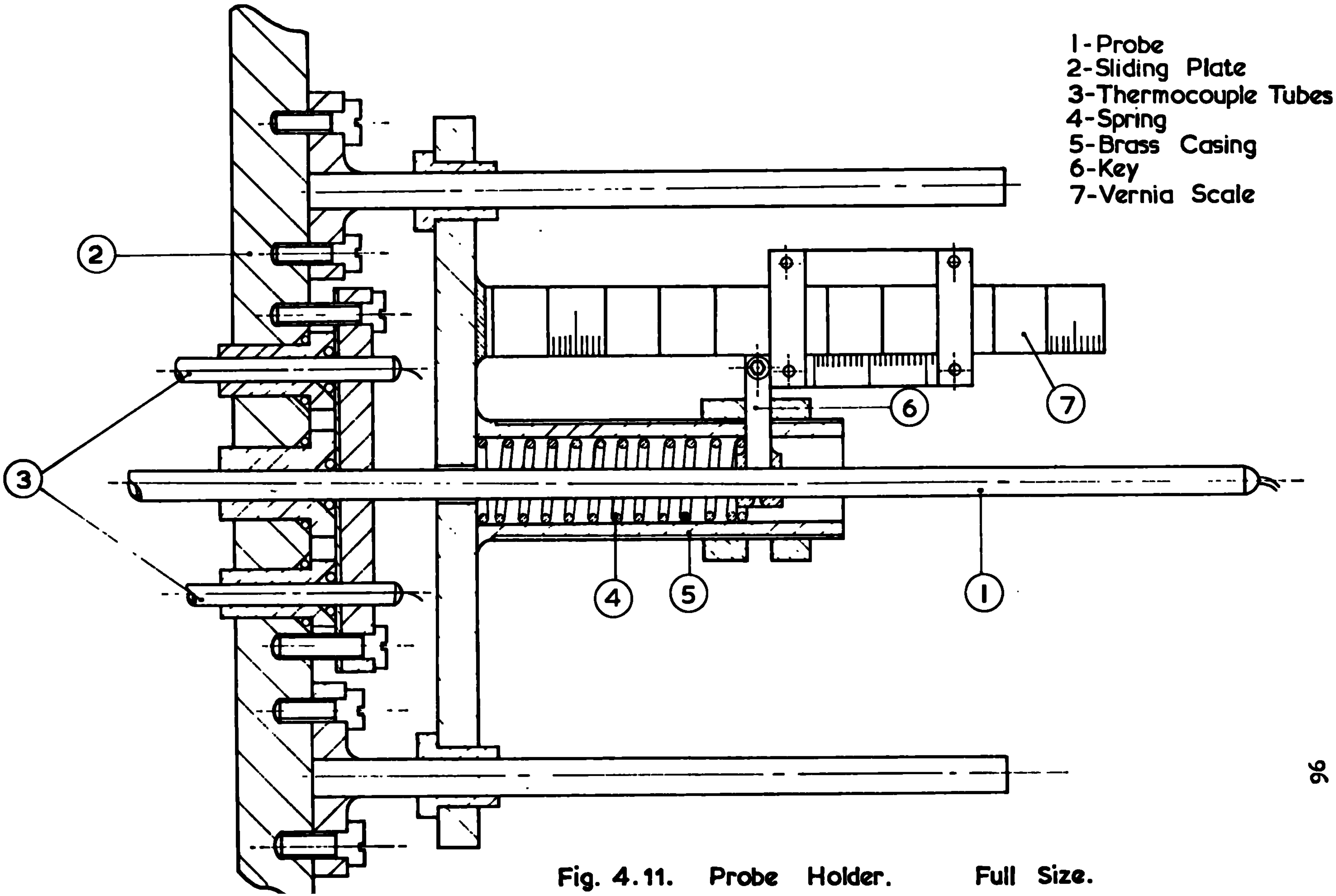

Fig. 4.11. Probe Holder. Full Size.

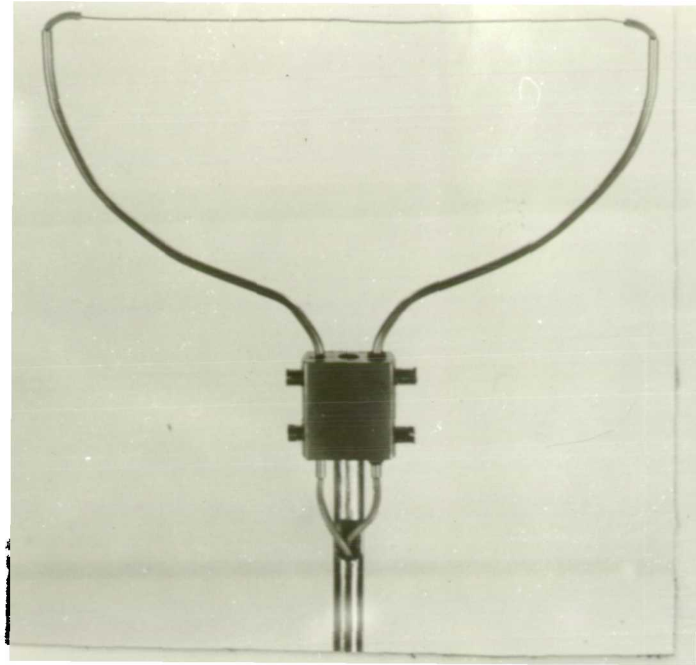

Fig. 4.12. THE PROBE.

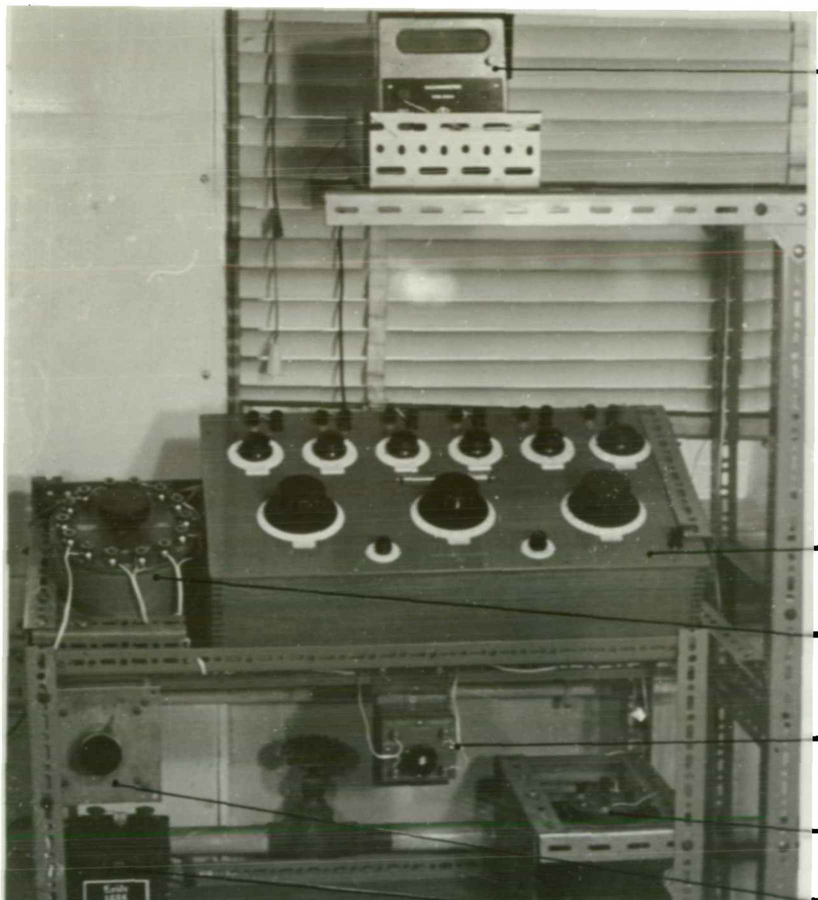

Fig 4.13. THE E.M.F MEASURING INSTRUMENT PANEL.

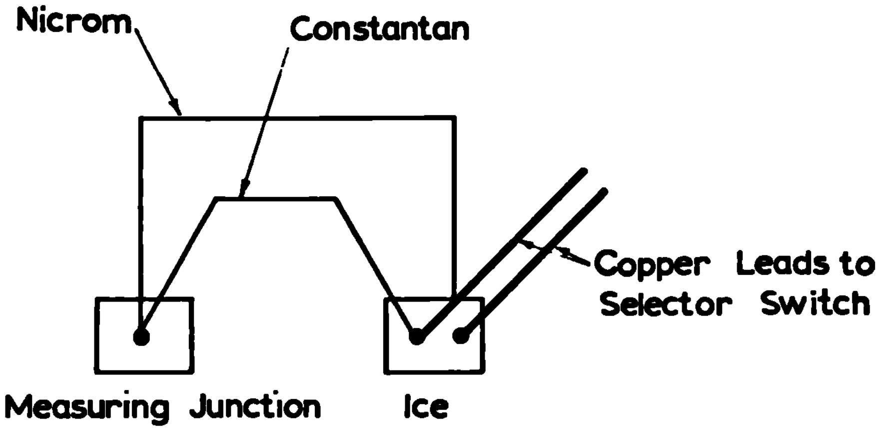

Fig. 4.14. THERMOCOUPLE ARRANGEMENT.

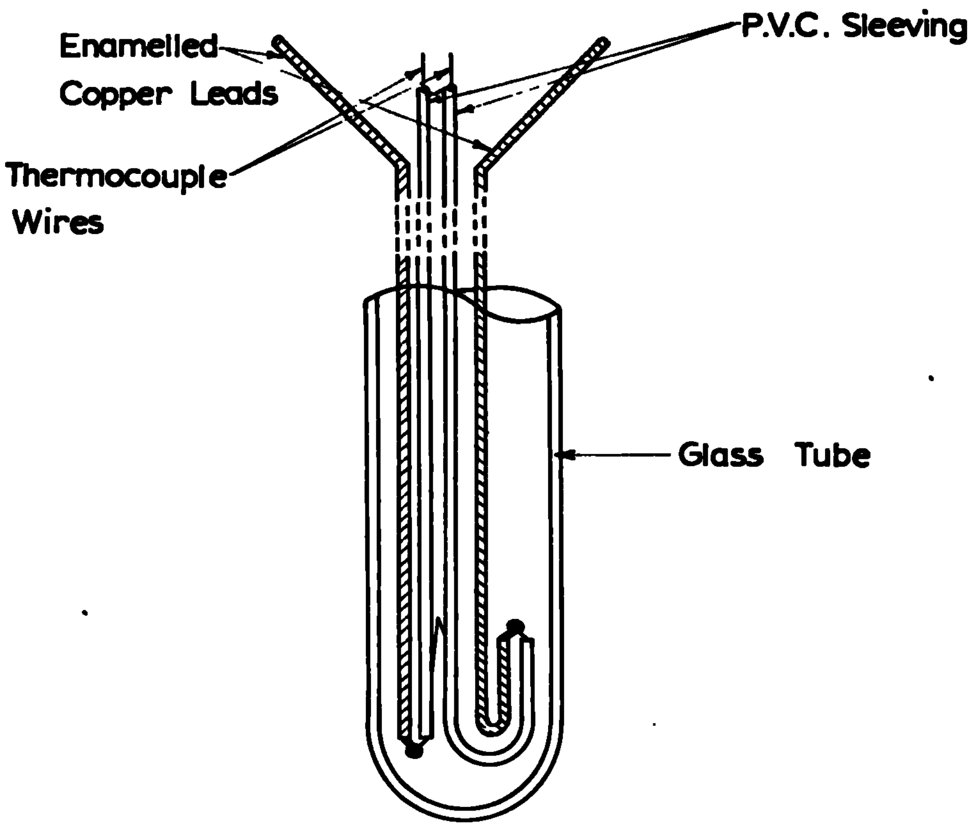

Fig. 4.15. COLD JUNCTION TUBE. SCALE. 5 : 1

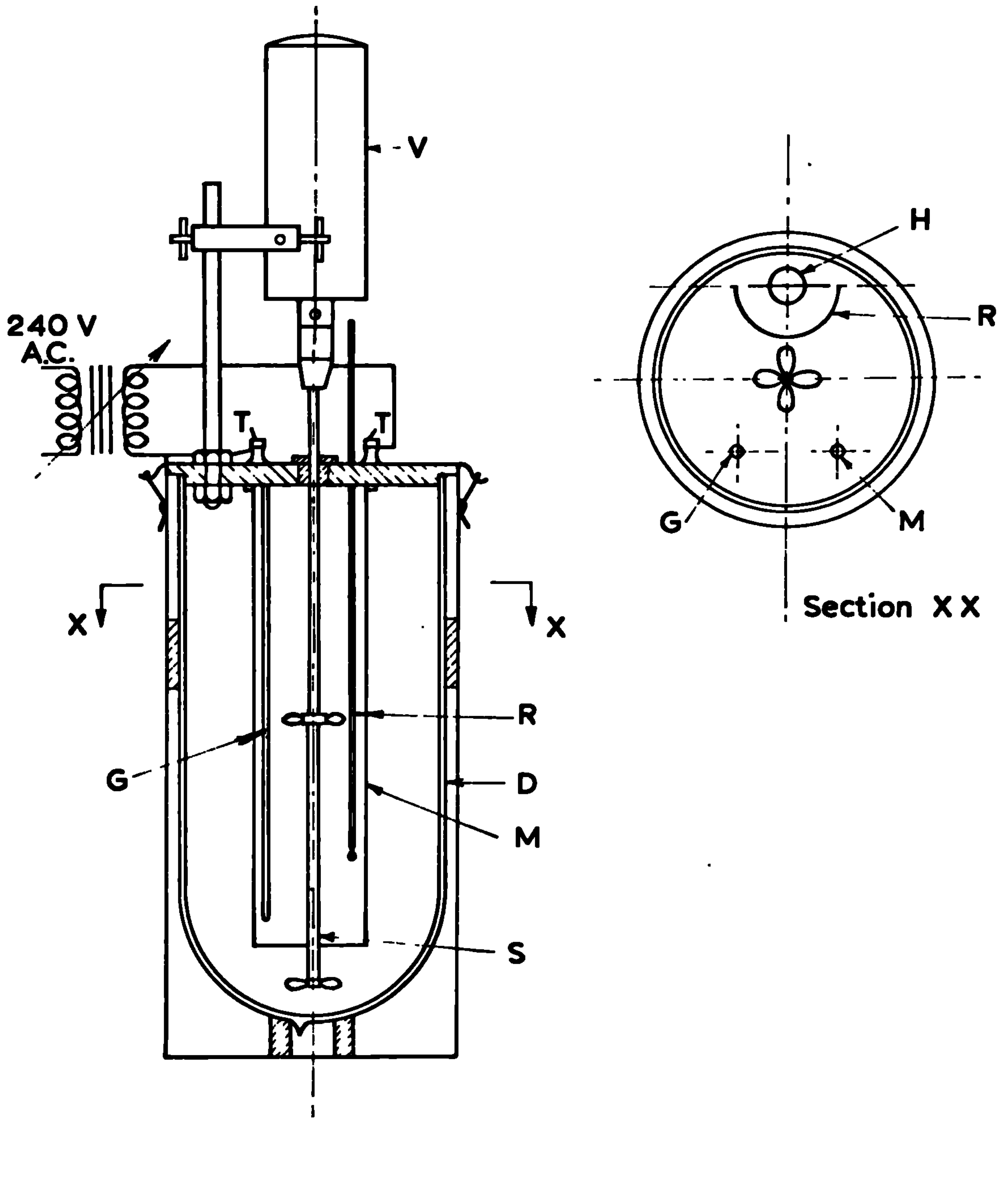

Fig. 4.16. THERMOCOUPLE CALIBRATING TANK. SCALE. 1:4

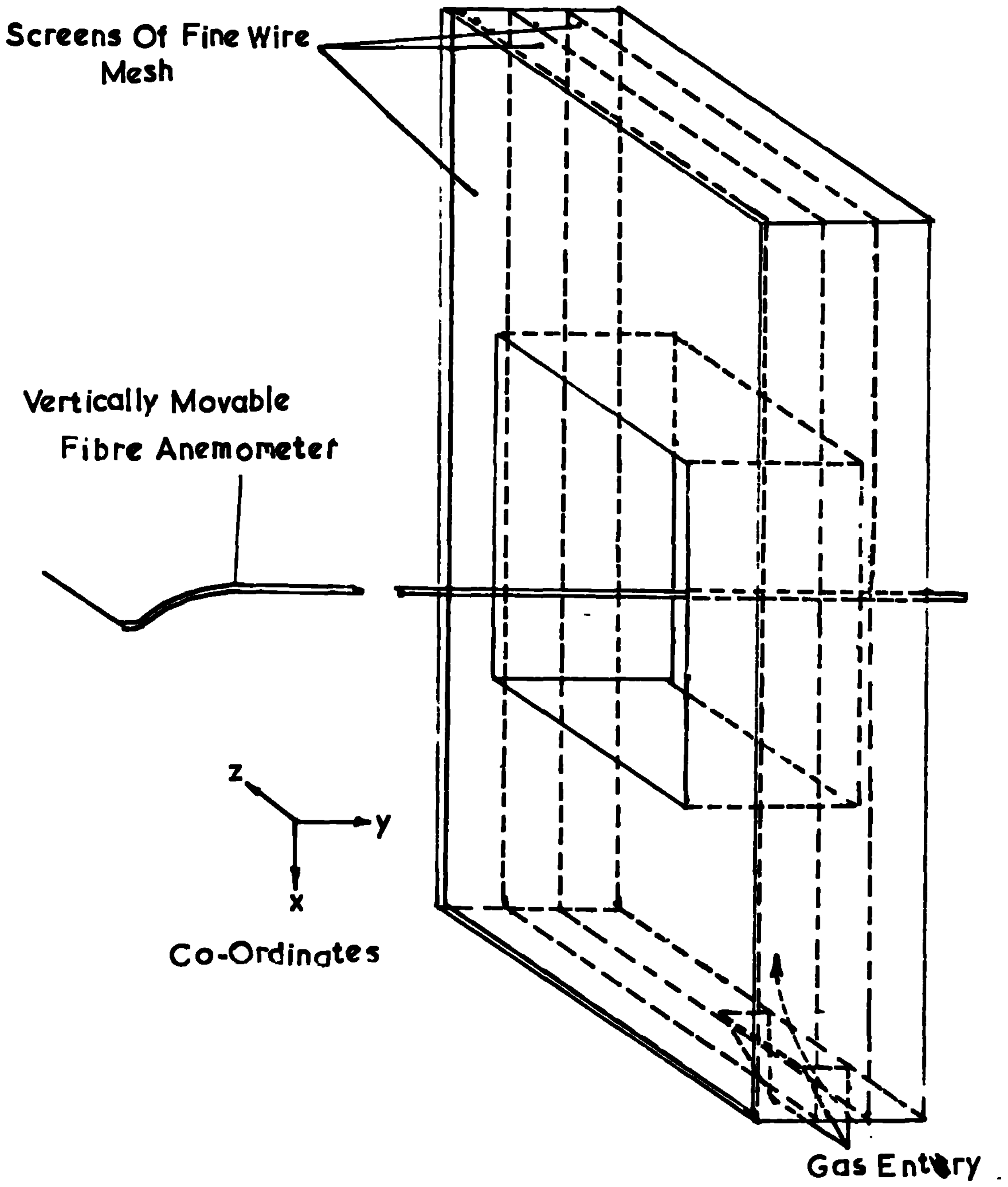

Fig. 4.17. Flow Dispersing Box

Chapter 5

Observations and Results

5.1 Experimental Procedure

a Temperature Profiles

b Variation of heat flux with temperature difference (i.e. between the steam-gas mixture and the metal surface)

5.2 Accuracy of Observations

a Plate Thermocouple Positions

b Temperatures

c Pressures

d Mean Gas Concentration

5.3 Results

5.1 Experimental procedure

Before each test the condensing surface of the test plate was "cleaned" as described in chapter 4. The boiler heaters were then switched on to maximum power and the test plate and the cooling chamber were assembled to the apparatus. To remove, as far as possible, gaseous contaminants including those dissolved in the water, the water was allowed to boil for at least two hours while purging with steam to atmosphere. The system was then closed and the coolant turned on to the maximum flow rate attainable. The boiler heaters were adjusted to give a steady pressure slightly higher than atmospheric. The plate and steam thermocouple readings, together with those of the barometer and the water manometer were observed.

To investigate the effect of a non-condensing gas, a pre-determined volume of the gas was injected as described in chapter 4. The boiler heaters were re-adjusted to maintain a steady pressure and the readings of plate and mixture thermocouples, the manometer and the barometer were observed again.

Temperature profiles

To determine the temperature profiles in the mixture near the condensing surface, the probe thermocouple readings and the probe position were observed as the probe was moved in steps of 0.5mm towards the test plate. The final probe readings were observed when the thermocouple sleeving touched the condensing surface (The junction was then about 2 mm from the plate). The probe was then withdrawn until it was outside the temperature boundary layer (i.e. when there was no change in the temperature readings with further withdrawal). The readings of the thermocouples in the test plate and those in the gas-vapour mixture, manometer, and barometer were observed again. The temperature profiles were determined in horizontal planes of depths, below the top of the plate, of approximately 3cm, 5cm, and [illegible]cm. The adjustment of the probe level to these horizontal planes was made by moving the sliding plate vertically.

If the condensate remained completely filmwise after performing the above procedure, (at the end of some tests mixed condensation occured at the vertical edges of the test plate), a further quantity of gas was injected and the above procedure was repeated.

<u>Variation of heat flux with temperature difference (i.e. between the steam-gas mixture and the metal surface)</u>.

To investigate the variation of heat flux with surface-to-mixture temperature difference, the level of the thermocouple probe was adjusted so that it was in a horizontal plane passing through the middle of the plate, the thermocouple junction being outside the temperature boundary layer. The cooling-water heaters were switched on and the reading of the mixture and test plate thermocouples, the water manometer and the barometer were observed for various cooling water flowrates and temperature. Time was allowed to establish steady conditions before each test.

At the end of each day or in case of breakdown of complete filmwise condensation, all heaters were shut off, the system was opened to atmosphere and the level of the water in the boiler was observed (this was needed in the calculation of the mean gas concentration).

Five series of tests were carried out, the first was for pure steam (i.e. such as is found by the purging technique mentioned. The readings of pressure and temperature corresponded to saturation values to within precision of measurements. This indicates that the gas concentration was not more than 0.002) and the other four were for steam mixtures with air, argon, helium and neon respectively.

5.2 Accuracy of observations

a - plate thermocouple positions

The distances from the edge of the araldite strip of the six thermocouples were measured using a travelling microscope. These measurements were repeated at various distances along the length of the strip. The measured location of each thermocouple was repeatable to within ∓ 0.002mm along its length.

b - temperatures

The thermocouples were calibrated to within ∓ 1μV(≡ 0.02K (see section 4.7). However, when measuring the temperature of the steam-gas mixture, the potentiometer reading was found to fluctuate by about ∓ 4μV. Similiar fluctuations of about ∓ 2μV were observed when measuring the plate temperatures. It is thus estimated that the steam-gas mixture and the plate temperatures were measured respectively to within about ∓ 0.1K and about ∓ 0.06K.

c - pressures

Although the water manometer was graduated to 1mm, its readings fluctuated within ∓ 5mm. The water manometer readings were thus measured to within about ∓ 5mmH_2O. The atmospheric pressure was read to within ∓ 0.05mmHg.

d - mean gas-concentration

The graduations of the cylinder of the gas-injection system was accurate to within ∓ 5cm^3. It was estimated that the calculated volumes of the boiler and steam chamber occupied by the gas-vapour mixture, was accurate to within ∓ 250cm^3.

The errors in the experimental results are discussed in appendix 4.

5.3 Results

The experimental results obtained from the tests are tabulated at the end of this chapter. The temperatures of the gas-vapour mixture listed in these tables were measured by the two mixture thermocouples and the probe thermocouple. The positions of these thermocouples are shown in fig 5.01. The heat flux was determined from the temperature distribution across the plate. These distributions were linear (examples of these distributions are shown in figs 5.02 and 5.03). The surface temperature, t_o, was determined by extrapolation. The gas concentration outside the steam-gas mixture boundary layer was estimated by assuming saturation and using the ideal gas relations.

A specimen calculation for the heat transfer results and the gas concentrations is given in appendix 3.

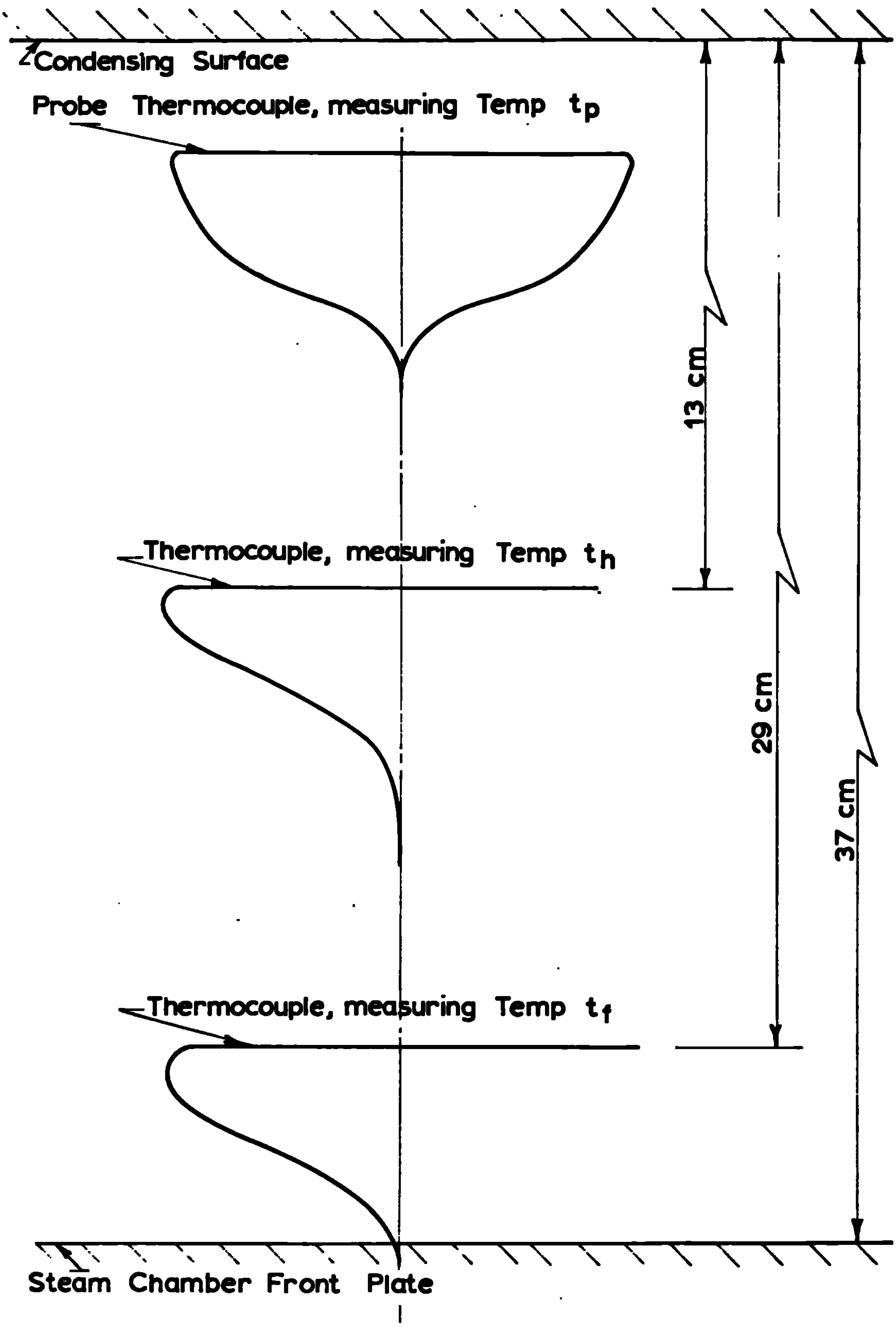

Fig. 5.01 POSITIONS OF THE MIXTURE THERMOCOUPLES.

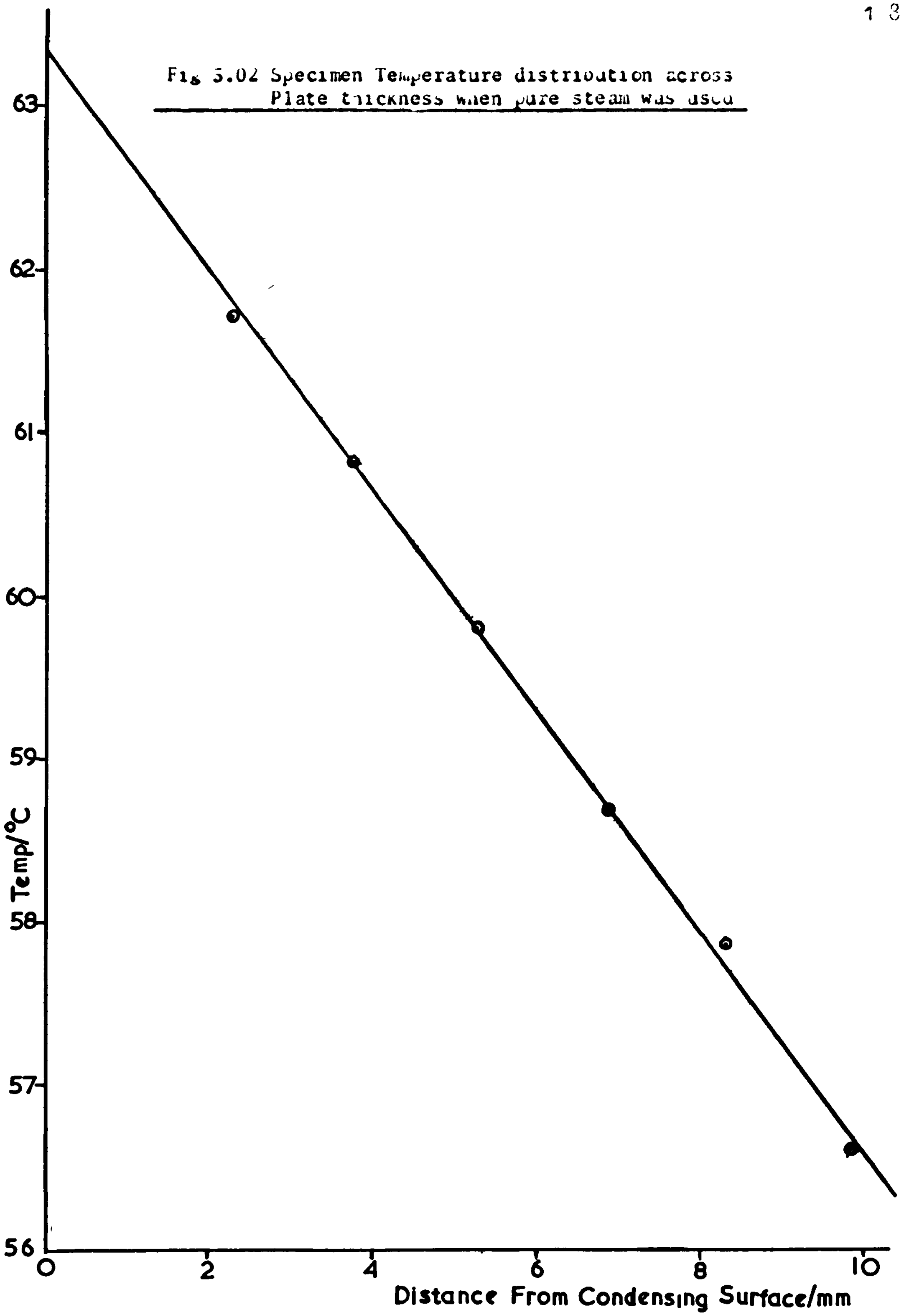

Fig 3.02 Specimen Temperature distribution across Plate thickness when pure steam was used

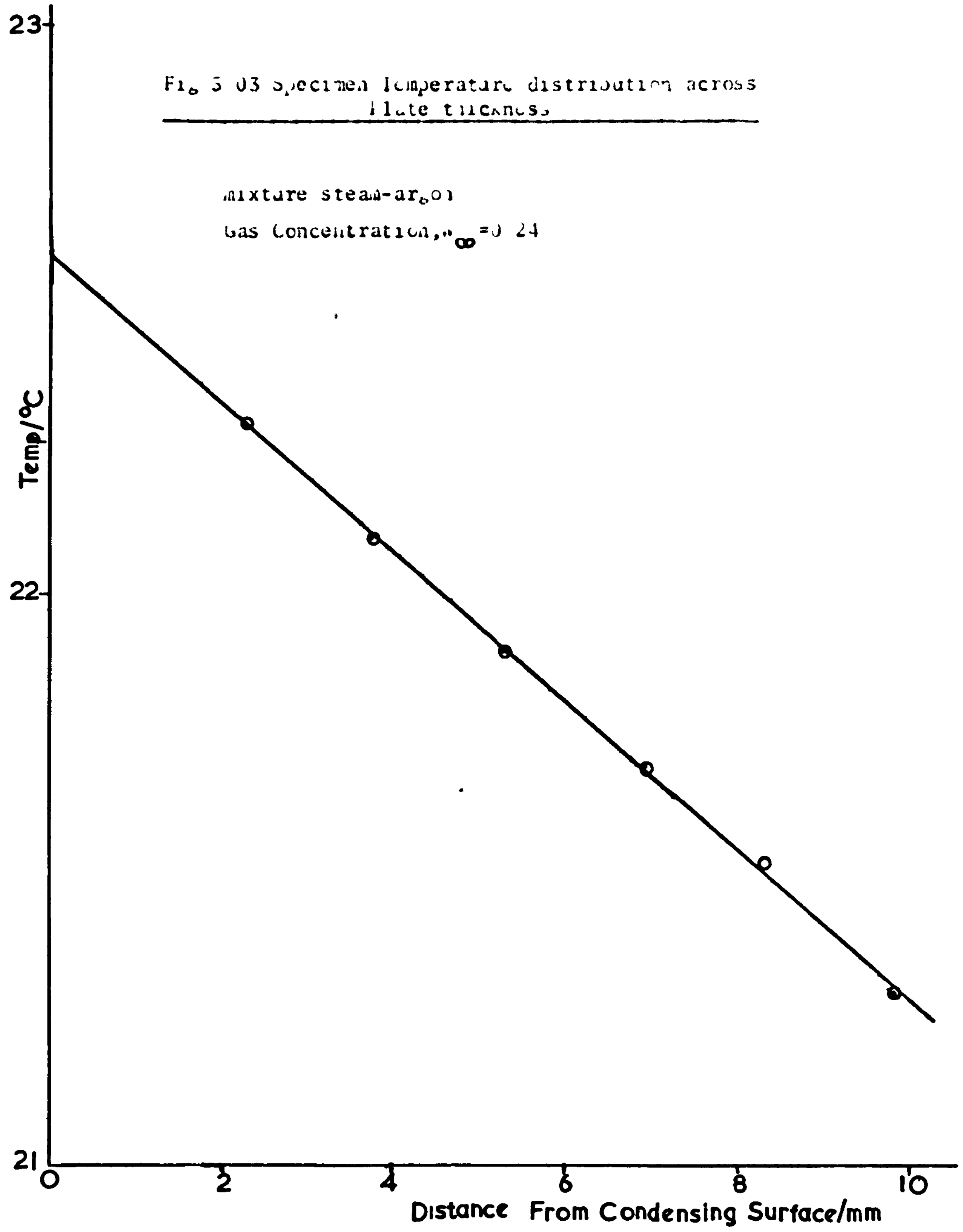

Fig. 5.03 Specimen Temperature distribution across Plate thickness

Table 5.01

Steam-Air Mixture, Full cooling water flowrate.

Test No	x/cm	t_p/C	t_h/C	t_f/C	t_w/C	$T_p - T_w$/K	Q/kW/m^2	Q/Qnu	W_n	W_m	Ptot/Bar
A.01	5.0	99.1	99.5	98.6	35.2	63.9	62	0.172	0.054	0.115	1.1660
A.02	5.0	99.5	99.7	99.3	38.1	61.5	68	0.195	0.035	0.093	1.0199
A.03	0.5	99.1	99.4	98.9	38.3	60.8	71	0.203	0.045	0.113	1.0103
	5.0	99.6	100.1	99.6	"	61.3	"	"	0.053	"	1.0357
	8.0	100.1	100.5	100.2	"	61.8	"	"	0.055	"	1.0529
A.04	8.8	98.8	99.0	97.8	30.7	68.1	45	0.123	0.108	0.211	1.0441
	5.8	99.2	99.3	98.1	"	68.5	"	"	0.132	"	1.0779
A.05	1.1	100.5	100.7	100.5	61.0	39.5	159	0.588	0.015	0.013	1.0427
	5.6	100.6	100.8	100.6	"	39.6	"	"	0.016	"	1.0466
	8.6	100.5	100.8	100.5	"	39.5	"	"	0.022	"	1.0447
A.06	1.1	101.0	101.0	101.0	46.5	54.5	114	0.345	0.015	0.029	1.0612
	5.6	100.8	100.9	100.8	"	54.3	"	"	0.021	"	1.0568
	8.6	100.7	100.9	100.7	"	54.2	"	"	0.026	"	1.0573
A.07	2.1	100.3	100.3	99.9	38.6	61.7	62	0.176	0.028	0.099	1.0426
	5.6	99.8	99.9	99.3	"	61.2	"	"	0.029	"	1.0269
	8.6	99.6	99.7	99.4	"	61.0	"	"	0.037	"	1.0215
A.08	2.6	100.6	100.6	100.5	43.3	57.3	62	0.181	0.018	0.055	1.0467
	5.6	101.1	101.1	100.9	"	57.8	"	"	0.020	"	1.0663
	8.6	101.1	101.2	101.1	"	57.8	"	"	0.020	"	1.0677
A.09	2.6	100.5	100.5	100.2	34.8	65.7	64	0.172	0.025	0.095	1.0503
	5.6	100.7	100.7	100.4	"	65.9	"	"	0.036	"	1.0626
	8.6	100.2	100.2	100.1	"	65.4	"	"	0.055	"	1.0589
A.10	8.6	98.4	98.1	98.4	29.7	68.7	37	0.100	0.126	0.159	1.0420
	5.6	100.0	99.7	100.0	"	69.3	"	"	0.084	"	1.0609
	2.2	100.5	100.5	100.5	"	69.8	"	"	0.058	"	1.0728
A.11	2.2	100.2	100.3	99.9	31.0	69.2	50	0.134	0.051	0.149	1.0529
	5.6	99.7	99.7	99.8	"	68.7	"	"	0.077	"	1.0554
	8.6	99.0	98.8	99.0	"	68.0	"	"	0.104	"	1.0490
A.12	8.6	98.2	97.9	97.8	31.3	66.9	37	0.101	0.137	0.164	1.0430
	5.6	99.3	99.0	99.4	"	68.0	"	"	0.088	"	1.0474
	2.2	100.0	100.0	100.2	"	68.7	"	"	0.057	"	1.0512

contd...........

Table 5.01

Steam–Air Mixture. Full cooling water rate.

Test No	x / cm	t_p / C	t_h / C	t_f / C	t_w / C	$T_p - T_w$ / K	Q / kW/m^2	Q/Qnu	W_I	W_m	P_{tot} / bar
A.13	2.2	99.1	98.9	99.2	29.1	70.0	32	0.087	0.080	0.221	1.0325
	5.0	98.0	97.6	98.3	"	69.1	"	"	0.129	"	1.0286
A.14	2.4	97.4	97.0	98.6	25.7	71.7	26	0.071	0.200	0.334	1.0657
	5.6	93.9	93.6	95.8	"	68.2	"	"	0.310	"	1.0515
	8.0	91.3	90.2	93.3	"	66.6	"	"	0.404	"	1.0508
A.15	8.0	99.5	99.6	99.5	43.6	55.7	123	0.370	0.012	0.030	1.0062
A.16	2.6	100.2	100.3	100.1	39.1	61.1	93	0.264	0.024	0.071	1.0357
	5.6	100.6	100.7	100.5	"	61.5	"	"	"	"	1.0539
	8.0	100.9	100.8	100.7	"	61.8	"	"	"	"	1.0632
A.17	5.0	100.4	100.4	100.4	38.7	61.7	90	0.255	0.024	0.073	1.0465
A.18	5.0	99.3	99.4	99.3	54.2	45.1	124	0.424	0.013	0.013	0.9958
A.19	5.0	101.4	101.4	101.4	41.0	60.4	68	0.133	0.019	0.051	1.0762
A.20	5.0	99.7	99.9	99.7	48.9	50.3	112	0.355	0.015	0.025	1.0154
A.21	2.4	99.8	99.7	99.5	32.7	67.1	61	0.166	0.035	0.121	1.0284
	5.7	[illegible]	[illegible]	[illegible]	"	[illegible]	"	"	0.054	"	1.0415
	7.1	99.6	99.6	99.7	"	66.9	"	"	0.075	"	1.0483
A.22	2.0	99.0	99.0	99.2	32.1	[illegible]	43	0.117	0.093	0.130	1.0407
	5.7	99.6	99.6	99.7	"	67.5	"	"	0.074	"	1.0473
	2.4	100.4	100.4	100.3	"	66.3	"	"	0.038	"	1.0534
A.23	2.4	99.0	99.0	99.8	32.0	66.9	37	0.102	0.043	0.153	1.0375
	5.7	99.1	99.2	99.3	"	67.1	"	"	0.077	"	1.0339
	8.0	98.7	98.5	99.7	"	66.7	"	"	0.096	"	1.0307
A.24	8.0	98.0	97.7	98.3	30.0	68.0	30	0.083	0.128	0.170	1.0278
	5.7	98.6	99.7	99.1	"	[illegible]	"	"	0.094	"	1.0340
	3.4	99.3	99.3	99.4	"	69.5	"	"	0.068	"	1.0347
A.25	2.7	100.2	100.1	100.0	34.4	65.6	60	0.164	0.029	0.103	1.0351
	5.7	100.3	100.2	100.1	"	66.0	"	"	0.042	"	1.0511
	7.3	99.9	99.9	99.9	"	65.5	"	"	0.059	"	1.0469
A.26	8.0	98.5	98.3	98.5	30.6	67.7	50	0.135	0.103	0.169	1.0307
	5.7	99.4	[illegible]	99.6	"	68.6	"	"	0.092	"	1.0541
	2.7	100.1	100.3	100.1	"	69.5	"	"	0.054	"	1.0540

contd.......

Table 5.01
Steam-Air Mixture. Full cooling water flowrate.

Test No	x / cm	t_p / C	t_h / C	t_f / C	t_w / C	T_p-T_w / K	Q / kW/m^2	Q/Qnu	W_p	W_m	Ptot / Bar
A.27	2.7	98.5	98.3	99.1	26.8	71.7	29	0.079	0.117	0.249	1.0410
	5.7	96.6	96.3	97.6	"	70.8	"	"	0.187	"	1.0266
	7.5	95.8	95.3	96.6	"	69.0	"	"	0.219	"	1.0220
A.28	7.5	94.2	93.5	95.4	25.5	68.7	21	0.058	0.300	0.284	1.0417
	5.7	95.8	95.3	97.2	"	70.3	"	"	0.249	"	1.0531
	3.4	97.9	97.3	98.6	"	72.4	"	"	0.169	"	1.0578
A.29	3.4	95.4	94.5	96.7					0.288	0.425	1.0392
	5.7	92.2	91.6	94.2					0.375	"	1.0249
	7.4	90.4	89.7	92.2					0.433	"	1.0228
A.30	7.4	86.2	85.0	88.5					0.528	0.520	1.0314
	5.7	89.2	88.1	91.7					0.458	"	1.0404
	3.4	93.1	92.0	95.1					0.346	"	1.0478
A.31	3.4	90.3	90.0	93.2					0.422	0.550	1.0333
	5.7	86.7	86.4	91.7					0.572	"	1.0221
	7.2	84.6	85.0	92.0					0.562	"	1.0268
A.32	7.2	76.5	81.0	88.4					0.718	0.635	1.0647
	5.7	78.7	82.0	87.9					0.636	"	1.0666
	3.4	83.5	83.6	88.9					0.605	"	1.0689
A.33	3.4	77.0	79.7	85.8					0.717	0.775	1.0821
	5.7	72.3	79.3	85.7					0.773	"	1.0809
	7.2	69.9	77.0	85.0					0.799	"	1.0801
A.34*	3.4	99.7	99.8	99.5					0.055	0.120	1.0389
	5.7	100.1	100.2	99.9					0.055	"	1.0523
	7.2	100.0	100.1	99.9					0.064	"	1.0561
A.35*	7.2	98.5	98.7	98.4					0.093	0.153	1.0219
	5.7	98.8	98.9	98.5					0.079	"	1.0219
	3.4	98.9	99.1	98.6					0.007	"	1.0219
A.36*	3.4	94.9	95.6	95.0					0.275	0.328	1.0440
	5.7	94.1	94.7	94.1					0.305	"	1.0420
	7.2	93.1	93.7	94.6					0.337	"	1.0401

* Zero cooling water flowrate.

contd......

Table 5.01

Steam-Air Mixture. Full cooling water flowrate.

Test No	x (cm)	t_p (C)	t_h (C)	t_f (C)	t_w (C)	T_p-T_w (K)	Q (kW/m²)	Q/Qnu	W_p	W_m	Ptot (Bar)
A.37*	7.2	87.2	87.8	91.9					0.500	0.463	1.0247
	5.7	88.6	89.3	91.9					0.465	"	1.0276
	3.4	89.8	90.7	91.8					0.430	"	1.0276
A.38*	3.4	84.7	85.7	8[illegible].7					0.572	0.601	1.0504
	5.7	83.5	84.3	89.4					0.596	"	1.0514
	7.2	82.0	82.9	89.1					0.625	"	1.0528
A.39*	7.2	58.3	59.0	59.8					0.881	0.880	1.0399
	5.7	59.6	60.0	61.0					0.874	"	1.0409
	3.4	60.9	60.8	63.0					0.865	"	1.0419
A.40	3.4	60.0	60.1	64.3					0.870	0.880	1.0300
	5.7	57.5	58.1	61.9					0.884	"	1.0231
	7.2	54.9	56.5	59.0					0.899	"	1.0259
A.41	7.2	99.9	100.0	99.8	43.0	56.9	133	0.312	0.018	0.019	1.0205
	5.7	100.2	100.4	100.1	"	57.2	"	"	0.017	"	1.0300
	3.4	100.4	100.6	100.2	"	57.4	"	"	0.016	"	1.0382
A.42	2.9	99.6	99.6	99.6	56.5	43.1	193	0.667	0.009	0.010	1.0100
	4.9	99.9	99.9	99.8	"	43.4	"	"	0.012	"	1.0150
	5.9	99.7	99.8	99.6	"	43.2	"	"	0.013	"	1.0088
A.43	5.9	99.3	99.3	99.3	38.5	60.8	119	0.341	0.014	0.029	0.9958
	4.9	99.6	99.7	99.6	"	61.1	"	"	0.015	"	1.0073
	2.9	99.8	99.9	99.8	"	61.3	"	"	0.015	"	1.0151
A.44	2.9	99.5	99.5	99.4	35.8	63.7	110	0.300	0.017	0.042	1.0048
	4.9	99.5	99.6	99.4	"	63.7	"	"	0.019	"	1.0060
	5.9	99.5	99.6	99.4	"	63.7	"	"	0.020	"	1.0058
A.45	5.9	99.8	99.7	99.0	32.4	67.4	74	0.200	0.032	0.070	1.0258
	4.9	100.2	100.3	99.7	"	67.8	"	"	0.024	"	1.0366
	2.9	100.5	100.6	100.1	"	68.1	"	"	0.021	"	1.0469
A.46	2.9	99.4	99.3	98.1	26.0	73.4	63	0.164	0.040	0.120	1.0147
	4.9	99.7	99.8	98.9	"	73.7	"	"	0.059	"	1.0406
	5.9	99.8	100.0	99.2	"	73.8	"	"	0.065	"	1.0479

* Zero cooling water flowrate.

contd......

Table 5.01

Steam-Air Mixture, Full cooling water flowrate.

Test No	x / cm	t_p / C	t_h / C	t_f / C	t_w / C	T_p-T_w / K	Q / kW/m^2	Q/Qnu	W_p	W_m	Ptot / Bar
A.47	5.9	97.1	97.3	96.2	22.3	74.4	51	0.133	0.123	0.170	0.9949
	4.9	98.1	98.3	97.1	"	75.4	"	"	0.100	"	1.0138
	2.9	99.0	99.3	97.7	"	76.3	"	"	0.079	"	1.0278
A.48	2.9	97.3	97.7	96.7	19.5	77.8	42	0.109	0.151	0.245	1.0233
	4.9	96.7	97.3	96.4	"	77.2	"	"	0.206	"	1.0449
	5.9	96.4	97.2	96.2	"	76.9	"	"	0.230	"	1.0579
A.49	5.9	99.8	99.8	99.8	43.7	56.1	133	0.396	0.012	0.022	1.0100
	4.9	100.3	100.5	100.4	"	56.6	"	"	0.021	"	1.0300
	2.9	100.1	100.3	100.2	"	56.4	"	"	0.021	"	1.0300
A.50	2.9	100.0	100.0	100.0	38.0	62.0	88	0.248	0.019	0.041	1.0200
	4.9	100.3	100.3	100.3	"	62.3	"	"	0.018	"	1.0300
	6.0	100.5	100.6	100.5	"	62.5	"	"	0.025	"	1.0400
A.51	6.0	100.3	100.3	100.3	34.8	65.5	66	0.181	0.020	0.060	1.0350
	4.9	100.5	100.5	100.5	"	65.7	"	"	0.020	"	1.0400
	2.9	100.4	100.4	100.4	"	65.6	"	"	0.021	"	1.0350
A.52	6.0	99.9	99.9	99.1	31.6	68.3	56	0.149	0.031	0.081	1.0250
	4.9	100.2	100.2	99.6	"	68.6	"	"	0.028	"	1.0300
	2.9	100.2	100.3	99.8	"	68.6	"	"	0.026	"	1.0350
A.53	2.9	100.1	100.0	99.1	29.0	71.1	42	0.111	0.030	0.099	1.0300
	4.9	100.2	100.2	99.3	"	71.2	"	"	0.037	"	1.0400
	6.0	100.1	100.2	99.3	"	71.1	"	"	0.040	"	1.0400
A.54	6.0	99.3	99.5	98.7	26.8	72.5	39	0.103	0.063	0.118	1.0300
	4.9	99.6	99.9	98.8	"	72.8	"	"	0.053	"	1.0300
	2.9	99.8	100.0	98.9	"	73.0	"	"	0.042	"	1.0300
A.55	2.9	99.5	99.7	98.4	25.1	74.4	35	0.093	0.056	0.138	1.0300
	6.9	99.2	99.5	98.7	"	74.1	"	"	0.072	"	1.0300
	6.0	99.0	99.3	98.6	"	73.9	"	"	0.081	"	1.0300
A.56	6.0	98.7	98.9	98.3	24.0	74.4	38	0.099	0.100	0.157	1.0300
	4.9	99.0	99.4	98.2	"	74.7	"	"	0.088	"	1.0300
	2.9	99.4	99.7	98.1	"	75.4	"	"	0.066	"	1.0300

contd........

Table 5.01
Steam-Air Mixture. Full cooling water flowrate.

Test No	$\frac{x}{cm}$	$\frac{t_p}{C}$	$\frac{t_h}{C}$	$\frac{t_f}{C}$	$\frac{t_w}{C}$	$\frac{T_p-T_w}{K}$	$\frac{Q}{kW/m^2}$	Q/Qnu	W_p	W_m	$\frac{Ptot}{Bar}$
A.57	2.9	98.7	99.0	97.4	22.0	76.7	32	0.082	0.096	0.195	1.0300
	4.9	98.1	98.4	97.0	"	76.1	"	"	0.123	"	1.0300
	6.0	97.6	98.0	96.7	"	75.6	"	"	0.145	"	1.0300
A.58	6.0	96.3	97.0	96.1	20.5	75.8	29	0.075	0.206	0.229	1.0300
	4.9	97.0	97.6	96.5	"	76.5	"	"	0.177	"	1.0300
	2.9	98.2	98.6	97.1	"	77.7	"	"	0.125	"	1.0300

Table 5.02
Steam-Air Mixture. Variable $(T_\infty - T_w)/K$.

Test No	$\frac{x}{cm}$	$\frac{t_p}{C}$	$\frac{t_h}{C}$	$\frac{t_f}{C}$	$\frac{t_w}{C}$	$\frac{T_\infty-T_w}{K}$	$\frac{Q}{kW/m^2}$	Q/Qnu	W_∞	W_m	$\frac{Ptot}{Bar}$
A.59	5.0	101.7	101.8	101.7	90.2	11.5	53	0.467	0.015	0.100	1.0904
	5.0	101.3	101.4	101.4	77.4	24.0	50	0.257	"	"	1.0708
	5.0	100.6	100.6	100.6	67.8	32.8	62	0.259	"	"	1.0335
	5.0	100.2	100.1	100.2	59.8	40.4	61	0.223	"	"	1.0109
	5.0	99.4	99.3	99.4	55.9	43.45	100	0.350	"	"	0.9737
A.60	5.0	100.5	100.7	100.5	43.4	57.2	58	0.171	0.024	0.048	1.0484
	5.0	100.9	101.1	100.0	51.8	48.9	24	0.170	"	"	1.0602
	5.0	100.5	100.7	100.0	63.6	36.8	42	0.163	"	"	1.0484
	5.0	100.8	100.9	100.2	81.7	18.9	42	0.255	"	"	1.0592
	5.0	101.1	101.2	100.6	92.9	8.1	37	0.411	"	"	1.0705
A.61	5.0	99.1	99.3	99.0	36.9	62.3	43	0.123	0.040	0.095	1.0062
	5.0	99.3	99.5	99.5	47.0	52.4	38	0.118	"	"	1.0121
	5.0	99.3	99.9	99.9	54.6	45.3	33	0.112	"	"	1.0308
	5.0	99.8	100.0	99.9	72.6	27.3	35	0.164	"	"	1.0337
	5.0	100.0	100.1	100.0	86.7	13.3	33	0.259	"	"	1.0415

contd.........

Table 5.02

Steam-Air Mixture. Variable $(T_\infty - T_w)/Y$.

Test No	$\frac{x}{cm}$	$\frac{t_p}{C}$	$\frac{t_h}{C}$	$\frac{t_f}{C}$	$\frac{t_w}{C}$	$\frac{T_\infty - T_w}{K}$	$\frac{\dot q}{kW/m^2}$	$\sqrt{/\Im nu}$	W_∞	W_m	$\frac{Ptot}{Bar}$
A.62	5.0	99.8	100.2	99.6	34.5	65.4	38	0.105	0.068	0.130	1.0491
	5.0	100.7	100.9	100.6	48.2	52.5	32	0.098	"	"	1.0848
	5.0	100.7	101.0	100.6	59.1	41.7	30	0.109	"	"	1.0888
	5.0	100.8	101.1	100.7	69.1	31.6	27	0.116	"	"	1.0917
	5.0	100.7	101.0	100.7	83.2	17.5	23	0.152	"	"	1.0873
A.63	5.0	97.7	98.1	97.0	31.9	65.7	30	0.083	0.120	0.178	1.0030
	5.0	97.9	98.4	97.5	42.5	55.4	24	0.072	"	"	1.0157
	5.0	98.2	98.7	97.8	58.9	39.3	19	0.072	"	"	1.0324
	5.0	98.7	99.2	98.6	79.2	19.7	17	0.104	"	"	1.0559
A.64	5.0	96.2	96.9	95.2	30.9	65.2	24	0.067	0.190	0.224	1.0059
	5.0	96.2	97.0	95.2	37.2	58.9	20	0.060	"	"	1.0137
	5.0	96.5	97.2	95.4	63.5	32.8	18	0.075	"	"	1.0255
	5.0	96.8	97.5	95.5	78.8	17.8	15	0.096	"	"	1.0422
A.65	5.0	94.6	95.6	95.2	29.4	65.7	18	0.052	0.254	0.334	1.0088
	5.0	94.6	95.5	95.2	35.9	59.2	16	0.048	"	"	1.0108
	5.0	94.7	95.8	95.1	62.1	33.1	14	0.061	"	"	1.0177
	5.0	94.9	95.9	95.0	79.0	16.3	11	0.078	"	"	1.0265

Table 5.03

Steam-Argon Mixture. Full cooling water flowrate.

Test No	x (cm)	t_p (C)	t_h (C)	t_f (C)	t_w (C)	T_p-T_w (K)	Q (kW/m^2)	Q/Qnu	W_p	W_m	Ptot (Bar)
R.01	2.9	100.1	100.0	100.0	55.5	44.6	232	0.784	0.005	0.005	1.0175
	4.9	100.0	99.9	99.9	"	44.5	"	"	0.004	"	1.0136
	6.9	99.9	99.9	99.9	"	44.4	"	"	0.005	"	1.0126
R.02	6.9	100.4	100.4	100.3	51.8	48.6	202	0.670	0.014	0.010	1.0337
	4.9	100.1	100.0	100.0	"	48.3	"	"	0.012	"	1.0209
	2.9	99.8	99.8	99.7	"	48.0	"	"	0.005	"	1.0097
R.03	6.9	101.5	101.[illegible]	101.4	43.[illegible]	57.6	140	0.410	0.011	0.015	1.0734
	4.9	101.2	101.1	101.1	"	57.3	"	"	0.009	"	1.0591
	2.9	100.8	100.9	100.8	"	[illegible]	"	"	0.015	"	1.0459
R.04	6.9	100.5	100.6	100.5	46.4	54.1	172	0.523	0.016	0.010	1.0401
	4.9	100.0	100.1	100.0	"	53.6	"	"	0.009	"	1.0186
	2.9	99.9	99.7	99.8	"	53.4	"	"	0.005	"	1.0038
R.05	6.9	100.9	100.9	100.9	45.9	55.0	157	0.475	0.015	0.015	1.0521
	4.9	100.7	100.7	100.7	"	54.[illegible]	"	"	0.009	"	1.0427
	2.9	100.5	100.4	100.5	"	54.4	"	"	0.008	"	1.0349
R.06	6.9	99.4	99.8	98.9	29.4	70.0	63	0.169	0.133	0.165	1.0612
	4.9	99.7	100.0	99.1	"	70.3	"	"	0.085	"	1.0449
	2.9	99.7	100.0	99.3	"	70.3	"	"	0.063	"	1.0330
R.07	2.9	100.8	100.9	100.5	41.2	59.6	119	0.345	0.021	0.020	1.0534
	4.9	100.4	100.5	100.3	"	59.2	"	"	0.022	"	1.0390
	6.9	100.1	100.1	99.9	"	58.9	"	"	0.024	"	1.025[illegible]
R.08	6.9	[illegible]	99.9	99.5	35.8	64.0	77	0.215	0.045	0.053	1.0284
	4.9	99.8	99.7	99.2	"	64.0	"	"	0.020	"	1.0135
	2.9	[illegible]	99.8	99.3	"	64.0	"	"	0.020	"	1.0149
R.09	2.9	100.3	100.5	99.7	30.7	69.6	75	0.201	0.058	0.158	1.0525
	4.9	[illegible]	100.1	99.0	"	69.1	"	"	0.077	"	1.0430
	6.9	99.3	99.5	[illegible]	"	[illegible]	"	"	0.097	"	1.0295
R.10	6.9	98.3	98.6	97.5	28.3	70.0	62	0.167	0.113	0.177	1.0189
	4.9	99.0	99.3	98.3	"	70.7	"	"	0.088	"	1.0200
	2.9	99.5	99.7	97.3	"	71.[illegible]	"	"	0.059	"	1.0232

contd......

Table 5.03

Steam-Argon Mixture. Full cooling water flowrate.

Test No	x / cm	t_p / C	t_m / C	t_f / C	t_w / C	$T_p - T_w$ / K	Q / kW/m^2	Q/Qnu	W_p	W_m	Ptot / Bar
R.11	2.9	100.4	100.4	100.0	27.8	72.3	65	0.170	0.076	0.199	1.0528
	4.9	99.7	100.0	99.3	"	71.9	"	"	0.107	"	1.0560
	6.9	98.9	99.3	98.1	"	71.1	"	"	0.160	"	1.0577
R.12	6.9	97.8	98.6	97.5	25.6	72.2	58	0.151	0.239	0.251	1.0704
	4.9	99.3	99.8	98.9	"	72.7	"	"	0.148	"	1.0655
	2.9	100.1	100.5	99.9	"	73.5	"	"	0.093	"	1.0635
R.13	2.9	96.7	97.6	96.4	20.1	76.6	33	0.087	0.274	0.383	1.0542
	4.9	94.7	95.9	94.4	"	74.6	"	"	0.364	"	1.0542
	6.9	92.2	93.6	91.5	"	72.1	"	"	0.459	"	1.0542
R.14	2.9	100.4	100.5	100.4	44.9	55.5	181	0.531	0.014	0.041	1.0358
	4.9	100.6	100.8	100.6	"	55.7	"	"	0.027	"	1.0491
	6.9	100.4	100.5	100.4	"	55.5	"	"	0.022	"	1.0373
R.15	2.9	101.1	101.1	100.6	35.4	75.7	91	0.294	0.026	0.075	1.0672
	4.9	101.1	101.1	100.1	"	75.7	"	"	0.029	"	1.0692
	6.9	101.1	101.1	100.6	"	75.7	"	"	0.030	"	1.0692
R.16	6.9	100.9	101.1	100.6	32.5	68.4	91	0.245	0.073	0.096	1.0821
	4.9	100.8	101.0	100.3	"	68.3	"	"	0.056	"	1.0589
	2.9	100.5	100.6	99.8	"	68.0	"	"	0.041	"	1.0497
R.17	2.9	100.7	100.8	100.5	39.0	61.7	133	0.381	0.027	0.045	1.0498
	4.9	100.3	100.3	100.1	"	61.3	"	"	0.030	"	1.0296
	6.9	100.2	100.2	100.0	"	61.2	"	"	0.030	"	1.0336
R.18	6.9	100.3	100.4	99.9	32.6	67.7	94	0.254	0.060	0.090	1.0527
	4.9	100.7	100.7	100.1	"	68.1	"	"	0.041	"	1.0584
	2.9	100.9	100.9	100.2	"	68.3	"	"	0.032	"	1.0613
R.19	2.9	100.8	100.9	100.3	34.4	66.4	111	0.305	0.029	0.079	1.0580
	4.9	100.7	100.7	100.1	"	66.3	"	"	0.035	"	1.0551
	6.9	100.4	100.5	100.0	"	66.0	"	"	0.048	"	1.0534
R.20	6.9	100.1	100.4	99.7	27.9	72.2	76	0.200	0.123	0.181	1.0833
	4.9	100.5	100.8	99.8	"	72.6	"	"	0.094	"	1.0784
	2.9	100.8	101.0	100.4	"	72.9	"	"	0.064	"	1.0738

contd......

Table 5.03

Steam-Argon Mixture. Full cooling water flowrate.

Test No	y / cm	t_p / C	t_h / C	t_f / C	t_w / C	$\Gamma_p - \Gamma_w$ / k	Q / kW/m^2	Q/Qnu	W_p	W_m	Ptot / Bar
R.21	2.9	100.7	100.8	100.1	28.4	72.3	77	0.204	0.059	0.174	1.0661
	4.9	100.1	100.4	99.2	"	71.7	"	"	0.087	"	1.0595
	6.9	99.5	99.8	98.6	"	71.1	"	"	0.111	"	1.0529
R.22	6.9	99.5	99.6	99.0	30.0	69.5	93	0.250	0.082	0.132	1.0350
	4.9	99.6	99.7	98.9	"	69.6	"	"	0.063	"	1.0289
	2.9	99.6	99.8	99.1	"	69.6	"	"	0.051	"	1.0235
R.23	2.9	99.8	99.8	99.2	31.3	68.5	89	0.238	0.038	0.115	1.0225
	4.9	99.8	100.0	99.2	"	68.5	"	"	0.059	"	1.0362
	6.9	100.0	100.2	99.6	"	68.7	"	"	0.075	"	1.0509
R.24	6.9	100.4	100.6	99.9	33.6	66.8	116	0.317	0.064	0.083	1.0600
	4.9	100.9	100.9	100.2	"	67.3	"	"	0.043	"	1.0661
	2.9	101.1	101.1	100.5	"	67.5	"	"	0.032	"	1.0700
R.25	2.9	97.6	98.2	97.3	21.3	76.3	42	0.112	0.202	0.361	1.0348
	4.9	96.3	97.2	95.8	"	75.0	"	"	0.281	"	1.0441
	6.9	94.4	95.6	94.3	"	73.1	"	"	0.374	"	1.0512
R.26	6.9	96.1	97.0	95.9	22.7	73.4	50	0.131	0.250	0.317	1.0465
	4.9	97.5	98.2	97.2	"	74.8	"	"	0.183	"	1.0465
	2.9	98.8	99.2	98.5	"	76.1	"	"	0.123	"	1.0470
R.27	2.9	99.2	99.4	98.8	23.5	75.7	53	0.140	0.166	0.284	1.0416
	4.9	97.9	98.5	97.5	"	74.4	"	"	0.193	"	1.0401
	6.9	96.3	97.2	96.1	"	72.8	"	"	0.272	"	1.0396
R.28	6.9	98.2	98.6	97.6	25.0	73.2	58	0.151	0.170	0.227	1.0372
	4.9	99.2	99.4	98.4	"	74.2	"	"	0.124	"	1.0475
	2.9	99.9	100.1	99.3	"	74.9	"	"	0.092	"	1.0541
R.29	2.9	99.8	100.1	99.4	26.4	73.4	63	0.168	0.085	0.215	1.0504
	4.9	99.7	99.9	98.9	"	73.3	"	"	0.106	"	1.0539
	6.9	99.2	99.5	98.6	"	72.8	"	"	0.136	"	1.0558
R.30	6.9	99.4	99.7	98.9	26.4	73.0	65	0.171	0.123	0.191	1.0558
	4.9	99.8	100.0	98.9	"	73.4	"	"	0.097	"	1.0558
	2.9	100.1	100.4	99.6	"	73.7	"	"	0.080	"	1.0573

contd......

Table 5.03

Steam-Argon Mixture. Full cooling water flowrate.

Test No	x/cm	t_p/C	t_h/C	t_f/C	t_w/C	T_p-T_w/K	Q/kW/m^2	Q/Qnu	W_p	W_m	Ptot/Bar
R.31	2.9	100.3	100.5	99.4	29.1	71.2	87	0.219	0.057	0.164	1.0546
	4.9	100.2	100.3	99.3	"	71.1	"	"	0.060	"	1.0472
	6.9	99.5	99.8	99.1	"	70.4	"	"	0.079	"	1.0350
R.32	6.9	71.9	73.9	84.5					0.818	0.675	1.0240
	4.9	76.5	78.5	84.3					0.772	"	1.0382
	2.9	82.3	84.2	84.2					0.697	"	1.0619
R.33	2.9	85.8	87.7	86.5					0.633	0.655	1.0648
	4.9	82.1	84.0	86.3					0.703	"	1.0662
	6.9	78.4	80.2	87.2					0.756	"	1.0694
R.34	6.9	83.3	85.2	93.0					0.668	0.584	1.0329
	4.9	87.4	89.3	89.5					0.585	"	1.0410
	2.9	90.9	92.3	90.6					0.500	"	1.0551
R.35	2.9	94.1	95.3	93.8					0.386	0.455	1.0508
	4.9	91.6	93.2	91.4					0.482	"	1.0608
	6.9	88.9	90.7	92.1					0.568	"	1.0779
R.36	6.9	92.0	93.7	93.4					0.472	0.387	1.0652
	4.9	94.6	95.8	94.3					0.380	"	1.0639
	2.9	96.8	97.8	96.7					0.289	"	1.0688
R.37	2.9	97.6	98.5	97.5	21.0	76.6	45	0.177	0.219	0.333	1.0488
	4.9	96.0	97.0	95.8	"	75.0	"	"	0.307	"	1.0356
	6.9	94.1	95.4	94.1	"	73.1	"	"	0.395	"	1.0400
R.38	6.9	98.4	96.4	98.0	24.6	73.8	46	0.120	0.156	0.270	1.0352
	4.9	98.7	96.9	97.9	"	74.1	"	"	0.136	"	1.0379
	2.9	99.5	99.7	98.8	"	74.9	"	"	0.098	"	1.0428
R.39*	2.9	98.7	98.7	98.7					0.089	0.197	1.0098
	4.9	98.6	98.6	98.6					0.101	"	1.0118
	6.9	98.5	98.5	98.5					0.108	"	1.0133
R.40*	2.9	95.7	95.9	95.7					0.297	0.365	1.0337
	4.9	95.3	95.5	95.2					0.317	"	1.0307
	6.9	94.6	94.9	94.5					0.344	"	1.0307

*Zero cooling water flowrate.

contd......

Table 5.03
Steam-Argon Mixture. Full cooling water flowrate.

Test No	x / cm	t_p / C	t_h / C	t_f / C	t_w / C	$t_p - t_w$ / K	q / kW/m^2	α/α_{Nu}	W_p	W_m	Ptot / Bar
R.41*	6.0	87.3	87.[illegible]	89.6					0.578	0.530	1.0209
	4.0	85.4	86.4	89.8					0.555	"	1.0155
	2.0	[illegible]	83.2	[illegible]					0.530	"	1.0141
R.42x	6.0	80.1	80.7	83.4					0.723	0.700	1.0375
	4.0	79.0	79.6	83.5					0.739	"	1.0350
	2.0	[illegible]	78.6	82.7					0.755	"	1.0336
R.43x	2.0	71.9	66.0	71.9					0.786	0.790	1.0367
	4.0	7[illegible].1	67.0	73.1					0.793	"	1.0377
	6.0	74.[illegible]	6[illegible].9	74.2					0.79[illegible]	"	1.0392
R.44*	2.0	59.0	58.4	58.7					0.909	0.910	1.0477
	4.0	55.4	58.2	58.2					0.912	"	1.0477
	6.0	57.7	57.[illegible]	56.6					0.915	"	1.0497
R.45	6.0	51.5	53.4	54.7					0.938	0.910	1.0443
	4.0	51.7	53.1	54.7					0.939	"	1.0450
	2.0	52.7	53.2	[illegible]					0.935	"	1.04[illegible]3
R.46	2.0	100.3	100.2	9[illegible].7	30.7	69.6	70	0.184	0.038	0.148	1.039[illegible]
	4.0	99.7	9[illegible].8	[illegible]	"	69.0	"	"	0.0[illegible]6	"	1.0315
	6.0	9[illegible].2	9[illegible].3	[illegible]	"	6[illegible].5	"	"	0.091	"	1.0303
R.47	6.0	9[illegible].8	99.9	[illegible].8	42.0	56.9	136	0.513	0.014	0.026	1.0135
	4.0	100.2	100.2	100.1	"	57.3	"	"	0.014	"	1.0245
	2.0	100.3	100.4	100.[illegible]	"	57.4	"	"	0.014	"	1.0297
R.48	2.0	9[illegible].9	100.0	99.9	48.8	51.1	127	0.414	0.021	0.040	1.0194
R.49	6.0	100.2	100.2	100.1	50.3	49.9	187	0.623	0.015	0.010	1.0247
	4.0	100.1	100.2	100.1	"	49.8	"	"	0.015	"	1.0238
	2.0	100.5	10[illegible].5	10[illegible].5	"	50.2	"	"	0.012	"	1.0353
R.50	2.0	100.5	10[illegible].5	10[illegible].2	38.8	61.7	123	0.349	0.020	0.054	1.0409
	4.0	100.4	100.4	99.9	"	61.6	"	"	0.023	"	1.0350
	6.0	100.1	100.0	9[illegible]	"	61.3	"	"	0.026	"	1.0273
R.51	6.0	9[illegible].4	[illegible].5	9[illegible].1	3[illegible].2	6[illegible]	77	0.[illegible]49	0.053	0.026	1.0169
	4.0	99.2	9[illegible].5	98.6	"	64.0	"	"	0.048	"	1.0259
	2.0	98.9	98.[illegible]	9[illegible]	"	65.7	"	"	0.030	"	0.9870

* Zero cooling water flowrate.

contd......

Table 5.03

Steam-Argon Mixture. Full cooling water flowrate.

Test No	x / cm	t_p / C	t_h / C	t_f / C	t_w / C	$T_p - T_w$ / K	Q / kW/m^2	Q/Q_{ru}	W_p	$-W_m$	Ptot / Bar
R.52	2.9	98.9	98.9	99.2	26.1	72.8	64	0.169	0.079	0.222	1.0117
	4.9	98.8	98.8	99.1	"	72.7	"	"	0.110	"	1.0229
	6.0	98.4	98.4	98.8	"	72.3	"	"	0.138	"	1.0242
R.53	6.0	98.5	99.0	98.9	57.9	40.6	174	0.591	0.019	0.015	0.9836
	4.9	98.8	98.9	98.8	"	40.9	"	"	0.017	"	0.9772
	2.9	98.9	98.9	98.9	"	41.0	"	"	0.016	"	0.9801
R.54	2.9	99.8	99.9	99.8	54.5	45.3	150	0.455	0.016	0.031	1.0147
R.55	2.9	100.6	100.6	100.3	37.2	63.4	114	0.318	0.023	0.059	1.0441
	4.9	100.6	100.6	100.4	"	63.4	"	"	0.025	"	1.0480
	6.0	100.8	100.8	100.5	"	63.6	"	"	0.026	"	1.0539
R.56	6.0	99.1	99.2	98.8	28.4	70.7	69	0.184	0.076	0.126	1.0166
	4.9	99.4	99.4	98.9	"	71.0	"	"	0.057	"	1.0195
	2.9	99.7	99.7	99.	"	71.3	"	"	0.039	"	1.0207
R.57	2.9	99.2	99.3	98.4	26.4	72.8	65	0.170	0.069	0.164	1.0157
	4.9	99.4	99.6	98.9	"	73.0	"	"	0.084	"	1.0323
	6.0	99.3	99.6	99.1	"	72.9	"	"	0.097	"	1.0372
R.58	6.0	97.9	98.3	97.3	24.5	73.4	55	0.145	0.158	0.207	1.0200
	4.9	98.9	99.2	98.1	"	74.4	"	"	0.120	"	1.0335
	2.9	99.6	99.9	99.0	"	75.1	"	"	0.087	"	1.0414
R.59	2.9	98.6	98.8	98.2	23.0	75.6	48	0.126	0.112	0.253	1.0167
	4.9	98.0	98.5	97.4	"	75.0	"	"	0.160	"	1.0245
	6.0	97.5	98.2	96.9	"	74.5	"	"	0.196	"	1.0294
R.60	5.9	96.1	97.0	95.9	21.3	74.8	39	0.101	0.271	0.299	1.0289
	4.9	97.3	98.0	96.9	"	76.0	"	"	0.218	"	1.0343
	2.9	98.6	99.1	98.3	"	77.3	"	"	0.145	"	1.0367
R.61	2.9	97.4	98.2	97.3	19.6	79.8	32	0.085	0.220	0.354	1.0396
	4.9	96.2	97.3	95.9	"	78.6	"	"	0.296	"	1.0526
	5.9	95.0	96.3	94.9	"	77.4	"	"	0.352	"	1.0541
R.62	5.9	91.8	93.5	91.8					0.459	0.415	1.0403
	4.9	93.9	95.4	93.8					0.392	"	1.0501
	2.9	96.7	97.8	96.5					0.279	"	1.0599

Table 5.04

Steam-Argon Mixture. Variable $(T_\infty - T_w)$/K.

Test No	x/cm	t_p/C	t_h/C	t_f/C	t_w/C	$T_\infty - T_w$/K	Q/kW/m²	Q/Qnu	W_∞	W_m	Ptot/Bar
R.63	5.0	100.7	100.7	100.7	49.5	51.2	179	0.564	0.010	0.005	1.0442
	5.0	100.8	100.7	100.8	64.8	35.7	147	0.577	"	"	1.0466
	5.0	101.5	101.5	101.5	57.2	44.3	151	0.518	"	"	1.0759
	5.0	100.7	100.7	100.7	46.0	54.7	157	0.475	"	"	1.0432
R.64	5.0	98.2	98.3	98.2	59.6	38.6	90	0.341	0.030	0.072	0.9610
	5.0	98.4	98.5	98.5	70.8	27.6	79	0.374	"	"	0.9678
	5.0	98.8	99.0	98.9	77.9	20.9	65	0.371	"	"	0.9845
	5.0	99.3	99.4	99.5	84.6	14.7	52	0.383	"	"	1.0022
	5.0	99.6	99.8	99.7	93.9	5.7	31	0.460	"	"	1.0169
	5.0	99.7	99.8	99.8	54.5	45.2	105	0.315	"	"	1.0137
R.65	5.0	99.1	99.3	99.2	51.1	48.0	60	0.199	0.061	0.124	1.0086
	5.0	98.9	99.1	98.9	68.2	30.7	49	0.214	"	"	1.0027
	5.0	99.0	99.2	99.1	79.7	19.3	41	0.248	"	"	1.0067
	5.0	99.3	99.5	99.3	83.9	15.4	36	0.258	"	"	1.0204
	5.0	99.3	99.5	99.3	93.5	5.8	27	0.390	"	"	1.0184
R.66	5.0	98.1	98.4	98.1	47.7	50.4	47	0.152	0.101	0.180	0.9906
	5.0	97.6	97.9	97.8	58.1	39.5	39	0.147	"	"	0.9750
	5.0	97.6	98.0	97.8	70.6	27.0	30	0.146	"	"	0.9808
	5.0	98.0	98.3	98.1	78.4	19.6	24	0.146	"	"	0.9926
	5.0	98.2	98.5	98.4	87.5	10.7	19	0.173	"	"	1.0034
R.67	5.0	96.6	97.2	96.6	45.1	51.5	30	0.095	0.153	0.230	0.9727
	5.0	97.2	97.8	97.4	63.6	33.6	26	0.106	"	"	0.9923
	5.0	97.7	98.3	97.9	78.5	19.2	21	0.129	"	"	1.0080
	5.0	97.8	98.5	97.9	88.5	9.4	14	0.139	"	"	1.0198

Table 3.05

Steam-Neon Mixture. Full cooling water rate.

Test No	x/cm	t_p/C	t_h/C	t_f/C	t_w/C	T_p-T_w/K	Q/kW/m^2	Q/Qnu	W_p	W_m	Ptot
N.01	5.9	100.0	100.1	100.0	41.4	58.6	105	0.130	0.012	0.008	1.0230
	4.9	100.3	100.3	100.3	"	58.9	"	"	0.009	"	1.0314
	2.9	100.4	100.5	100.4	"	59.0	"	"	0.010	"	1.0368
N.02	5.9	99.9	100.2	100.1	39.4	60.5	80	0.230	0.019	0.013	1.0265
	4.9	99.9	100.2	100.1	"	60.5	"	"	0.017	"	1.0255
	2.9	100.0	100.2	100.1	"	60.6	"	"	0.016	"	1.0267
N.03	2.9	99.5	99.9	99.9	34.4	65.1	56	0.154	0.024	0.021	1.0159
	4.9	99.6	100.0	99.9	"	65.2	"	"	0.024	"	1.0210
	6.0	99.7	100.0	100.0	"	65.3	"	"	0.024	"	1.0230
N.04	6.0	99.6	99.9	99.8	33.3	66.3	60	0.164	0.019	0.025	1.0166
	4.9	99.8	100.1	100.0	"	66.5	"	"	0.022	"	1.0247
	2.9	99.9	100.2	100.1	"	66.6	"	"	0.023	"	1.0293
N.05	2.9	99.4	99.7	99.6	32.5	66.9	54	0.147	0.022	0.033	1.0107
	4.9	99.7	100.0	99.8	"	67.2	"	"	0.023	"	1.0214
	6.0	99.8	100.1	100.0	"	67.3	"	"	0.024	"	1.0273
N.06	6.0	99.7	100.0	99.9	32.5	67.2	52	0.140	0.024	0.039	1.0241
	4.9	100.2	100.5	100.4	"	67.7	"	"	0.025	"	1.0440
	2.9	100.3	100.7	100.5	"	67.8	"	"	0.027	"	1.0506
N.07	2.9	99.5	99.7	99.4	30.5	69.0	56	0.151	0.025	0.047	1.0155
	4.9	99.6	99.8	99.6	"	69.1	"	"	0.025	"	1.0200
	6.0	99.7	99.8	99.7	"	69.2	"	"	0.025	"	1.0200
N.08	6.0	99.8	99.9	99.8	44.8	55.0	137	0.415	0.016	0.004	1.0205
	4.9	99.8	99.9	99.9	"	55.0	"	"	0.013	"	1.0191
	2.9	99.9	100.0	100.0	"	55.1	"	"	0.011	"	1.0215
N.09	6.0	99.7	99.9	99.9	44.5	55.2	110	0.330	0.016	0.011	1.0151
	4.9	100.2	100.2	100.2	"	55.7	"	"	0.013	"	1.0203
	2.9	100.6	100.7	100.5	"	56.1	"	"	0.012	"	1.0439
N.10	2.9	99.8	99.9	99.9	38.9	60.9	95	0.271	0.014	0.018	1.0181
	4.9	100.1	100.3	100.3	"	61.2	"	"	0.019	"	1.0330
	6.0	100.1	100.5	100.3	"	61.2	"	"	0.019	"	1.0367

contd.......

Table 5.05

Steam-Neon Mixture. Full cooling water rate

Test No	x/cm	t_p/C	t_h/C	t_f/C	t_w/C	$T_p - T_w$/K	Q/kW/m^2	Q/Qnu	W_p	W_m	Ptot/Bar
N.11	6.0	100.1	100.4	100.3	35.2	64.9	82	0.224	0.010	0.024	1.0358
	4.9	100.2	100.4	100.3	"	65.0	"	"	0.010	"	1.0363
	2.9	100.1	100.4	100.3	"	64.9	"	"	0.010	"	1.0360
N.12	2.9	99.7	100.0	99.8	33.3	66.4	80	0.218	0.024	0.032	1.0228
	4.9	99.9	100.2	100.1	"	66.6	"	"	0.024	"	1.0302
	6.0	100.1	100.4	100.3	"	66.8	"	"	0.022	"	1.0341
N.13	6.0	99.8	100.0	99.9	32.3	67.5	67	0.180	0.021	0.038	1.0231
	4.9	100.0	100.2	100.1	"	67.7	"	"	0.019	"	1.0277
	2.9	100.0	100.3	100.1	"	67.7	"	"	0.022	"	1.0351
N.14	2.9	99.7	99.9	99.4	31.0	68.7	63	0.170	0.022	0.047	1.0205
	4.9	99.9	100.1	99.9	"	68.9	"	"	0.023	"	1.0293
	6.0	100.0	100.2	100.0	"	69.0	"	"	0.023	"	1.0342
N.15	6.0	100.0	100.3	100.1	30.3	69.7	68	0.180	0.025	0.045	1.0377
	4.9	100.2	100.6	100.3	"	69.9	"	"	0.026	"	1.0461
	2.9	100.3	100.6	100.3	"	70.0	"	"	0.025	"	1.0483
N.16	2.9	99.4	99.5	99.4	28.7	70.7	58	0.153	0.026	0.055	1.0145
	4.9	99.9	99.9	99.9	"	71.2	"	"	0.024	"	1.0300
	6.0	99.9	99.9	99.9	"	71.2	"	"	0.024	"	1.0292
N.17	6.0	99.6	99.6	99.5	27.5	72.1	53	0.140	0.033	0.072	1.0291
	4.9	100.2	100.2	99.9	"	72.7	"	"	0.033	"	1.0499
	2.9	100.3	100.5	99.9	"	72.8	"	"	0.033	"	1.0551
N.18	2.9	99.4	99.3	98.2	25.7	73.7	44	0.116	0.036	0.086	1.0243
	4.9	99.9	99.8	98.5	"	74.2	"	"	0.034	"	1.0405
	6.0	100.1	99.9	98.6	"	74.4	"	"	0.034	"	1.0469
N.19	6.0	99.2	98.9	97.2	24.3	74.9	38	0.100	0.043	0.100	1.0249
	4.9	99.4	99.3	97.6	"	75.1	"	"	0.046	"	1.0352
	2.9	99.6	99.6	97.8	"	75.3	"	"	0.048	"	1.0426
N.20	2.9	98.9	98.8	97.0	23.1	75.8	33	0.087	0.053	0.115	1.0215
	4.9	99.2	99.0	97.3	"	76.1	"	"	0.052	"	1.0326
	6.0	99.4	99.3	97.6	"	76.3	"	"	0.052	"	1.0413

contd.......

Table 5.05

Steam-Neon Mixture. Full cooling water rate.

Test No	x / cm	t_p / C	t_h / C	t_f / C	t_w / C	$T_p - t_w$ / K	Q / kW/m^2	Q/Qnu	W_p	W_m	Ptot / Bar
N.21	6.0	98.3	98.3	96.9	21.7	76.6	31	0.081	0.095	0.140	1.0491
	4.9	98.6	98.7	97.4	"	76.9	"	"	0.096	"	1.0555
	2.9	98.9	98.9	97.2	"	77.2	"	"	0.087	"	1.0563
N.22	2.9	96.0	96.7	95.4					0.170	0.206	1.0387
	4.9	96.3	96.1	95.6					0.173	"	1.0529
	6.0	96.0	95.8	95.2					0.180	"	1.0500
N.23	6.0	93.0	92.4	92.3					0.275	0.272	1.0489
	4.9	93.9	94.4	94.0					0.268	"	1.0753
	2.9	93.7	94.6	94.5					0.257	"	1.0547
N.24	2.9	89.8	90.9	91.2					0.363	0.340	1.0473
	4.9	90.5	91.3	91.1					0.362	"	1.0733
	6.0	90.1	99.6	90.6					0.369	"	1.0719
N.25	6.0	83.4	84.2	86.0					0.501	0.431	1.0300
	4.9	83.7	84.9	87.1					0.499	"	1.0430
	2.9	84.6	86.7	88.4					0.485	"	1.0453
N.26	2.9	99.7	99.8	99.5	28.8	70.9	63	0.167	0.026	0.052	1.0256
	4.9	100.2	100.2	100.1	"	71.4	"	"	0.036	"	1.0500
	6.0	100.2	100.2	100.1	"	71.4	"	"	0.036	"	1.0500
N.27	6.0	99.5	99.3	98.6	26.8	72.7	59	0.155	0.027	0.065	1.0165
	4.9	99.8	99.7	99.1	"	73.0	"	"	0.031	"	1.0300
	2.9	99.8	99.8	99.2	"	73.0	"	"	0.033	"	1.0355
N.28	2.9	99.3	99.1	98.2	25.3	74.0	54	0.140	0.039	0.078	1.0155
	4.9	99.5	99.4	98.2	"	74.2	"	"	0.037	"	1.0263
	6.0	99.6	99.4	98.3	"	74.3	"	"	0.036	"	1.0300
N.29	6.0	98.9	98.6	97.3	24.2	74.7	49	0.129	0.047	0.091	1.0100
	4.9	99.2	99.1	97.6	"	75.0	"	"	0.048	"	1.0250
	2.9	99.5	99.4	98.1	"	75.3	"	"	0.048	"	1.0350
N.30	2.9	98.5	98.6	97.2	23.0	75.5	44	0.115	0.063	0.104	1.0150
	4.9	99.0	98.9	97.4	"	76.0	"	"	0.059	"	1.0300
	6.0	98.4	98.5	97.1	"	75.4	"	"	0.063	"	1.0150

contd.......

Table 5.05

Steam-Neon Mixture. Full cooling water flowrate.

Test No	x/cm	t_p/C	t_h/C	t_f/C	t_w/C	T_p-T_w/K	Q/kW/m^2	Q/Qnu	W_p	W_m	Ptot/Bar
N.31	6.0	98.3	98.1	96.9	22.3	76.0	45	0.117	0.075	0.118	1.0200
	4.9	98.5	98.4	97.1	"	76.2	"	"	0.077	"	1.0255
	2.9	97.9	98.0	98.3	"	75.6	"	"	0.074	"	1.0000
N.32	2.9	97.9	97.9	96.4	21.1	76.8	38	0.098	0.085	0.132	1.0100
	4.9	98.0	98.0	96.6	"	76.9	"	"	0.086	"	1.0200
	6.0	98.1	98.0	96.6	"	77.0	"	"	0.090	"	1.0300
N.33	6.0	96.4	96.4	95.3	20.0	76.4	36	0.093	0.126	0.149	1.0000
	4.9	96.8	96.9	95.7	"	76.8	"	"	0.125	"	1.0105
	2.9	97.1	97.3	96.1	"	77.1	"	"	0.118	"	1.0208
N.34	5.0	98.7	98.5	96.9	23.3	75.4	57	0.139	0.058	0.073	1.0155
N.35	5.0	99.5	99.4	97.8	25.0	74.5	66	0.172	0.044	0.059	1.0300
N.36	5.0	100.1	100.1	99.2	28.3	71.7	75	0.199	0.027	0.049	1.0336
N.37	5.0	99.8	100.0	99.8	33.1	66.7	110	0.300	0.020	0.035	1.0176
N.38	5.0	99.8	99.9	99.8	37.4	62.4	129	0.364	0.013	0.006	1.0189
N.39	5.0	100.9	100.9	100.9	41.3	69.6	130	0.377	0.006	0.007	1.0500
N.40	5.0	100.8	100.9	100.8	40.8	60.0	135	0.388	0.005	0.007	1.0467
N.41	5.0	100.3	100.5	100.3	37.8	62.5	104	0.294	0.015	0.014	1.0300
N.42	5.0	99.9	100.2	100.1	34.0	65.9	78	0.230	0.019	0.021	1.0267
N.43	5.0	100.0	100.2	100.1	30.7	69.3	83	0.223	0.022	0.028	1.0269
N.44	5.0	100.4	100.5	100.4	29.8	70.6	64	0.170	0.019	0.035	1.0408
N.45	5.0	100.0	100.0	100.0	29.2	70.8	62	0.165	0.018	0.040	1.0255
N.46	5.0	99.9	100.0	99.9	28.9	71.0	63	0.168	0.021	0.021	1.0200
N.47	5.0	99.9	100.0	100.0	28.6	71.3	70	0.185	0.023	0.047	1.0300

Table 5.06

Steam-Neon Mixture. Variable $(T_\infty - T_w)/K$

Test No	x / cm	t_p / C	t_h / C	t_f / C	t_w / C	$T_\infty - T_w$ / K	Q / kW/m^2	Q/Qnu	W_∞	W_m	Ptot / Bar
N.48	5.0	99.2	99.3	99.2	72.1	27.1	93	0.444	0.012	0.007	0.9942
	5.0	99.5	99.6	99.5	81.8	17.7	69	0.443	"	"	0.9942
	5.0	99.9	100.0	100.0	86.0	13.9	57	0.433	"	"	1.0197
	5.0	100.4	100.5	100.5	92.2	8.2	50	0.556	"	"	1.0422
	5.0	100.5	100.7	100.5	96.3	4.2	36	0.670	"	"	1.0462
N.49	5.0	99.3	99.4	99.3	65.4	33.9	70	0.288	0.018	0.017	1.0020
	5.0	99.1	99.2	99.2	73.3	25.8	51	0.252	"	"	0.9971
	5.0	99.1	99.2	99.2	80.0	19.1	42	0.258	"	"	0.9961
	5.0	99.2	99.4	99.3	87.3	11.9	34	0.289	"	"	1.0010
	5.0	99.6	99.7	99.9	93.8	5.8	25	0.368	"	"	1.0137
N.50	5.0	98.7	98.8	98.8	55.6	43.1	63	0.221	0.022	0.037	0.9890
	5.0	98.6	98.8	98.8	67.4	31.2	48	0.210	"	"	0.9812
	5.0	99.2	99.3	99.3	75.1	24.1	37	0.194	"	"	1.0008
	5.0	99.5	99.6	99.6	83.7	15.8	27	0.190	"	"	1.0165
	5.0	99.9	100.0	99.6	92.4	7.5	21	0.246	"	"	1.0322
N.51	5.0	98.4	100.6	98.5	51.8	47.4	58	0.195	0.044	0.064	0.9848
	5.0	99.4	99.4	99.3	64.8	34.6	43	0.176	"	"	1.0172
	5.0	99.3	99.3	99.1	77.2	22.1	32	0.176	"	"	1.0260
	5.0	99.3	99.4	99.2	89.2	10.1	21	0.206	"	"	1.0309
N.52	5.0	98.0	97.9	97.9	47.4	50.6	47	0.152	0.088	0.102	0.9946
	5.0	97.6	97.8	97.5	56.6	41.0	40	0.144	"	"	0.9956
	5.0	97.5	97.8	97.5	74.1	23.4	23	0.121	"	"	1.0064
	5.0	97.6	97.8	97.6	86.3	11.3	19	0.166	"	"	1.0172
N.53	5.0	96.8	96.9	96.8	44.2	52.6	34	0.107	0.130	0.135	0.9995
	5.0	96.3	96.6	96.3	67.0	29.3	22	0.102	"	"	0.9995
	5.0	96.4	96.5	96.4	74.0	22.4	17	0.094	"	"	1.0113
	5.0	96.5	96.8	96.5	88.6	7.9	12	0.136	"	"	1.0270

Table 5.07
Steam-Helium Mixture, Full cooling water flowrate

Test No	x (cm)	t_p (C)	t_h (C)	t_f (C)	t_w (C)	T_p-T_w (K)	Q (kW/m^2)	Q/Qnu	W_p	W_m	Ptot (Bar)
H.01	2.9	86.8	89.3	95.3	21.6	65.2	32	0.092	0.135	0.121	1.0550
	4.9	88.4	91.5	95.9	"	67.2	"	"	0.117	"	1.0544
	6.9	90.5	92.8	96.5	"	68.9	"	"	0.093	"	1.0514
H.02	6.9	92.0	93.7	96.1	22.7	69.3	38	0.107	0.076	0.103	1.0379
	4.9	90.1	93.2	95.5	"	67.4	"	"	0.095	"	1.0423
	2.9	89.1	92.5	95.4	"	66.4	"	"	0.106	"	1.0438
H.03	2.9	91.8	93.7	95.6	24.1	67.7	40	0.112	0.076	0.073	1.0330
	4.9	92.7	94.8	96.0	"	68.6	"	"	0.070	"	1.0369
	6.9	94.1	95.5	96.3	"	70.0	"	"	0.057	"	1.0400
H.04	6.9	95.9	97.3	97.2	26.3	69.6	47	0.128	0.040	0.048	1.0396
	4.9	95.4	96.8	97.1	"	69.1	"	"	0.046	"	1.0420
	2.9	94.7	96.2	97.1	"	68.4	"	"	0.052	"	1.0436
H.05	2.9	95.7	97.4	97.7	28.6	67.1	61	0.167	0.038	0.036	1.0265
	4.9	96.1	97.7	97.7	"	67.5	"	"	0.034	"	1.0203
	6.9	96.8	97.9	97.7	"	68.2	"	"	0.027	"	1.0176
H.06	6.9	97.9	98.6	98.5	30.0	66.9	52	0.174	0.020	0.025	1.0222
	4.9	97.8	99.1	98.9	"	66.8	"	"	0.025	"	1.0470
	2.9	97.6	98.9	99.0	"	67.6	"	"	0.028	"	1.0521
H.07	2.9	99.6	100.0	100.1	38.6	61.0	112	0.320	0.006	0.009	1.0260
	4.9	99.7	100.4	100.4	"	61.1	"	"	0.008	"	1.0391
	6.9	100.0	100.6	100.5	"	61.4	"	"	0.008	"	1.0489
H.08	6.9	98.3	99.4	99.3	34.7	63.6	108	0.336	0.017	0.013	1.0282
	4.9	98.5	99.4	99.1	"	63.8	"	"	0.014	"	1.0238
	2.9	99.2	99.4	99.2	"	64.5	"	"	0.009	"	1.0233
H.09	2.9	99.3	99.9	99.7	42.5	56.8	132	0.394	0.005	0.003	1.0131
	4.9	99.6	100.0	100.0	"	57.1	"	"	0.004	"	1.0170
	6.9	99.9	100.2	100.2	"	57.4	"	"	0.003	"	1.0261

contd...

Table 5.07

Steam-Helium Mixture. Full cooling water flowrate.

Test No	x / cm	t_p / C	t_h / C	t_f / C	t_w / C	$T_p - T_w$ / K	Q / kW/m^2	Q/Qnu	W_p	W_m	Ptot / Bar
H.10	6.9	100.9	101.1	101.0	38.4	62.5	94	0.264	0.005	0.007	1.0697
	4.9	100.4	100.7	100.6	"	62.0	"	"	0.007	"	1.0692
	2.9	99.7	100.3	100.3	"	61.3	"	"	0.010	"	1.0535
H.11	2.9	98.7	99.8	99.5	35.9	62.8	74	0.208	0.015	0.013	1.0332
	4.9	98.8	99.7	99.4	"	62.9	"	"	0.012	"	1.0254
	6.9	99.3	99.6	99.4	"	63.4	"	"	0.006	"	1.0185
H.12	6.9	98.7	99.5	99.1	32.1	66.6	59	0.163	0.015	0.023	1.0368
	4.9	98.1	99.1	98.8	"	66.0	"	"	0.020	"	1.0312
	2.9	97.6	98.8	98.6	"	65.5	"	"	0.023	"	1.0260
H.13	2.9	99.8	100.4	100.3	41.5	58.4	105	0.309	0.007	0.006	1.0370
	4.9	99.5	100.0	100.1	"	58.0	"	"	0.006	"	1.0214
	6.9	99.8	100.1	100.2	"	58.3	"	"	0.004	"	1.0253
H.14	6.9	52.0	56.5	73.3					0.605	0.675	1.0775
	4.9	49.0	52.4	70.4					0.644	"	1.0732
	2.9	44.9	50.9	66.8					0.694	"	1.0691
H.15	2.9	65.8	68.4	84.9					0.404	0.367	1.0584
	4.9	69.7	71.0	88.0					0.353	"	1.0671
	6.9	73.0	73.0	88.5					0.305	"	1.0581
H.16	6.9	77.5	77.3	90.0					0.246	0.273	1.0500
	4.9	74.4	77.1	90.4					0.253	"	1.0640
	2.9	73.2	75.8	87.5					0.273	"	1.0771
H.17	2.9	84.4	83.2	90.0					0.158	0.139	1.0430
	4.9	86.2	85.5	90.8					0.139	"	1.0514
	6.9	88.1	87.6	91.7					0.123	"	1.0655
H.18	6.9	90.6	90.7	93.0					0.097	0.119	1.0688
	4.9	89.5	89.5	93.3					0.110	"	1.0754
	2.9	86.9	88.0	93.0					0.133	"	1.0774

contd.....

Table 5.07

Steam-Helium Mixture. Full cooling water flowrate

Test No	x / cm	t_p / C	t_h / C	t_f / C	t_w / C	T_s-T_w / K	Q / kW/m^2	Q/Q_{nu}	W_p	W_m	Ptot / Bar
H.19	2.9	90.2	89.5	93.8					0.105	0.103	1.0817
	4.9	91.4	91.5	94.3					0.093	"	1.0837
	6.9	92.5	92.5	94.4					0.083	"	1.0881
H.20	6.9	94.8	94.7	95.1	22.3	72.5	30	0.083	0.057	0.069	1.0707
	4.9	93.7	93.5	95.0	"	72.4	"	"	0.066	"	1.0635
	2.9	92.6	92.2	94.8	"	72.3	"	"	0.076	"	1.0631
H.21	2.9	94.5	94.3	95.5	23.3	71.2	33	0.090	0.055	0.052	1.0484
	4.9	95.1	94.9	95.7	"	71.8	"	"	0.050	"	1.0493
	6.6	95.5	95.4	95.9	"	72.2	"	"	0.046	"	1.0489
H.22	6.6	97.7	97.6	97.4	26.2	71.5	41	0.110	0.027	0.031	1.0479
	4.9	97.9	97.8	98.0	"	71.7	"	"	0.029	"	1.0671
	2.9	97.9	97.8	98.3	"	71.7	"	"	0.034	"	1.0864
H.23	2.9	85.1	88.9	93.1	18.7	66.4	24	0.068	0.157	0.115	1.0669
	4.9	86.8	89.3	95.0	"	68.1	"	"	0.135	"	1.0644
	6.9	86.5	89.3	92.9	"	69.8	"	"	0.115	"	1.0563
H.24	6.9	89.9	89.9	94.7	19.3	70.6	27	0.074	0.099	0.125	1.0445
	4.9	88.1	89.3	94.0	"	68.8	"	"	0.116	"	1.0433
	2.9	86.3	88.3	92.9	"	67.0	"	"	0.135	"	1.0411
H.25	2.9	90.7	90.3	94.5	21.1	69.6	30	0.083	0.092	0.087	1.0509
	4.9	92.5	93.0	95.4	"	71.4	"	"	0.082	"	1.0845
	6.9	93.7	93.6	95.5	"	72.6	"	"	0.071	"	1.0845
H.26	6.9	95.5	95.5	96.0	22.8	72.7	34	0.092	0.047	0.057	1.0541
	4.9	94.7	94.6	95.9	"	71.9	"	"	0.053	"	1.0511
	2.9	93.7	93.5	95.7	"	71.1	"	"	0.062	"	1.0497
H.27	2.9	95.9	95.9	96.8	24.7	71.2	39	0.103	0.042	0.039	1.0447
	4.9	96.8	96.8	97.3	"	72.1	"	"	0.036	"	1.0549
	6.9	97.4	97.4	97.6	"	72.7	"	"	0.033	"	1.0618

contd.....

Table 5.07

Steam-Helium Mixture. Full cooling water flowrate

Test No	x / cm	t_p / C	t_h / C	t_f / C	t_w / C	$T_p - T_w$ / k	Q / kW/m^2	Q/Qru	W_p	W_m	Ptot / Bar
H.28	6.9	98.9	99.0	98.9	27.8	71.1	52	0.139	0.020	0.026	1.0621
	4.9	99.1	99.2	99.5	"	71.3	"	"	0.023	"	1.0835
	2.9	99.0	99.1	99.5	"	71.2	"	"	0.025	"	1.0923
H.29	2.9	99.7	99.7	99.8	30.6	69.1	62	0.167	0.016	0.018	1.0743
	4.9	99.8	99.8	99.9	"	69.2	"	"	0.014	"	1.0692
	6.9	100.1	100.0	99.9	"	69.5	"	"	0.011	"	1.0648
H.30	6.9	100.1	100.1	99.8	32.5	67.6	76	0.208	0.007	0.011	1.0477
	4.9	99.7	99.8	99.7	"	67.2	"	"	0.010	"	1.0473
	2.9	99.5	99.5	99.6	"	67.0	"	"	0.012	"	1.0468
H.31	2.9	100.2	100.2	100.4	36.3	63.9	82	0.229	0.006	0.007	1.0455
	4.9	100.8	100.8	100.8	"	64.5	"	"	0.004	"	1.0622
	6.9	100.2	101.3	101.2	"	63.9	"	"	0.004	"	1.0757
H.32	2.9	76.2	84.0	92.5					0.262	0.274	1.0567
	4.9	79.0	84.4	92.8					0.225	"	1.0538
	6.9	81.6	84.7	92.4					0.192	"	1.0513
H.33	6.9	75.9	81.4	89.4					0.265	0.312	1.0539
	4.9	72.6	80.2	89.3					0.308	"	1.0520
	2.9	69.3	78.5	88.4					0.353	"	1.0471
H.34	2.9	58.4	69.6	80.4					0.507	0.456	1.0439
	4.9	62.3	71.0	81.6					0.451	"	1.0439
	6.9	66.5	72.4	82.8					0.390	"	1.0439
H.35	6.9	59.0	67.3	77.3					0.507	0.571	1.0733
	4.9	54.5	65.5	76.6					0.570	"	1.0723
	2.9	50.2	63.2	75.6					0.627	"	1.0704
H.36*	2.9	54.4	63.1	74.3					0.570	0.515	1.0697
	4.9	59.7	65.4	73.8					0.495	"	1.0697
	2.9	62.8	66.7	74.2					0.453	"	1.0760

*Zero cooling water flowrate.

contd....

Table 5.07

Steam-Helium Mixture, Full cooling water flowrate

Test No	x/cm	t_p/C	t_h/C	t_f/C	t_w/C	T_p-T_w/K	Q/kW/m^2	Q/Qnu	W_p	W_m	Ptot/Bar
H.37*	6.9	70.0	71.9	80.9					0.339	0.367	1.0324
	4.9	68.5	70.9	77.8					0.357	"	1.0265
	2.9	66.9	70.3	77.0					0.380	"	1.0255
H.38*	2.9	78.1	77.5	86.8					0.230	0.255	1.0343
	4.9	81.1	80.0	87.3					0.197	"	1.0461
	6.9	83.3	82.4	88.3					0.175	"	1.0598
H.39*	6.9	89.3	88.8	92.6					0.107	0.127	1.0530
	4.9	88.6	87.8	92.8					0.117	"	1.0657
	2.9	87.6	86.9	93.0					0.131	"	1.0804
H.40*	2.9	93.7	93.2	95.3					0.063	0.066	1.0505
	4.9	94.2	93.9	96.0					0.059	"	1.0669
	6.9	94.8	94.6	96.1					0.056	"	1.0657
H.41*	6.9	96.7	96.7	97.4					0.037	0.045	1.0579
	4.9	96.4	96.2	97.4					0.041	"	1.0647
	2.9	96.0	95.8	96.7					0.046	"	1.0711

Table 5.08

Steam-Helium Mixture, Variable $(T_\infty - T_w)$/K

Test No	x/cm	t_p/C	t_h/C	t_f/C	t_w/C	$T_\infty-T_w$/K	Q/kW/m^2	Q/Qnu	W_∞	W_m	Ptot/Bar
H.42	5.0	100.1	100.2	100.1	59.7	40.4	66	0.240	0.003	0.003	1.0320
	5.0	100.3	100.4	100.3	66.1	34.2	67	0.274	"	"	1.0369
	5.0	100.8	100.9	100.8	77.5	23.3	62	0.329	"	"	1.0565
	5.0	100.6	100.7	100.6	87.4	13.2	47	0.371	"	"	1.0516
	5.0	100.7	100.8	100.7	96.5	4.2	41	0.755	"	"	1.0545

*Zero cooling water flowrate.

contd.....

Table 5.08

Steam-Helium Mixture, Variable $(T_\infty - T_w)/K$.

Test No	x / cm	t_p / C	t_h / C	t_f / C	t_w / C	$T_\infty - T_w$ / K	Q / kW/m^2	Q/Q_{nu}	W_∞	W_m	Ptot / Bar
H.43	5.0	98.6	98.7	98.6	46.9	51.7	58	0.182	0.012	0.015	1.0196
	5.0	99.0	99.1	99.0	62.3	36.7	54	0.211	"	"	1.0338
	5.0	99.6	99.7	99.6	79.7	19.9	37	0.218	"	"	1.0544
	5.0	99.6	99.7	99.6	84.0	15.6	31	0.218	"	"	1.0554
	5.0	99.7	99.9	99.7	94.0	5.7	26	0.377	"	"	1.0613
H.44	5.0	97.9	97.9	97.9	44.5	53.4	44	0.136	0.020	0.024	1.0139
	5.0	98.4	98.4	98.4	52.2	46.2	44	0.148	"	"	1.0326
	5.0	99.0	98.9	99.0	73.8	25.2	31	0.158	"	"	1.0704
	5.0	98.5	98.5	98.5	80.3	18.2	26	0.166	"	"	1.0636
	5.0	98.2	98.3	98.2	90.7	7.5	21	0.257	"	"	1.0596
H.45	5.0	94.7	94.8	94.7	39.9	54.8	40	0.123	0.043	0.042	1.0069
	5.0	95.1	95.1	95.1	58.2	36.9	36	0.143	"	"	1.0216
	5.0	95.5	95.5	95.3	73.1	22.4	21	0.118	"	"	1.0382
	5.0	95.4	95.4	95.4	85.8	9.6	20	0.200	"	"	1.0402
H.46	5.0	91.7	91.6	91.7	36.9	54.8	34	0.106	0.070	0.063	1.0057
	5.0	91.9	91.8	91.9	56.0	45.9	27	0.111	"	"	1.0135
	5.0	92.5	92.5	92.5	68.2	24.3	21	0.113	"	"	1.0331
	5.0	92.6	92.5	92.6	86.8	5.8	13	0.191	"	"	1.0361
H.47	5.0	88.2	88.3	88.2	34.3	53.9	29	0.095	0.103	0.089	1.0008
	5.0	88.5	88.4	88.5	51.5	37.0	19	0.077	"	"	1.0071
	5.0	88.8	88.8	88.8	65.7	23.1	15	0.084	"	"	1.0155
	5.0	89.1	89.2	89.1	82.1	7.0	12	0.158	"	"	1.0262

Table 5.09

Representative temperature profiles. Steam-Air Mixture.

W_m=0.017

x = 8.6cm

y/mm	1.35	2.35	3.35	4.35	5.35
t_p/°C	97.1	99.4	100.1	100.3	100.5

x = 5.6cm

y/mm	1.35	2.35	4.00	6.00
t_p/°C	99.3	100.3	100.4	100.6

x = 2.1cm

y/mm	2.45	2.80	4.00	6.00
t_p/°C	100.2	100.4	100.6	100.6

W_m=0.055

x = 8.6cm

y/mm	1.35	2.35	3.35	4.35	5.35	6.35
t_p/°C	86.6	96.7	99.5	100.1	100.5	100.5

x = 5.6cm

y/mm	1.35	2.35	3.35	4.35	5.35	6.35
t_p/°C	93.6	99.7	100.6	100.9	101.1	101.1

x = 2.6cm

y/mm	1.35	2.35	3.35	4.35	5.35	6.35
t_p/°C	96.1	99.9	100.8	101.0	101.1	101.1

W_m=0.075

x = 8.6cm

y/mm	1.40	2.40	4.00	5.40	6.60	7.40	8.40
t_p/°C	83.4	93.8	98.2	99.3	99.8	100.0	100.2

x = 5.6cm

y/mm	1.35	2.35	4.00	5.40	7.40
t_p/°C	85.2	96.4	99.7	100.3	100.6

x = 2.6cm

y/mm	1.35	2.35	4.35	5.35	6.35	7.35
t_p/°C	90.1	98.1	100.1	100.4	100.5	100.5

contd............

Table 5.09

Representative temperature profiles, Steam-Air Mixture.

W_m =0.095

x = 8.6cm										
y/mm	1.35	2.35	3.35	4.35	5.35	6.35	7.35	8.35		
t_p/°C	78.2	90.3	94.8	96.7	97.5	97.9	98.1	98.2		
x = 5.6cm										
y/mm	1.55	2.55	3.55	4.55	5.55	6.55	7.55			
t_p/°C	85.9	95.4	98.4	99.2	99.7	99.8	99.9			
x = 2.2cm										
y/mm	1.60	2.60	3.60	4.60	5.60	6.60	7.60			
t_p/°C	90.7	98.0	99.6	100.0	100.4	100.4	100.5			

W_m =0.149

x = 8.6cm										
y/mm	1.35	1.85	2.35	2.85	3.35	4.35	5.35	6.35	7.35	8.35
t_p/°C	77.5	85.0	90.2	93.6	95.4	97.6	98.4	98.7	98.9	99.0
x = 5.6cm										
y/mm	1.35	1.85	2.35	2.85	3.35	4.35	5.35	6.35	7.35	8.35
t_p/°C	83.7	90.1	94.9	97.0	98.2	99.1	99.4	99.6	99.7	99.8
x = 2.2cm										
y/mm	1.35	1.85	2.35	2.85	3.35	4.35	5.35	6.35	7.35	
t_p/°C	92.2	96.4	97.8	99.0	99.5	99.9	100.0	100.1	100.1	

W_m =0.164

x = 8.6cm										
y/mm	1.35	1.85	2.35	2.85	3.35	4.35	5.35	6.35	7.35	8.35
t_p/°C	76.2	84.3	89.0	92.2	94.2	96.4	97.3	97.7	97.9	98.1
x = 5.6cm										
y/mm	1.45	1.95	2.45	2.95	3.45	4.45	5.45	6.45	7.45	
t_p/°C	83.6	89.9	93.9	96.0	97.5	98.4	98.8	99.0	99.2	
x = 2.2cm										
y/mm	1.60	2.10	2.60	3.10	3.60	4.60	5.60	6.60		
t_p/°C	90.5	95.2	97.3	98.3	99.0	99.6	99.8	99.9		

contd........

Table 5.09

Representative temperature profiles. Steam-Air Mixture.

W_m=0.221										
x = 5.0cm										
y/mm	1.40	1.90	2.40	2.90	3.40	4.40	5.40	6.40	7.40	8.40
t_p/°C	81.2	87.0	91.2	93.8	95.5	96.7	97.4	97.6	97.7	97.8
x = 2.2cm										
y/mm	1.40	1.90	2.40	2.90	3.40	4.40	5.40	6.40	7.40	
t_p/°C	87.0	92.0	95.5	96.9	97.8	98.5	98.8	99.0	99.0	
W_m=0.550										
x = 7.3cm										
y/mm	1.70	2.70	3.70	4.70	5.70	6.70	7.70			
t_p/°C	76.6	81.0	82.8	83.9	84.3	84.6	84.6			
x = 5.7cm										
y/mm	1.70	2.70	3.70	4.70	5.70	6.70	8.70			
t_p/°C	79.7	83.3	85.3	86.1	86.5	86.6	86.7			
x = 3.3cm										
y/mm	1.70	2.70	3.70	4.70	5.70	6.70	7.70			
t_p/°C	84.4	87.2	88.9	89.7	90.1	90.3	90.3			

Table 5.10

Representative temperature profiles. Steam-Argon Mixture.

W_m=0.015

x = 6.9cm							
y/mm	2.30	3.00	4.00	5.00	6.00		
t_p/°C	90.9	94.6	97.4	98.2	98.7		
x = 4.9cm							
y/mm	2.25	2.50	3.00	4.00	5.00	6.00	
t_p/°C	94.7	95.1	97.0	98.3	98.9	99.2	
x = 2.9cm							
y/mm	2.25	2.50	3.00	4.00	5.00	6.00	
t_p/°C	97.4	97.7	98.6	99.0	99.3	99.5	

W_m=0.075

x = 6.9cm							
y/mm	2.35	3.00	4.00	5.00	6.00	7.00	8.00
t_p/°C	89.1	93.3	96.8	97.9	98.3	98.5	98.7
x = 4.9cm							
y/mm	2.25	3.00	4.00	5.00	6.00	7.00	8.00
t_p/°C	93.5	96.3	98.2	98.9	99.1	99.3	99.4
x = 2.9cm							
y/mm	2.30	3.00	4.00	5.00	6.00	7.00	8.00
t_p/°C	95.7	97.7	99.1	99.5	99.7	99.8	99.9

W_m=0.132

x = 6.9cm					
y/mm	2.25	3.00	4.00	5.00	6.00
t_p/°C	97.8	99.0	99.7	99.9	100.0
x = 4.9cm					
y/mm	2.25	3.00	4.00	5.00	6.00
t_p/°C	97.3	98.8	99.8	100.1	100.2
x = 2.9cm					
y/mm	2.25	3.00	4.00	5.00	6.00
t_p/°C	99.0	99.7	100.1	100.2	100.3

contd...........

Table 5.10

Representative temperature profiles. Steam-Argon Mixture.

$W_m = 0.317$

$x = 6.9$cm

y/mm	1.50	1.95	3.00	4.00	5.00	6.00	7.00
t_p/°C	84.5	86.2	91.0	94.5	95.9	96.2	96.3

$x = 4.9$cm

y/mm	1.60	3.00	4.00	5.00	6.00	7.00
t_p/°C	90.3	95.4	97.1	97.6	97.8	97.9

$x = 2.9$cm

y/mm	1.00	2.00	3.00	4.00	5.00	6.00
t_p/°C	91.3	95.7	97.8	98.4	98.7	98.8

$W_m = 0.270$

$x = 6.9$cm

y/mm	1.50	2.00	3.00	4.00	5.00	6.00
t_p/°C	92.6	94.7	96.8	97.6	97.9	98.1

$x = 4.9$cm

y/mm	1.50	2.00	3.00	4.00	5.00	6.00	7.00
t_p/°C	94.2	96.0	97.8	98.3	98.5	98.6	98.7

$x = 2.9$cm

y/mm	1.50	2.00	3.00	4.00	5.00	6.00	7.00
t_p/°C	97.1	98.3	98.9	99.2	99.4	99.4	99.4

$W_m = 0.333$

$x = 6.9$cm

y/mm	1.75	2.00	3.00	4.00	5.00	6.00	7.00
t_p/°C	88.2	89.4	92.1	93.3	93.8	94.0	94.1

$x = 4.9$cm

y/mm	1.75	2.00	3.00	4.00	5.00	6.00	7.00
t_p/°C	91.2	92.1	94.5	95.4	95.8	95.9	96.0

$x = 2.9$cm

y/mm	1.60	2.00	3.00	4.00	5.00	6.00	7.00
t_p/°C	93.4	94.7	96.5	97.1	97.4	97.5	97.5

contd.........

Table 5.10

Representative temperature profiles, Steam-Argon Mixture.

W_m=0.455								
x = 6.9cm								
y/mm	1.75	2.00	3.00	4.00	5.00	6.00	7.00	
t_p/°C	81.0	82.3	86.1	87.9	88.6	88.8	89.0	
x = 4.9cm								
y/mm	1.70	2.00	3.00	4.00	5.00	6.00	7.00	
t_p/°C	84.9	85.7	89.2	90.7	91.3	91.6	91.7	
x = 2.9cm								
y/mm	2.00	3.00	4.00	5.00	6.00	7.00		
t_p/°C	88.8	92.0	93.3	93.8	94.0	94.1		
W_m=0.655								
x = 6.9cm								
y/mm	1.55	2.00	3.00	4.00	5.00	6.00		
t_p/°C	69.6	70.9	75.0	77.2	78.1	78.4		
x = 4.9cm								
y/mm	1.70	2.00	3.00	4.00	5.00	6.00	7.00	
t_p/°C	73.0	74.9	79.0	80.9	81.8	82.1	82.4	
x = 2.9cm								
y/mm	1.75	2.00	3.00	4.00	5.00	6.00		
t_p/°C	77.1	79.2	83.1	84.7	85.4	85.8		
W_m=0.761								
x = 6.9cm								
y/mm	1.65	3.00	4.00	5.00	6.00	7.00		
t_p/°C	57.1	64.9	68.6	70.8	71.7	72.0		
x = 4.9cm								
y/mm	1.80	2.00	3.00	4.00	5.00	6.00	7.00	8.00
t_p/°C	62.3	63.9	70.5	74.0	75.8	76.5	76.9	77.0
x = 2.9cm								
y/mm	1.75	2.00	3.00	4.00	5.00	6.00	7.00	8.00
t_p/°C	73.9	75.5	79.4	81.2	82.1	82.5	82.6	82.6

Table 5.11

Representative temperature profiles. Steam-Neon Mixture.

W_m = 0.047

x = 6.0cm								
y/mm	1.50	3.00	4.00	5.00	6.00	7.00		
t_p/°C	88.6	98.3	99.1	99.3	99.5	99.6		
x = 4.9cm								
y/mm	1.50	3.00	4.00	5.00	6.00	7.00	8.00	
t_p/°C	93.3	97.8	98.7	99.2	99.5	99.6	99.7	
x = 3.9cm								
y/mm	1.50	3.00	4.00	5.00	6.00	7.00	8.00	
t_p/°C	93.1	97.7	98.7	99.2	99.4	99.6	99.7	

W_m = 0.011

x = 6.0cm								
y/mm	1.50	3.00	4.00	5.00	6.00			
t_p/°C	97.0	98.7	99.5	99.6	99.7			
x = 4.9cm								
y/mm	1.50	3.00	4.00	5.00	6.00	7.00	8.00	
t_p/°C	98.5	99.9	100.1	100.3	100.3	100.3	100.4	
x = 2.9cm								
y/mm	1.50	3.00	4.00	5.00	6.00	7.00	8.00	
t_p/°C	98.6	100.0	100.3	100.5	100.5	100.5	100.6	

W_m = 0.068

x = 6.0cm								
y/mm	1.50	3.00	4.00	5.00	6.00	7.00	9.00	14.00
t_p/°C	91.5	96.9	98.3	99.1	99.6	99.6	99.9	99.9
x = 4.9cm								
y/mm	1.50	3.00	4.00	5.00	6.00	7.00	9.00	
t_p/°C	93.1	98.2	99.3	99.9	100.1	100.3	100.4	
x = 2.9cm								
y/mm	1.50	3.00	4.00	5.00	6.00	7.00	9.00	
t_p/°C	94.5	98.8	99.8	100.1	100.2	100.4	100.4	

contd............

Table 5.11

Representative temperature profiles, Steam-Neon Mixture.

W_m=0.134										
x=6.0cm										
y/mm	1.50	3.00	4.00	5.00	6.00	7.00	9.00	14.00		
t_p/°C	85.5	93.6	95.8	97.2	97.7	98.2	98.4	98.6		
x=4.9cm										
y/mm	1.50	3.00	4.00	5.00	6.00	7.00	9.00	14.00		
t_p/°C	86.0	94.1	96.1	97.4	97.8	98.2	98.4	98.6		
x=2.9cm										
y/mm	1.50	3.00	4.00	5.00	6.00	7.00	9.00	14.00		
t_p/°C	88.1	95.0	97.1	97.9	98.5	98.7	98.8	99.0		
W_m=0.200										
x=6.0cm										
y/mm	1.50	3.00	4.00	5.00	6.00	7.00	9.00	14.00		
t_p/°C	79.8	88.9	91.3	93.2	94.0	94.8	95.5	95.9		
x=4.9cm										
y/mm	1.50	3.00	4.00	5.00	6.00	7.00	9.00	14.00		
t_o/°C	80.0	90.0	92.2	93.9	94.8	95.5	96.0	96.3		
x=2.9cm										
y/mm	1.50	3.00	4.00	5.00	6.00	7.00	9.00	14.00		
t_p/°C	80.8	90.7	92.7	94.4	95.2	95.9	96.3	96.4		
W_m=0.265										
x=6.0cm										
y/mm	1.50	3.00	4.00	5.00	6.00	7.00	9.00	12.00	14.00	17.00
t_p/°C	73.2	83.7	86.8	89.0	90.5	91.5	92.6	93.0	93.4	93.5
x=4.9cm										
y/mm	1.50	3.00	4.00	5.00	6.00	7.00	9.00	12.00		
t_p/°C	77.3	86.4	89.4	91.2	92.3	93.0	93.6	93.9		
x=2.9cm										
y/mm	1.50	3.00	4.00	5.00	6.00	7.00	9.00	12.00		
t_p/°C	79.6	87.8	90.4	91.7	92.4	92.9	93.3	93.4		

contd.........

Table 5.11

Representative temperature profiles. Steam-Neon Mixture.

$W_m = 0.340$

x=6.0cm									
y/mm	1.50	3.00	4.00	5.00	6.00	7.00	9.00	12.00	
$t_p/^{o}C$	69.4	79.3	82.9	85.0	86.7	87.7	88.6	89.4	
x=4.9									
y/mm	1.50	3.00	4.00	5.00	6.00	7.00	9.00	12.00	
$t_p/^{o}C$	72.3	81.4	84.6	86.7	88.2	89.3	89.9	90.6	
x=2.9cm									
y/mm	1.50	3.00	4.00	5.00	6.00	7.00	9.00	12.00	
$t_p/^{o}C$	73.8	83.0	85.9	87.5	88.8	89.5	90.1	90.3	

$W_m = 0.425$

x=6.0cm									
y/mm	1.50	3.00	4.00	5.00	6.00	7.00	9.00	12.00	13.00
$t_p/^{o}C$	60.9	71.3	75.1	77.3	79.3	80.3	81.8	82.9	83.3
x=4.9cm									
y/mm	1.50	3.00	4.00	5.00	6.00	7.00	9.00	12.00	13.00
$t_p/^{o}C$	63.4	73.1	75.8	79.2	80.7	81.4	82.9	83.6	83.7
x=2.9cm									
y/mm	1.50	3.00	4.00	5.00	6.00	7.00	9.00	12.00	13.00
$t_p/^{o}C$	67.2	76.6	79.7	81.8	83.0	83.7	84.4	84.6	84.6

Table 5.12
Representative Temperature profiles. Steam-Helium Mixture.

W_m=0.087

. x=2.9cm

y/mm	1.50	3.00	4.00	5.00	6.00	7.00	12.00	14.00
t_p/°C	69.4	78.2	82.5	85.0	86.8	87.9	90.2	90.3

. x=4.9cm

y/mm	1.50	3.00	4.00	5.00	6.00	7.00	12.00	14.00
t_p/°C	72.7	82.2	85.9	88.3	89.6	90.5	92.4	92.6

. x=6.9cm

y/mm	1.50	3.00	4.00	5.00	6.00	7.00	12.00	14.00
t_p/°C	75.6	84.8	68.3	90.1	91.3	92.1	93.5	93.7

W_m=0.026

. x=6.9cm

y/mm	1.50	3.00	4.00	5.00	6.00	7.00	12.00	14.00
t_p/°C	86.4	93.7	95.8	97.0	97.7	98.0	99.0	99.0

. x=4.9cm

y/mm	1.50	3.00	4.00	5.00	6.00	7.00	12.00	14.00
t_p/°C	85.1	93.0	95.3	96.7	97.5	98.2	99.2	99.3

. x=2.9cm

y/mm	1.50	3.00	4.00	5.00	6.00	7.00	12.00	14.00
t_p/°C	83.0	92.0	94.5	96.0	97.1	97.8	99.0	99.2

contd.............

Table 5.12

Representative temperature profiles. Steam-Helium Mixture.

W_m=0.139									
x=2.9cm									
y/mm	1.50	3.00	5.00	7.00	12.00	22.00	32.00	42.00	
t_p/°C	57.1	68.9	76.7	80.7	84.3	84.3	84.3	84.3	
x=4.9cm									
y/mm	1.50	3.00	5.00	7.00	12.00	17.00	32.00	42.00	
t_p/°C	60.8	71.6	78.9	82.4	85.1	85.9	86.2	86.2	
x=6.9cm									
y/mm	1.50	3.00	5.00	7.00	12.00	22.00	32.00	42.00	
t_p/°C	63.7	75.5	82.4	85.4	87.3	87.9	87.9	88.0	
W_m=0.119									
x=6.9cm									
y/mm	1.50	3.00	4.00	5.00	6.00	7.00	10.00	12.00	15.00
t_p/°C	71.1	80.4	83.8	86.0	87.5	88.5	89.9	90.3	90.7
x=4.9cm									
y/mm	1.50	3.00	5.00	7.00	15.00	17.00			
t_p/°C	66.2	77.8	83.9	86.9	88.9	89.5			
x=2.9cm									
y/mm	1.50	3.00	5.00	7.00	12.00	17.00			
t_p/°C	65.7	76.0	82.4	85.9	88.0	88.4			
W_m=0.069									
x=6.9cm									
y/mm	1.50	3.00	5.00	7.00	12.00	17.00			
t_p/°C	76.8	84.8	90.3	92.5	94.3	94.8			
x=4.9cm									
y/mm	1.50	3.00	4.00	5.00	7.00	12.00	17.00		
t_p/°C	73.0	83.0	86.9	89.1	91.6	93.3	93.7		
x=2.9cm									
y/mm	1.50	3.00	4.00	5.00	6.00	7.00	12.00	17.00	
t_p/°C	71.6	81.0	85.2	87.5	89.6	90.4	92.2	92.6	

contd...........

Table 5.12

Representative temperature profiles. Steam-Helium Mixture.

$W_m = 0.675$

x=6.9cm

y/mm	1.35	3.00	5.00	7.00	12.00	22.00	32.00	42.00	82.00
$t_p/^oC$	27.0	33.6	39.8	43.7	48.1	49.5	50.3	50.7	52.6

x=4.9cm

y/mm	1.15	3.00	5.00	7.00	12.00	22.00	32.00	42.00	82.00
$t_p/^oC$	19.9	20.4	31.8	35.9	40.9	43.1	44.4	45.5	49.2

x=2.9cm

y/mm	1.25	3.00	5.00	7.00	12.00	22.00	32.00	42.00	82.00
$t_p/^oC$	20.4	23.0	27.2	30.7	35.7	38.4	39.6	41.0	44.5

$W_m = 0.367$

x=6.9cm

y/mm	1.50	3.00	5.00	7.00	12.00	22.00	32.00	42.00	82.00
$t_p/^oC$	46.2	55.9	64.0	67.6	70.8	71.5	71.8	72.0	72.4

x=4.9cm

y/mm	1.30	3.00	5.00	7.00	12.00	22.00	32.00	42.00	82.00
$t_p/^oC$	41.4	53.3	58.5	64.2	67.9	68.8	69.1	69.1	69.5

x=2.9cm

y/mm	1.20	3.00	5.00	7.00	12.00	22.00	32.00	42.00	82.00
$t_p/^oC$	34.6	46.5	54.9	59.0	63.3	64.6	65.0	65.2	65.8

$W_m = 0.273$

x=6.9cm

y/mm	1.50	3.00	5.00	7.00	12.00	22.00	32.00	42.00	82.00
$t_p/^oC$	51.7	61.6	69.5	73.0	76.1	77.0	77.2	77.3	77.5

x=4.9cm

y/mm	1.30	3.00	5.00	7.00	12.00	22.00	32.00	42.00	82.00
$t_p/^oC$	46.1	58.8	66.9	70.7	73.6	74.9	76.5	77.5	77.4

x=2.9cm

y/mm	1.50	3.00	5.00	7.00	12.00	22.00	32.00	42.00	82.00
$t_p/^oC$	44.6	56.2	63.3	67.3	71.1	72.1	72.9	73.1	73.4

Chapter 6

Discussion

6.1 Mechanism of condensation in the presence of a non-condensing gas.

6.2 Comparison of present and other approximate analyses [43,44] with the "exact variable property" analysis [22].

6.3.1 Condensation of steam from steam-gas mixtures when maximum coolant flowrate was used.

6.3.2 Effect of steam-gas mixture-to-surface temperature difference on fractional reduction in heat flux.

6.3.3 Effect of variation of mixture temperature with height on heat flux.

6.4 Comments on the different gases used.

6.5 Comparison between present experimental results and equation 3.27 with earlier experimental work.

6 Discussion

6.1 Mechanism of condensation in the presence of a non-condensing gas

Theoretical and experimental investigations on the condensation from vapour-gas mixtures indicate that the presence of non-condensing gases causes reductions in heat flux (see chapter 2). The physical mechanism by which the reduction in heat flux occurs may be explained as follows:-

When a vapour, containing a non-condensing gas, condenses on a cooled surface, the concentration of the gas in the immediate vicinity of the surface is greater than that in the remoter vapour (this is because, as the vapour is removed by condensation, the gas is left behind). This in turn, results in a density difference in the vapour-gas mixture which gives rise to free convection. If the molecular weight of the gas exceeds that of the vapour, the density of the mixture near the surface is greater than that farther away and the vapour-gas mixture moves downwards near the surface. Alternatively if the gas has the smaller molecular weight, the tendency would be for the vapour-gas mixture to move upwards near to the condensation surface. This upward movement, however, would be opposed by the downward dragging action of the condensate at the interface.

As a result of the increased gas concentration, the partial pressure, and hence temperature, of the vapour near the surface, is diminished. This, in turn, reduces the temperature difference across the condensate layer, and thereby diminishes the heat flux.

6.2 Comparison of present and other approximate analyses with the "exact variable property" analysis

Minkowycz and Sparrow [22] have obtained "exact" numerical solutions for steam-air mixtures under various conditions. The fractional reduction in heat flux (Q/Q_{nu}) for the highest and lowest bulk temperatures considered (i.e. 373.15 K and 299.82 K) are reproduced in figs 6.01 and 6.02. For the same two bulk temperatures and using equation 3.27, the approximate solution of Rose [43] and Sledgers' analysis (see appendix 6), values of Q/Q_{nu} were obtained for steam-air mixtures. These results are also shown in figs 6.01 and 6.02. To avoid overcrowding in fig 6.02, only the results for the highest and lowest gas concentrations, obtained from the solutions of Rose and Sledgers, are shown.

In obtaining the curves based on the approximate analyses, the steam-gas mixtures and the condensate properties were evaluated as indicated in appendix 7. In figs 6.01 and 6.02 it may be observed that the approximate solutions follow the same general trends as those given by the exact solution. Results of equation 3.27 and Rose [43] analysis virtually coincide, indicating that the effect of including the thickening of the condensate layer is very small. At lower concentrations (i.e. $W \lesssim 0.02$), equation 3.27 and Rose's analysis both underestimate the heat flux as given by the exact solution. The discrepancy increases with decreasing concentration and to a lesser extent with increasing bulk-to-surface temperature differences. At higher concentrations (i.e. $W \gtrsim 0.02$) the results given by equation 3.27 and Rose's solution virtually coincide with those of the exact analysis. The curves obtained using Sledgers analysis (see appendix 6), shows the same general trends but deviates further from the exact solution.

It may be noted from figs 6.01 and 6.02 that the exact and all approximate solutions indicate that the gas causes a larger drop in heat flux at the lower bulk temperature (i.e. lower pressure).

6.3 Present experimental results

Preliminary experiments were performed to determine the variation of heat flux with steam-to-surface temperature difference for pure steam at atmospheric pressure. In fig 6.03 a comparison is made between the experimental and theoretical variations of heat flux with steam-to-surface temperature differences. The theoretical values were computed using the Nusselt expression [1]. Fig 6.03 indicates that the Nusselt analysis is satisfactory for the condensation of pure steam under the conditions which prevailed in the present tests. It would thus be expected that the approximations of the simple Nusselt theory would be valid for the condensate film in subsequent tests when non-condensing gases were present in the steam.

6.3.1 Condensation of steam from steam-gas mixtures when maximum coolant flowrate was used

The results for the various steam-gas mixtures when maximum coolant flowrate was used are presented in figs 6.04-6.10 the ranges of steam-to-surface temperature difference, $T_\infty - T_w$, occurring in these tests were different for the different gases and are indicated on the graphs. No systematic dependance of the results on $(T_\infty - T_w)$ could be detected and no attempt has been made to distinguish between the different points on the graphs. Moreover, the theory indicates that the effect of $(T_\infty - T_w)$ is quite small (see figs 6.01 and 6.02).

In figs 6.04, 6.05 and 6.06 the fractional reductions in heat flux (Q/Q_{nu}) were plotted against the mean gas concentration W_m. This concentration was based on the measured mass of the injected gas (see appendix 3). In figs 6.07-6.10, these fractional reductions were plotted against the gas concentration outside the steam-gas mixture boundary layer, W_∞. W_∞ was calculated from the mixture temperature and pressure and using the ideal gas relations and assuming saturation of conditions in the mixture (see appendix 3). Since the temperature outside the mixture layer was found to be a function of height (see appendix 2), the calculation of W_∞ was based on the mean temperature of the steam-gas mixture (i.e. the temperature corresponding to the mid-height of the test plate). For helium, Q/Q_{nu} has been plotted only against W_∞ since the differences between W_m and W_∞ of helium were small. The relationship between W_m and W_∞ for steam-air, steam-argon and steam-neon are shown in figs 6.11-6.13. Values of Q/Q_{nu} were calculated, using equation 3.27, at the highest and lowest values of $(T_\infty - T_w)$ used in the tests. These theoretical results are shown in figs 6.07-6.09.

It may be seen from figs 6.04-6.09 that

(a) The heat flux decreases most rapidly with gas concentration at the lowest concentrations.

(b) Generally, the values of Q/Q_{nu} obtained using equation 3.27 are lower than the experimental values at the lower gas concentrations (i.e. in the range $0<W_\infty<0.03$ for air, $0<W_\infty<0.1$ for argon and $0<W_\infty<0.02$ for neon). These discrepancies between theory and experiment are discussed in section 6.3.2.

For the case where the non-condensing gas has the smaller molecular weight, no theoretical solution has yet been developed. In Chapter 3 a semi-empirical equation was given. Here the approximate analysis was carried out as in the case where the molecular weight of the gas was the larger except that the velocity of the liquid-vapour interface was set to zero. It was then suggested that the values of Q/Q_{nu} so found should be multiplied by a correction factor which involved the ratio of the interface velocity to the maximum velocity in the vapour-gas mixture. The form of the correction factor was chosen so that it tended to unity as the above-mentioned ratio tended to zero. The single disposable constant in the correction factor was determined by fitting the present experimental data for helium. In fig 6.10 the results of this procedure are shown for the highest and lowest values of $T_\infty-T_w$ used in the steam-helium tests. The closeness of fit is clearly quite satisfactory. It should be pointed out that the procedure for calculation of heat transfer in the case where the non-condensing component has the smaller molecular weight is only a tentative proposal. Further tests should be made with different gases and different plate heights before any claims could be made regarding the reliability of such a procedure.

It may be seen from figs 6.11-6.13 that, at the lower gas concentrations, the values of W_m are higher than the corresponding values of W_∞. This is a reflection of the fact that the gas concentration is greatest near the condensing surface and that the variation of gas concentration with distance from the plate is greatest at the lower concentrations.

6.3.2 Effect of mixture-to-surface temperature difference on the fractional reduction in heat flux

In the previous section it was seen that Q/Q_{nu} was only weakly dependant on $(T_\infty - T_w)$ for the ranges covered (see figs 6.04-6.10). Tests, however, were carried out using different heated coolant flowrates with fixed gas concentrations.

The variation of the fractional reduction in heat flux with mixture-to-surface temperature differences are represented in figs 6.14-6.17. The gas concentration was based on the mean temperature of steam-gas mixture outside the boundary layer. Results given by equation 3.27, for the same conditions prevailed in experiments are also shown in figs 6.14, 6.16 and 6.20. In fig 6.17 the curves are based on the semi-empirical procedure discussed earlier.

It may be seen from figs 6.14-6.16 that at low gas concentrations, equation 3.27 gives lower Q/Q_{nu} results than those obtained experimentally.

In fig 6.14 it may be seen that, except for few experimental points, good agreement was obtained between theory and experiment for steam-air mixtures. For steam-argon mixture of gas concentration o:

0.01, the theoretical Q/Q_{nu} results are lower than the experimental results by about 30%, fig 6.15. This discrepancy between theoretical and experimental results decreases rapidly with increasing argon concentration and virtual coincidence was obtained for concentration >0.1. For the steam-neon mixtures again good agreement was obtained for gas concentrations >0.018, (fig 6.16).

In figs 6.14-6.16, both theory and experiment demonstrate the weak dependance of Q/Q_{nu} on $T_{\infty}-T_w$. The discrepancy between theory and experiment at the low gas concentrations, shown in figs 6.07-6.09 is again seen in figs 6.14-6.16. As has been seen earlier, the only significant discrepancy between the exact and approximate solutions (for air-steam mixtures) occured at the low gas concentrations. The results given by Sparrow and Minkowycz [22] corresponding to the lowest experimental gas concentration, are shown in fig 6.14. This suggests that the most probable reason for the discrepancy between experiment and the approximate theory lie in the approximations of the solution. The present experimental results seemed to the present author adequate confirmation of the theory and it did not seem necessary to carry out the laborious and expensive processes of evaluating the numerical exact solutions for the other gas-vapour combinations.

Fig 6.17 compares the results for helium with the lines obtained from the semi-empirical procedure discussed earlier. The agreement is less satisfactory than might have been expected from fig 6.10. The discrepancies are more serious at the lowest gas concentrations and temperature differences.

6.3.3 Effect of variation of mixture temperature with height on heat flux

The temperature of the steam-gas mixture outside the boundary layer was found to vary with height in the present experiments (see appendix 2). This temperature was taken as constant in all analyses including that yielding equation 3.27. However, for the range of gas concentration used to obtain the experimental Q/Q_{nu} results, these temperature variations were small compared with the experimental mixture-to-surface temperature differences. Therefore the effect of these variations on the heat flux is expected to be small, this is confirmed by the good agreement between theory and experiment.

6.4 Comments on the different gases used

In deciding which are the important gas properties, from the view point of reducing heat-flux, it is easier to compare theoretical results for the different gases than experimental ones. Since the approximate theory has been found generally satisfactory except at the very low gas concentrations, this theory has been used. Clearly all of the parameters in the theory play a role. The objective here is to try to assess which of these are the most important.

Sets of results for steam-argon and steam-neon mixtures were obtained using equation 3.27, (see figs 6.18 and 6.19). These results show the same trends as those of steam-air mixture, (fig 6.01).

To compare the effect of various gases on the heat flux, the

Q/Q_{nu} results of steam-argon, steam-air and steam-neon corresponding to gas concentrations of 0.001 and 0.1 are reproduced in fig 6.20. These results show marked differences from one gas to another. These differences result from the different properties of the mixtures. However, since the steam is common to all mixtures used, then these differences in Q/Q_{nu} are dependant on the properties of the gases used. These gases were assumed to be perfect gases when evaluating their densities. Therefore, the gas density is directly proportional to its molecular weight. The gas viscosity, μ, and the steam-gas mixture coefficient of diffusion, D, were evaluated as follows [81]:

$$\mu = 0.0000026693 \times M_g T/(\sigma^2 \psi) \qquad 6.03$$

$$D = (3.64 \times 10^{-8}/P_{tot})\left[(M_v + M_g)/(M_v M_g)\right]^{\frac{1}{2}} \times$$

$$(P_{cv} P_{cg})^{\frac{1}{3}} (T_{cv} T_{cg})^{-0.75} T^{2.334} \qquad 6.04$$

where M_g & M_v are the molecular weights of the gas and vapour respectively

T & P_{tot} are the temperature and pressure of the mixture respectively

P_{cv} & P_{cg} are the critical pressures (in atmosphere) of the steam and gas respectively

T_{cv} & T_{cg} are the critical temperatures (in K) of the steam and gas respectively

σ is the hard sphere diameter (in A)

ψ is the collision integral based on Lennard-Jones potential and is a function of temperature.

Equations 6.03 and 6.04 indicate that, apart from the gas molecular weight, μ is dependent on $(\sigma^2)^{-1}$ and D is dependant on $P_{cg}^{1/3}/[T_{cg}^{0.75}]$. However, for a given temperature, $(\sigma^2)^{-1}$ and $P_{cg}^{1/3}/[T_{cg}^{0.75}]$ are functions of molecular weight. Thus the gas molecular weight may be considered as the main factor in influencing these differences in the reduction of heat flux.

It may be seen from fig 6.20 that the reduction in heat flux decreases with increasing gas molecular weight. This is because the difference in mixture density at the bulk and at interface (for given bulk temperature and gas concentration) increases with increasing gas molecular weight. This increase in density difference results in an increase in the natural convection flow which in turn causes an increase in heat flux (i.e. decrease in the reduction in heat flux). It may also be seen from fig 6.20 that the differences in Q/Q_{nu} (for any given mixture-to-surface temperature difference) from one steam-gas mixture to another decrease with increasing gas concentration.

6.5 Comparison between present experimental results and equation 3.27 with earlier experimental work

Among the few experimental data reported for flat plates, only those of Hampson[45], Akers, Davis and Crawford[47] and Sledgers[44] were made using vertical plane surfaces.

In Hampson's investigation, both drop and film condensation of steam from steam-nitrogen mixtures were examined. The heat-transfer data obtained, covered a range of small nitrogen concentration (i.e. $W_{\infty} \leq 0.02$). In fig 6.21 the heat transfer results of Hampson[45] (i.e. the variation of steam side-heat transfer coefficient, α, with heat flux for various nitrogen concentration) are reproduced and are compared with those computed, using equation 3.27. It may be seen from fig 6.21 that the theoretical results show similiar general trends to those of Hampson's experimental results. However, at a given heat-transfer coefficient, the theoretical values of heat flux are much lower than those obtained by Hampson. These differences might be attributable to the presence of significant forced convection in the experimental work.(in Hampson's experiments the gas was continously fed to the apparatus, and vented along with the excess steam and condensate at the bottom of the test plate).

A semi-empirical equation was given by Akers, Davis and Crawford[47] which fitted their measurements (for mixtures of ethanol with nitrogen, helium and carbon dioxide and carbon tetrachloride with nitrogen and carbon dioxide) very closely. This equation is compared with the present experimental and theoretical results in fig 6.22 and 6.23. These comparisons show that.-

(a) In contrast to Aker's results, the theoretical results (equation 3.27) do not lie close to a single line (i.e. the variation of the mass transfer parameter, $(k_g LRT/D) \times (P_{bm}/P)$, with the product of the Grashof and Schmidt number, Gr x Sc assumes different lines for different steam-gas mixtures).

(b) For given (Gr x Sc) the values of mass transfer parameter found by Akers is roughly an order of magnitude higher than those given by equation 3.27.

This difference in results may again be attributed to the experimental arrangement used. The size of the condenser chamber was small compared with the condensing surface area. In addition, the condensing surface was directly about and close to the evaporating surface. Although a baffle, in the form of a disc attached to the bottom of the condensing plate, separated the "boiler" from the condenser, it seems possible that this may not have been adequate to prevent disturbances of the free convective flow in the condenser. Such disturbances would enhance the heat transfer and thus lead to the above mentioned discrepancies between these and the present results.

Sledger's experimental results were obtained for steam-air mixtures with small gas concentration (i.e. $0<W_{\infty}<0.01$) and at low pressures. Therefore it was not possible to make a direct comparison between Sledger's data and the present experimental results. In figs 6.24-6.26, Sledger's results are compared with the corresponding values obtained using the exact solution [22], Sledger's approximate solution and equation 3.27. It may be seen from these figs that, for a given air concentration and bulk temperature, experimental Q/Q_{nu} results are generally higher than the corresponding theoretical results. These differences between theory and experiment decrease with increasing gas concentration. However, Sledger's results are much closer to the theory than the earlier measurements and these together with the present results give support to boundary layer treatment to the problem.

Fig. 6.01 Comparison of heat transfer results between exact and approximate solutions

Mixture: steam-air. Bulk temperature: 373.15 K.

- ——— exact solutions
- - - - - Rose approximate analysis
- —·+— Sledgers approximate analysis (see appendix 6)
- — — — equation 3.27

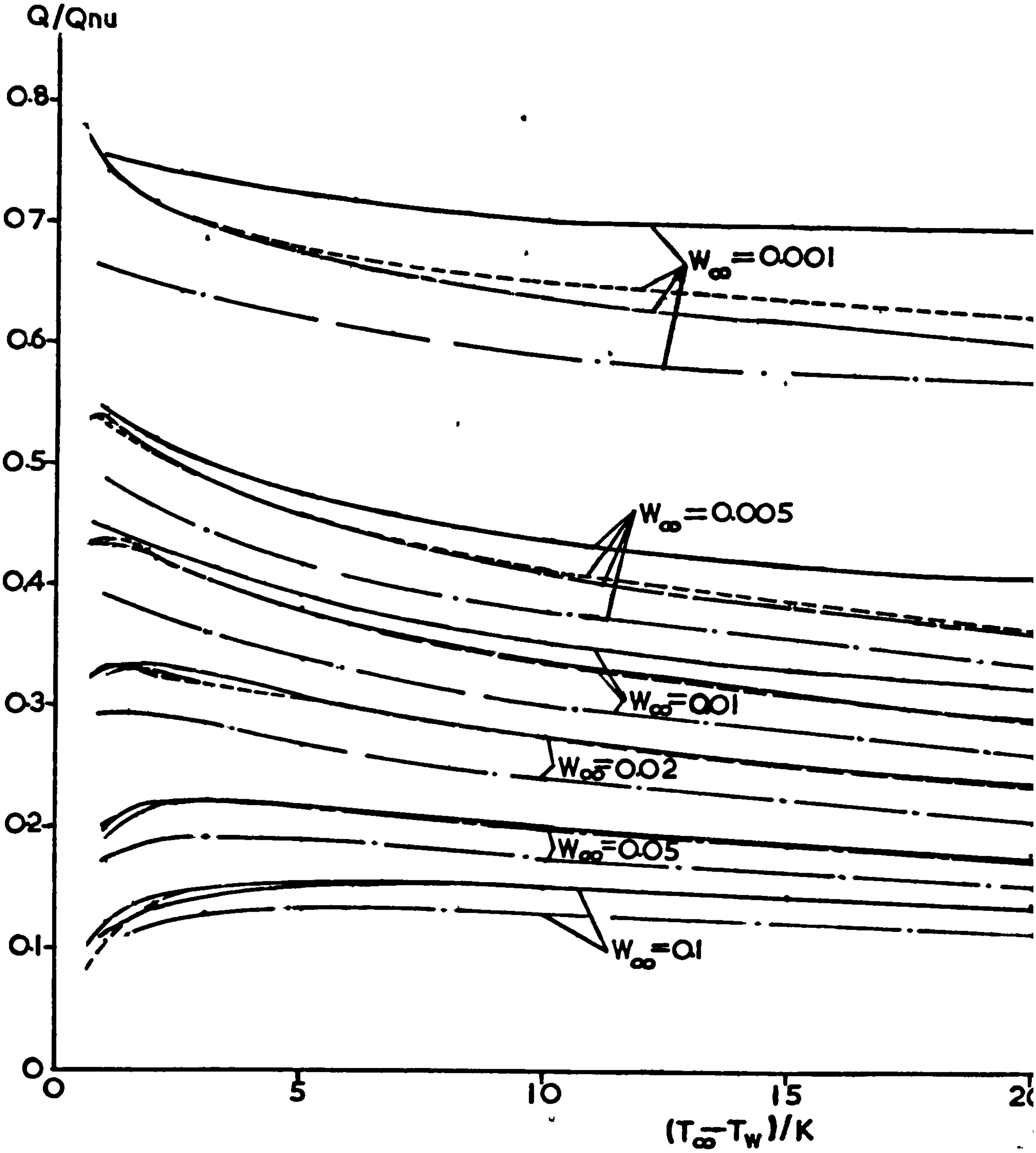

Fig 6.02 Comparison of heat transfer results between exact and approximate solutions

Mixture: steam-air. Bulk temperature: 299.82 K

——————— exact solutions

- - - - - - - Rose approximate analysis

——·—— Sledgers approximate analysis (see appendix 6)

——— — ——— equation 3.27

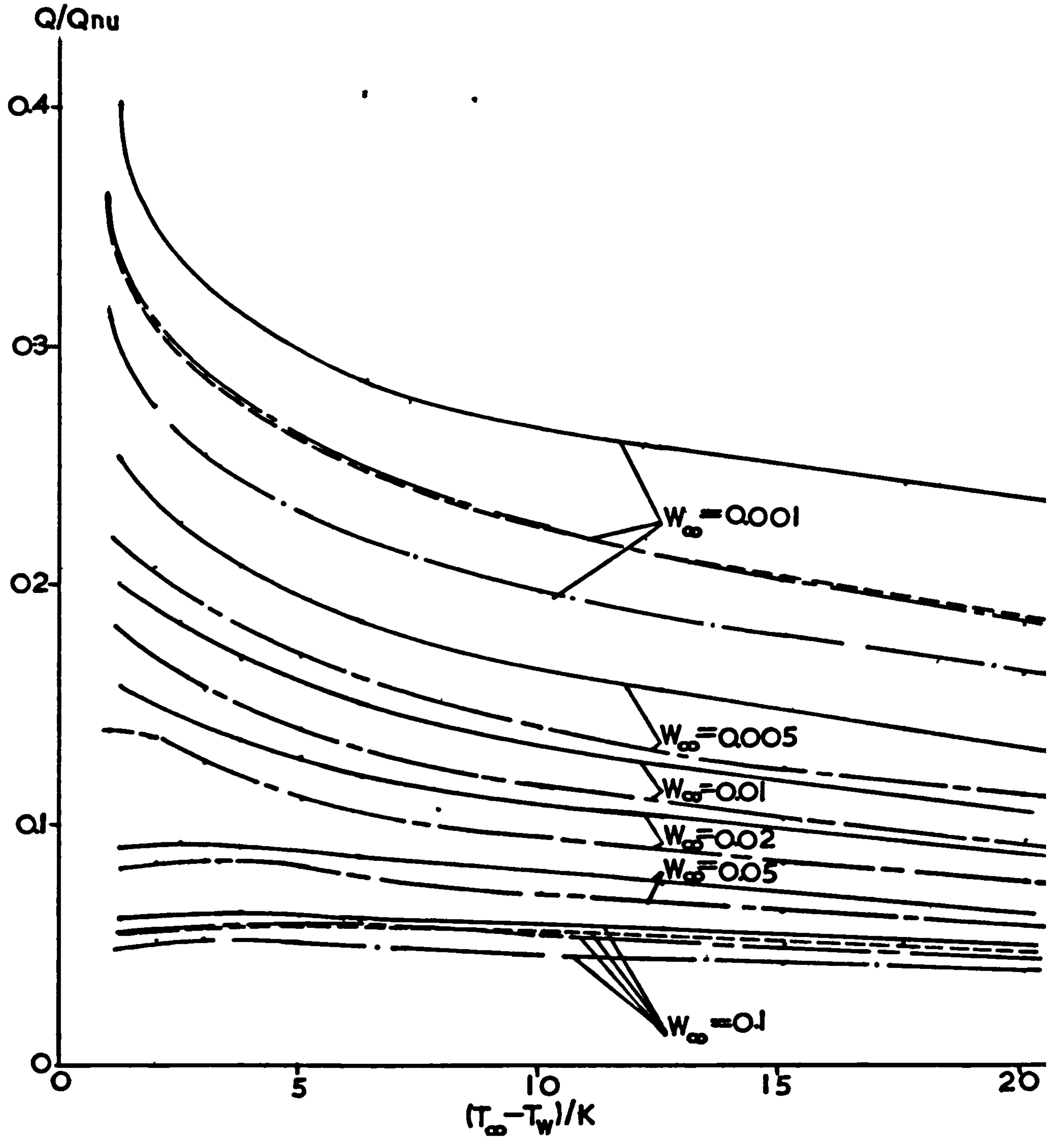

Fig 6 03 Condensation of Pure Steam at Atmospheric Pressure

Steam-to-Condensing Surface Temperature Difference against Heat Flux

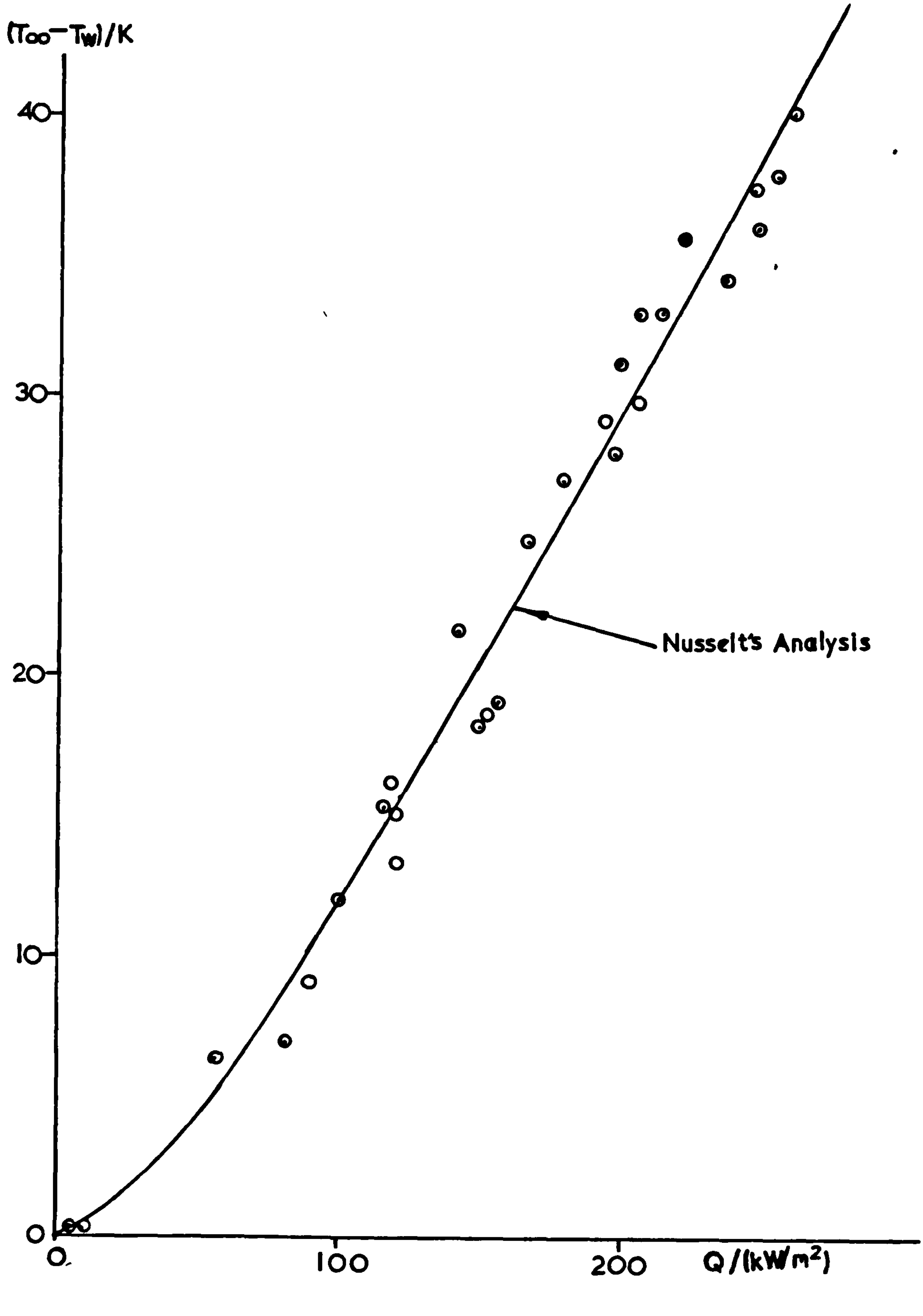

Fig 6.04 Fractional Reduction in Heat Transfer against Mean Gas Concentration

Non-Condensing Gas: Air

$40 < \left(\frac{T_\infty - T_w}{\kappa}\right) < 80$

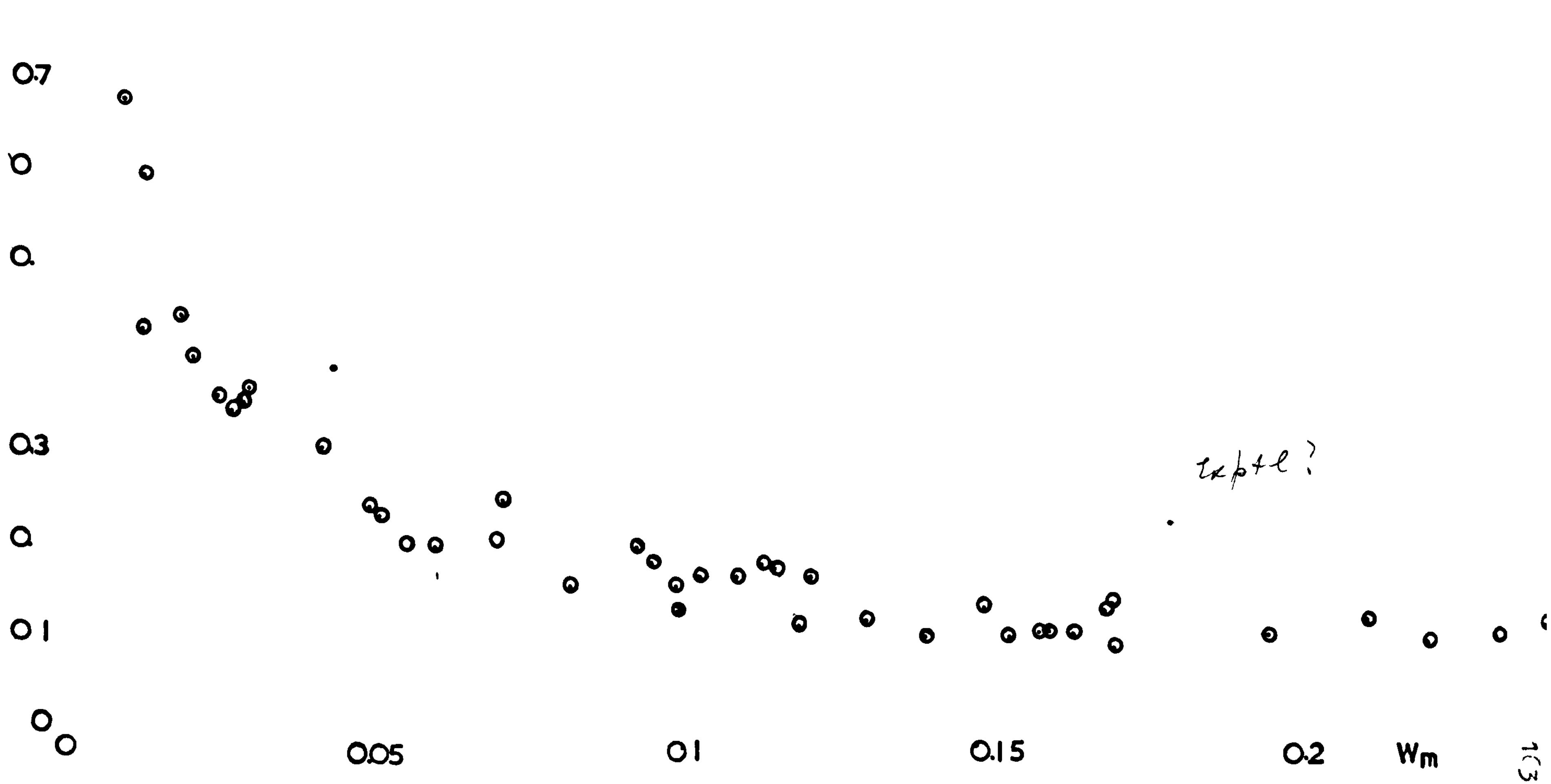

Fig 6.05 Fractional Reduction in Heat Transfer against
Mean Gas Concentration ~~outside the Mixture Boundary Layer~~

Non-Condensing Gas Argon

$45 < \left(\frac{T_\infty - T_w}{K}\right) < 75$

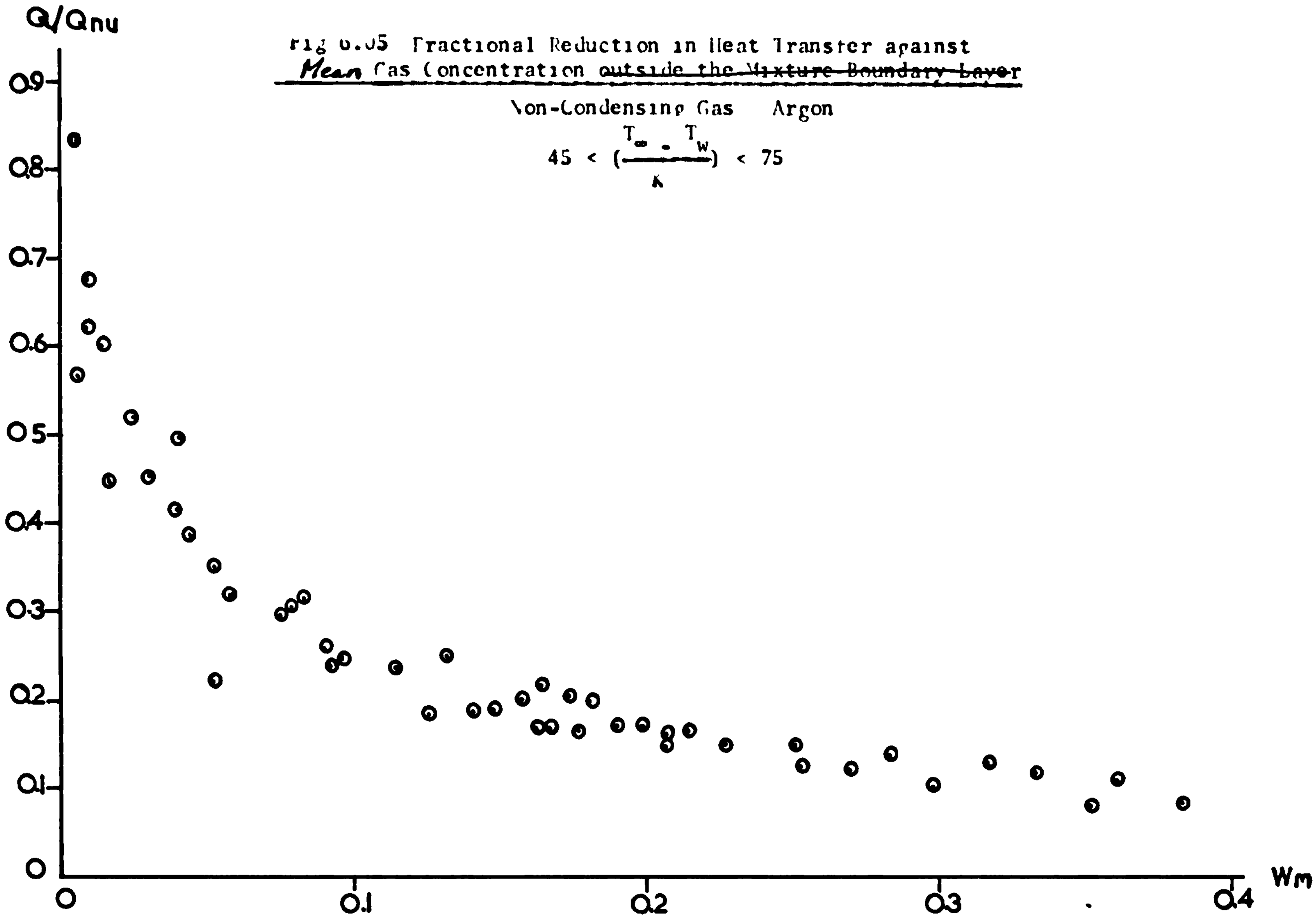

Fig 6.06 Fractional Reduction in Heat Transfer against Mean Gas Concentration

Non-Condensing Gas: Neon

$$55 < \left(\frac{T_{\infty} - T_{w}}{K}\right) < 80$$

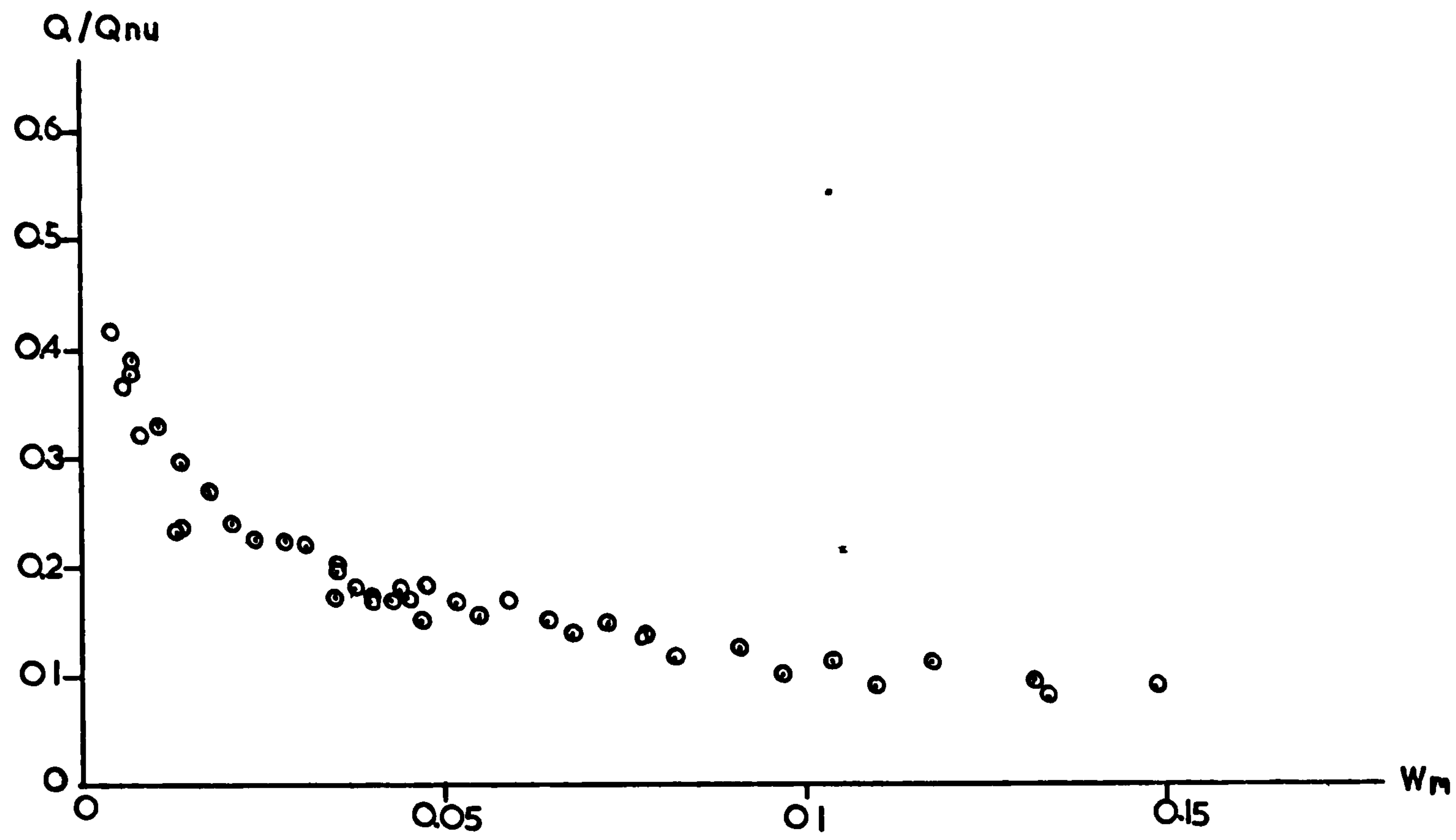

Fig 6.07 Fractional Reduction in Heat Transfer against Gas Concentration outside the Mixture Boundary Layer

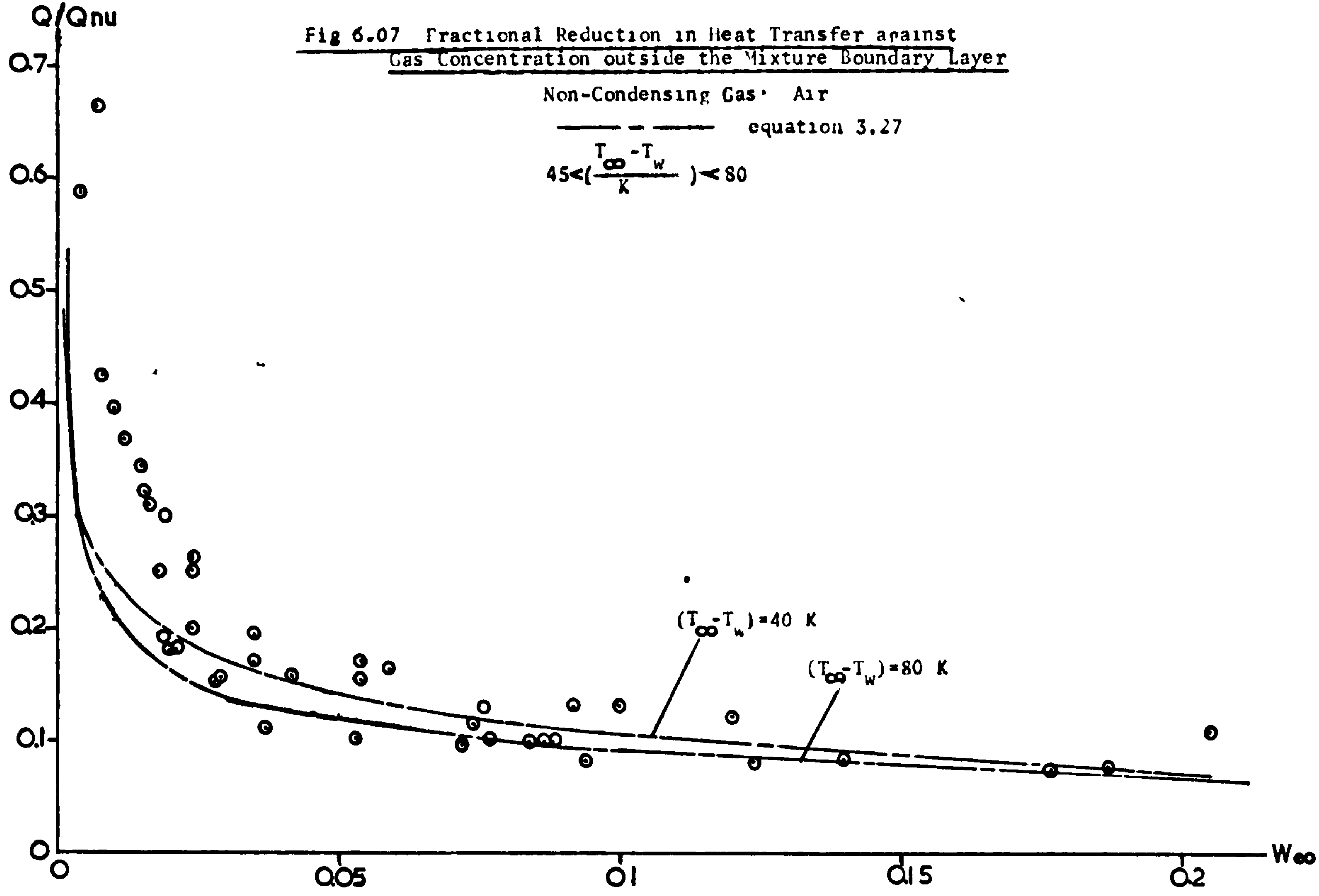

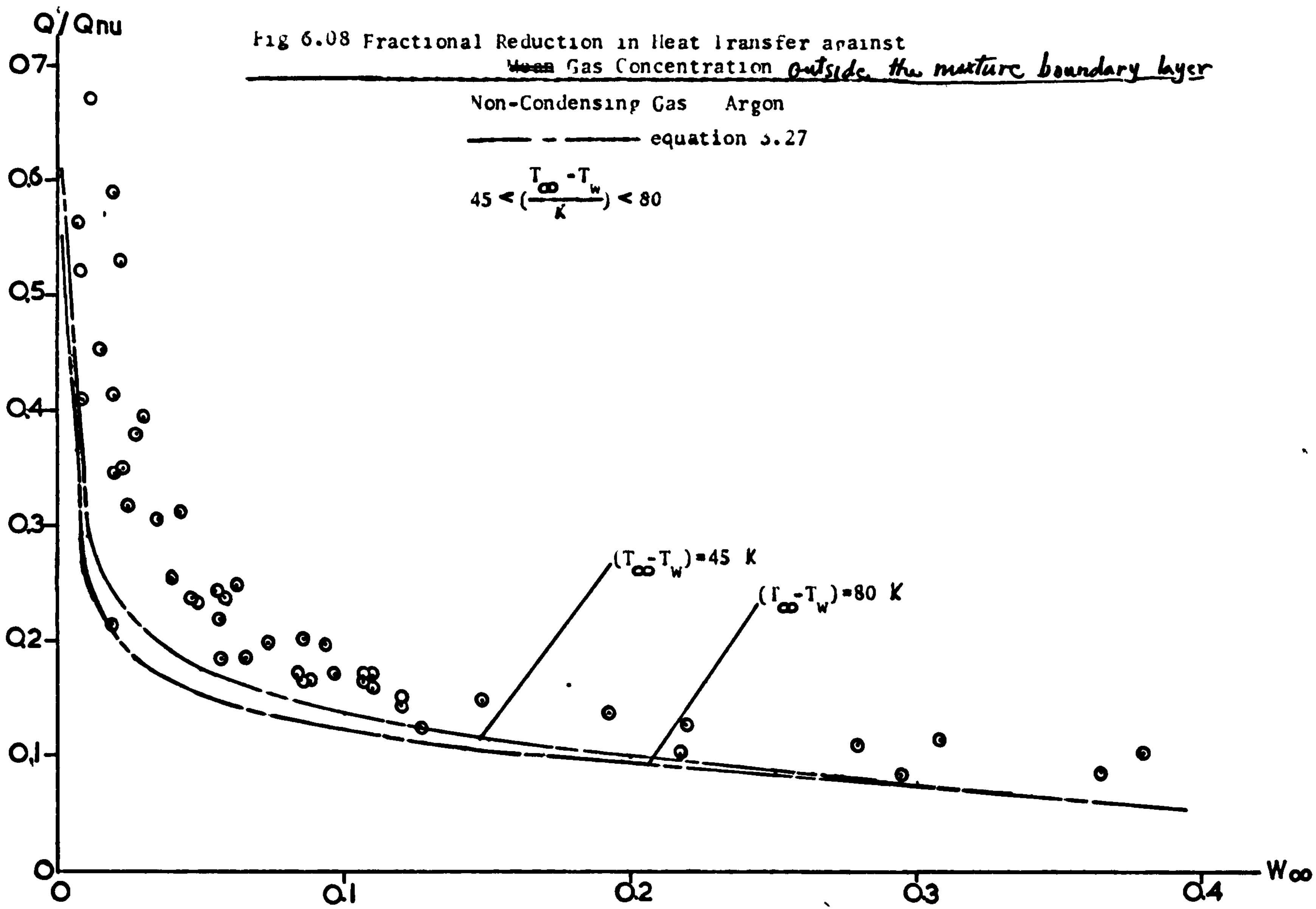

Fig 6.08 Fractional Reduction in Heat Transfer against ~~Wcon~~ Gas Concentration *outside the mixture boundary layer*

Fig 6.09 Fractional Reduction in Heat Transfer against Gas Concentration outside the Mixture Boundary layer

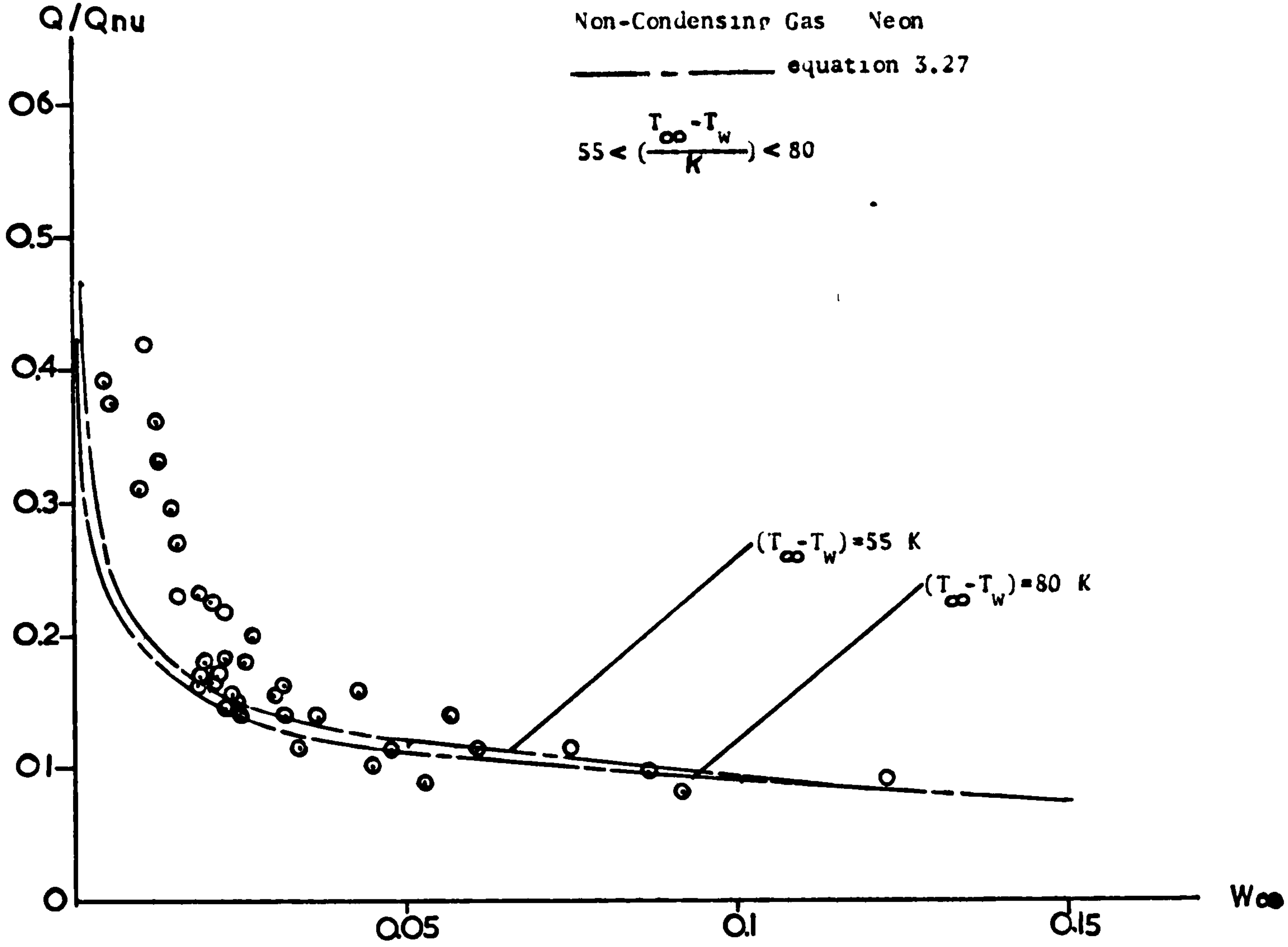

Fig 6 10 Fractional Reduction in Heat Transfer against Gas Concentration outside the Mixture Boundary Layer

Non-condensing Gas: Helium

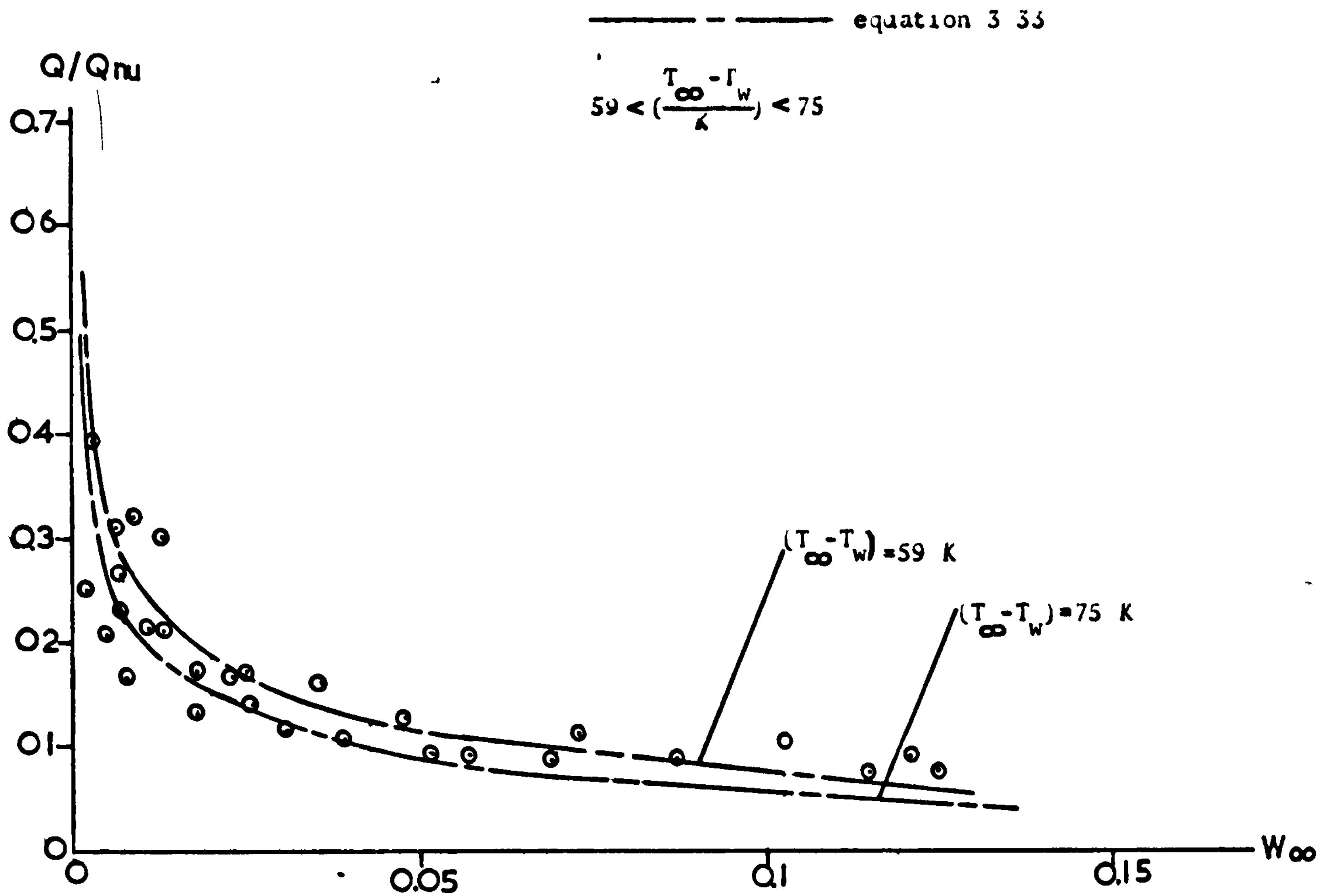

Fig 6.11 Relation between observed lean Gas Concentration and that calculated from Temperature measurement outside Boundary Layer

Non-Condensing Gas: air

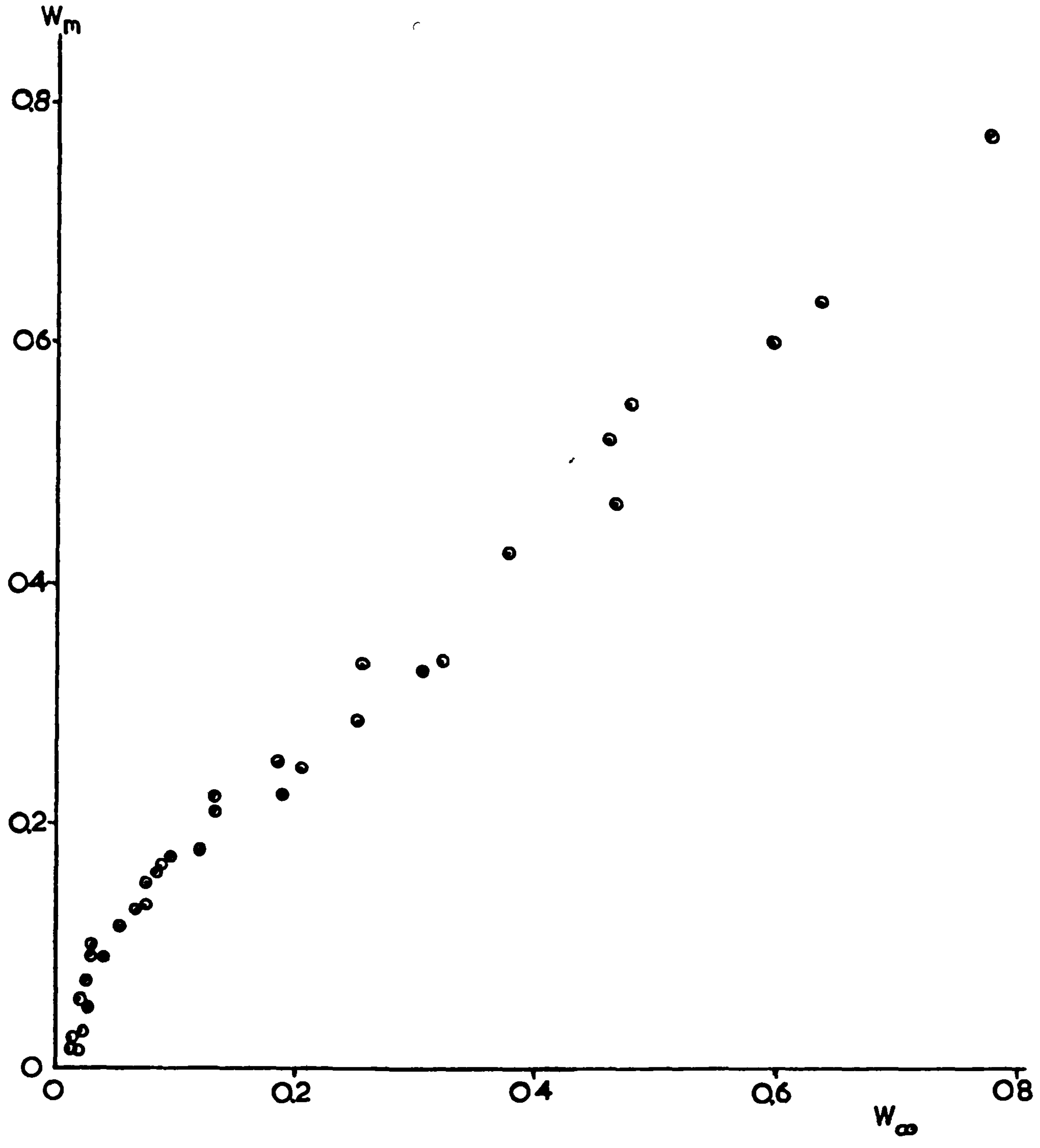

Fig 6.12 Relation between observed Mean Gas Concentration and that calculated from Temperature measurement outside boundary Layer

Non-Condensing Gas.argon

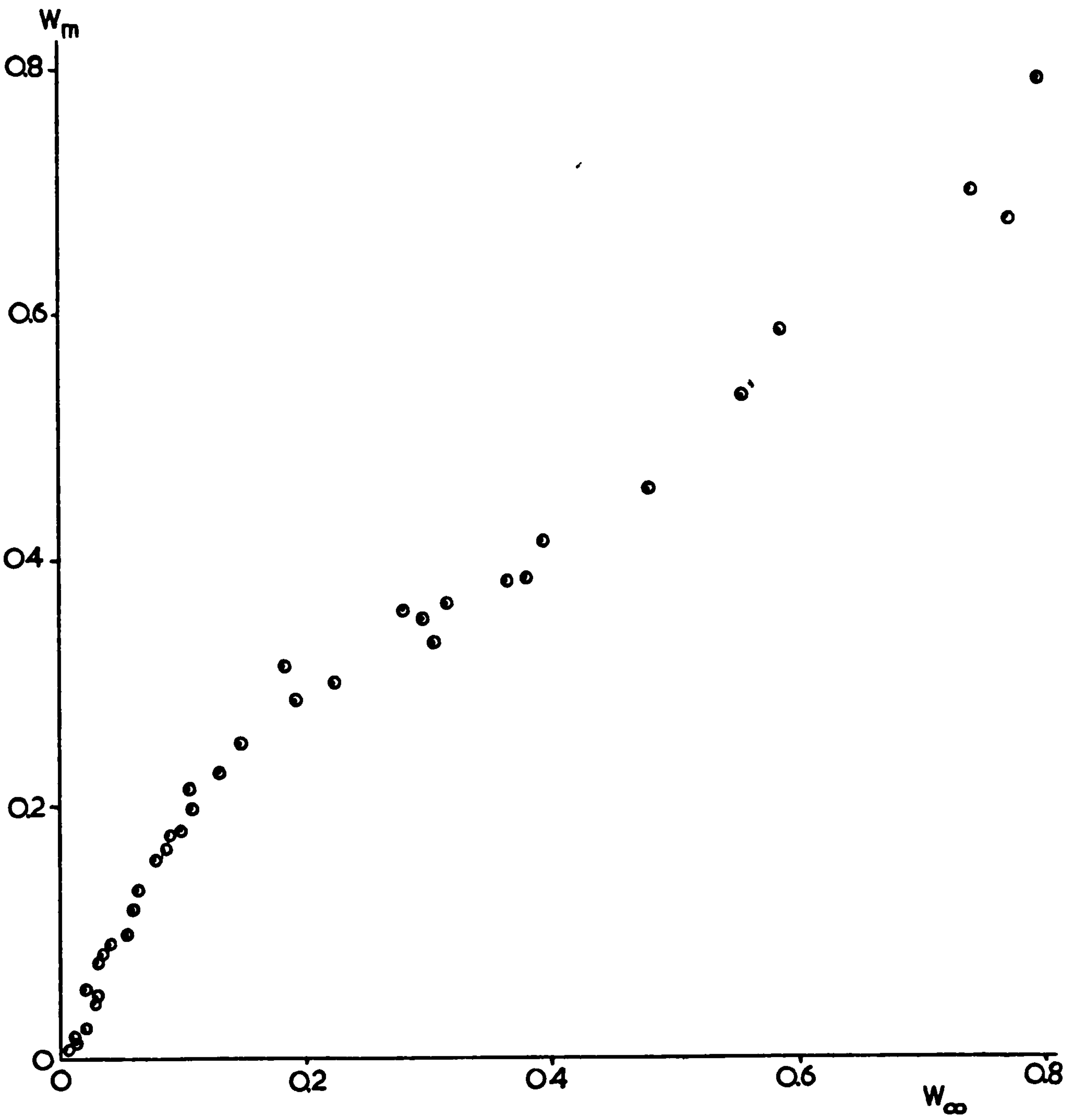

Fig 6.13 Relation between observed Mean Gas Concentration and that calculated from Temperature measurement outside Boundary Layer

Non-Condensing Gas. neon

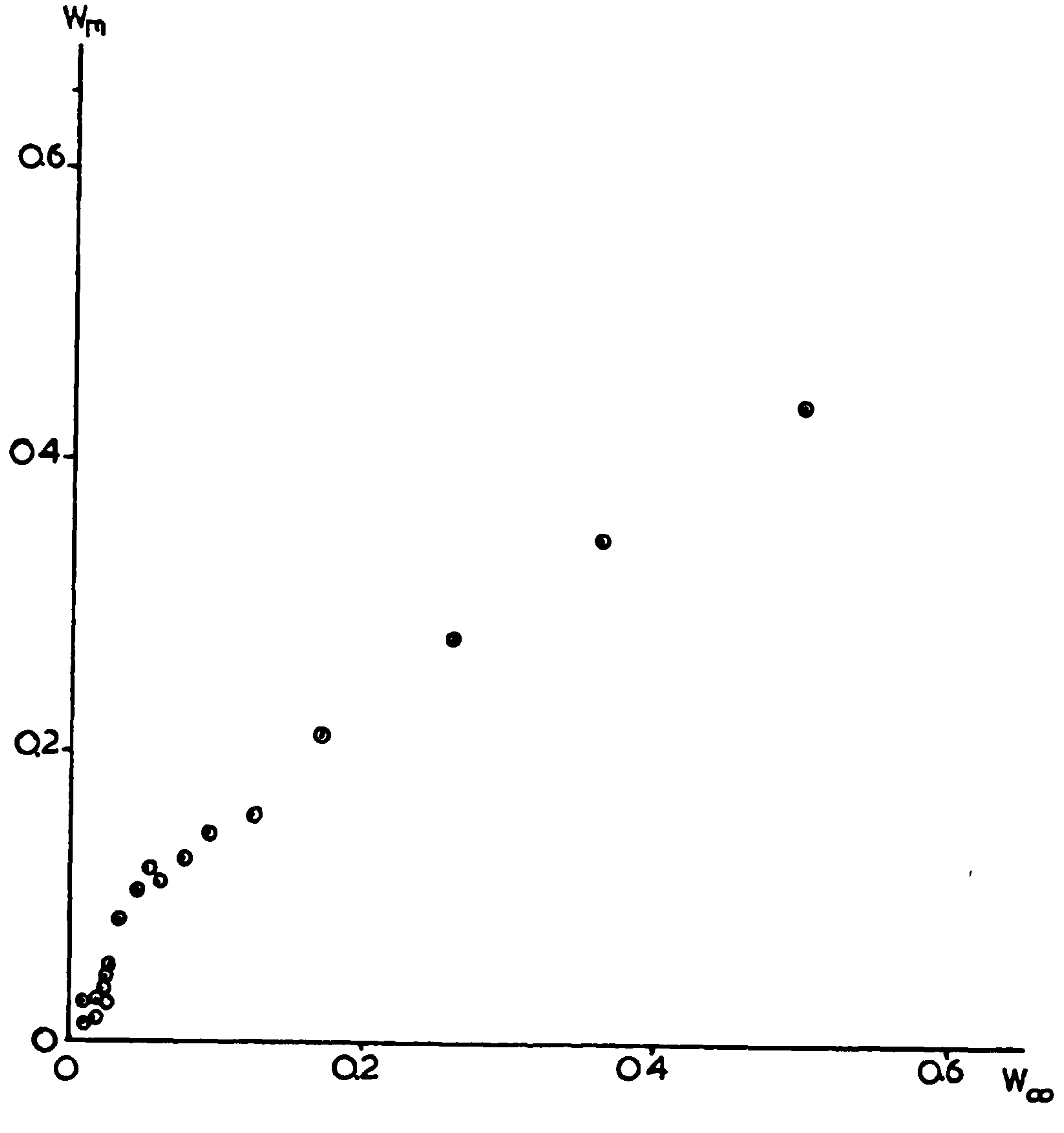

Fig 6.14 Fractional Reduction in Heat Transfer against Vapour-to-Condensing Surface Temperature Difference

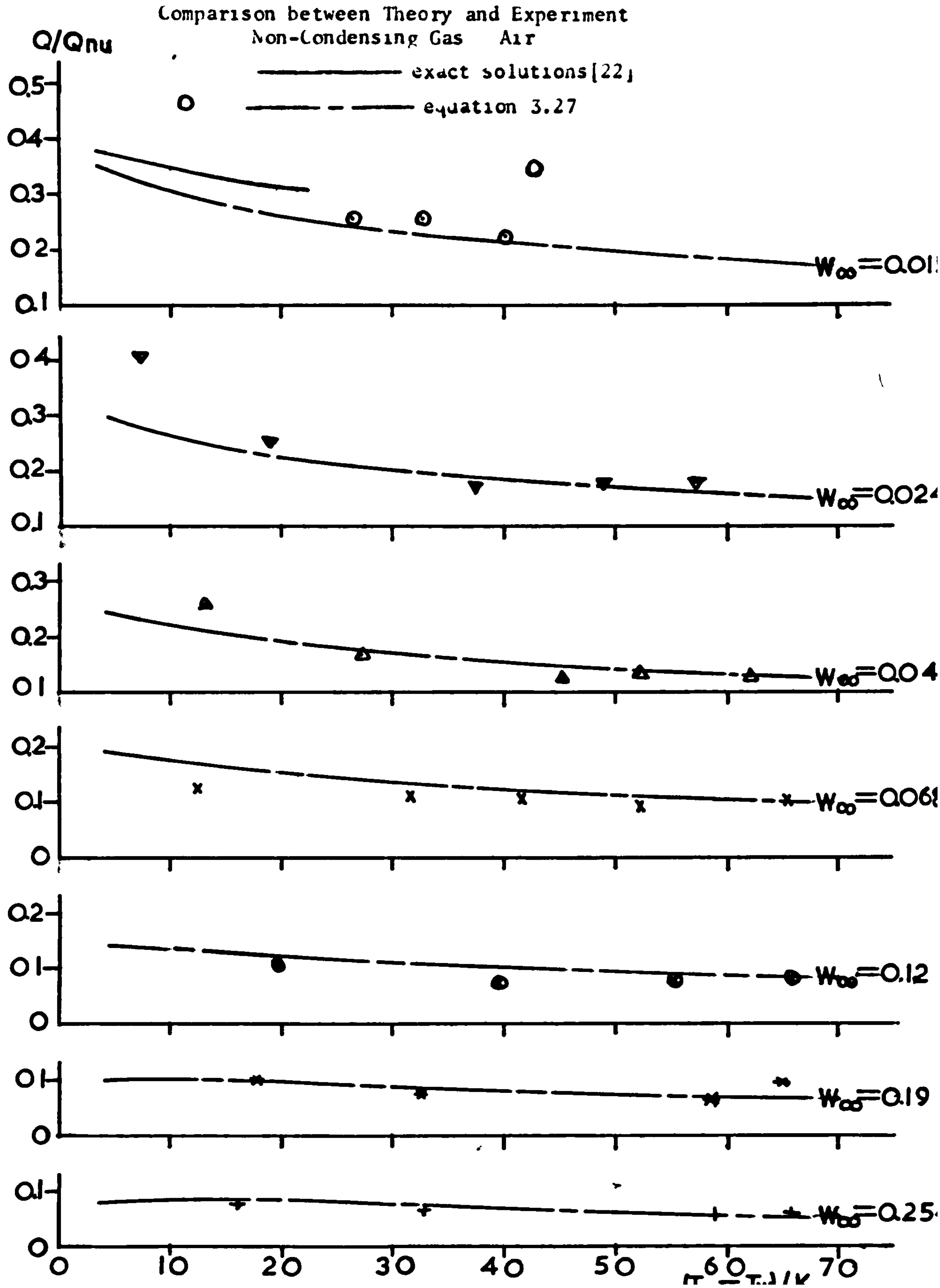

Fig 6.15 Fractional Reduction in Heat Transfer against Vapour-to-Condensing Surface Temperature Difference

Comparison between Theory and Experiment

Non-condensing gas: Argon

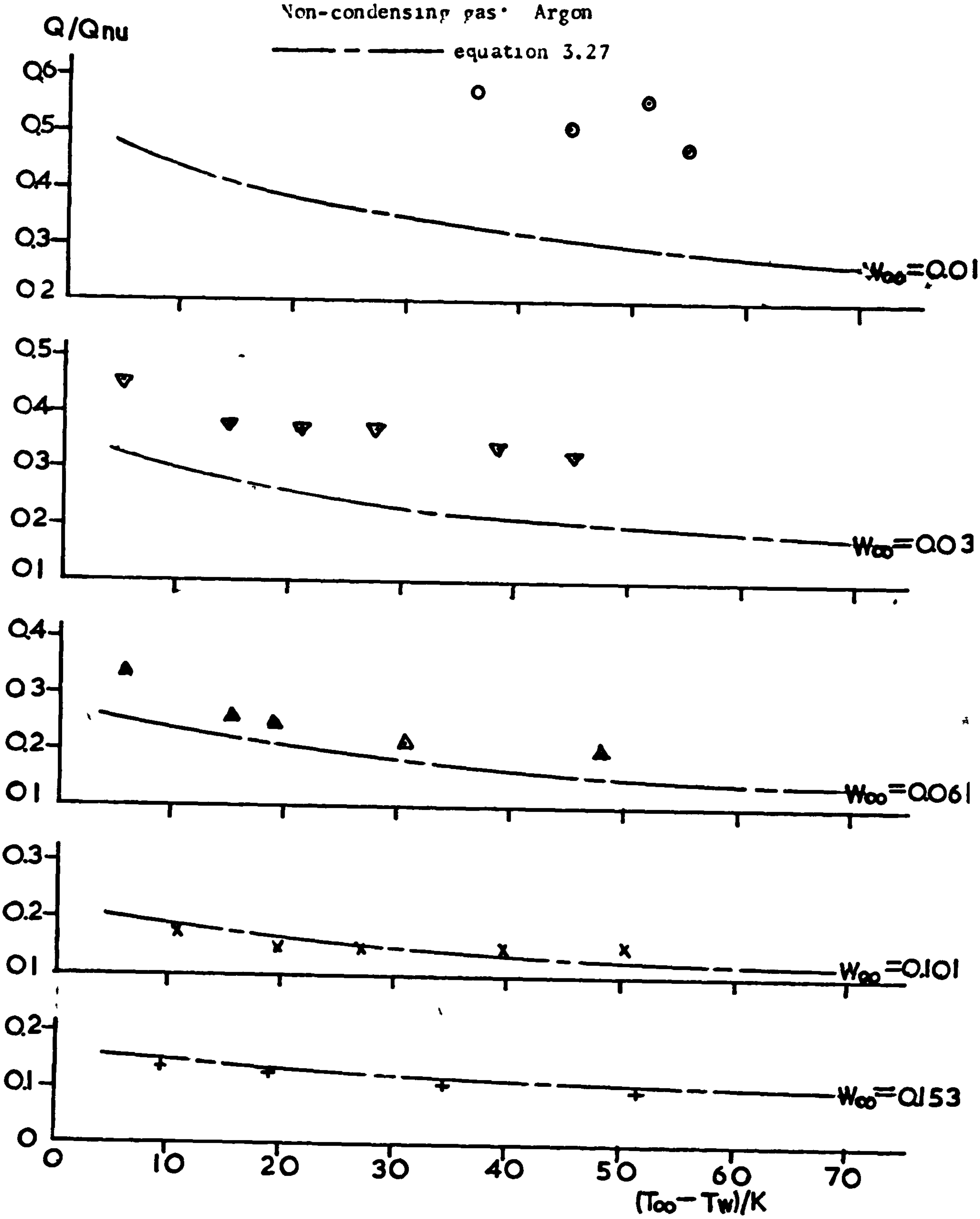

Fig 6 16 Fractional Reduction in Heat Transfer against Vapour-to-Condensing Surface Temperature Difference

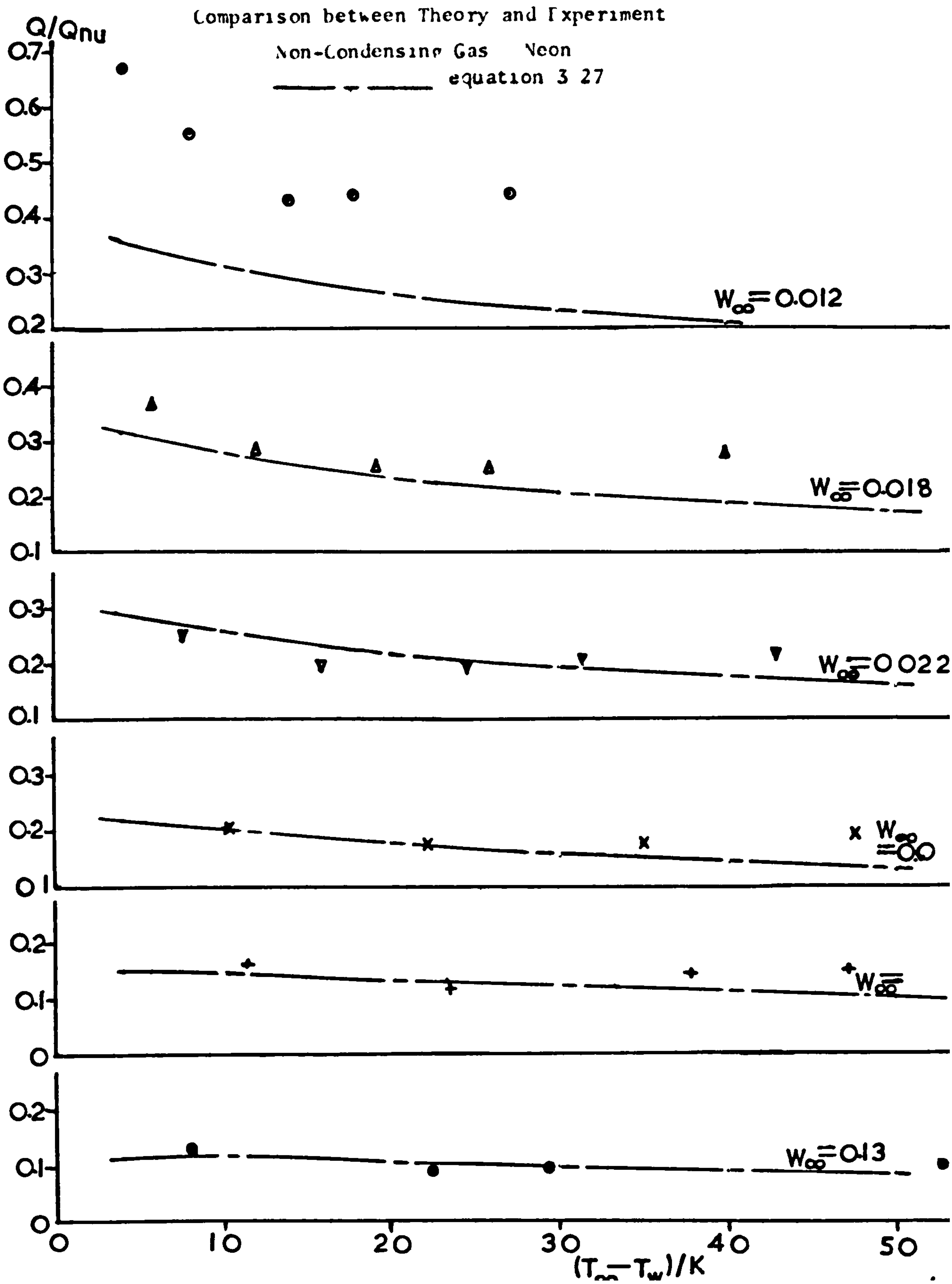

Fig 6.17 Fractional Reduction in Heat Transfer against Vapour-to-Condensing Surface Temperature Difference

Comparison between Theory and Experiment

Non-condensing gas Helium

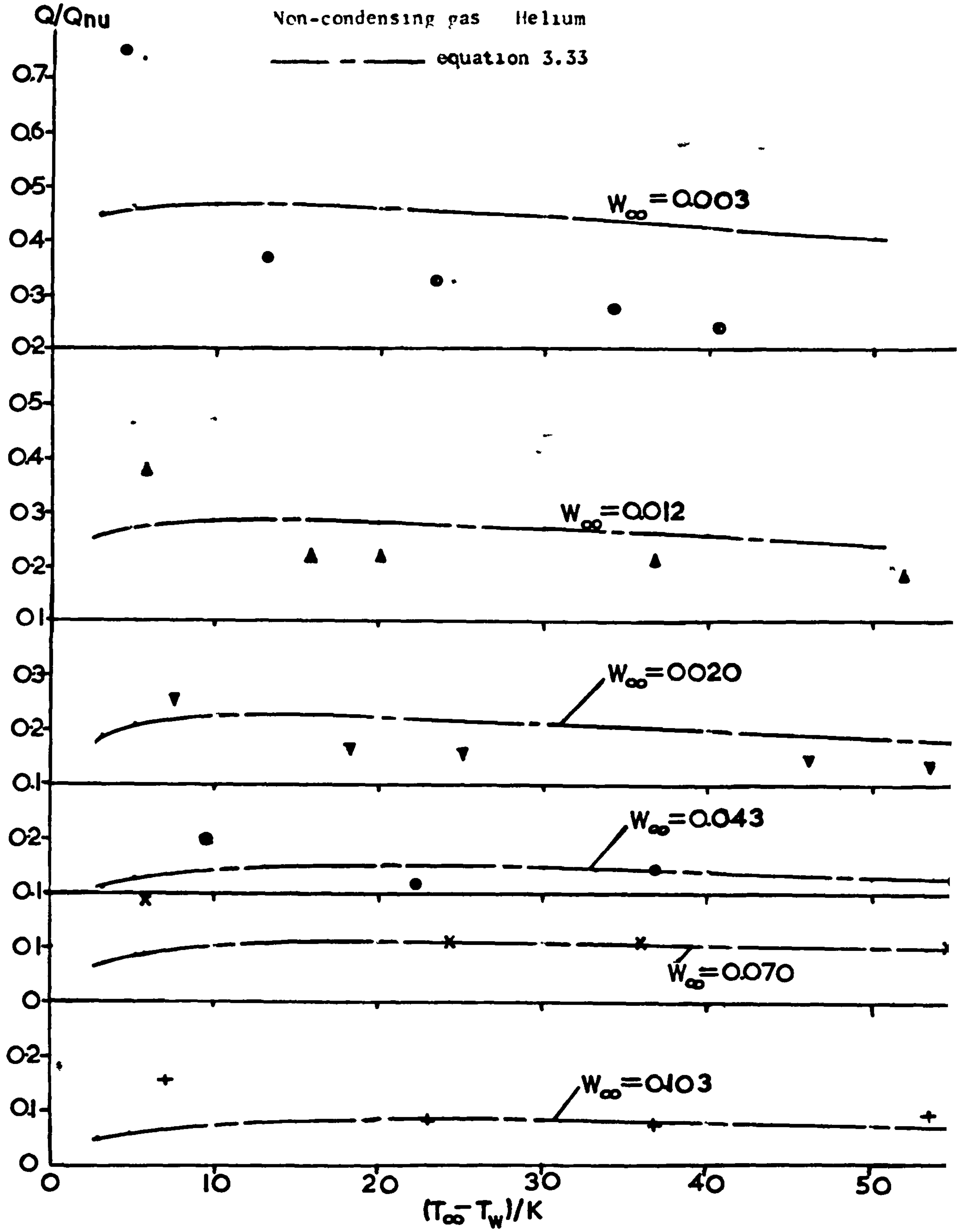

Fig 6.18 Theoretical heat transfer results given by equation [illegible]

Mixture: steam-argon
Bulk temperature: 373.15 K

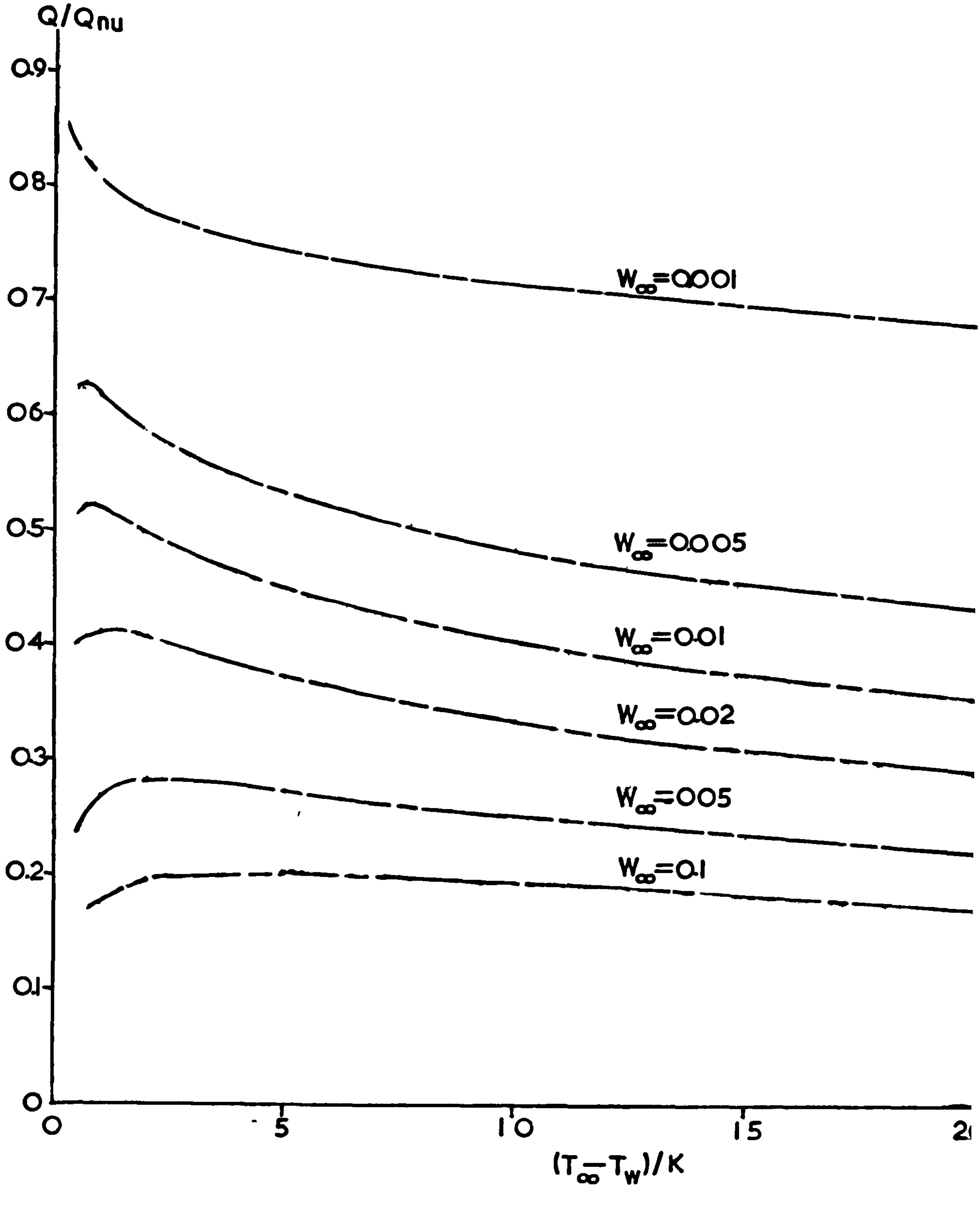

Fig. 6.19 Theoretical heat transfer results given by equation 3.27

Mixture: steam-neon
Bulk temperature: 373.15 K

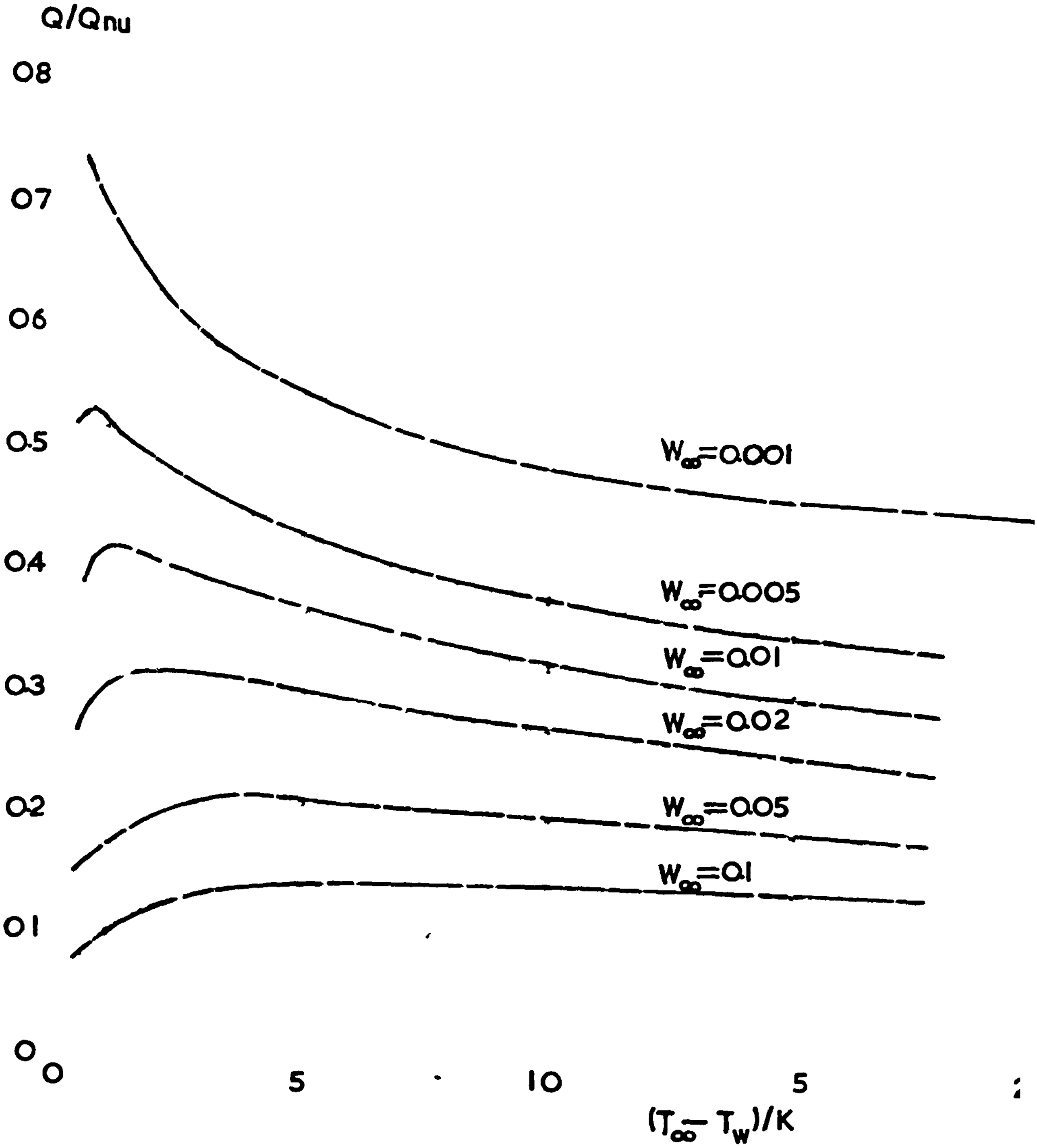

Fig. 6.20 Comparison of the theoretical heat transfer results for various steam-gas mixtures

Bulk temperature: 373.15 K
——- - —— equation 3.27

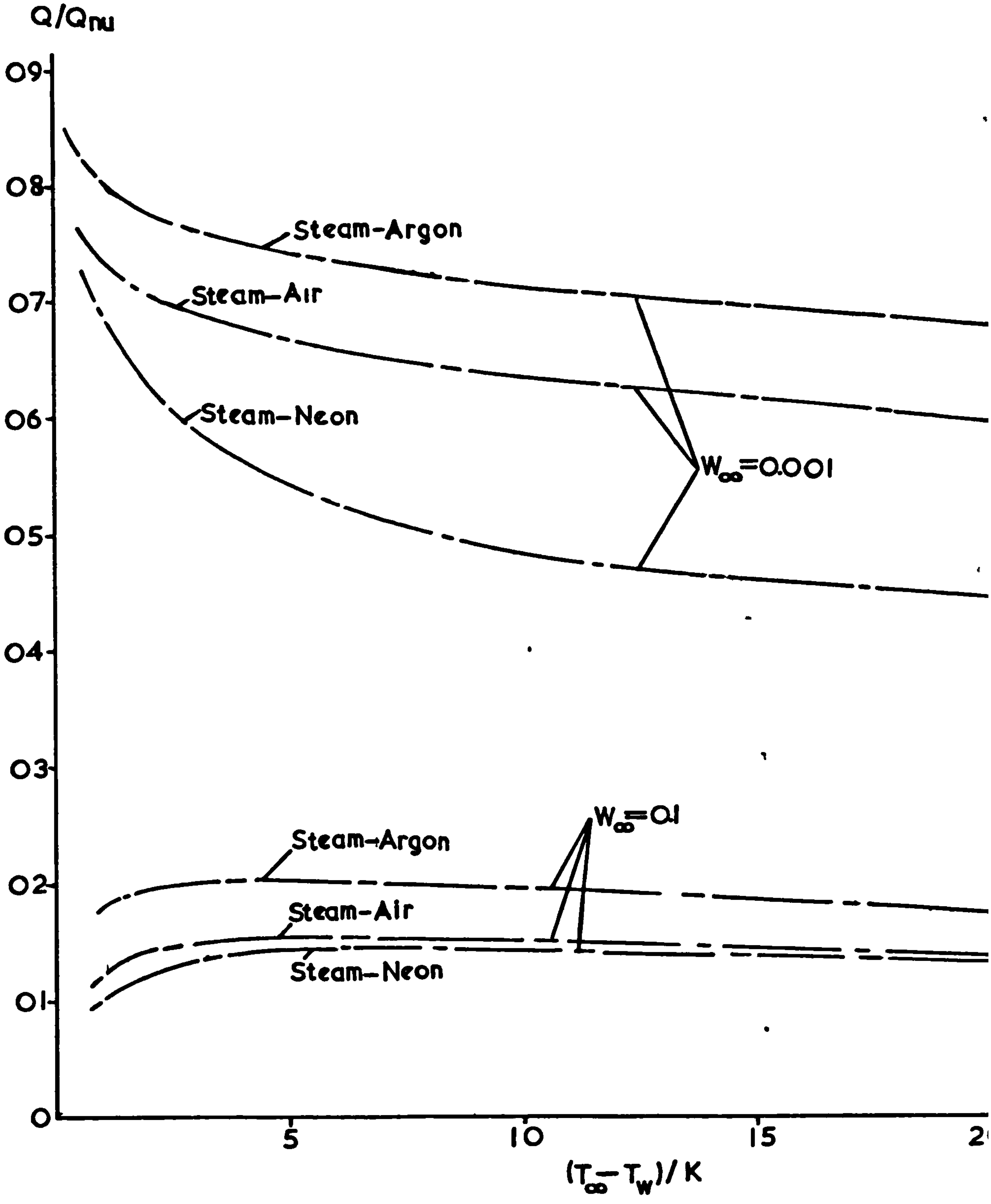

Fig 6.21 Comparison of heat transfer results between equation 3.27 and Hampson's experimental data [45]

Mixture: steam-nitrogen. Bulk temperature: 374.5 K

——— Hampson's results)the numbers refer to the

— - — equation 3.27)nitrogen concentrations

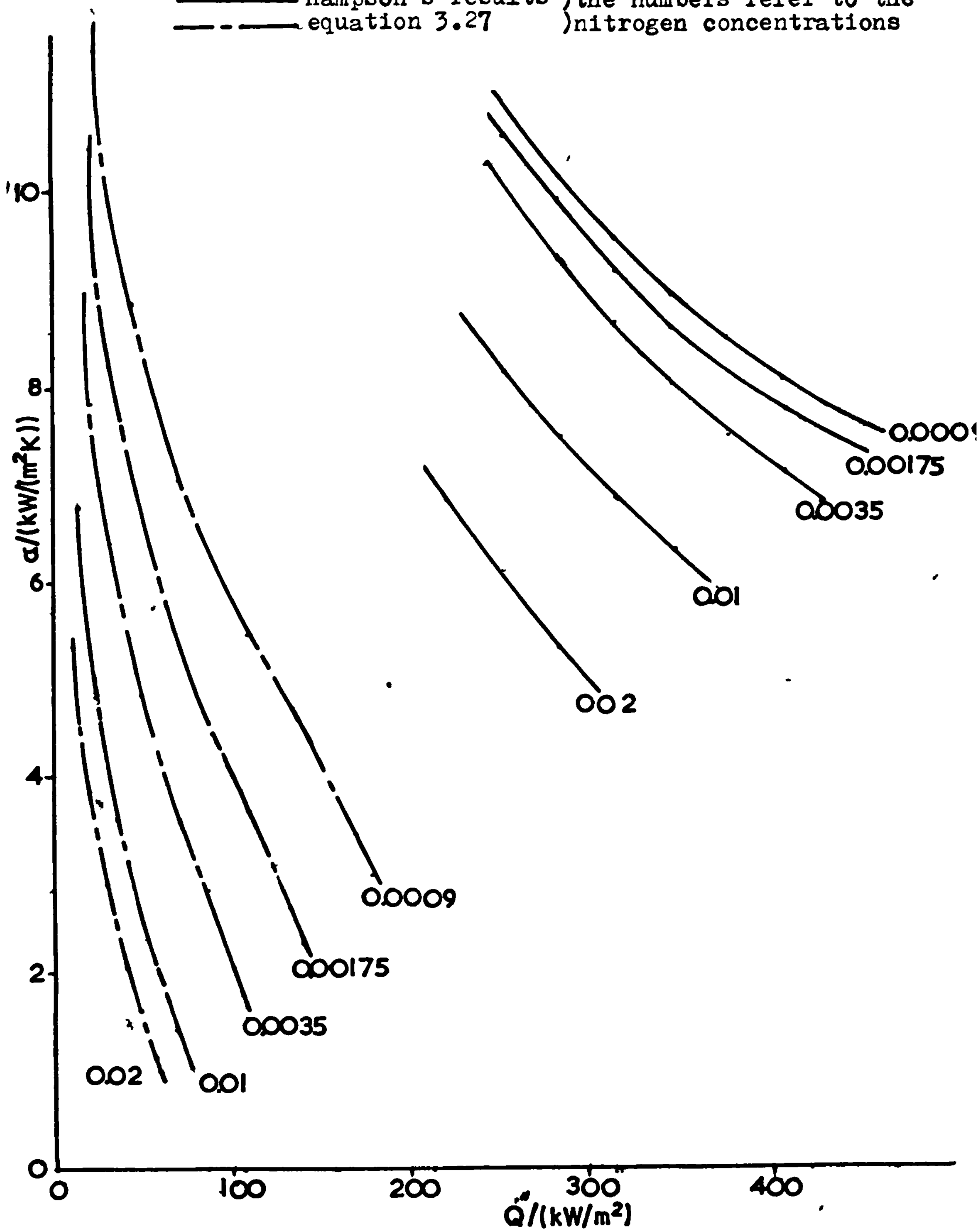

Fig 6.22 Comparison of heat transfer results between equation 3.27 and Akers, Davis&Crawford equation [47]

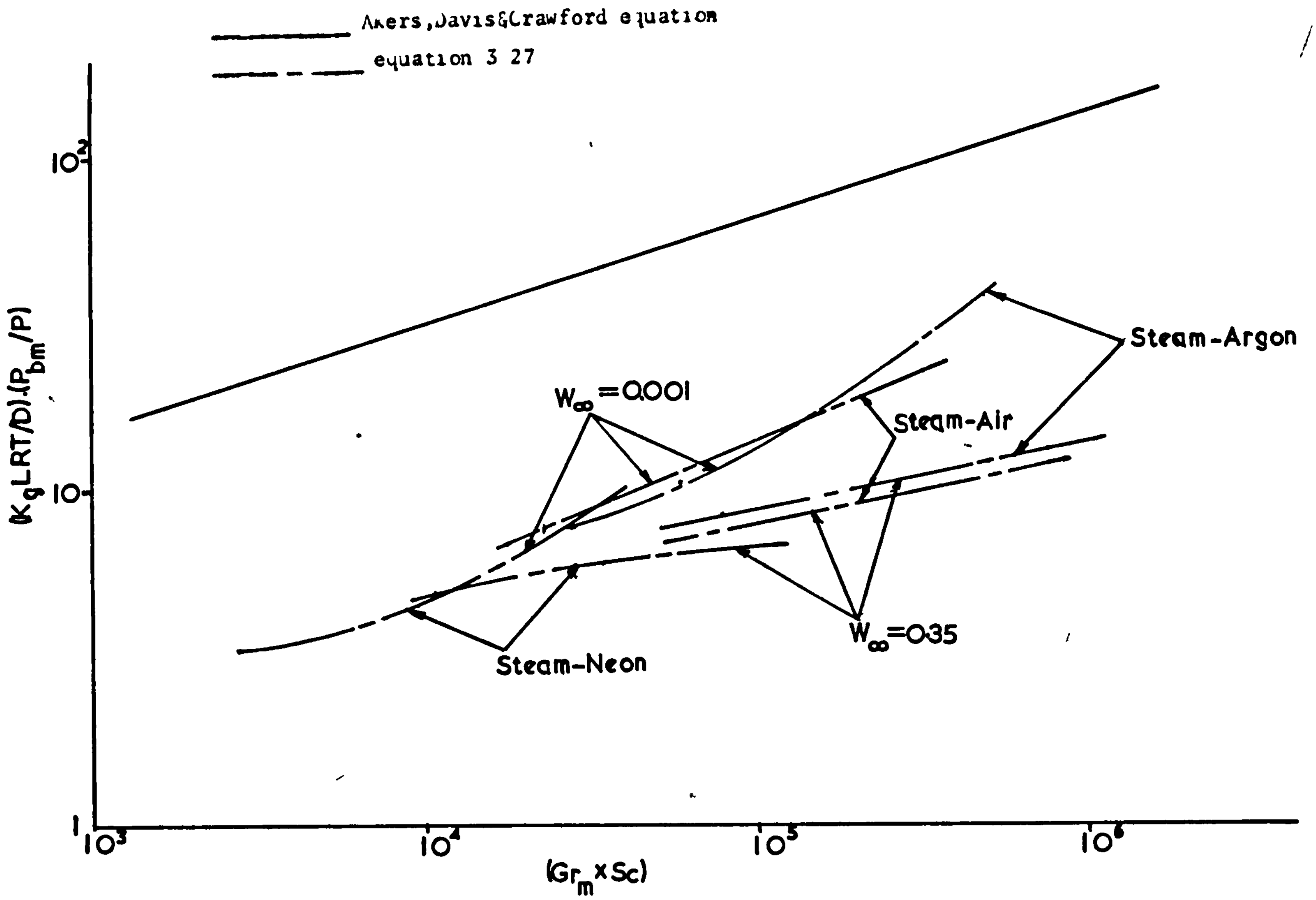

Fig. 6 23 Comparison between present experimental data and Akers, Davis&Crawford equation[47]

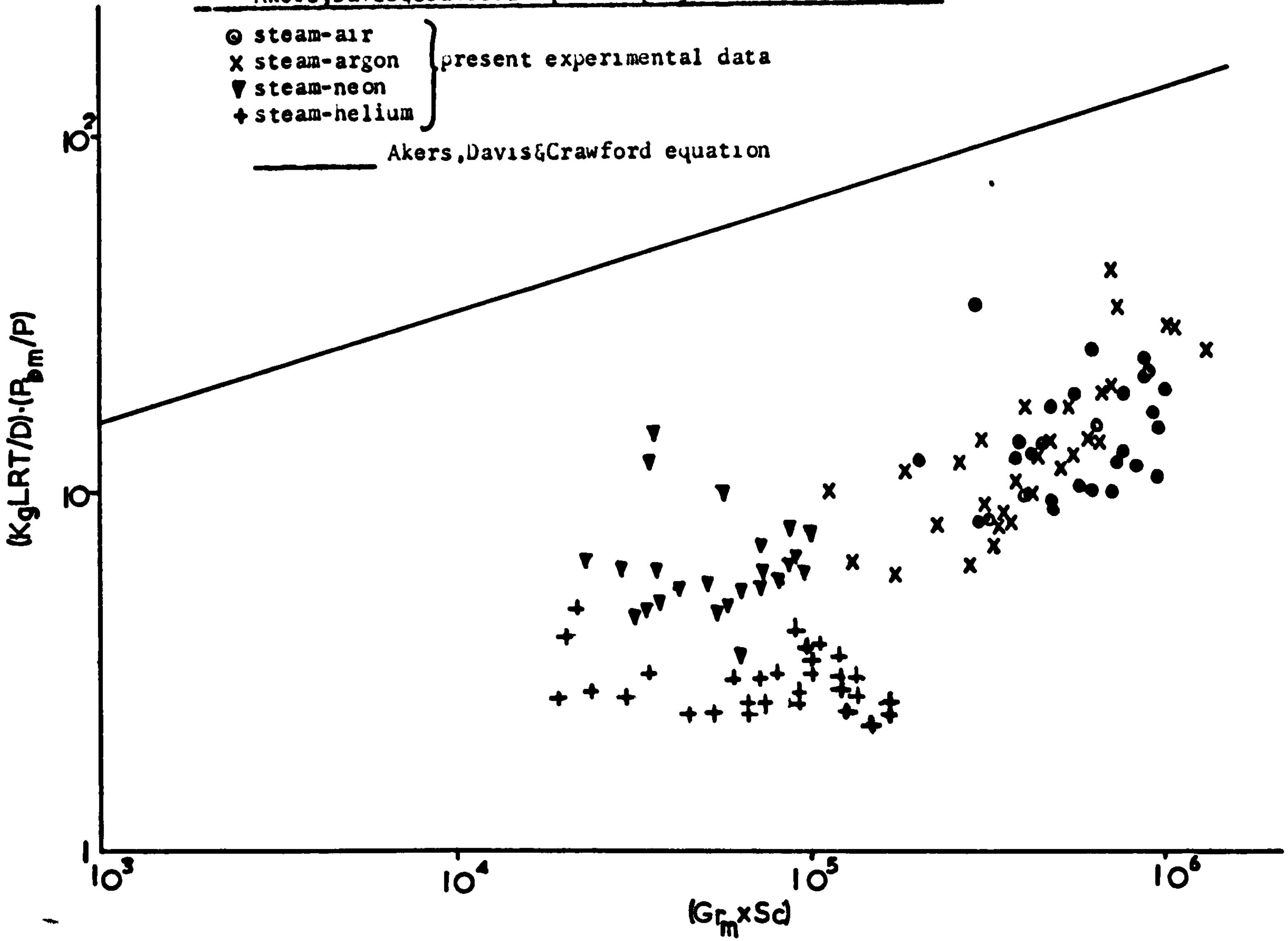

Fig 6.24 Comparison of heat transfer results between theory and Sledgers experimental data [44]

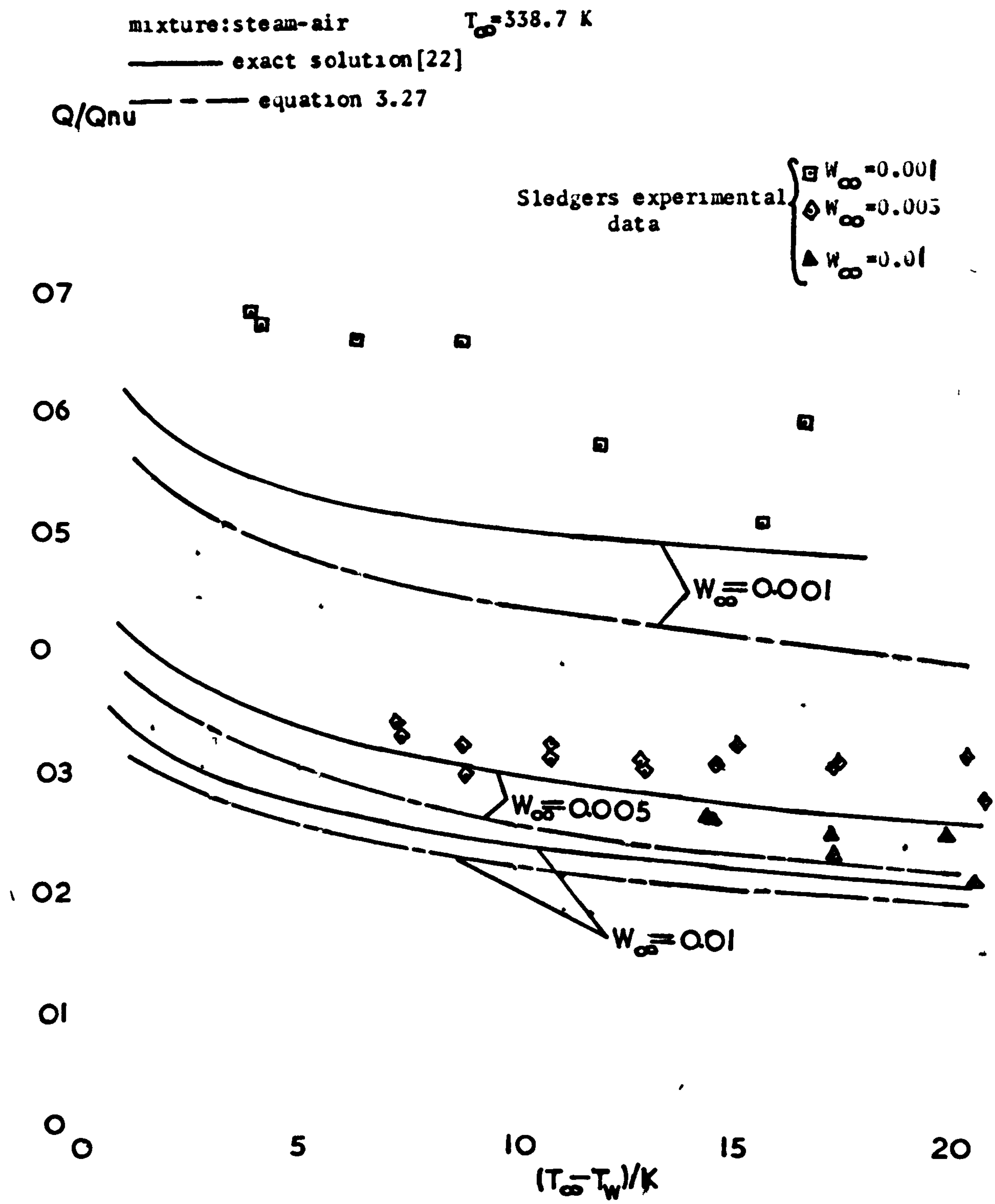

Fig 6.25 Comparison of heat transfer results between theory and Sledgers experimental data [44]

mixture:steam-air T_∞=319.3

——— exact solutions [22]

— — — equation 3.27

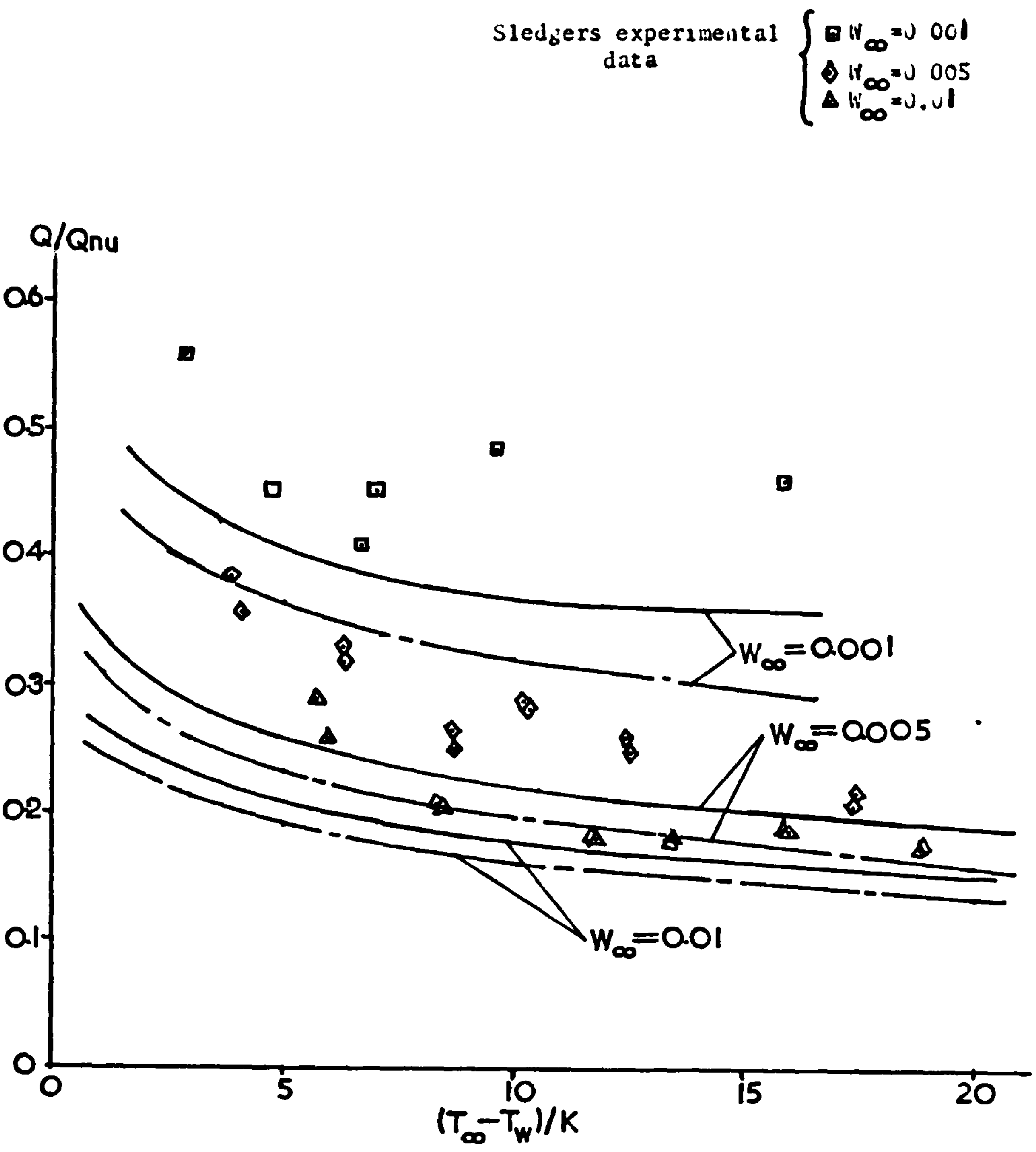

Fig 6.26 Comparison of heat transfer results between theory and Sledgers experimental data [44]

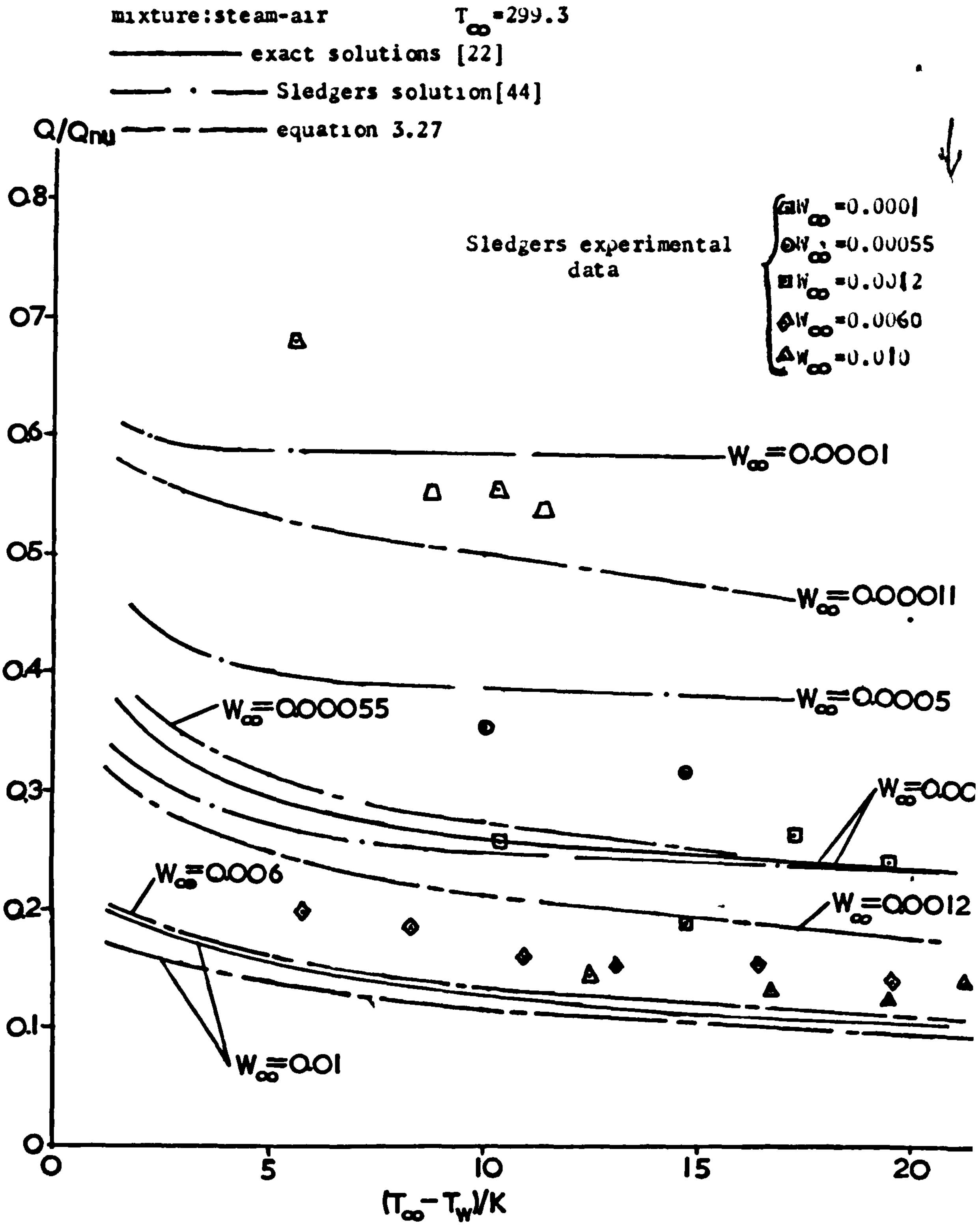

Chapter 7

Concluding Remarks

For film condensation in the presence of a non-condensing gas, the existing boundary-layer solutions for plane vertical surfaces under conditions of free convection have been reviewed. These solutions are valid only for the case where the non-condensing gas has a higher molecular weight than the vapour. "Exact" numerical solutions have, to date, only been evaluated for air-steam mixtures [22, 37]. The numerical work involved is such that the time requirement, even with modern computers, is considerable. Approximate "integral" solutions have also been given [43, 44], leading to closed-form results, which may be readily applied to any gas-vapour combination where the gas is heavier than the vapour.

In the course of the present work the approximate solution [43] was modified to include the variation with height of the condensate layer thickness, formerly omitted. The heat-transfer results for air-steam mixtures using the new result differed very little from the original, both agreeing satisfactorily with the "exact" solution. In the case of the other approximate solution [44] the present author was unable to confirm that the method adopted led to the result given [44]. However, the analysis was re-worked by the present author (see appendix 6) and the results obtained agreed fairly well with the "exact" solution for air-steam mixtures but not so closely as either version of the alternative approximate approach.

Prior to the present work little experimental work had been carried out in this field using flat plates. Such results as were available were not in good agreement with the above-mentioned theoretical results. The present results for mixture of air, argon and neon with steam, however, together with others obtained independently during the course of the present work [44] (using steam-air mixture at low pressures) are in satisfactory agreement with the theory. Moreover, the observed temperature profiles in the present study (see appendix 1), help to confirm that the boundary layer approximation is valid in this case, (it is suggested that in the case of the earlier results effects of forced convection may have been significant).

There is at present no satisfactory solution for the case where the non-condensing gas has a molecular weight smaller than that of the vapour. In the present work, experiments have been carried out with such a combination (steam-helium) and a semi-empirical correlation proposed.

The case of condensation on a horizontal tube has, on account of the greater practical importance, received more attention from experimenters. however, there exists at present no satisfactory theoretical solution for the case. It is thought that the present work, in removing doubts regarding the validity of the boundary-layer approach to this problem, may contribute towards a solution for the case of the horizontal tube.

Appendices

Appendix 1 Velocity measurements and temperature profiles in the steam-gas mixture

Appendix 2 Vertical temperature variation in the steam chamber

Appendix 3 Specimen Calculations

Appendix 4 Experimental errors

Appendix 5 Condensation of steam from steam-carbon dioxide mixture

Appendix 6 Consideration of Sledger's analysis [44]

Appendix 7 Computation of the theoretical results

Appendix 1

Velocity measurement and temperature profiles in the steam-gas mixtures

Initially it had been planned to observe the steam-gas mixture temperature, and velocity and the gas concentration profiles within the mixture boundary layer. The object being to verify the profiles assumed in the approximate analysis of chapter 3.

The temperature profiles were determined as indicated in chapter 5. These profiles will be discussed later.

Measurement of gas concentration involves sampling the mixture. However, this technique is laborious and was considered to be outside the scope of this thesis.

The fibre anemometer was considered for use to measure the steam-gas mixture velocity.

A1.1 Velocity measurement using the fibre anemometer

This technique was used by Schmidt and Beckman [74] to determine the velocity profiles in natural convection flow, in air, along a heated flat plate. The anemometer was chosen in preference to the hot wire anemometer on account of the low velocities to be measured. The technique was further developed by Tritton [75, 76] and was used to measure small velocities in wind tunnels. The technique entails the measurement of the deflection of the free end of a very thin uniform quartz fibre, subtended in the flow. The other end is secured in a rigid base so that the fibre acts as a cantilever. The deflection of the fibre is caused by the drag of the fluid. This technique was adopted here because of its simplicity and precision (Tritton [76] estimated that the accuracy of his velocity measurements was within 2%).

Precision of the fibre anemometer

To test the precision of the anemometer measurements, air was passed through a long channel (6ft) of a rectangular cross section (6in x 0.5in) made out of perspex. The anemometer was situated near the outlet of the channel so as to determine the air velocity profiles across the thickness of the channel (i.e. across the 0.5in side). The air mean flow rates estimated from these profiles (in these estimations the velocity across the width of the channel was assumed to be constant) agreed very well with the observed flow rates from the flow meter inserted at the inlet of the channel.

The use of the fibre anemometer in the present problem

Initially the apparatus was fitted with the fibre anemometer which was used to determine the shape of the flow dispersing section (see section 4.3).

To examine the applicability of the fibre anemometer in measuring the mixture velocity in the present problem, tests were carried out in which steam was allowed to condense on the test plate while visually observing the effect of steam on the fibre performance. These observations were made through the telescopes described in section 4.3. The steam was observed to condense on the fibre in the form of drops. To obviate this effect, an electrical heater was installed, fig A1.01. The steam was again allowed to condense on the test plate. The heater was switched on as soon as the drops began to appear on the fibre. The heater was then switched off when these drops evaporated. Within a few minutes new drops appeared on the fibre.

This behaviour indicated that in order to prevent condensation on the fibre, the fibre has to be heated continously. However, if heating of the fibre was to be provided, the heater would have had to be controlled so that the heater temperature would be the same as the local temperature of the mixture (this is to avoid affecting the condition of the mixture).Such provision was considered to be outside the scope of this thesis, thus steam-gas mixture velocity measurement was abandoned.

A1.2 Temperature profiles in the steam-gas mixture boundary layer

In each of the steam-gas mixtures investigated and for a selective number of tests, the temperature distributions within the mixture boundary layer (i.e. temperature profiles) were determined. In these tests the plate was cooled with maximum water flowrates. These temperature profiles were obtained at three depths from the condensing surface leading edge. Owing to the construction of the probe(see section 4.4), these profiles were determined to about 2mm from the condensing surface. Some of these profiles are shown in figs A1.02-A1.16. The corresponding values of the theoretical boundary layer thickness, for steam-air, steam-argon and steam-neon mixtures, calculated using the analysis of chapter 3, are shown in figs A1.02-A1.12.

It may be seen from figs A1.02-A1.16 that:

(a) Big temperature drops in the steam-gas mixtures occured within small distances from the interface. A similar tendency is indicated by the analyses based on the boundary layer theory [e.g. 22,43] for the present problem.

(b) Further away from the leading edge, the variation of the steam-gas mixture boundary layer thickness with height is very small.

(c) At any given height, the steam-gas boundary layer thickness increases with increasing gas concentration.

(d) For any given gas concentration, the steam-gas mixture boundary layer thickness increases with decreasing gas molecular weight. This thickness becomes large at high helium concentrations (i.e. at $W \geq 0.6$).

Similiar trends to (b),(c) and (d) are indicated by the analyses based on the boundary layer approach. This is shown by the good agreement between the theoretical and the experimental values for the steam-air, steam-argon and steam-neon mixture boundary layer thicknesses.

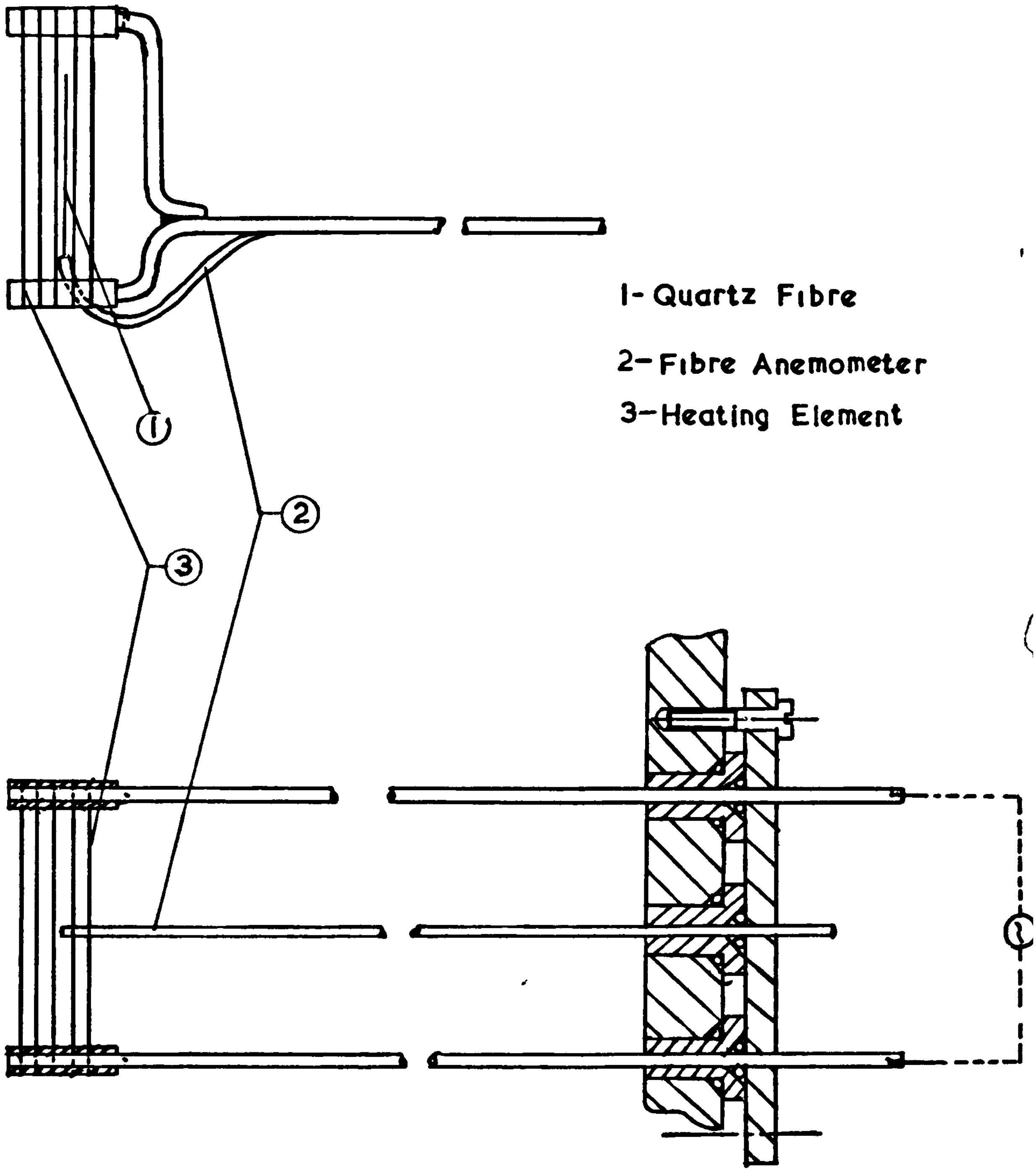

Fig A1 O1 The Fibre Anemometer's Heater

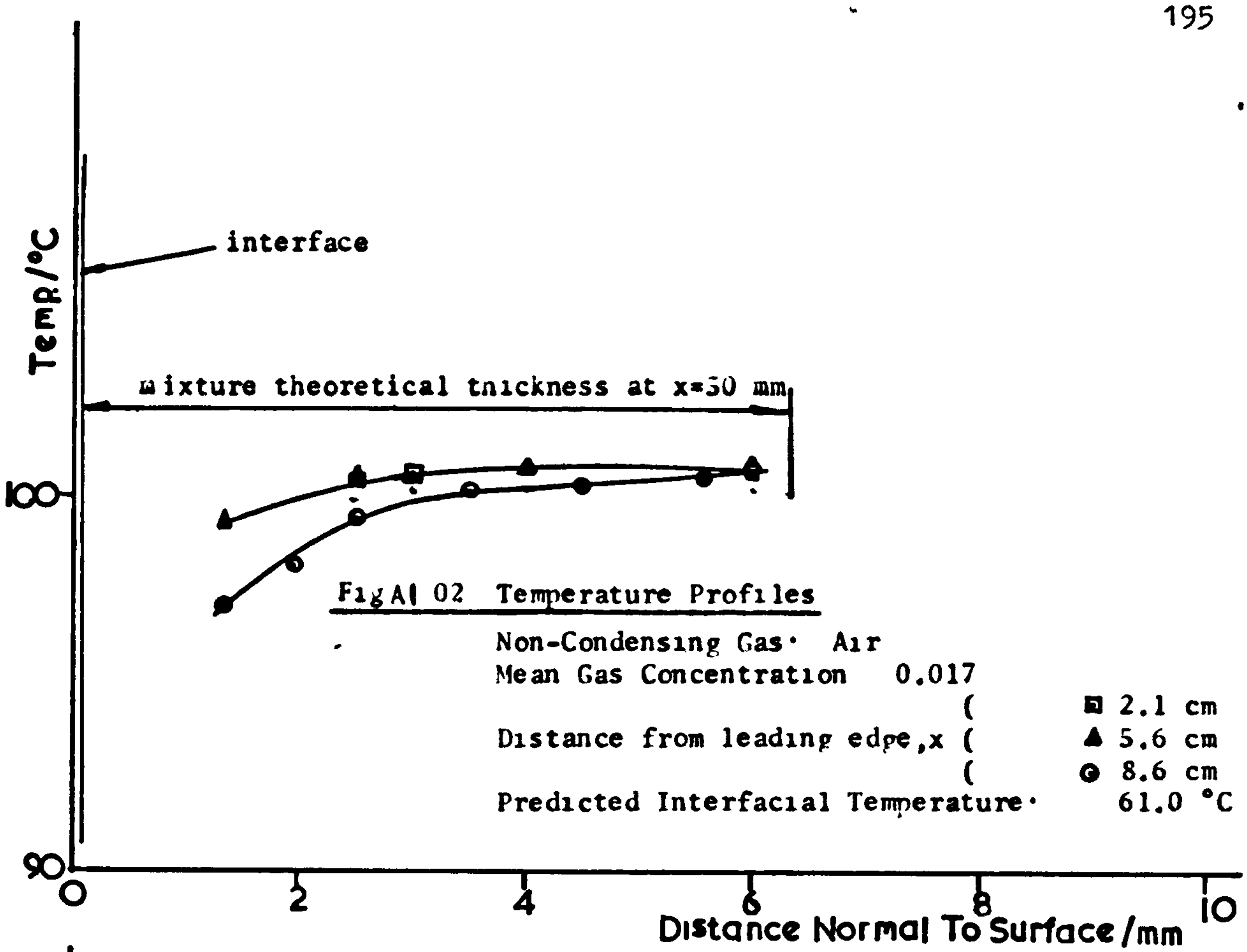

Fig A1 02 Temperature Profiles

Non-Condensing Gas: Air
Mean Gas Concentration 0.017

Distance from leading edge, x (■ 2.1 cm; ▲ 5.6 cm; ⊙ 8.6 cm)

Predicted Interfacial Temperature: 61.0 °C

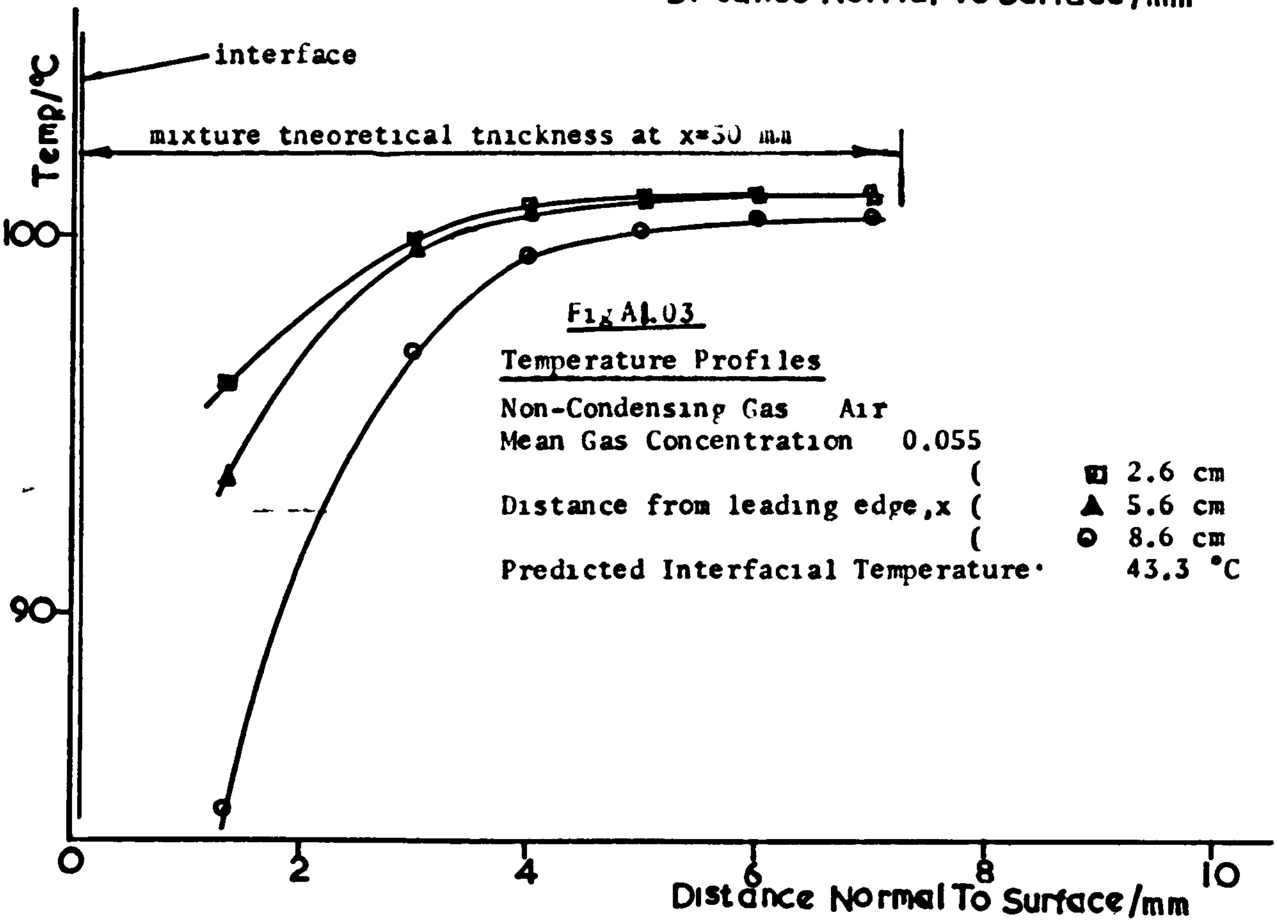

Fig A1.03

Temperature Profiles

Non-Condensing Gas Air
Mean Gas Concentration 0.055

Distance from leading edge, x (■ 2.6 cm; ▲ 5.6 cm; ⊙ 8.6 cm)

Predicted Interfacial Temperature: 43.3 °C

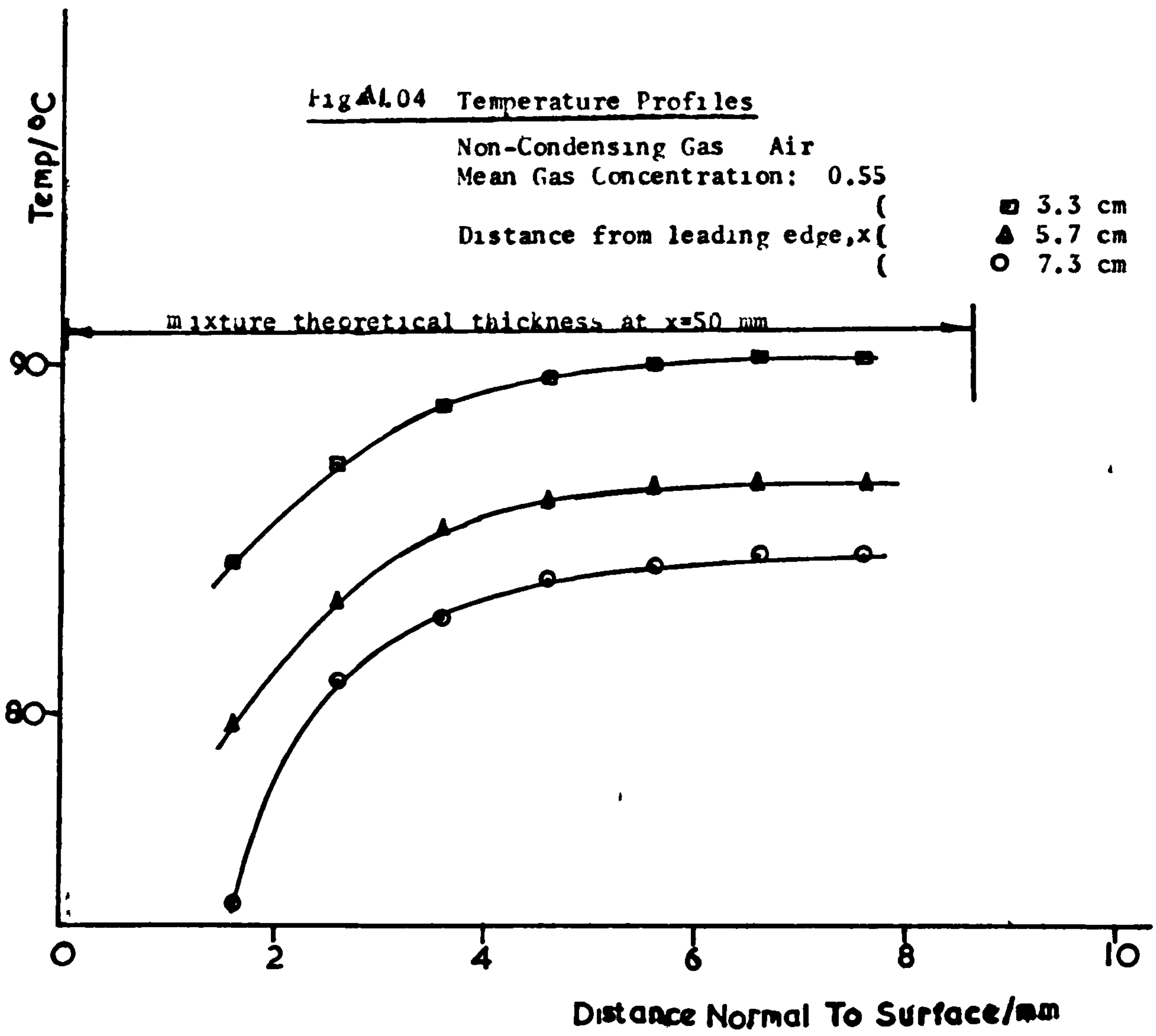
Fig A1.04 Temperature Profiles
Non-Condensing Gas Air
Mean Gas Concentration: 0.55
Distance from leading edge,x
3.3 cm
5.7 cm
7.3 cm
mixture theoretical thickness at x=50 mm
Temp/°C
90
80
0
2
4
6
8
10
Distance Normal To Surface/mm

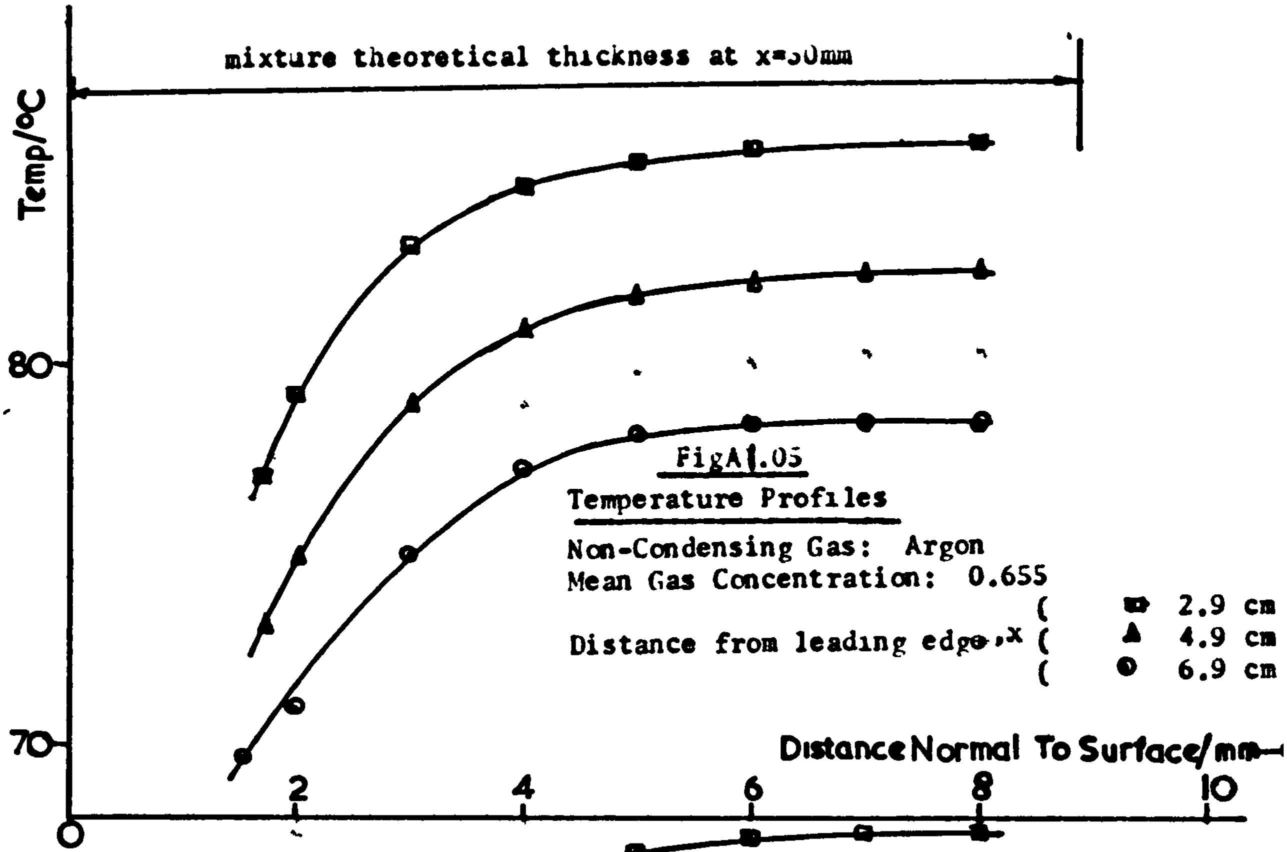

FigA1.05

Temperature Profiles

Non-Condensing Gas: Argon

Mean Gas Concentration: 0.655

Distance from leading edge, x (■ 2.9 cm (▲ 4.9 cm (● 6.9 cm

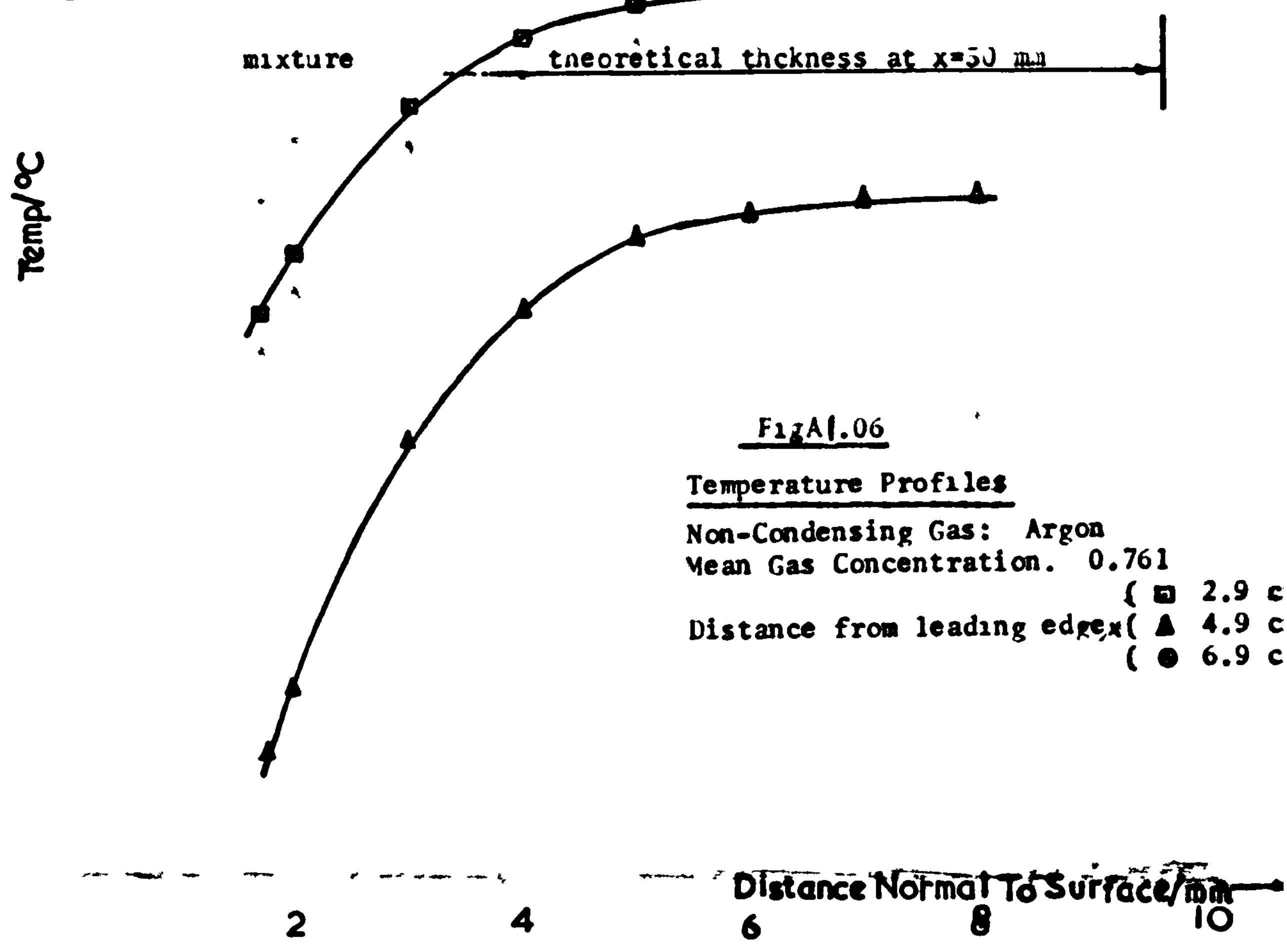

FigA1.06

Temperature Profiles

Non-Condensing Gas: Argon

Mean Gas Concentration. 0.761

Distance from leading edge x (■ 2.9 c (▲ 4.9 c (● 6.9 c

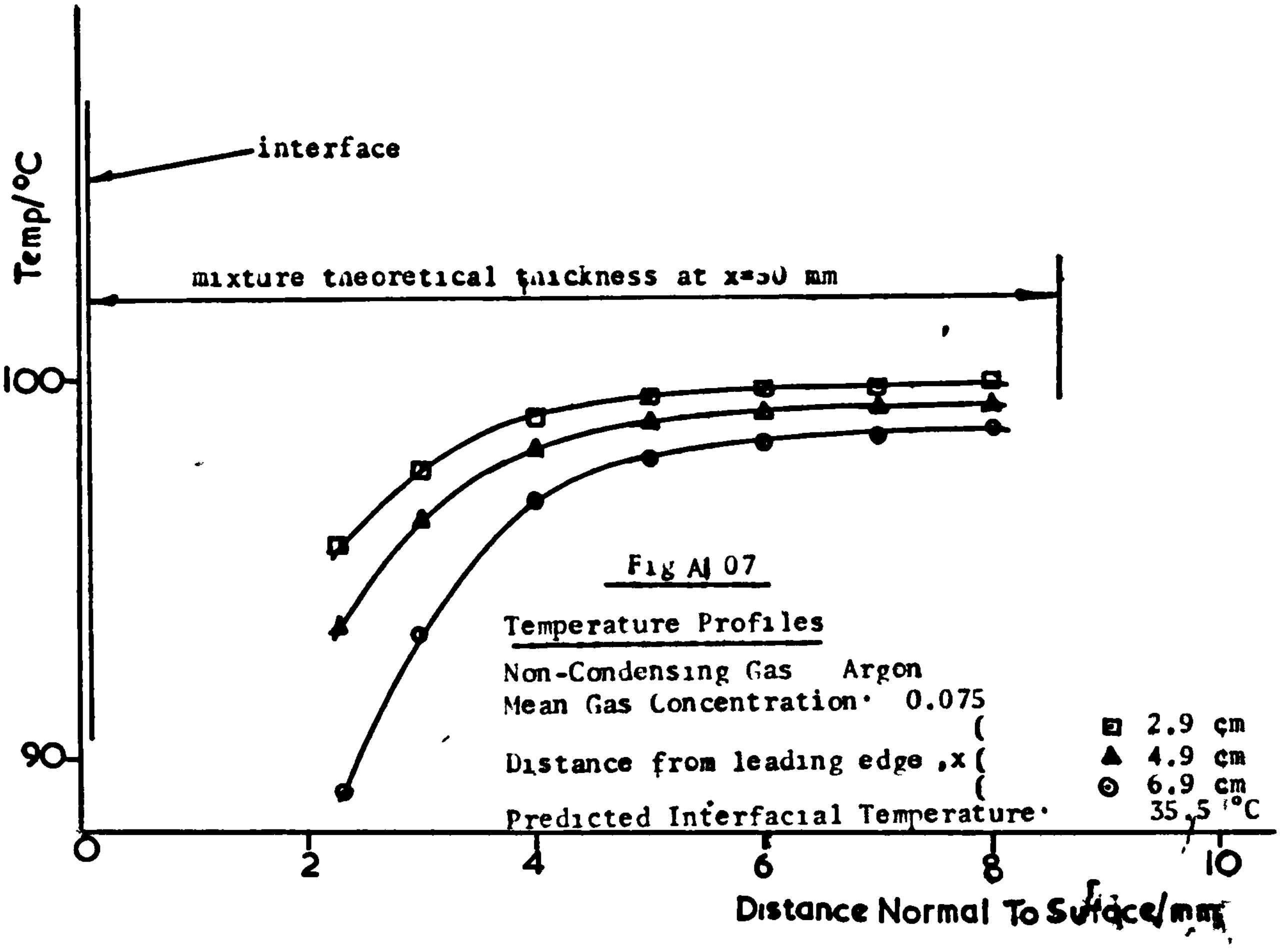

Fig A1 07

Temperature Profiles

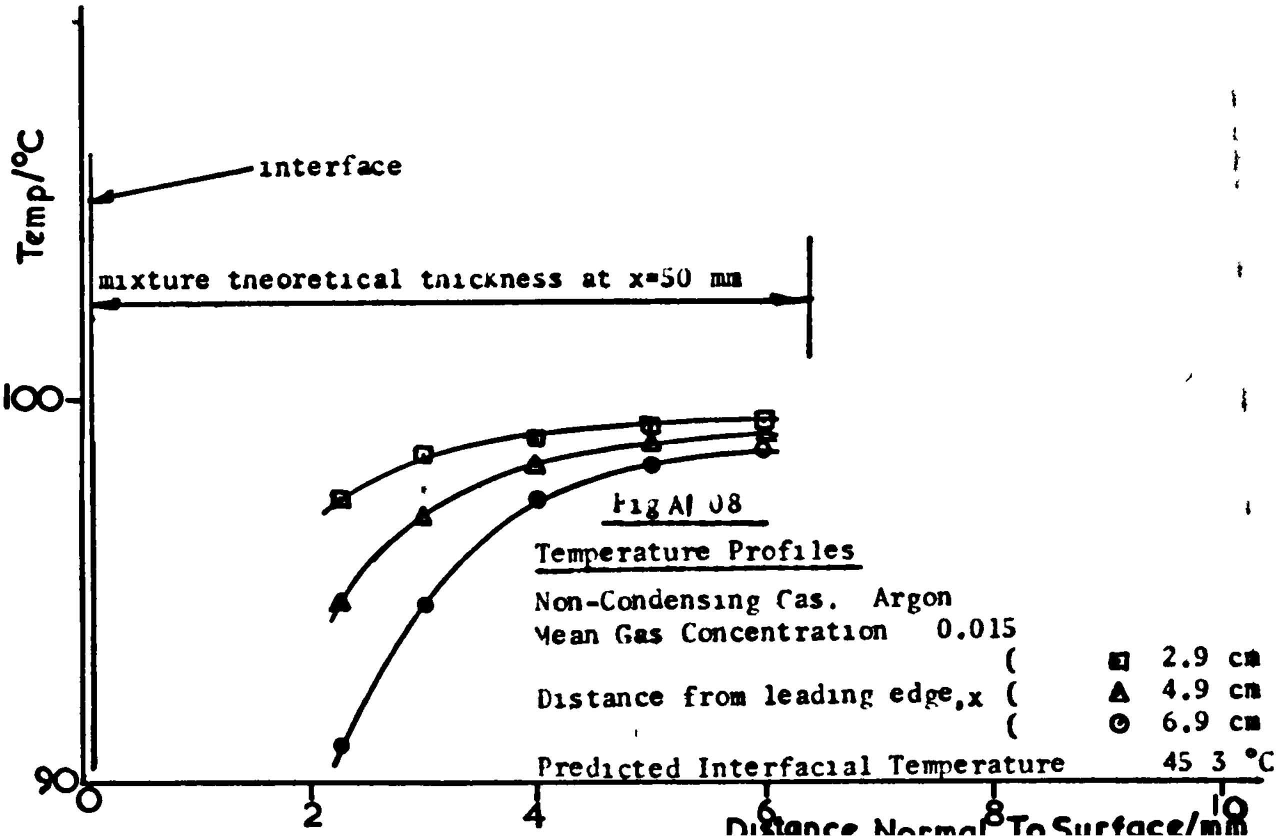

Fig A1 08

Temperature Profiles

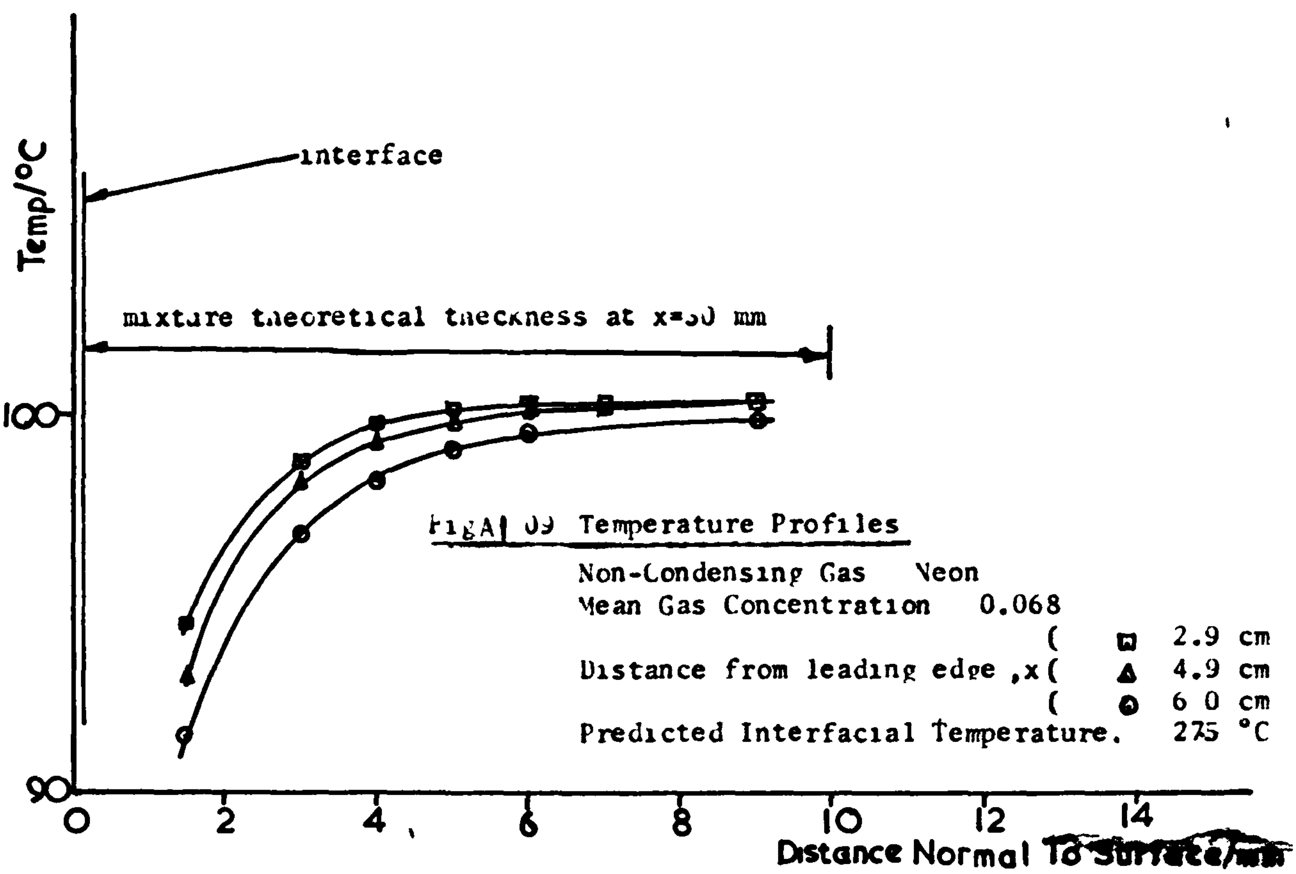

Fig A1 09 Temperature Profiles

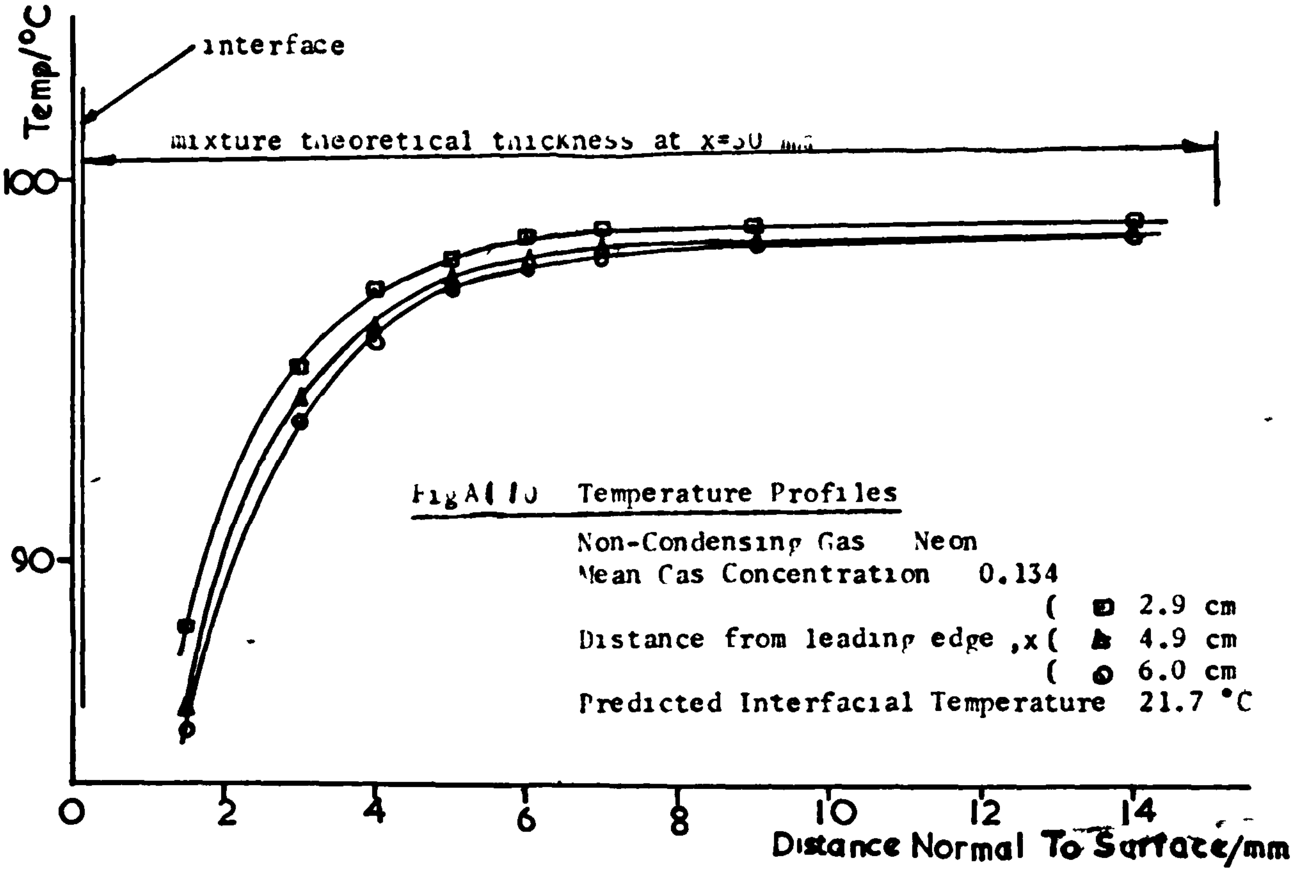

Fig A1 10 Temperature Profiles

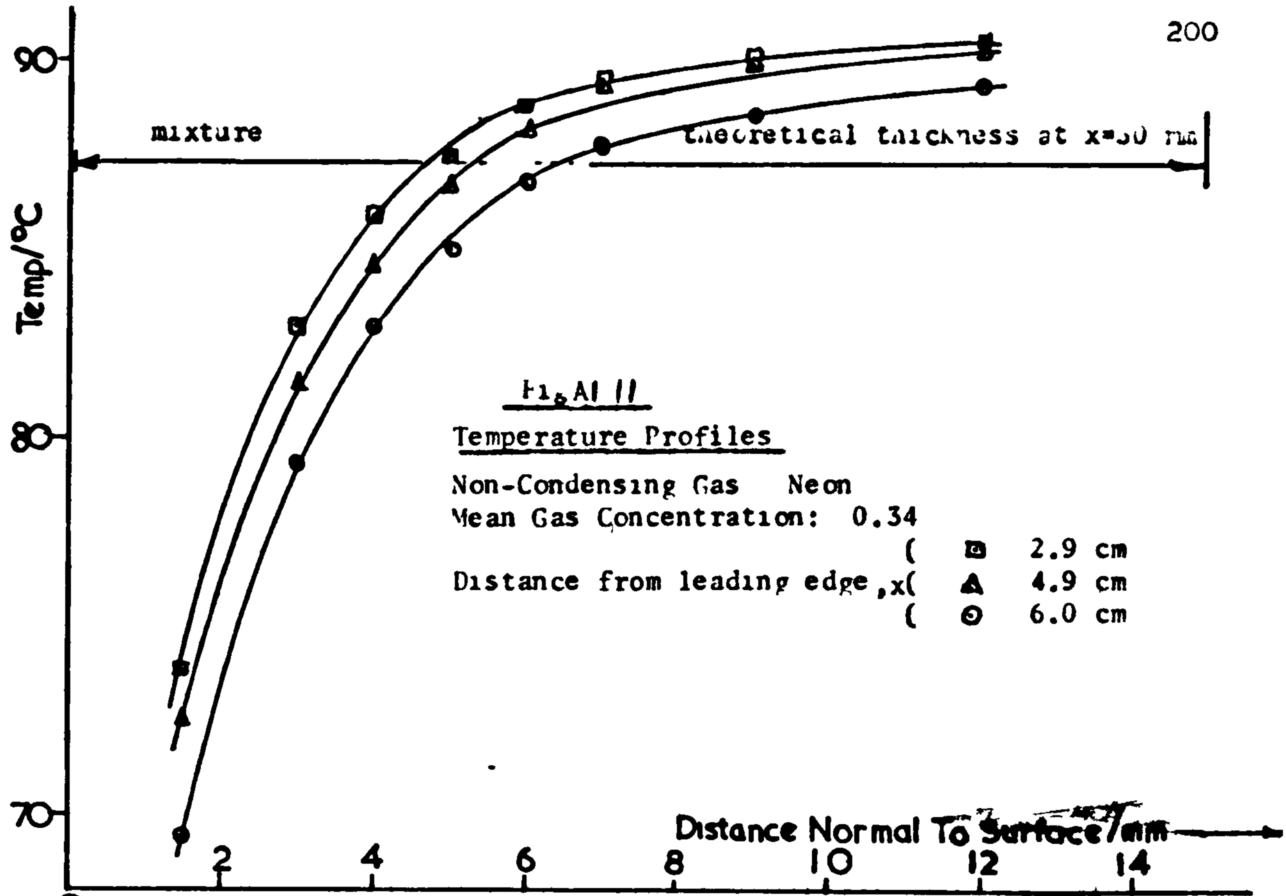
90
80
70
Temp/°C
mixture
theoretical thickness at x=50 mm
Fig A1 11
Temperature Profiles
Non-Condensing Gas Neon
Mean Gas Concentration: 0.34
Distance from leading edge, x (2.9 cm (4.9 cm (6.0 cm
Distance Normal To Surface/mm
2 4 6 8 10 12 14

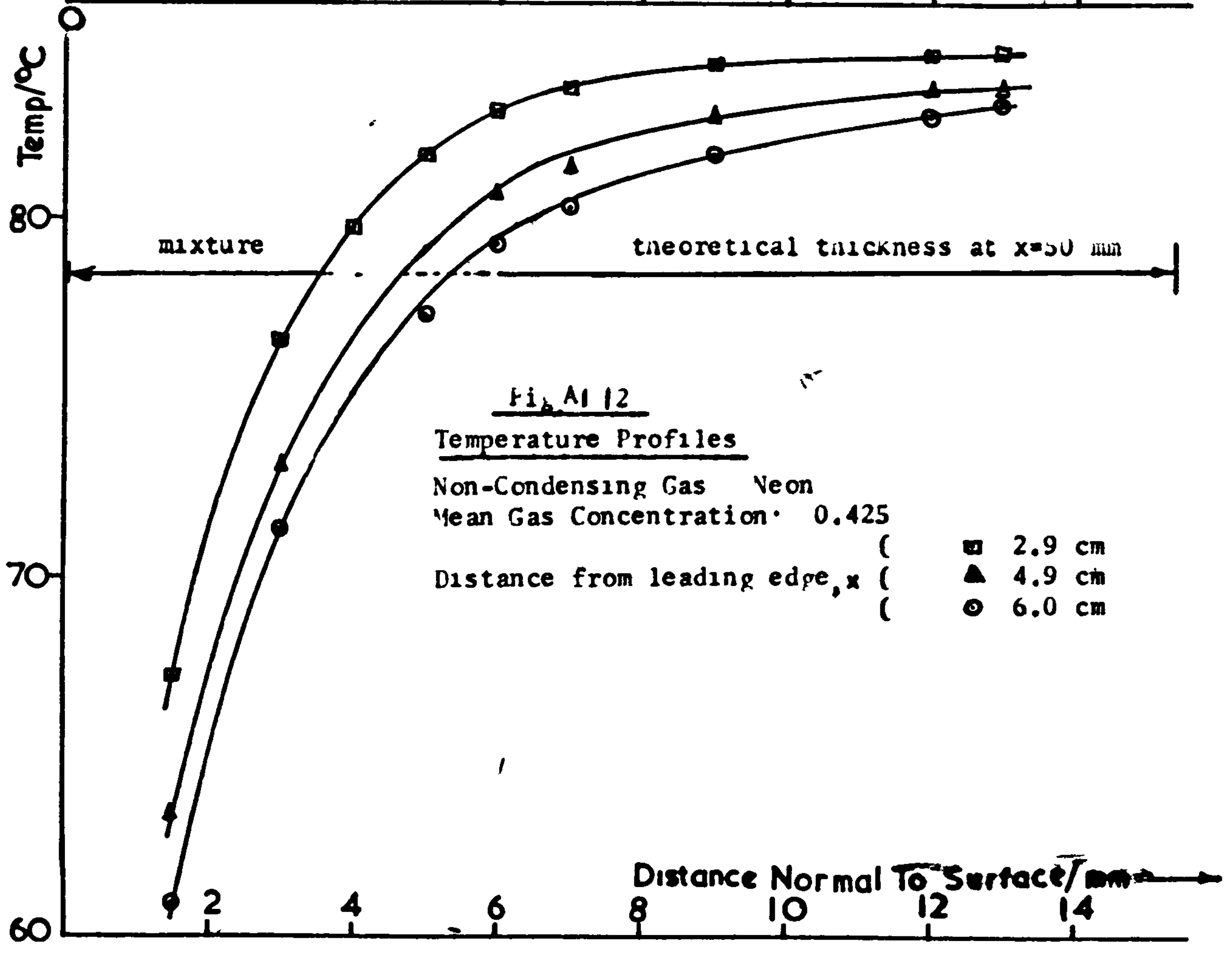
0
80
70
60
Temp/°C
mixture
theoretical thickness at x=50 mm
Fig A1 12
Temperature Profiles
Non-Condensing Gas Neon
Mean Gas Concentration: 0.425
Distance from leading edge, x (2.9 cm (4.9 cm (6.0 cm
Distance Normal To Surface/mm
2 4 6 8 10 12 14

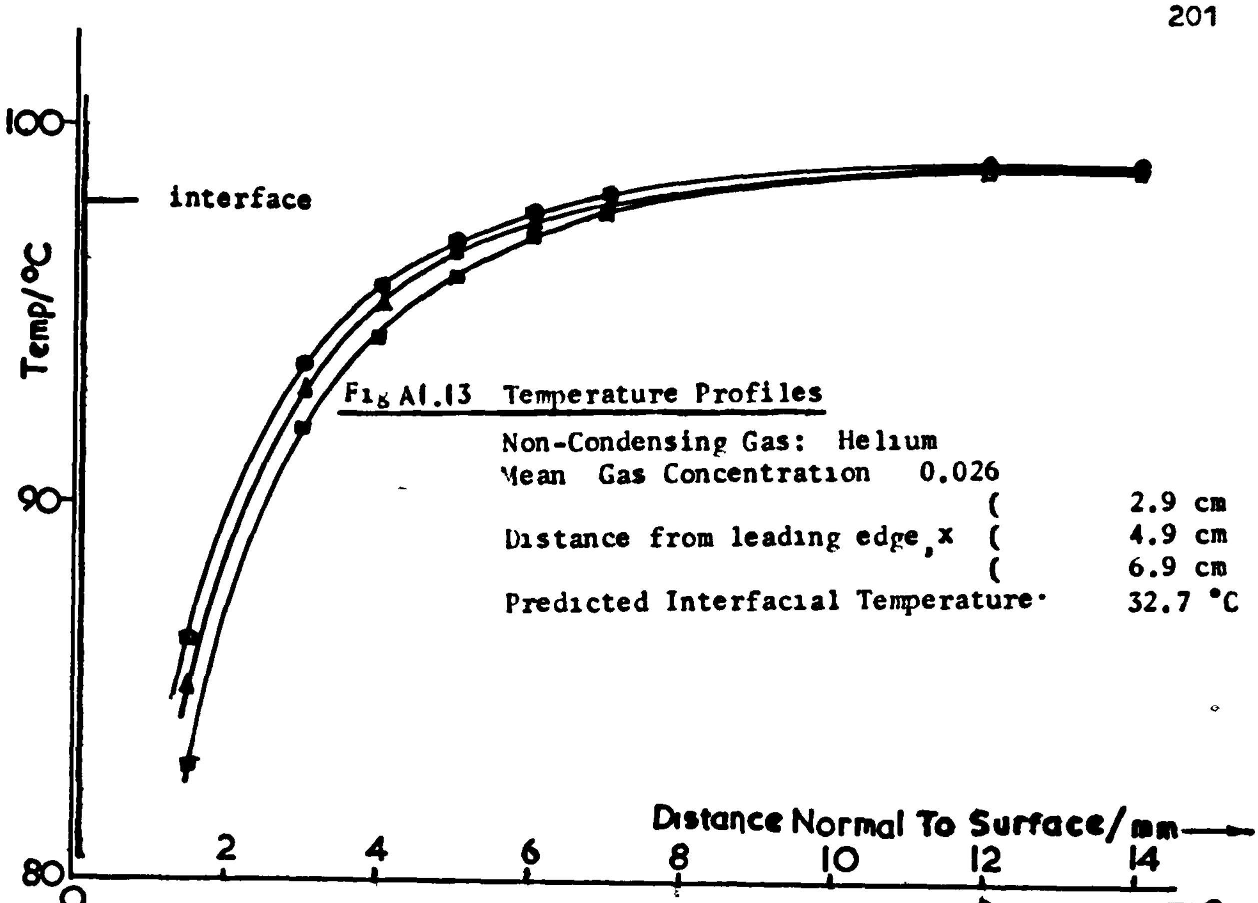

Fig A1.13 Temperature Profiles

Non-Condensing Gas: Helium
Mean Gas Concentration 0.026
Distance from leading edge, x (2.9 cm (4.9 cm (6.9 cm
Predicted Interfacial Temperature: 32.7 °C

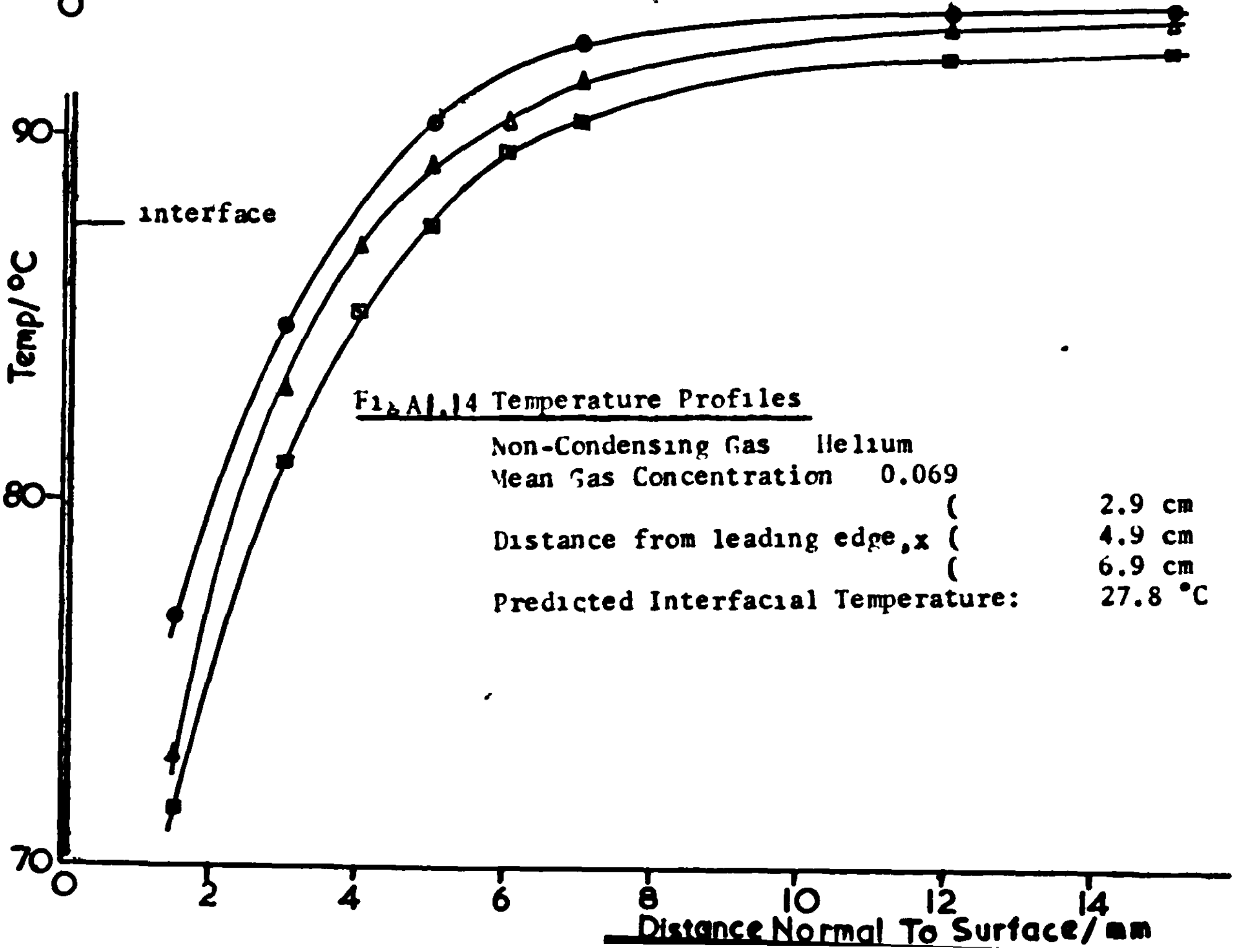

Fig A1.14 Temperature Profiles

Non-Condensing Gas Helium
Mean Gas Concentration 0.069
Distance from leading edge, x (2.9 cm (4.9 cm (6.9 cm
Predicted Interfacial Temperature: 27.8 °C

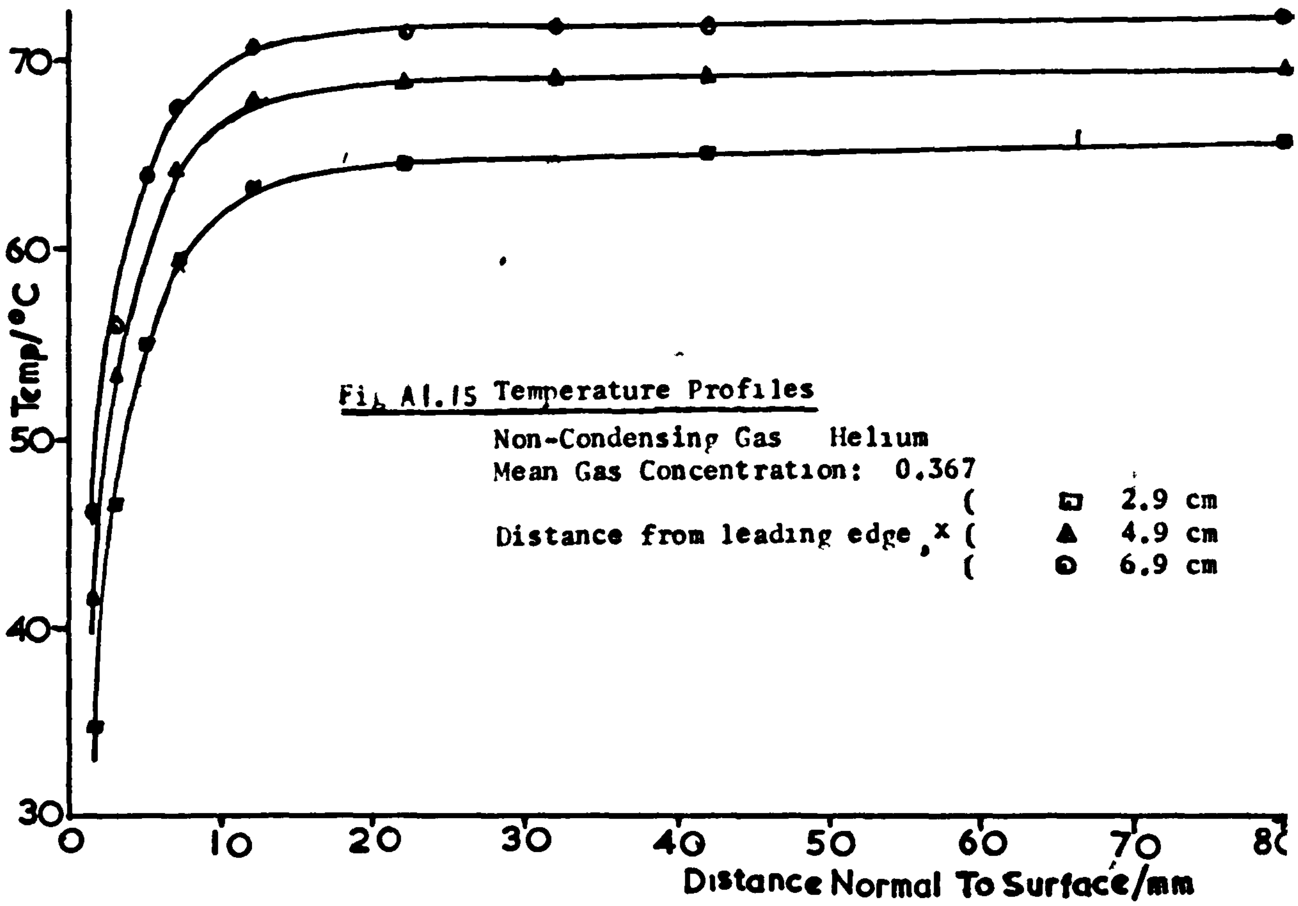

Temp/°C
70
60
50
40
30
0
10
20
30
40
50
60
70
80
Distance Normal To Surface/mm
Fig. A1.15 Temperature Profiles
Non-Condensing Gas Helium
Mean Gas Concentration: 0.367
Distance from leading edge, x
2.9 cm
4.9 cm
6.9 cm

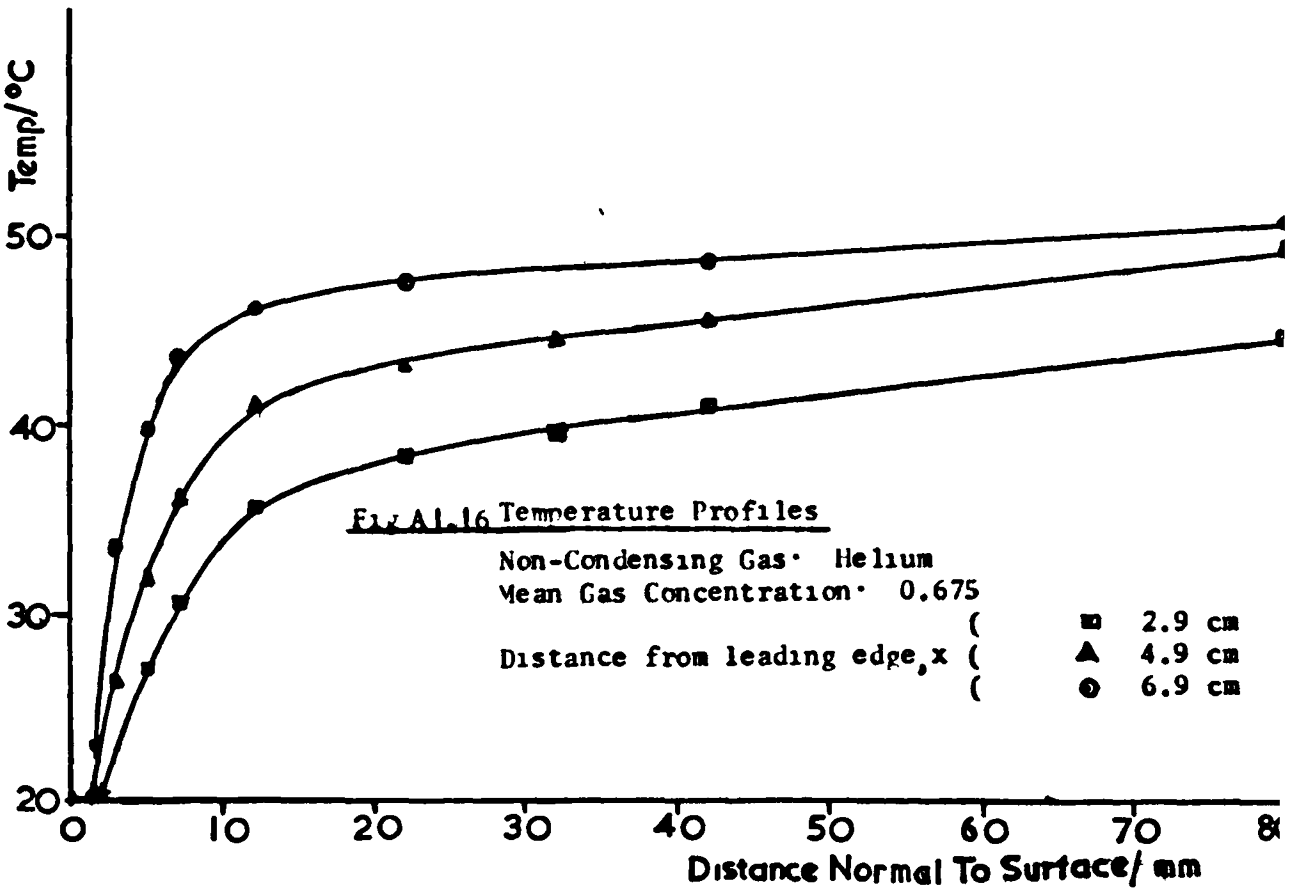

Temp/°C
50
40
30
20
0
10
20
30
40
50
60
70
80
Distance Normal To Surface/ mm
Fig A1.16 Temperature Profiles
Non-Condensing Gas· Helium
Mean Gas Concentration· 0.675
Distance from leading edge, x
2.9 cm
4.9 cm
6.9 cm

Appendix 2

Vertical temperature variation in the steam chamber.

The steam-gas mixture temperature in the steam chamber was found to vary with height. Initially it was thought that these variations were due to gravity field. Consequently an equation was used to estimate the steam partial pressure, and hence mixture temperature as follows:-

A2.1 Variation of partial pressure of steam, (when present in steam-gas mixtures), in a gravity field.

For a stagnant mixture of gases in a gravity field, the conditions for equilibrium are uniformity of the total potential (μ_i) and the temperature of each component [77]. This total potential is defined as the sum of the chemical potential of the gas and its gravity potential.

i.e. $\mu_i = \mu_{ci} + hg$ A2.01

for perfect gases the chemical potential of component i may be written as follows [77],

$$\mu_{ci} = \frac{RT}{M_i} \ln P_i + \frac{H_i}{M_i} \qquad \text{A 2.02}$$

where R is the universal gas constant

M_i is the gas molecular weight

P_i is the gas partial pressure

H_i is the enthalpy

∴ For equilibrium at any two different heights in the mixture we have

$$\frac{RT}{M_i} \ln P_i + \frac{H_i}{M_i} + hg = \frac{RT}{M_i} \ln P_{io} + \frac{H_i}{M_i} + h_o g \qquad \text{A2.03}$$

where P_i and P_{io} are the gas partial pressures at heights h and h_o respectively

$$\therefore \quad P_i = P_{io} \exp\left[\frac{-g(x) M_i}{RT} \right] \qquad \text{A2.04}$$

where $x = h - h_o$

For a Gibbs Dalton mixture, the total pressure, P, at any point is given by

$$P = \sum P_i$$

$\therefore$ For a two component mixture:-

$$P = P_v + P_g$$

(in the present work subscript v relates to condensing component (vapour) and subscript g relates to non-condensing component (gas)), hence

$$P_v = \frac{P_{vo} \exp\left[-M_v gx/(RT) \right]}{P_{vo} \exp\left[-M_v gx/(RT) \right] + P_{go} \exp\left[-M_g gx/(RT) \right]}$$

$$= \left[1 + \frac{P_{go}}{P_{vo}} \exp\left[\frac{gx\,(M_v - M_g)}{RT} \right] \right]^{-1} \qquad \text{A2.05}$$

For stagnant mixtures of steam with air, argon, neon and helium, at total pressure of 1.0125 bar and temperature range of 373.15-331.15 K, the difference in partial pressures of steam corresponding to the top and the bottom of the steam chamber, found using equation A2.05, would vary between 0.and 0.00036 bar. We can thus estimate the maximun temperature variation in the steam chamber, due to gravity, by assuming saturation conditions at the top and [illegible] bottom of the chamber. This gives maximum temperature difference of 0.01 K.

A.2.2 Vertical temperature distribution outside the steam-gas mixture boundary layer

These temperature distributions were determined in all tests in which the test plate was cooled with maximum coolant flowrate. In some other tests, these distributions were determined when the test plate was not cooled. For each gas concentration, the mixture temperature was measured, using the two steam thermocouples and the probe, at three different levels. Representative temperature distributions for steam-air, steam-argon and steam-helium which were determined using the probe thermocouple, are shown in figs A2.01-A2.03. The temperature distribution for the steam-neon mixture, though showing the same tendency as in the steam-air mixture was small therefore no representation was made for it.

It may be seen from figs A2.01-A2.02 that, up to high gas concentrations, the absolute difference in mixture temperature corresponding to the top and the bottom of the test plate (i.e. $|T_{top}-T_{bottom}|$) increases with increasing gas concentrations. These absolute differences are large compared with the estimated values for the variation in steam-gas temperature, due to gravity field (the estimated values were shown earlier to be within 0.1 K). This discrepancy between the estimated and the experimental values for the steam-gas temperature variations may be attributed mainly to the presence of natural convection flow in the steam chamber. This convection flow was caused by the heat transfer through the steam chamber wall and end plates.

It may also be seen from figs A2.01-A2.02 that the mixture temperature difference in the steam-gas mixture were smaller in cases where the plate was not cooled than when it was cooled. This is because the effect of the natural convection was greater when the plate was cooled (since more heat was lost to the surroundings, thus larger density differences existed between the bulk and the vicinity of the plate).

Figs A2.01 and A2.02 indicate that in the cases of steam-argon and steam-air mixtures, the mixture temperature decreases with increasing depth from the test plate leading edge level. This is because the air and argon are heavier than steam, thus causing the gas concentration to increase with increasing depth (since the mixture becomes richer with gas at increasing depths). Therefore, if the steam is at its saturation state in the mixture, thetemperature decreases with increasing depth. Fig A2.02 indicates that steam-helium mixture temperature increased with increasing depth from the plate leading edge, this is to be expected since the helium is lighter than the steam. Thus the reverse situation to that of steam-air mixture,existed in the steam-helium. The absence of large variation in the steam-neon mixture may be attributed to the small difference between the densities of steam and neon (the neon is slightly heavier than steam). Thus the variation in the steam-neon mixture density, and hence in its temperature, with height is small compared with other steam-gas mixtures.

Fig. A2.01 Representative Vertical Temperature Distributions in Steam Chamber

Non-condensing gas Air

---------- zero cooling water flow rate) The numbers refer to average concentrations
——— maximum cooling water flow rate)

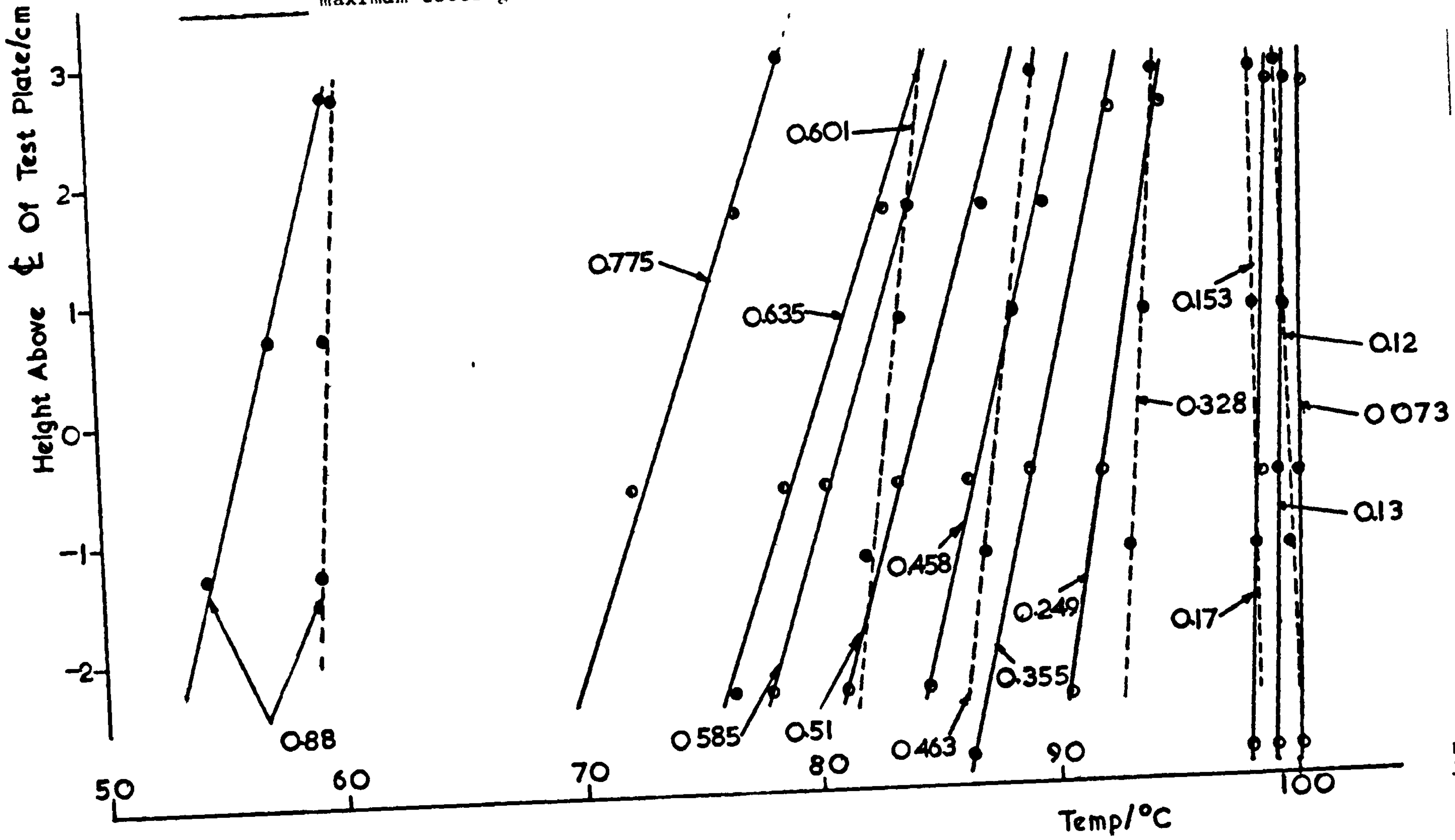

Fig A2.02 Representative Vertical Temperature Distributions in Steam Chamber

Non-condensing gas. Argon

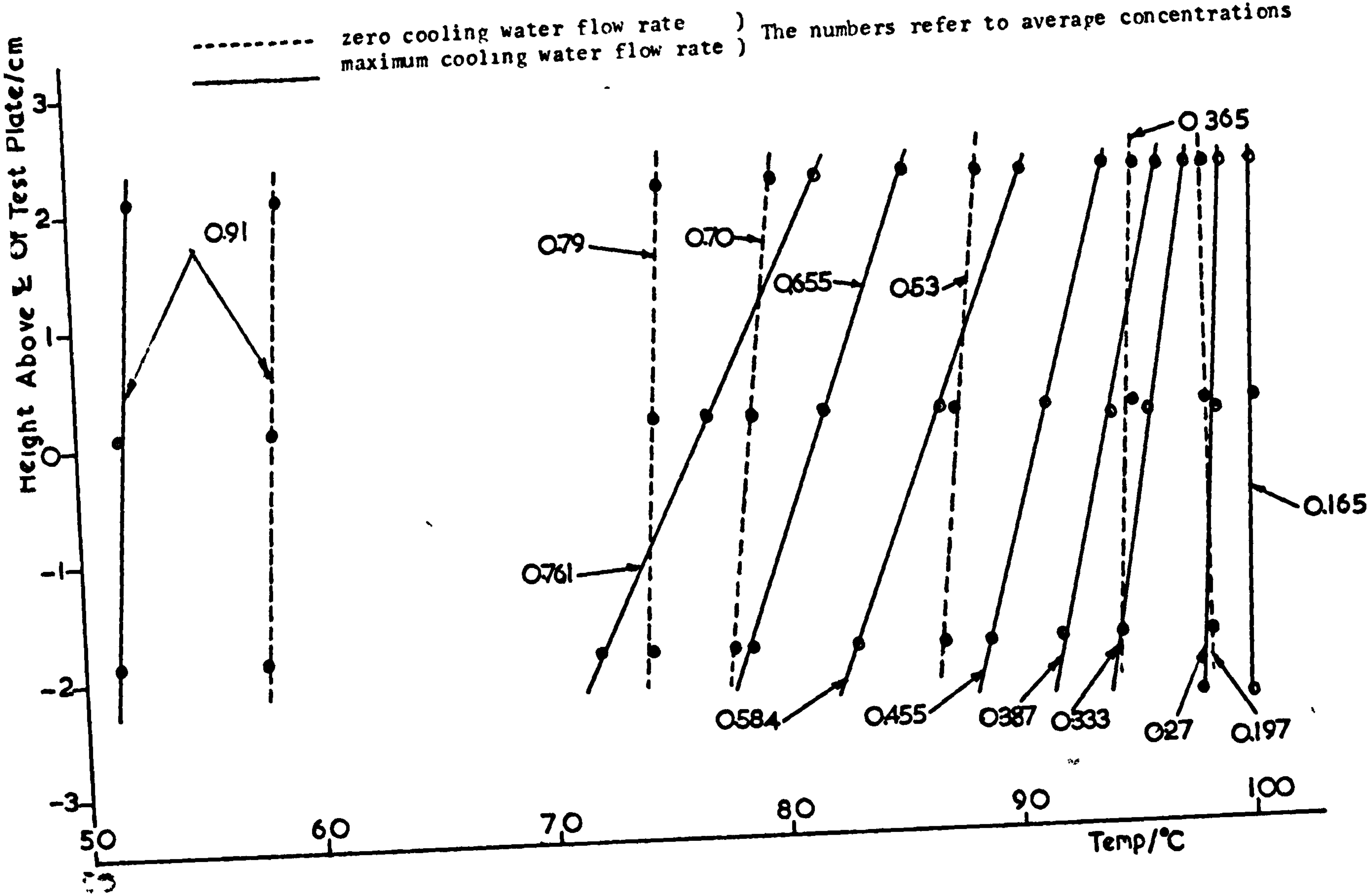

Fig. A2 03 Representative Vertical Temperature Distributions in Steam Chamber

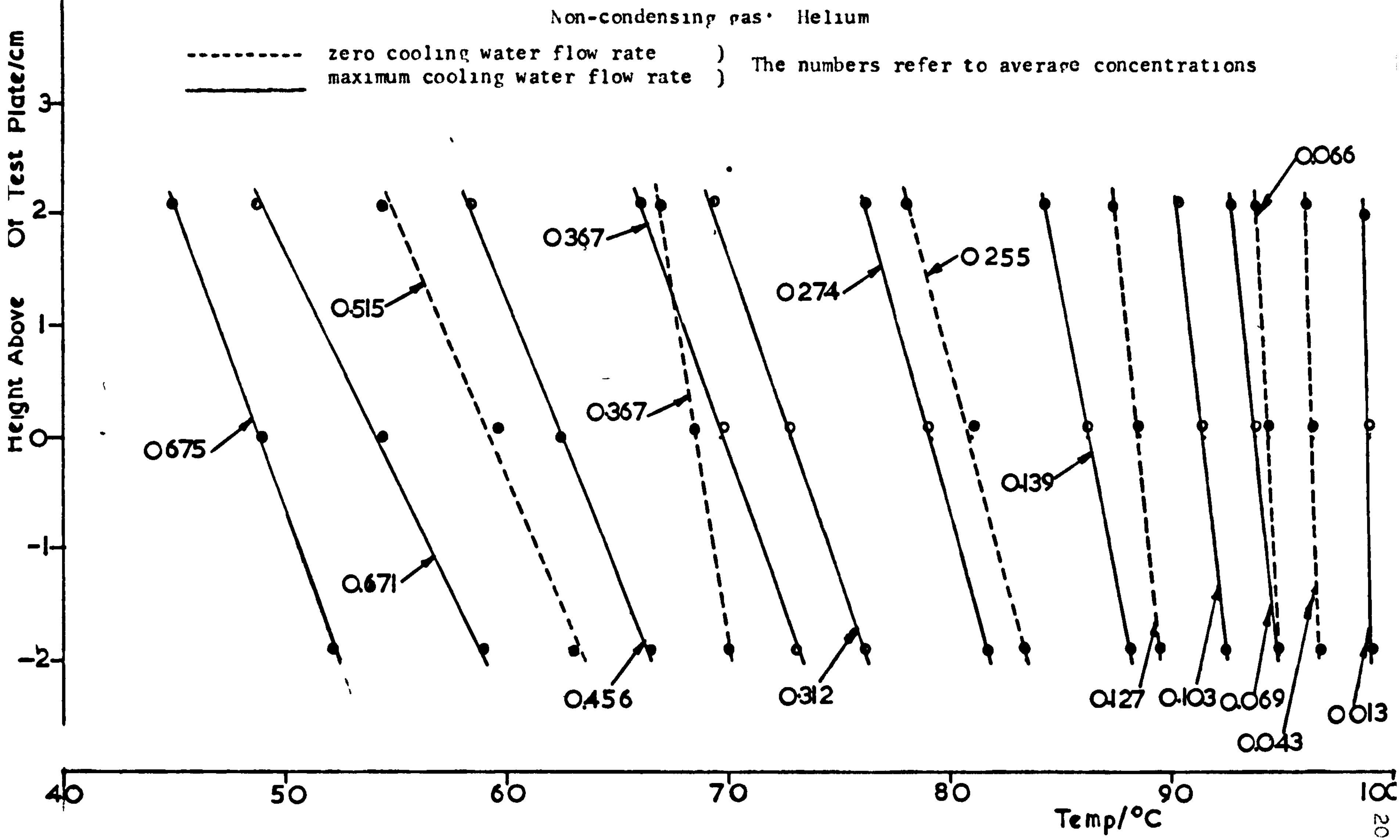

Appendix 3

Specimen calculation

The experimental data obtained in test R.51* are used in the following calculations.

a - calculation of the heat flux and the mixture-to-surface temperature difference

For a linear temperature distribution:-

$\therefore\ t = ax + t_o$

where t is the temperature at distance x from condensing surface

t_o is the condensing surface temperature

a is the temperature gradient

t_o and Q may be found by linear regression of t on x, thus:-

$$a = \frac{n\Sigma(xt) - \Sigma(x)\ \Sigma(t)}{n\Sigma(x^2) - \Sigma(x)\ \Sigma(x)}$$

$$t_o = \frac{\Sigma(t)\ \Sigma(x^2) - \Sigma(x)\ \Sigma(xt)}{n\Sigma(x^2) - \Sigma(x)\ \Sigma(x)}$$

where n is the number of the temperature observations through the plate. The terms in the above equations are calculated as shown in the following table

x/cm	t/^{o}C	x^2/cm^2	xt/cmK
0.236	32.57	0.055696	7.60652
0.373	32.23	0.139129	12.02179
0.527	31.86	0.277729	16.79022
0.688	31.44	0.473344	21.63072
0.830	31.20	0.688900	25.89600
0.980	30.90	0.960400	30.28200
3.634	190.20	2.595198	114.22725

Thus:

$$a = \frac{6x114.22725 - 3.634x190.20}{6x2.595198 - 3.634^2} \frac{K}{cm} = -2.000 \frac{K}{cm}$$

Since

$$Q = -ka, \quad k = 3.85 \ W/(cmK)$$

$$\therefore \frac{Q}{kw/m^2} = \frac{3.85x2.000x10^4}{10^3} = \underline{77.0}$$

and

$$t_o = \frac{190.20 \ x \ 2.595198 - 3.634x114.22725}{6 \ x \ 2.595198 - 3.634^2} \ ^oc = 33.24^oc$$

$$T_\infty - T_o = t_{p_{50m}} - t_o = 99.2 - 33.2 = \underline{66.0K}$$

From reference 1 :-

$$Q = \left[\frac{k^3 \rho_f^2 g \ h_{fg} \ (\Delta T)^3}{4 \mu_f x}\right]^{\frac{1}{4}} \qquad A2.01$$

$$= \left[\frac{k_f^3 g \ h_{fg} \ (\Delta T)^3}{4 v_f^2 \mu_f x}\right]^{\frac{1}{4}}$$

The properties in equation A2.01 are determined at the reference temperature [22]:-

$T^* = T_w + 0.31\,(T_\infty - T_w)$

$\therefore\; T^* = 33.24 + 0.31 \times 66 = 53.7\text{K}$

From the steam table ,

$h_{fg_{99.2}} = 2257$ J/gm, $v_{f_{53.7}} = 1.014 \times 10^{-6}\ \text{m}^3/\text{g}$

$\mu_{f_{53.7}} = 0.514$ gm/(m.s), $k_{f_{53.7}} = 0.651$ J/(m.s.K)

Since Q was determined at mid point of the plate (x = 4.84cm

$$\therefore\quad Qnu = \left[\frac{0.651^3 \times 9.81 \times 2257 \times (53.7)^3}{4(1.014\times10^{-6})^2 \times 0.514 \times 0.0484}\right]^{\frac{1}{4}} \times 10^{-3} = \underline{310}$$

$$\therefore\quad \frac{Q}{Qnu} = 77/310 = \underline{0.249}$$

<u>b - calculation of the gas concentration</u>

The gas concentration, $W = \dfrac{m_g}{m_g+m_v} = \dfrac{1}{1+m_v/m_g}$,

where m_g is the mass of the injected gas

m_v is the mass of the steam in the mixture

To calculate the mean concentration,

$m_g = \dfrac{P_a\ V}{R_g\ T_a}$ (assuming the gas to be ideal)

where $m_v = \dfrac{V_{tot}}{v_g}$

P_a (the atmospheric pressure) $= \rho_m g\, H_b$

V is the injected gas volume

T_a is the room temperature

R_g (the gas constant) = .2086 J/(gmK) for argon

V_{tot} is the volume of the mixture in the apparatus

v_g is the steam specific volume

H_b is the barometric pressure

ρ_m is the mercury density

$$\therefore \quad W_m = 1 \Big/ \left[1 + \frac{V_{tot} \, R_g \, T_a}{P_a \, V \, v_g} \right]$$

To calculate the gas concentration outside the boundary layer,

$m_v/m_g = \rho_v/\rho_g$

but $\rho_g = P_g/R_g T$ (assuming the gas to be ideal)

$\rho_v = 1/v_g$

where P_g(is the gas partial pressure in the mixture) $= P_{tot} - P_v$

T_p is the mixture temperature

P_{tot} (the total pressure) $= \rho_m g H_b + \rho_a g H_m$

$$\therefore \quad W_\infty = 1 \Big/ \left[1 + \frac{R_g \, T_p}{P_g \, v_g} \right]$$

From test R51

$H_b = 760.30$ mmHg

$H_m = 120$ mmH_2O

$V_{tot} = 91620.3$ cm^3

$V_a = 3350$ cm^3

$t_a = 20$ ^oC

From steam tables v_g(corresponding to T_p) $= 1.721$ m^3/kg

$T_p = 99.2 + 273.15 = 372.35K$, $P_v = 1.00375$ bar

$\therefore$ $P_a = 13.5951 \times 980.665 \times 760.30/10^5 = 1.01436$ bar

$T_a = 20 + 273.15 = 293.15K$

$P_m = 1.01436 + 32 \times 980.665/10^6 = 1.02588$ bar

$P_g = 1.02588 - 1.00375 = 0.02263$ bar

$$\therefore \quad W_m = 1/\left[1 + \frac{91620.3 \times 0.2086 \times 293.15}{1.01436 \times 10^5 \times 3350 \times 1.721 \times 10^{-3}}\right] = \underline{0.096}$$

$$W_\infty = 1/\left[1 + \frac{0.2086 \times 372.35}{0.02263 \times 10^5 \times 1.72 \times 10^{-3}}\right] = \underline{0.048}$$

Appendix 4

Experimental Errors

A4.1 Summary of prior estimated errors:

Steam and plate temperatures	± 0.1 K
Depth in plate to which measured temperature relates	± 0.02mm
Barometer	± 0.05mm Hg
Water manometer	± 5mm H_2O
Total volume occupied by steam-gas mixture	± 250cm^3
Volume (at atmospheric temperature and pressure) of gas injected	± 5cm^3
Thermal conductivity of plate	± 2%

A4.2 Heat flux and vapour-to-surface temperature difference

The values of surface temperature and heat flux were found by linear regression of the temperatures on the distances. In a number of cases alternative estimates were made by regressing the distances on the temperatures. The difference between the two estimates of surface temperature and heat flux was negligible by comparison to the scatter on the graphs. Thus, apart from possible systematic errors we estimate the accuracies of these quantities from fig 6.03 (i.e. tests for pure steam)

Q ± 12 kW/m^2

$T_\infty - T_W$ ± 1 K

It is thought that the only significant source of systematic error was in the thermal conductivity of the plate, which would give a possible systematic error in Q of 2%.

A4.3 Mean gas concentration

These were calculated from the equation:-

$$W_m = \left[1 + V_{tot} \cdot R_g \cdot T_a / (P_a \cdot V \cdot v_g)\right]^{-1} \text{ (see appendix 3)}$$

Using the above prior estimates of error in the various quantities, the limits of error in W_m was found to vary between about 2% at the lower concentrations to about 1.5% at the higher concentrations used.

A4.4 Gas concentrations based on temperature and pressure measurements

These were calculated from the equation:-

$$W_\infty = \left[1 + R_g \cdot T_p / (P \cdot v_g)\right]^{-1} \text{ (see appendix 3)}$$

Using the above prior estimates of error, the limits of error in W_∞ were found to vary from about:

12×10^{-4} to 9×10^{-4} for argon

9×10^{-4} to 7×10^{-4} for air

6×10^{-4} to 5×10^{-4} for neon

1×10^{-4} to 2×10^{-4} for helium

(the first figure given above relates to lower concentrations and the second to the higher).

Appendix 5

Condensation of steam from steam-carbon dioxide mixture

Initially carbon dioxide was chosen for the investigation of mixtures with high gas-to-steam molecular weight ratio. When carbon dioxide was injected, however, into the steam, the condensate was observed to change from complete filmwise to a good dropwise within a short time of gas injection. The condensation was stopped by closing the cooling water tap. The valve at the bottom of the steam chamber back plate was then opened and the system flushed out with steam for about twenty minutes. When condensation was restarted, the condensate was again in the form of a complete film. This behaviour of the condensate suggested that the gas might have been contaminated when entering the system. Consequently the gas cylinder was changed and a series of vapour traps filled with sodium hydroxide solution was connected between the gas cylin and the gas injecting system.

When injecting, the carbon dioxide was allowed to bubble slowly through the sodium hydroxide in the traps. The change from film to dropwise condensation was, however, again observed. It was thus considered that the nature of the gas, and not contamination may have been responsible for the change in the condensation mode. To avoid further loss of time, carbon dioxide was abandoned and argon was used instead.

Appendix 6

Consideration of Sledgers analysis [44]

Sledgers [44] proposed an approximate analysis for the present problem. In this analysis integral solutions were obtained for the following mixture, continuity, momentum and energy equations respectively:-

$$\frac{\partial u}{\partial x} + \frac{\partial v'}{\partial y} = 0 \qquad \text{A6.01}$$

$$\frac{u\partial u}{\partial x} + \frac{v\partial u}{\partial y} = \frac{\nu \partial^2 u}{\partial y^2} \qquad \text{A6.02}$$

$$\frac{u\partial T}{\partial x} + \frac{v\partial T}{\partial y} = \frac{a \partial^2 T}{\partial y^2} \qquad \text{A6.03}$$

where $a = \frac{k}{\rho c_p}$

In these solutions the following profiles were assumed:-

velocity profile, $\frac{u}{u_o} = 1 - F(\eta) - \lambda G(\eta)$ A6.04

gas concentration and mixture temperature profiles,

$$\theta = \phi = 1 - F(\eta) \qquad \text{A6.05}$$

where $\eta = \frac{y - \Delta}{\delta}$

λ is a constant

$F(\eta) = 2\eta - 2\eta^3 + \eta^4$

$G(\eta) = 1/6\eta(1 - \eta)^3$

$\phi = \frac{T - T_\infty}{T_o - T_\infty}$

$\theta = \frac{W - W_\infty}{W_o - W_\infty}$

When using the above approach the present writer unable to confirm the results obtained by Sledgers. In integrating equations A6.01 and A6.02 Sledgers obtained the following equation

$$\frac{d}{dx}\left[\int_{\Delta}^{\delta+\Delta} u^2\, dy\right] + u_o\left[\underline{u_o \frac{d\Delta}{dx}} - v\right] = g\left[\int_{\Delta}^{\delta+\Delta} w\, \frac{\rho-\rho_\infty}{\rho}\, dy\right] - \nu\left[\frac{\partial u}{\partial y}\right]_{\Delta} \qquad \text{A6.06}$$

The underlined term in equation A6.06 could not be accounted for. Furthermore in computing the equation relating heat and mass transfer obtained by Sledgers, high heat fluxes were obtained for all gas concentrations (e.g. for air in steam concentration of 0.01 and at T =373.15 and ΔT=10K, the fractional reduction in heat transfer was about 0.9, for the same conditions, this reduction was about 0.4 when computing equation 3.27). Therefore it was thought that a re-appraisal of Sledgers' analysis was desirable.

Basically in his solution, Sledgers followed the same steps as those followed in chapter 3. The difference between Sledgers' approach and that followed in chapter 3 is that Sledgers employed different profiles and solved the mixture energy equation instead of the gas diffusion equation. Sledgers, however, assumed, the Lewis number (i.e. D/α) to be unity, in addition to assigning the same profiles for the mixture temperature and the gas concentration. The application of these conditions leads to the same solution for both the energy and diffusive equations

After integrating the mixture, continuity, momentum and diffusion equations, and employing the profiles, A6.04 and A6.05, the following equations were obtained:-

$$\frac{d}{dx}\left[\delta u_o^2\left(\frac{23}{126}+\frac{11\lambda}{1512}-\frac{\lambda^2}{9072}\right)\right]-u_o^2\frac{d\Delta}{dx}-\frac{2u_o}{\delta}\frac{Dw_o}{W_o}$$

$$=\frac{16}{5}X\,W_o\,\delta+\frac{12+\lambda}{68}u_o \qquad \text{A6.06}$$

$$\frac{d}{dx}\left[\delta u_o\left(\frac{23}{126}-\frac{\lambda}{354}\right)\right]-u_o\frac{d\Delta}{dx}=\frac{2\,DW_\infty}{\delta\,W_o}, \qquad \text{A6.07}$$

where $w_o = W_o - W_\infty$

$X = (M_g - M_v)/[M_g - (M_g - M_v)\,W_\infty]$

In solving equation A6.06 and A6.07 the following equation was obtained:-

$$Sp^2\left[1-2\left(\frac{\rho_f}{\rho}\right)+\left(2+\frac{\lambda}{6}\right)\left(\frac{\rho_f}{\rho}\right).Sc\left(\frac{W_o}{w_o}\right)\right]-10\,x\,.$$

$$\frac{Sp}{Sc}(\mu/\mu_f)\frac{w_o}{W_o}\left(\frac{23}{126}-\frac{11\lambda}{1512}+\frac{\lambda^2}{9072}\right)+\frac{12}{5}(\mu/\mu_f)\frac{w_o^2}{W_o}\frac{X}{Sc}=0$$

where $\lambda = \frac{1357}{21} - 118\,\frac{\mu_f}{\mu}\cdot\frac{W_o}{w_o}\cdot Sp.\,Sc\left(\frac{W_\infty}{W_o}\frac{\rho_f}{\rho_o}\cdot\frac{W_o}{w_o}+\frac{1}{2}\right)$

These results are discussed in chapter 6.

Appendix (7)

Computation of the theoretical results

In the approximate analyses for the present problem, equations relating the thermal and transport properties of both the condensate and the mixture were obtained. Using these equations with the appropriate properties, heat transfer results may be obtained by the use of suitable computer programmes.

A7.1 The thermal and transport properties

a - the steam and water properties

The water and steam properties were taken from the steam tables, [78,79]. These properties are in SI units

Within the range 0-100°c, the water saturation properties were assumed to be functions of temperature only. Therefore, by curve fitting, suitable equations were obtained for these properties. These equations are:-

$$v_f = 0.0009917 + t(6.5 \times 10^{-6} + 3.833333 \times 10^{-7} \times t)$$

$$k_f = 0.563 + (t - 5)\,(11.655 + 0.229(155 - t))/18900$$

$$\mu_f = 0.001 \exp(-1.62515 - T(1138.885 - 474754.6 \times T))$$

where t is temperature in Celsius

$T = t + 273.15$ K

v_f, k_f and μ_f are the water specific volume, thermal conductivity and viscosity respectively.

Equations of steam saturation pressure as a function of temperature and its saturation specific volume as a function of temperature and pressure were taken from the international steam tables [78]. For the saturated steam viscosity, the equation given in ref [81] to determine the gas viscosity was adjusted so as to give values within 2% of those given in the steam table [79] in the range 0-150°c. This adjusted equation is:-

$$\mu_v = 0.0000026693\, M_v T/(11.1503238 \times \psi)$$

where M_v is the steam molecular weight

ψ is collision integral based on the Lennard-Jones potential. This value is dependant on the temperature and may be obtained from appropriate tables, [81].

b - the gas properties

To obtain the non-condensing gas density, the gas was assumed to be ideal. To determine the gas viscosity, μ, the following equation was used, [81]:-

$$\mu = 0.0000026693 \times M_g T/(\sigma^2 \psi) \quad \text{(in SI units)}$$

M_g is the gas molecular weight

where σ is the hard-sphere diameter in angstroms. The value of σ varies from one gas to another and may be obtained from appropriate tables, [81].

c - the mixture **diffusion coeficient and viscosity**

The mixture viscosity and diffusion coefficient may be determined as follows, [81]:-

$$\mu_m = \mu_v/[1 + (y_2/y_1)\theta_{12}] + \mu/[1 + (y_1/y_2)\theta_{21}]$$

where μ_m is mixture viscosity in SI units

y_1 and y_2 are the mole fractions of the steam and gas respectively

$$\theta_{12} = 1 + (\mu_v/\mu)^{\frac{1}{2}}(M_g/M_v)^{\frac{1}{4}} \; 2/\left[\sqrt{8}(1 + M_v/M_g)^{\frac{1}{2}}\right]$$

$$\theta_{21} = \theta_{12}(\mu/\mu_v)\;(M_v/M_g)$$

$$D_{12} = (3.64 \times 10^{-8}/P_{mix})\left[(M_v + M_g)/M_v\,M_g\right]^{\frac{1}{2}} \times (P_{cv}\,P_{cg})^{\frac{1}{3}}\;(T_{cv}\,T_{cg})^{-\frac{5}{4}}\;T^{\,2.334}$$

where D_{12} is the coefficient of diffusion in SI units

P_{mix} is the mixture total pressure

P_{cv} and P_{cg} are the steam and gas critical pressures respectively

T_{cv} and T_{cg} are the steam and gas critical temperature respectively

<u>2.d-Steam-Gas mixtur and condensate properties</u>

The condensate properties(except viscosity)were taken as the arithmatic means of their values at the condensing surface and the interface, and the latent heat of vapourization at the interface temperature. The mixture properties(except viscosity)were taken as the arithmatic means of their values at the interface and in the bulk. In expressing the condensate viscosity as a polynomial in distance perpendicular to the test plate, and solving the Nusselt equation for the equilibrium of forces in the condensate, LeFevre[80] obtained the following expression for the condensate mean viscosity, μ_f:-

$$\mu_f = 3/(2/\mu_{fw} + 1/\mu_{fo}) \qquad \text{———— A}$$

where μ_{fw} and μ_{fo} are the condensate viscosities corresponding to the condensing surface and interfacerespectively

By making an analogy beteewan the governing equations, of the condensate and the vapour-gas mixture layers, LeFevre[80] concluded that the mean viscosity of the mixture μ_m, may be taken as:-

$$\mu_m = 3/(1/\mu_\infty + 2/\mu_o) \quad \text{—— B}$$

where μ_∞ and μ_o are the vapour-gas mixture viscosity at the bulk and interface respectively

Expressions A and B were used in evaluating the condensate and the steam-gas mixture viscosities.

A7.2 The computer programme

A typical programme used, is given below. The language used in the programme is "ALGOL". All computations were made on the University of London Atlas computer.

To compute heat transfer results using equation 3.27, procedures were set up to determine the various thermal and transport properties. Procedure (f) states equation 3.27. With the aid of procedure "find" which was written by LeFevre [80], equation 3.27 may be called with the appropriate input parameters to obtain an output of fractional reduction of heat transfer, mean mixture Schmidt and Grashof numbers and the temperature difference across the condensate film.

The same programme may be used to evaluate the results of other approximate solutions (i.e. Rose's equation [43] and Sledgers' analysis (appendix 6)). This is done by suitably adjusting procedure (f).

The programme

```
begin real delt,zin,cin,molg,ci,ai,pci,zci,roseratio,gr,sc,deltf;
   integer j,ii;Boolean boo;


procedure heatratio(delt,zin,cin,molg,ci,ai,pci,zci,roseratio,sc,gr,deltf);
   value delt,zin,cin,molg,ci,ai,pci,zci;
   real delt,zin,cin,molg,ci,ai,pci,zci,roseratio,sc,gr,deltf;

comment The parameters of procedure heatratio are as follows:-
         INPUT
         delt is mixture to surface temp. diff. (K)
         zin and cin are mixture bulk temp,and gas concentration
         molg is gas molecular weight
         ci and ai are gas Lennard Jones potentials
         pci and zci are gas critical pressure and temp.
           OUTPUT
         roseratio is Q/Qnu
         sc and gr are mixture mean Schmidt and Grashoff numbers
         deltf is temp. diff.across condensate;
begin
real wetparameters,
   zw,pw,vgw,hfgw,vfw,mufw,kfw,mugw,
   z,p,vg,hfg,vf,muf,kf,mug,
   pin,vgin,hfgin,vfin,mufin,kfin,mugin,
   gasparamaters,
   roegas,mu,
   roegasin,muin,
   mixparameters,pmix,
   c,mum,dee,roe,
   mumin,deein,roein,scin,
   constants,
   rmol,ln10,
   readconstants,
   mj,pcj,zcj,xi,rgas,
   v;
```

```
realprocedureomega(tee);valuetee;realtee;
beginowninteger i;ownrealarraya,b,c[1:81];
iftee>0thengotonormal;
a[ 1 ]:=-1.2040 ;b[ 1 ]:= 1.0242 ;a[ 2 ]:=-1.0498 ;b[ 2 ]:= 0.0662
a[ 3 ]:=-0.0163 ;b[ 3 ]:= 0.0131 ;a[ 4 ]:=-0.7985 ;b[ 4 ]:= 0.8620
a[ 5 ]:=-0.6031 ;b[ 5 ]:= 0.8140 ;a[ 6 ]:=-0.5078 ;b[ 6 ]:= 0.7683
a[ 7 ]:=-0.5108 ;b[ 7 ]:= 0.7251 ;a[ 8 ]:=-0.4308 ;b[ 8 ]:= 0.6841
a[ 9 ]:=-0.3567 ;b[ 9 ]:= 0.6461 ;a[ 10 ]:=-0.2877 ;b[ 10 ]:= 0.6103
a[ 11 ]:=-0.2231 ;b[ 11 ]:= 0.5766 ;a[ 12 ]:=-0.1625 ;b[ 12 ]:= 0.5452
a[ 13 ]:=-0.1054 ;b[ 13 ]:= 0.5158 ;a[ 14 ]:=-0.0513 ;b[ 14 ]:= 0.4880
a[ 15 ]:= 0.0000 ;b[ 15 ]:= 0.4618 ;a[ 16 ]:= 0.0488 ;b[ 16 ]:= 0.4376
a[ 17 ]:= 0.0953 ;b[ 17 ]:= 0.4148 ;a[ 18 ]:= 0.1398 ;b[ 18 ]:= 0.3934
a[ 19 ]:= 0.1823 ;b[ 19 ]:= 0.3720 ;a[ 20 ]:= 0.2231 ;b[ 20 ]:= 0.3535
a[ 21 ]:= 0.2624 ;b[ 21 ]:= 0.3358 ;a[ 22 ]:= 0.3001 ;b[ 22 ]:= 0.3158
a[ 23 ]:= 0.3365 ;b[ 23 ]:= 0.3023 ;a[ 24 ]:= 0.3716 ;b[ 24 ]:= 0.2874
a[ 25 ]:= 0.4055 ;b[ 25 ]:= 0.2731 ;a[ 26 ]:= 0.4383 ;b[ 26 ]:= 0.2593
a[ 27 ]:= 0.4700 ;b[ 27 ]:= 0.2461 ;a[ 28 ]:= 0.5008 ;b[ 28 ]:= 0.2343
a[ 29 ]:= 0.5306 ;b[ 29 ]:= 0.2215 ;a[ 30 ]:= 0.5596 ;b[ 30 ]:= 0.2103
a[ 31 ]:= 0.5878 ;b[ 31 ]:= 0.1997 ;a[ 32 ]:= 0.6152 ;b[ 32 ]:= 0.1898
a[ 33 ]:= 0.6419 ;b[ 33 ]:= 0.1798 ;a[ 34 ]:= 0.6678 ;b[ 34 ]:= 0.1706
a[ 35 ]:= 0.6931 ;b[ 35 ]:= 0.1613 ;a[ 36 ]:= 0.7419 ;b[ 36 ]:= 0.1450
a[ 37 ]:= 0.7885 ;b[ 37 ]:= 0.1293 ;a[ 38 ]:= 0.8329 ;b[ 38 ]:= 0.1151
a[ 39 ]:= 0.8755 ;b[ 39 ]:= 0.1017 ;a[ 40 ]:= 0.9163 ;b[ 40 ]:= 0.0890
a[ 41 ]:= 0.9555 ;b[ 41 ]:= 0.0779 ;a[ 42 ]:= 0.9933 ;b[ 42 ]:= 0.0667
a[ 43 ]:= 1.0296 ;b[ 43 ]:= 0.0564 ;a[ 44 ]:= 1.0647 ;b[ 44 ]:= 0.0460
a[ 45 ]:= 1.0986 ;b[ 45 ]:= 0.0383 ;a[ 46 ]:= 1.1314 ;b[ 46 ]:= 0.0296
a[ 47 ]:= 1.1632 ;b[ 47 ]:= 0.0218 ;a[ 48 ]:= 1.1939 ;b[ 48 ]:= 0.0139
a[ 49 ]:= 1.2238 ;b[ 49 ]:= 0.0070 ;a[ 50 ]:= 1.2528 ;b[ 50 ]:=-0.0001
a[ 51 ]:= 1.2809 ;b[ 51 ]:=-0.0068 ;a[ 52 ]:= 1.3083 ;b[ 52 ]:=-0.0131
a[ 53 ]:= 1.3350 ;b[ 53 ]:=-0.0191 ;a[ 54 ]:= 1.3610 ;b[ 54 ]:=-0.0249
a[ 55 ]:= 1.3863 ;b[ 55 ]:=-0.0305 ;a[ 56 ]:= 1.4110 ;b[ 56 ]:=-0.0357
a[ 57 ]:= 1.4351 ;b[ 57 ]:=-0.0408 ;a[ 58 ]:= 1.4586 ;b[ 58 ]:=-0.0457
a[ 59 ]:= 1.4816 ;b[ 59 ]:=-0.0506 ;a[ 60 ]:= 1.5041 ;b[ 60 ]:=-0.0551
a[ 61 ]:= 1.5261 ;b[ 61 ]:=-0.0595 ;a[ 62 ]:= 1.5476 ;b[ 62 ]:=-0.0639
a[ 63 ]:= 1.5686 ;b[ 63 ]:=-0.0680 ;a[ 64 ]:= 1.5892 ;b[ 64 ]:=-0.0720
a[ 65 ]:= 1.6094 ;b[ 65 ]:=-0.0759 ;a[ 66 ]:= 1.7918 ;b[ 66 ]:=-0.1095
a[ 67 ]:= 1.9459 ;b[ 67 ]:=-0.1362 ;a[ 68 ]:= 2.0794 ;b[ 68 ]:=-0.1581
a[ 69 ]:= 2.1972 ;b[ 69 ]:=-0.1769 ;a[ 70 ]:= 2.3026 ;b[ 70 ]:=-0.1933
a[ 71 ]:= 2.9957 ;b[ 71 ]:=-0.2868 ;a[ 72 ]:= 3.4012 ;b[ 72 ]:=-0.3560
a[ 73 ]:= 3.6889 ;b[ 73 ]:=-0.3978 ;a[ 74 ]:= 3.9120 ;b[ 74 ]:=-0.4302
a[ 75 ]:= 4.0943 ;b[ 75 ]:=-0.4565 ;a[ 76 ]:= 4.2485 ;b[ 76 ]:=-0.4700
a[ 77 ]:= 4.3820 ;b[ 77 ]:=-0.4982 ;a[ 78 ]:= 4.4998 ;b[ 78 ]:=-0.5152
a[ 79 ]:= 4.6052 ;b[ 79 ]:=-0.5307 ;a[ 80 ]:= 5.2983 ;b[ 80 ]:=-0.6311
a[ 81 ]:= 5.9915 ;b[ 81 ]:=-0.7317 ;
fori:=1step1until80doc[i]:=(b[i+1]-b[i])/(a[i+1]-a[i]);i:=40;tee:=exp(a[i]);
normal:tee:=ln(tee);step:ififtee<a[i]theni>1elsefalsetheni:=i-1else
ififtee>a[i+1]theni<80elsefalsetheni:=i+1elsegotoset,gotostep;set:
omega:=exp(b[i]+(tee-a[i])*c[i]);
end which states variation of collision integrals with temp.
 and determines the integral for a given temp.;
```

```
procedure wet(z,p,vg,hfg,vf,kf,muf,mug);
   value z;      real z,p,vg,hfg,vf,kf,muf,mug;
   begin         real t,T,x;
   if z<273.16 then z:=273.16 else if z>623.15
        then z:=623.15;
   hfg:=2477200-2450*(z-283.15);
   z:=z+0.01;
   if z<373.16 then
   p:=exp((28.59051+0.0024804*z-3142.31/z)*ln10-8.2*ln(z))
   else
   for x:=z*z-293700 do
   p:=10exp(5.432368-2005.1/z+(1.3869v-4*x/z)*(10exp(1.1965v-11*x*x)-1)
      -0.0044*10exp(-0.0057148*(647.26-z)exp1.25));
   T:=500/z;     t:=Texp6;
   vg:=(4.6152*z/p+0.512004+T*(-1.101807+T*(2.500832+T*
      (-21.433083+T*(15.281761+T*(-2.527165-2.454047*T)))))
      +p*t*(0.661366+T*(-3.258346+T*(6.303115+T*
      (-6.447504+T*(3.202128+T*(-0.514045-0.120102*T)))))
      +(p*t)exp3*0.000001*(8.44104+T*(28.86344+T*(-270.10366+
      T*(624.08835+T*(-675.70455+T*(363.16788-79.26405*T))))))))*0.001;
   p:=p*100000; z:=z-0.01;
   t:=z-273.15;
   kf:=0.563+(t-5)*(11.655+0.229*(155-t))/18000;
   vf:=0.01*(0.090017+t*(6.5v-6+3.833333v-7*t));
   mug:=0.0000026693*sqrt(18.016*z)/(11.15032376184*omega(z/416.419407));
   z:=1/z;
   muf:=0.001*exp(-1.62515-z*(1198.885-474754.6*z));
   end wet which gives properties of water substance at saturation
      when T=z K, all in SI units,from 0 to 100 Celsius;


real procedure ptot(zin,cin,rgas);
  value zin,cin,rgas; real zin,cin,rgas;
  begin wet(zin,pin,vgin,hfgin,vfin,kfin,mufin,mugin);
        ptot:=if cin=1 then pin else
              rgas*zin*cin/(vgin*(1-cin))+pin;
  end which,given bulk temperature and gas concentration
     determines the total pressure in SI units;


  procedure gasprop(z,p,roegas,mu,molg,rgas);
        value z,p,molg,rgas; real z,p,roegas,mu,molg,rgas;
        begin       roegas:=p/(rgas*z);
              mu:=0.0000026693*sqrt(molg*z)/(si*omega(z/ci));
        end which gives noncondensing gas density and viscosity
           in SI units.z is T,molg is M,rgas is Rgas;
```

```
procedure mixprop(z,c,mum,dee,roe,sc);
   value z; real z,c,mum,dee,roe,sc;
   begin real kij,kji;
   wet(z,p,vg,hfg,vf,kf,muf,mug);
   gasprop(z,pmix-p,roegas,mu,molg,rgas);
   c:=vg*roegas;c:=c/(c+1);
    roe:=roegas+1/vg;
   comment end of thermodynamic properties.
         begin transport properties.
   kji:=mu/mug. mum.=mj/molg; dee.=1/mum.
   kij:=(1+sqrt(kji*sqrt(mum)))exp2/sqrt(8*(1+dee));
   kji:=kij*dee/kji c:=rgas*z*c/(rgas*z*c+p*(1-c)*vg).
   mum:=c*mu/(c+(1-c)*kij)+(1-c)*mug/(1-c+c*kji);
   dee:=0.000000364*zexp2.334*101325/pmix*sqrt((molg+mj)/(molg*mj))*pci.
   sc:=mum/(roe*dee);c =p*vg*c/(rgas*z*(1-c)+c*p*vg);
   end which,for a given temperature,determines all
      mixture properties at that tenerature;in SI units.


procedure setup;
   begin
   ln10:=ln(10);xi:=omega(-1);
   rmol:=8314.3;mj =18.016;
   pcj.=22120000/101325;pci =(pci*pcj)exp0.333333333333.
   zcj.=647.3.pci:=pci*(zci*zcj)exp(-0.75);
   ai:=ai*ai.rgas =rmol/molg;
   end which sets all the constants required to
      determine viscosity and coefficient of
      diffusion for the mixture;



real procedure f(z);
   value z;    real z;
   begin real sp,r,wi;
   mixprop(z,c,mum,dee,roe,sc);
   kf:=0.5*(kf+kfw);
   muf =3/(2/mufw+1/muf);
   vf:=0.5*(vf+vfw);
   sp =(z-zw)*kf/(hfg*muf);
   wi:=c-cin;
   sc.=0.5*(sc+scin);
   roe:=0.5*(roe+roein);
   mum.=3/(1/mumin+2/mum);
   r:=sp*sp*sp*sc*c*c;
   f:=r*muf*cin*(cin*200+210*sc*c)/(roe*mum*vf)+
      wi*wi*wi*wi*roe*mum*vf/(sc*muf)*(sp*30-56*xi*wi)+
      50*r*wi*wi*muf*roe*vf/mum+r*wi*muf*(sc*c*105+200*cin)/mum-
      71*sp*sp*wi*wi*wi*c*roe*vf+sp*sp*wi*wi*c*(wi*42-100*cin-168*sc*c);
```

```
end which states equation 3.27;


procedure find(e)within:(a) between:(b,c)nullifying:(f)within:(d,found)
value a,b,c,d; real a,b,c,d,e,f; Boolean found; comment f is f(e);
begin real g,h,i,j,k,l,m,n;Boolean o; integer p;
      e:=m:=b; g:=f; e:=n:=c;h:=f;found:=true;ifsign(g)=sign(h)then
      begin   i:=abs(g); j:=abs(h);
              if i>d and j>d or i=j then go to fail;o:=i<j;
              k:= if o then b else c;e:= k+sign(c-b)*(ifothenaelse-a)
              if2*(ifothenjelsei)>abs(f)thengotofail;e:=k;goto exit;
      fail:           found:=i+j<d+d and abs(m-n)<a+a; e:=if found then (m+n)/2
              else if o then m else n; goto exit
      end solution or failure at bound; p:=0; j:=ln(abs(c-b)/a);
entry:  p:=p+1; i:=m+n; if p<j then
      begin   k:=(h+g)/(h-g); i:=i+(m-n)*k*abs(k)
      end;e:=k:=i/2;if abs(m-n)<a+a and abs(g+h)<d+d then goto exit;
      l:=f;if sign(l)≠sign(h) then
      begin       g:=l; m:=k
      endelse
      begin       h:=l; n:=k
      end;goto entry;
exit:
end find(e,a,b,c,f,d,found) which solves equation 3.27 to determine
     the interfacial temperature.


wet(zin,pin,vgin,hfgin,vfin,kfin,mufin,mugin);
setup;
xi:=(molg-mj)/(molg-cin*(molg-mj));
zw:=zin-delt;
vmix:=vtot(zin,cin,rgas);
wet(zw,pw,vgw,hfgw,vfw,kfw,mufw,mugw);
mixprop(zin,cin,mumin,dcoin,rooin,scin);
find(z,0.000025*(zw+zin),zw,zin,f(z),0.000000000001,hoo);
resratio:=if abs(zin-zw)<0.000001 then 1 else
      sqrt((vfin+vfw)/(vf+vfw)*sqrt(hfg↑/hfgin*((kf+kfw)*(z+zw)/
            ((kfin+kfw)*(zin+zw)))exp3*(mufin+mufw)/(muf+mufw)));
gr:=rooin*(roo-rooin)*0.05*0.05*0.05*0.980665/(mum*mum);
sc:=0.5*(sc+scin);
deltf:=z-zw;
end procedure heatratio;


comment begin of typical solution;
```

```
writetext(≮STEAM-AIR£MIXTURE£ALDIWNYS£VERTICAL≯);newline(2);
for cin:=0.001,0.01,0.05,0.1,0.2,0.3do
begin
writetext(≮GAS£CONC£AT£INF:≯);print(cin,1,3);newline(1);
writetext(≮£DELT/K≮5s≯Q/Qnu≮7s≯DELTF/K≮3s≯SC≮5s≯GR≯);newline(1);
fordelt:=5,10,20,50,70do
begin
heatratio(delt,373.15,cin,28.06,72.6,3.711,37.25,132.5,rosoratio,sc,gr,deltf
print(delt,2,3);print(rosoratio,1,3);print(deltf,6,3);print(sc,1,3);print(gr
newline(1);
end;
end;
end;
***Z
```

REFFRENCES

1. Nusselt N. — Z.Ver.deut.Ing., 60, 541 (1916a).

2. Nusselt N. — Z.Ver.deut.Ing., 60, 569 (1916).

3. Sparrow E.M. and Gregg J.L. — J.Heat Transfer, Trans.ASME,81,13 (1959).

4. Sparrow E.M. and Gregg J.L. — J.Heat Transfer, Trans.ASME,81,291 (1959).

5. Koh J.C.Y. Sparrow E.M. and Hartnett J.P. — Int.J.Heat & Mass Transfer,2,69, (1961).

6. Kirkbride C.G. — Ind.Eng.Chem.,26,425 (1934).

7. Hampson H. and Ozisik N. — Proc.Inst.Mech.Eng. (1953).

8. Tialby S.R. and Porlalskis — Trans.Instn.Chem.Engrs,38,324 (1960)

9. Zozulya M.V. — Dopovidi Akrd. Nauk Ukr.RSR,3,272 (1958).

10. Norman W.S. and McIntyre V. — Trans.Instn.Chem.Engrs,38,301 (1960)

11. Colburn A.P. — Ind.Eng.Chem.,26,432 (1934).

12. Rohsenow W.M. Webber J.H. and Ling A.T. — Trans.ASME.,78,1637 (1956).

13. Kutateladze S.S. — Fundamentals of Heat Transfer, Academic Press Inc., New York (1963)

14. Carpenter F.G. — Ph.D.Thesis,Dept.Chem.Engng.,Univ of Delaware (1948).

15. Gudemchuk V.A. and Konstantinov V.A. — Zlaur.Tekh.Fiz, 9 (1936).

16. Kututeladze S.S. — Heat Transmission in Condensation and Boiling,Mashgiz (1952).

17. Fuks S.N. — Teploenergelika,4,35 (1957).

× 18. Furman J. and Hampson H. — Proc.Instn.Mech.Engrs,173,147 (1959)

× 19. Mundelzweig S.I. — M.Sc.Thesis,Dept.Mech.Engng.,Queen Mary College (U.L.) (1961).

20. Rohsenow W.M. and Choi H.Y. — Heat,Mass and Momentum Transfer Prentice-Hall,New Jersey,PP 251 (1961).

× 21. Sparrow E.M. and Eckert E.R.G. — J.Heat Transfer, ASME,7,473 (1961).

22. Minkowycz W.J. and Sparrow E.M. — Int.J.Heat Mass Transfer,9,1125 (1966).

23. Merkel F. — Die Grun.Der War,T.Steinkopf, Leipzig (1966).

24. Sparrell J.K. — (Personal Communication in ref.20) Dynatch Corp. Camb. Mass.(1961).

× 25. Provan T.F. — N.E.L. Report No.219,(March 1966).

26. Schurge R.W. — Interphase Mass Transfer,Columbia University Press, New York (1953).

27. Sparrow E.M. Minkowycz W.J. and Saddy M. — Int.J.Heat Mass Transfer,10,1829 (1967).

28. Silver R.S. — Engineering, 161, 505 (1946).

29. Baer E. and McKelvey J.M. — J. A.I. Ch.E.,4,218 (1958).

30. Stefan J. — S.B. Akad. Wiss. Wien,63,63 (1871).

31. Stefan J. — Ann. Phys.,41,725 (1890).

32. Van der Held E.F.M. — Gesundheitzing,60,229 (1937).

× 33. Maxwell J.C. — Phil. Mag.,20,21, (1860).

× 34. Maxwell J.C. — Phil. Mag.,35,199 (1868).

× 35. Sparrow E.M. and Gregg J.I. — J.Heat Transfer,Trans.ASME,81,113 (1959).

× 36. Sparrow E.M. and Hartnett J.P. — J.Heat Transfer,Trans.ASME,83,101 (1961).

× 37. Sparrow E.M. and Lin S.H. — J.Heat Transfer,Trans.ASME,86,430 (1964).

× 38. Singer R.M. — Argonne National Lab.,ANL.6861 (July 1964).

× 39. Cess R.D. — Argew. Math. Phys.,11,426 (1960).

40. Sparrow E.M. — Ph.D.Thesis, Harvard Univ., Camb. Mass. (1956).

41. Minkowycz W.J. — Ph.D. Thesis, Univ. Minnesota, Minneapolis, Minn. (1965).

42. Othmer D.F. — Ind. Eng. Chem., 21, 577 (1929).

43. Rose J.W. — Int. J. Heat Mass Transfer, 12, 233 (1969).

44. Sledgers L. — Ph.D. Thesis, Univ. California, Berkeley (1968).

x 45. Hampson F. — Proc. Conf. on General Disc Heat Transfer, 58 (1951), London. Inst. Mech. Engrs (1952).

46. Brdlik P.M. — Inzh. Fiz. Zhur., 2, 3 (1959).

x 47. Akers W.W., Davis H. and Crawford J.E. — Chem. Engng. Progr. Symp. Ser., 56, 139 (1960).

x 48. Kroger D.G.C. and Rohsenow W.M. — Int. J. Heat Mass Transfer, 11, 15 (1968).

49. Thain W. — Ph.D. Thesis, Aberdeen Univ. (1967).

50. Colburn A.P. and Hougen O.A. — Ind. Eng. Chem., 26, 1178 (1934).

51. Cribb G.S. and Nelson E.T. — Gas Council, Research Commun. GC 32, London Gas Council (1956).

52. Votta K.A. and Walker C.A. — J. A.I. Ch.E., 4, 413 (1958).

53. Chilton J.H. and Colburn A.P. — Ind. Eng. Chem., 26, 1183 (1934).

54. Langen E. — Forschung, 2, 359 (1931).

55. Defriece A.N. — M.S. Thesis, The Rice Institute, Texas (1952).

x 56. Luder Z. — BIOS Final Report 1851, Item 31, 59, 68, London: H.M. Stationery Office (1947).

57. Tolubinskii V.I. and Yampolskii N.G. — Trady Inst. Teploenerget, 10, 24 (1953).

58. Mazyukevich I.V. — Zhur. Prik. Khi, 33, 1060 (1960).

59. Hampson H. — ASME. Int. Dev. in Heat Transfer, Part 2, 310 (1961).

60. Meisenburg S.I. Boats R.M. and Badger W.L. — Trans. A.I.Ch.E, 31,100 (1936).

61. Wetjen K.A. — Dissertation.Karlsuhe:Fak.Fur Mash.der Tech. Hoch (1953).

62. Renker W. — Wis.Zeit.der Tech.Hoch.Dresden,4, 1003 (1954/55).

63. Othmer D.F. — Ind.Eng.Chem.Anal.Ed.,1,46 (1929).

64. Mazyukevich I.V. — Teploenergetika, 7,53 (1955).

65. Mazyukevich I.V. — Trudy Len.Tekhn.Inst.Kholod.Prom., 11, 115 (1956).

66. Kelman J.S. — M.Sc. Thesis, Aberdeen Univ. (1962).

67. Gudemchuk V.A. — Izv. VTI, 12 (1935).

68. Smith C.S. and Palmer E.W. — Trans.Am.Inst.Min.Mteall.Engrs, 117 225 (1935).

69. Jakob M. — Heat Transfer, Vol.1, P109, John Wiley and Sons,New York (1964).

70. Squire H.B. — Modern Development in Fluid Dynamics,Ed. S.Goldstein,Vol.2,P641, Dover Publications (1965).

71. Ostrac h S. — NASA Report 1111 (1953).

72. Eckert E.R.G. and Drake K.A. — Heat and Mass Transfer, McGraw-Hill Inc (1959).

73. Cheesewright R. — Int.J.Heat Mass Transfer,10,1847 (1967).

74. Schmidt E.R. and Beckman W. — Tech. Mech and Ther., 1,11 (1930).

75. Tritton D.J. — Phil.Mag.,Vol IV 8th Series,780, June (1959).

76. Tritton D.J. — J.Fluid Mechanics, 6,547 (1959).

77. Hatsopoulos G.N. and Keenan J.T. — Principles of General Thermodynamics,John Wiley & Sons,Inc., New York (1965).

78. International Steam Tables — NEL, (1963).

79. VDI-Steam Tables — Springer-Varley (1963).

80. Le Fevre E.J. — Private Communications.

81. Reid R.C. and Sherwood T.K. — The Properties of Gases and Liquids, McGraw-Hill Inc.(1966).

82. Topping J. — Errors of Observation and Their Treatment, Chapman & Hall Ltd, London (1965).